UNIVERSITÀ DEGLI STUDI DI NAPOLI FEDERICO II

FACULTY OF MATHEMATICS
PHYSICAL AND NATURAL SCIENCES

SCUOLA DI DOTTORATO IN SCIENZE CHIMICHE
XXV ciclo

EXPERIMENTAL THESIS

SYNTHESIS AND CHARACTERIZATION OF NEW POLYMERIC BIOMATERIALS FOR PHARMACEUTICAL APPLICATIONS BY "CLICK CHEMISTRY"

SUPERVISORS
Prof. Giovanni Maglio
Co Supervisor
Prof.ssa Angelina Lombardi
COORDINATOR
PROF. LUCIO PREVITERA
EXAMINER
PROF. LUIGI PADUANO

CANDIDATE
Pasquale Tirino

ACADEMIC YEARS 2010-2013

INDEX

1.Introduction

2. Click chemistry strategy applied in low molecular weight range (from 1000 to 20000 dalton)

1. Introduction

1.1 Biomaterials

A biomaterial is a material that will interface with biological systems to evaluate, treat, augment or replace any tissue, organ or function of the organism[1]. In this second decade of 21st century, biomaterials constantly accompany everyone's life because are widely used throughout medicine, dentistry and biotechnology. Just 50 years ago biomaterial as we think of them today did not exist. The word “biomaterial” was not used. There were no medical device manufacturers (except for external prosthetics such as limbs, fracture fixation devices, glass eyes, and dental devices), no formalized regulatory approval processes, no understanding of biocompatibility, and certainly no academic courses on biomaterial. Yet, crude biomaterial have been used, generally with poor to mixed results, throughout history. The story of biomaterial use begins in the earliest days of human civilization to present days. It is convenient to organize the history of biomaterials into four eras: prehistory (until second industrial revolution), the era of the surgeon hero, designed biomaterials engineered devices(until 1980), and the contemporary era[2].

There is evidence that sutures may have been used as long as 32,000 years ago[3]. Large wounds were closed early in history by cautery or sutures. Linen sutures were used by the early Egyptians. The introduction of non-biological materials into the humanbody was noted far back in prehistory. The remains of a humanfound near Kennewick, Washington, USA (often referred to as the “Kennewick Man”) was dated (with some controversy) to be 9000 years old. This individual, described by archeologistas a tall, healthy, active person, wandered through the region now know as southern Washington with a spear point embedded

in his hip. It had apparently healed in and did not significantly impede his activity. This unintended implant illustrates the body's capacity to deal with implanted foreign materials. The spear points has little resemblance to modern biomaterial, but it was a "tolerated" foreign material implant, just the same. Unlike the spear point described above, dental implants were devised as implants and used early in history. The Mayan people fashioned nacre teeth from sea shells in roughly 600 A.D. and apparently achieved what we now refer to as bone integration, basically a seamless integration into the bone[4]. Similarly, an iron dental implant in a corpse dated 200 A.D. was found in Europe[5]. This implant was described as properly bone integrated. There were no materials science, biological understanding, or medicine behind these procedures. Their success (and longevity) is impressive and highlights two points: the forgiving nature of the human body and the pressing drive, even in prehistoric times, to address the loss of physiologic/anatomic function with an implant. In the year1508Leonardo da Vinci developed the contact lens concept while Rene Descartes is credited with the idea of the cortical contact lens in 1632.English physician William Harvey in 1628 espoused a relatively modern view of heart function when he wrote, "The heart's one role is the transmission of the blood and its propulsion, by means of the arteries, to the extremities everywhere." With the appreciation of the heart as a pump, it was a logical idea to think of replacing the heart with an artificial pump. Adolf Fick, best known for his laws of diffusion, was an optometrist and in 1860 invented the first contact lens offering a real success. Possibly the first study assessing the *invivo* bioreactivity of implant materials was performed by H. S. Leven 1829. Gold, silver, lead, and platinum specimens were studied in dogs and platinum, in particular, was found to be well tolerated. In1886, bone fixation plates of nickel-plated sheet steelwith nickel-plated screws were studied. In1924. A. Zierold published a study on tissue reaction to various materials in dogs. In 1938, aviator (and engineer) Charles Lindbergh and surgeon (and Nobel prize winner) Alexis Carrel wrote a visionary book, *The Culture of Organs*. They addressed issues of pump design (referred to as the

Lindbergh pump). sterility, blood damage, the nutritional needs of perfused organs and mechanics. This book must be considered a seminal document in the history of artificial organs.

After World War II, there was little precedent for surgeons to collaborate with scientists and engineers. Medical and dental practitioners of this era felt it was appropriate to invent (improvise) on their own where the life or functionality of their patient was at stake. Looking at a patient open on the operating table, they could imagine replacement; bridges, conduits, and even organ systems based on new materials originally manufactured for airplanes and automobiles. Many materials were tried on the spur of the moment. These early biomaterials include silicones. polyurethanes, tetrafluoroethylene (Teflon), nylon, methacrylates, titanium, and stainless steel. These were high-risk trials, but usually they took place where other options were not available. The term “surgeon hero” seems justified since the surgeon often had a lift (or a quality of life) at stake and was willing to take a huge technological and professional leap to repair the individual. This *laissez faire* biomaterials era quickly led to a new order characterized by scientific/engineering input, government quality controls, and a sharing of decisions prior to attempting high-risk, novel procedures. Still, a foundation of ideas and materials for the biomaterials field was built by courageous, fiercely committed, creative individuals and it is important to look at this foundation to understand many of the attitudes, trends, and materials common today.In 29thNovember, 1949 Sir Harold Ridky, M.D. (1906–2001) used ICI Perspex poly(methyl methacrylate) to fabricate plant lenses (intraocular lenses). For many years, Ridley was the center of fierce controversy because he challenged the dogma that spoke against implanting foreign materials in eyes. In this revolutionary period were invented and improved a lot of medical devices such as hip and knee prostheses, vascular graft, stents cardiovascular, pacemaker and heart valves.In contrast to the surgeon-hero era, the 1960s on saw the development of

materials designed specifically for biomaterials applications. The attention was focused on silicones rubber as component of artificial kidney or dialysis membrane, on polyurethanes as cardiovascular components, on Teflon for surgery and biotechnology applications, on titanium for implants in bony tissue, on hydroxyapatite for orthopedic applications, on polyethylene glycol also called polyethyleneoxide and polylactic-glycolic acid for controlled drug delivery.

It is likely that the modern era biomaterials engineered to control specific biological reactions, was ushered in by rapid developments in modern biology. In the 1960, when the field of biomaterials was laying down its foundation principles and ideas, concepts such as cell-surface receptors, growth factors, nuclear control of protein expression and phenotype, cell attachment proteins, and gene delivery were either controversial observations or undiscovered. On the other side new ideas in materials science grow in importance such as phase separation, anodization, self-assembly, surface modification and analysis. Since 1990 there has been a gradual integration between biology, chemistry and materials science that has provided a radically different approach to the design of new biomaterials.[6]This new approach is based on the modification of the physical-chemical properties of a material to obtain the desired final properties up to the concept of smart materials able to interact specifically with their biological environment. On these bases were founded new research field regarding tissue engineering and regenerative medicine, biospecific biomaterials, protein adsorption and controlled release. Polymeric materials are those which are best suited to this type of scenario because it is possible in principle to obtain any properties by modifying the molecular weight, the chemical structure, the degree of crystallinity.

1.2 Polymeric biomaterials

It is no accident that most of biomaterials currently produced is of a

polymeric nature or having polymeric components. Polymers are long-chain molecules (macromolecules) that consists of a large number of small repeating units A first great distinction in polymer universe, and consequently in polymeric biomaterials, concerns the way of obtaining a macromolecular chain: natural macromolecules or derived from organic synthesis process. In natural polymer can be included cellulose, alginate, chitosan, hyaluronic acid and genetic materials such as DNA or RNA. Synthetic polymeric biomaterials range from hydrophobic, non water absorbing materials such as silicone rubber (SR), polyethylene (PE), polypropylene (PP), poly(ethylene terephthalate) (PET), polytetrafluoroethylene (PTFE), polymethyl methacrylate (PMMA) to somewhat more polar materials such as polyvinylchloride (PVC), copoly(lactic glycolic acid) (PLGA) and nylons, to water swelling materials such as poly(hydroxyethyl methacrylate) (PHEMA), to water soluble material such as polyethyleneoxyde (PEO or PEG). A polymer is usually synthetized with a distribution of molecular weights, for this reason it is useful define an average molecular weight. The number average molecular weight, Mn (Equation 1), is an average over the number of molecules. The weight average molecular weight , Mw (Equation 2), is an average over the weight of each molecular chain

$$(1) \quad Mn = \frac{\sum NiMi}{\sum Ni} \quad (2) \quad Mw = \frac{\sum NiMi^2}{\sum NiMi}$$

Where N*i* is the number of mole of species *i* and M*i* is the molecular weight of species *i*

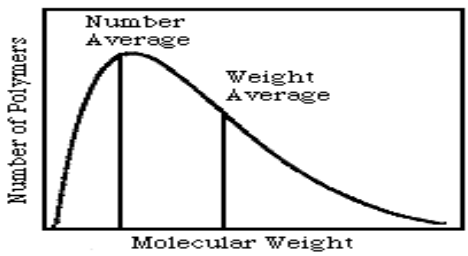

Fig 1.1 Example of molecular weight distribution

The ratio between Mn and Mw is known as the polydispersity index (Pi) and is used as measure of breadth of molecular weight distribution. Usually the Mn of polymeric biomaterials have a range from 5000 to 200000 Daltons and Mw from 8000 to 300000, but in exceptional case, such as PE used in hip joint, Mw can reach a million of Dalton. In general increasing molecular weight increase mechanical properties but increase melt viscosity also making more difficult manipulate the materials. The general requirement for polymeric biomaterials (or not) is biocompatibility. Biocompatibility was first defined, on the proposal of Williams,[7] during 9thInternational Conference on Biomaterials, (Chester, Great Britain, 1991) as "The ability of a material to perform with an appropriate host response in a specific application". This means that biomaterials must interact without recognizing of immune system which can eject it through inflammatory processes and without absorbing mechanism which can produce toxic or carcinogenic substances. The biocompatibility depends on both material properties (mechanical and chemical-physical properties), and the conditions of the host organism (tissue type, place of implantation, age, sex, general health, pharmaceutical regime). In particular, great importance have chemical-physical surface characteristics of biomaterial: the chemical structure of the surface, the hydrophilicity, hydrophobiciy, the presence of ionic groups, the morphology, the degree of surface roughness are factors that exert a strong influence on the characteristics of biocompatibility of the material. This still emphasizes the attention whereby are designed synthetic strategies to obtain polymer with a high degree of purity and very high stability during the phases of processing, sterilization and storage.

1.3 Polymeric biomaterials applications

Regenerated cellulose, for many years, was the most widely used dialysis membrane. Different kind of cellulose, such as cellulose acetate (CA) or microbial cellulose (MC), are also used as hollow fibers for kidney dialyser, in osmotic drug delivery devices and tissue engineering[8]. Chitosan is a linear polysaccharide composed of randomly distributed β-(1-4)-linked D-glucosamine (deacetylated unit) and N-acetyl-D-glucosamine (acetylated unit). It is made by treating shrimp and other crustacean shells with the alkali sodium hydroxide and find a lot of application in pharmaceutical chemistry from drugs for body weight control to fine system for controlled release[9]. Alginate, also called Alginic acid, is an anionic polysaccharide distributed widely in the cell walls of brown algae, where it, through binding water, forms a viscous gum. In extracted form it absorbs water quickly; it is capable of absorbing 200-300 times its own weight in water. It is used extensively as an impression-making material in dentistry and, due to alginate's biocompatibility and simple gelation with divalent cations such as Ca^{2+}, it is widely used for cell immobilization and drugs encapsulation.[10,11] Hyaluronic acid (also called Hyaluronan or hyaluronate or HA) is an anionic, nonsulfated glycosaminoglycan distributed widely throughout connective, epithelial, and neural tissues. It is unique among glycosaminoglycans in that it is nonsulfated, forms in the plasma membrane instead of the Golgi, and can be very large, with its molecular weight often reaching the millions. One of the chief components of the extracellular matrix, hyaluronan contributes significantly to cell proliferation and migration, and may also be involved in the progression of some malignant tumors. Hyaluronan has been used in the synthesis of biological scaffolds for wound-healing applications and as targeting or shielding agent in drugs controlled release[12].

PMMA it is a hydrophobic, linear chain polymer that is transparent, amorphous, and glassy at room temperature and may he more easily recognized by such trade name as Lucite or Plexiglas. It is a major ingredient in hone cement for orthopedic implants. In addition to toughness and stability, it has excellent light transmittance, making it a good material for intraocular lenses and hard contact lenses. The monomers are polymerized in the shape of a rod from which buttons are cut. The button or disk is then mounted on a lathe, and the posterior and anterior surfaces machined to produce a lens with defined optical power. The substitution of the methyl ester group in methylmethacrylate with a hydroxyethyl group (2-hydroxyethyl methacrylate or HEMA) produces a very hydrophilic polymer. For soft contact lenses, the polyHEMA is slightly cross-linked with ethylene glycol dimethyacrylate (EGDMA) to retain dimensional stability for its use as a lens. Fully hydrated, is a swollen hydrogel. PHEMA is glassy when dried, and therefore, soft lenses are manufactured in the same way as hard lenses; however, for the soft lens a swelling factor must he included when defining the optical specifications. Polyacrylamide is another hydrogel polymer that is used in biomedical separations (e.g., polyacrylamide gel electrophoresis or PAGE). The mechanical properties and the degree of swelling can be controlled by cross-linking with methylene-bis-acrylamide (MBA). Poly(N-alkylacrilamides) are environmentally sensitive, and the degree of swelling can be altered by changes in temperature and acidity. Polyacrylic acids also have applications in medicine. They are used as dental cements, e.g., as glass ionomers. In this use, they are usually mixed with inorganic salts, where the cation interacts with the carboxyl groups of the acid to form physical cross-links. Polyacrylic acid is also used in a covalently cross-linked form as a mucoadhesive additive to mucosal drug delivery formulations (Sec Chapter 7.14). Polymethacrylic acid may also be incorporated in small quantities into contact lens polymer formulations to improve wettability[13]. PE is used in its high-density form in biomedical applications because low-density

material cannot withstand sterilization temperatures. It is used as tubing for drains anti catheters, and in ultrahigh MW form as the acetabular component in artificial hips and other prosthetic joints. The material has good toughness and wear resistance and is also resistant to lipid absorption. Radiation sterilization in an Inert atmosphere may also provide some covalent cross-linking that strengthens the PE. PP is an isotactic crystalline polymer with high rigidity, good chemical resistance, and good tensile strength. Its stress cracking resistance is excellent, and it is used for sutures and hernia repair. PTFE, also known as Teflon, has the same structure as PE, except that the four hydrogens in the repeat unit of PE are replaced by fluorines. PTFE is a very high melting polymer (Tm= *327° C)* and as a result it is very difficult to process. It is very hydrophobic, has excellent lubricity, and is used to make catheters. In microporous form, known generically as the commercial product Gore- Tex, it is used in vascular grafts. Because of its low friction, it was the original choice by dr John Charnley for the acetabular component of the first hip joint prosthesis, but it failed because of as low wear resistance and the resultant inflammation caused by wear particles. PVC is used mainly as tubing and blood storage bags in biomedical applications. Typical tubing uses include blood transfusion, feeding, and dialysis. Pure PVC is a hard, brittle, material, but with the addition of plasticizers, it can be made flexible and soft. PVC can pose problems for long-term applications because the plasticizers can be extracted by the body[14]. Poly(dimethylsiloxane) PDMS or SR is an extremely vet· polymer, although Its use is often limited by its relatively poor mechanical strength. it is unique in that it has a silicon-oxygen backbone instead of a carbon backbone. Its properties are less temperature sensitive than other rubbers because of its very low Tg. In order to improve mechanical properties, SR is usually formulated with reinforcing silica filler and sometimes the polysiloxane backbone is also modified with aromatic rings that can toughen it. Because of its excellent flexibility and stability. SR is used in a variety of prostheses such as finger

joints, heart valves, and breast implants, and in ear, chin, and nose reconstruction. It is also used as catheter and drainage tubing and in insulation for pacemaker leads. It has also been used in membrane oxygenators because of its high oxygen permeability, although porous polypropylene or polysulfone polymers have recently become more used as oxygenator membranes. PET is one of the highest volume polymeric biomaterials. It is a polyester, containing rigid aromatic rings in a "regular" polymer backbone, which produces a high-melting (Tm=267°C) crystalline polymer with very high tensile strength. It may be fabricated in the forms of knot, velour, or woven fabrics and fabric tubes, and also as nonwoven felts. Dacron is a common commercial form of PET used in large-diameter knit, velour, or woven arterial grafts. Other uses of PET fabrics are for the fixation of implants and hernia repair. PET and more often poly(butylenterephtalate) (PBT) can also be used in ligament reconstruction and as a reinforcing fabric for tissue reconstruction with soft polymers such as SR[15]. Polymerization of bisphenol A and phosgene produces poly-carbonate, a clear, tough material. Its high impact strength dictates its use as lenses for eyeglasses and safety glasses, and housings for oxygenators and heart–lung bypass machine. Polycarbonate macrodiols have also been used to prepare copolymers such as polyurethanes. Poly-carbonate segments may confer enhanced biological stability to a material[16]. Nylon is the name originally given by Du Pont to a family of polyamides, the name is now generic, and many other companies make nylons. Nylons arc formed by the reaction of diamines with dibasic acids or by the ring opening polymerization of lactams. Nylons are used as surgical sutures. PLGA is a random copolymer used in resorbable surgical sutures, drug delivery systems, and orthopedic appliances such as fixation devices. The degradation products are endogenous compounds (lactic and glycolic acids) and as such are non toxic. PLGA polymerization occurs via a ring-opening reaction of a glycolide and a lactide. The presence of ester linkages in the polymer back bone allows gradual

hydrolytic degradation (resorption). The rare of degradation can be controlled by the ratio of poly(glycolic) to poly(lactic) acid [17]. Copolymers are another important class of biomedical materials. A copolymer of tetrafuoroethylene with a small amount of hexafluoropropylene (FEP Teflon) is used as a tubing connector and catheter. FEP has a crystalline melting point near 265°C (for PTFE is 327°C). This enhances its processability, compared with PTFE, while maintaining the excellent chemical inertness and low friction characteristics. Polyurethanes are block copolymers containing "hard" and "soft" blocks. The "hard" blocks, having T_g values above room temperature and acting as glassy or semicrystalline reinforcing blocks, are composed of a diisocyanate and a chain extender. The diisocyanates most commonly used are 2,4-toluene diisocyanate (TDI) and methylene di(4-phenyl isocyanate) (MDI), with MDI being used in most biomaterials. The chain extenders are usually shorter aliphatic glycol or diamine materials with two to six carbon atoms. The "soft" blocks in polyurethanes arc typically polyether or polyester polyols whose Tg values are much lower than room temperature, allowing them to give a rubbery character to the materials. Polyether polyols are more commonly used for implantable devices because they are stable to hydrolysis. Polyurethanes are tough elastomers with good fatigue and blood-containing properties. They are used in pacemaker lead insulation, catheters, vascular grafts, heart assist balloon pumps, artificial heart bladders. and wound dressings. A great importance for biomedical variety of uses and strong biocompatibility is covered by PEG or PEO. PEG is used in drug delivery as conjugates with low solubility drug and with immunogenic or fairly unstable protein drugs, to enhance the circulation times and stabilities of the drugs[18]. It is also used as PEG-phospholipid conjugates to enhance the stability and circulation time of drug-containing liposomes[19]. In both cases it serves to "hide" the circulating drug system from immure recognition, especially in the liver[20]. PEG has also been immobilized on polymeric

biomaterials surface: to make them "nonfouling." PEGs usually exist in a highly hydrated state on the polymer surfaces, where they can exhibit steric repulsion based on an osmotic or entropic mechanism. This phenomenon contributes to the protein and cell-resistant properties of surfaces containing PEGs[21,22].

1.4 Polymeric biomaterials synthesis

As mentioned above, appropriate structural changes allow to obtain from polymer new materials with specific mechanical properties, biocompatibility, and with controllable degradation rates. That is why it is possible to use different strategies to achieve these materials:

a) Modification of the polymer repeat unit: for example, shifting from poly(lactic) to (poly)glycolic acid, slower degradation and better workability is observed; while shifting from poly(glycolic) to poly(malic) acid a more hydrophilic character and the presence of functional groups in the chain is instead obtained.

b) Copolymerization: in this way it is possible to modify the physical and chemical properties of a given polymer as a function of nature of the comonomer, the composition, microstructure and architecture of the macromolecule. An example are the poly(caprolactone-polyethylene glycol) copolymers.

c) Mixing: the formation of alloys between two immiscible polymers allows to combine, possibly in a synergistic way, the desired properties of both components. Typical examples are alloys consisting of poly(L-lactide)/poly(ethylenglycol) and poly(DL-lactide)/poly(caprolactone).

d) Curing: ensure the dimensional stability of flexible, amorphous or extremely hydrophilic or water-soluble polymers

e) Modification of surface properties: an increase of 'hydrophilicity surface by grafting of groups -COOH, -OH, $-NH_2$, or by coating with hydrophilic polymers such as poly(ethyleneglycol), reduces cell adhesion, in particular of platelets.

As regard to chemical modifications, the synthetic strategies are based mainly on the formation of ester or amide bonds between the hydroxyl or amine terminals of the macromolecular chains or, more frequently, on "click chemistry" reactions. In his landmark review in 2001, Dr. Sharpless defined "click chemistry" as a group of reactions that "must be modular, wide in scope, give very high yields, generate only inoffensive byproducts that can be removed by nonchromatographic methods, and be stereospecific (but not necessarily enantioselective)". The required process characteristics include simple reaction conditions (ideally, the process should be insensitive to oxygen and water), readily available starting materials and reagents, the use of no solvent or a solvent that is benign (such as water) or easily removed, and simple product isolation. Purification, if required, must be by non chromatographic methods, such as crystallization or distillation, and the product must be stable under physiological conditions"[23]. To date, four major classifications of click reactions have been identified:

- Nucleophilic ring-openings—these refer to the openings of strained heterocyclic electrophiles, such as aziridines, epoxides, cyclic sulfates, aziridinium ions, episulfonium ions, etc

- Carbonyl chemistry of the non-aldol type-examples include the formations of ureas, thioureas, hydrazones, oxime ethers, amides, aromatic heterocycles, etc.. Carbonyl reactions of the aldol type generally have low thermodynamic driving forces, hence they have longer reaction times and give side products, and therefore cannot be considered click reactions

- Additions to carbon-carbon multiple bonds-examples include epoxidations, aziridinations, dihydroxylations, sulfenyl halide additions, nitrosyl halide additions, and certain Michael additions
- Cycloadditions, these primarily refer to 1,3-dipolar cycloadditions, but also include hetero-Diels-Alder cycloadditions

Among the four major classifications, cycloadditions, particularly the Cu(I)-catalyzed Huisgen 1,3-dipolar cycloaddition (HDC) of azides and terminal alkynes to form 1,2,3-triazoles, are the most widely used. Based on the literature search mentioned earlier, nearly 100% of the publications referred to this click reaction. The Cu(I)-catalyzed Huisgen 1,3-dipolar cycloaddition of azides and terminal alkynes to form 1,2,3-triazoles is the model example of a click reaction. It fulfills all of the criteria of click chemistry perfectly, no matter how subjective they may be, and is therefore extremely reliable and easy to use. This reaction exclusively forms 1,4-substituted products, making it regiospecific. It typically does not require temperature elevation but can be performed over a wide range of temperatures (0–160°C), in a variety of solvents(including water), and over a wide range of pH values (5 through 12). It proceeds as much as 10^7 times faster than the uncatalyzed version, and purification essentially consists of product filtration. Furthermore, it is unaffected by steric factors.

1.5 Biomaterial for pharmaceutical application

One of most important application of biomaterials is in pharmaceutical area. In fact new materials available, the large amount of innovative technologies and the high specificity achieved by the analytical techniques has enabled the development of new forms of administration for low and high molecular weight drugs with considerable therapeutic advantages, such as modified-controlled release systems. The formulations specifically defined "controlled release", are characterized by the accuracy with which the drug is released in order that obtaining the desired kinetics, generally, but not necessarily zero order, it is no longer an occasional fact, but a benefit rigidly guaranteed. In “Official pharmacopeia XI Edition” are more properly defined "modified-release pharmaceutical forms" those preparations in which the rate and/or the site of release of the active principles are different from that of a conventional pharmaceutical form administered by the same route. Ideally, a system defined “controlled release substance” (CRS) allows a single administration of the drug for the entire duration of therapy, ensuring the release of the same to the site of action and guarantees the spatial limitation and temporal monitoring of the bioactive substance . The design of such system of transport and release of drugs aims to satisfy various requirements, including:

- maintain plasma drug levels in the therapeutic range ;
- maintain the therapeutic efficacy throughout the programmed cycle;
- reduce the amount of drug administered;
- try to eliminate the side effects;
- avoid to patient inconveniences derived from repeated administration.

This deliberate modification is achieved with a special project formulation and/or method of manufacture. In all cases, the most important therapeutic advantage is represented by an effective medication, prolonged in time and without interruption throughout the duration of the programmed cycle, as shown in fig 1.2. This allows the optimal expression of the clinical potential of the active substance

by not exposing the patient to periods of ineffectiveness, typical of the conventional pharmaceutical forms, in proximity of the periods of ingestion. These duration extensions without solution of continuity are also achieved with a daily dose of medication generally less than that used in the therapy with the traditional pharmaceutical forms.

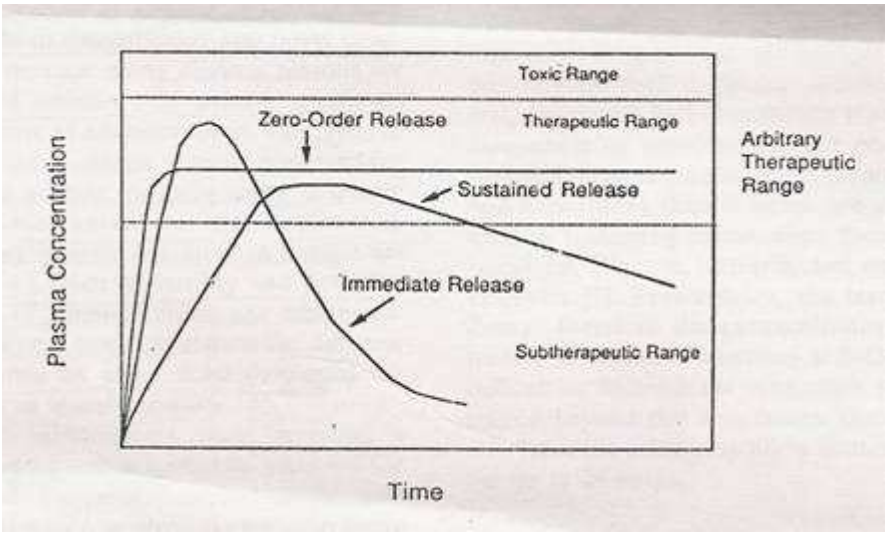

Fig 1.2 plasma concentration of drug versus time: immediate release curve is referred to a traditional pharmaceutical form; it is possible to note that sustained release drug remain more in therapeutic range.

Typically in new fomulations the drug is dispersed in a polymeric biomaterial. If a drug is dispersed in the polymer matrix, this must first be reached by the solvent to dissolve and subsequently diffusing through polymer layer, before reaching the external environment. In chemical controlled systems are also involved erosion processes and/or biodegradation of the polymer matrix that causes the progressive dissolution of the polymer of the outermost layer; in the latter case the chemical composition of the polymer is decisive. For the reasons described above, a biodegradable polymer result effective in controlling the release of drugs must be:

- Permeable to water;
- Semicrystalline: since only the amorphous phase is accessible to water
- In rubbery state: because the release media does not penetrate into polymer if not when the macromolecular chains reach a certain mobility (the temperature at which the transition occurs glass-rubber is referred to Tg)

Listed below are some types of matrices for release controlled bioactive substances:

FILM: loaded with drugs, subcutaneous implants or periodontal.

HYDROGELS are materials characterized by high hydrophilicity, high crosslinking density, discrete porosity. The drug is trapped in the polymer matrix or is chemically bonded to a component of hydrogel. When the system is in contact with aqueous biological fluids the hydrogel swells and the active substance diffuses out of the polymer glass matrix.

MICROSPHERES (d = 1-100 μm): uploaded with drugs or proteins, for oral use or injectable subcutaneously or intramuscularly.

NANOPARTICLES (MICELLES) (d = 10-100 nm) loaded with drugs or proteins for aqueous solutions for intramuscular injections or intravenous (also in blood vessels of reduced size).

1.6 Scope of research

This research is included in wider field of synthesis and characterization of polymeric biomaterials for pharmaceutical applications. In particular, has been developed a general synthetic strategy based on click chemistry suitable for a very large molecular weight range: from 1000 to 200000 dalton. The main advantages of this strategy is to be found in the simplicity of the characterization of synthetic intermediates, essentially ^{1}H-NMR and FT-IR, and the possibility to make useful as point of couplig any functional group generally present in polymers such as –OH, -NH_2 or -COOH. This ease of use has enabled to solve different problems related to

heterogeneous areas and different molecular weight range. In the first range, low molecular weight (from 1000 to 20000 dalton), described in chapter 1, can be inserted the synthesis and characterization of amphiphilic diblock copolymer of hydrophobic poly-ε-caprolactone (PCL) and hydrophilic poly(ethylenglycol) (PEG) block with non linear architecture. In aqueous environment amphiphilic copolymers self assembly in core shell micelles and hydrophilic and hydrophobic blocks form the corona and the core of micelles, respectively. Such systems have been investigated as nanocarriers of lipophilic drugs. Thanks to click coupling strategy has been possible to achieve copolymer with different architecture and to evaluate the influence of this parameter on copolymer bulk and self assembly properties. Furthermore has been possible to synthesize diblock and triblock copolymer with functional molecules coupled onto terminal of both block such as rhodamine, folic acid or cathechol. Function of these molecules will be discussed in chapter 1. Medium molecular weight range, discussed in chapter 2, (from 20000 to 50000 dalton) includes functionalization of poly(lactic-co-glycolic acid) copolymer with rhodamine used as polymeric matrix to realize microsphere for drug controlled release and the modification of –OH terminal into azide group of poly(ethyleneoxyde-polystyrene) diblock copolymer used in nano-technological application. As regard high molecular weight range, chapter 3, (50000-200000) it was possible to synthesize, in collaboration with group of professor Jean Cristophe Leroux of ETH in Zurich, conjugates polymer-protein using α-chimotrypsin as initiator in polymerization of PEG methacrylate and azidate monomer and focus attention on the peculiar features of these systems. It also was possible to synthesize chitosan chemical crosslinked by PEO. This product has showed good swelling properties useful in transdermal drug release.

References

[1] *Consensus Conference*, Chester, UK, 1991.

[2]*Biomat. Science: An Introd. to Materials in Medicine 2nd ed*., 2004, 8; Elsevier

[3]*Nat. News*, 1983, 20(5): 15-7)

[4]Bobbin, *Biomat. Science: An Introd. to Materials in Medicine 2nd ed*., 2004, 10; Elsevier

[5]Crubezy, *Biomat. Science: An Introd. to Materials in Medicine 2nd ed*., 2004, 10 Elsevier

[6]Daniel G. Anderson et all, *Science* 2004, 305, 1923,

[7]DF Williams, *Journal of biomedical engineering*, 1989, 11, Issue 3, pp 185-191;Elsevier

[8]Czaja et all *Biomacromolecules*, 2007, Vol.8, 1;

[9]Peniche C. et all, *Macromol. Biosci*. 2003, 3, 511–520

[10] Kuen Yong Lee, David J. Mooney, *Progress in Polymer Science*, 2012, 37, 106-126

[11] Alexander D. Augst et all, *Macromolecular Bioscience*, 2006, May, 623-634

[12] Na S.J. et all, *Int J Pharm*., 2008, Nov 3;363(1-2):149-54

[13] Giulia Bonacucina et all, *Polymers*, 2011, *3*(2), 779-811

[14] Joel A. Tickner, *American Journal of Industrial Medicine January*, 2001, pp. 100–111,

[15] Prowans P. et all, *Biomaterials*, 2002, 23, 2973-2978

[16] Maria Hanshella R. Magno et all, *Journal of Materials Chemistry*, 2010, 20, 8885–8893

[17] Ghanashyam Acharya et all, *Journal of Controlled Release*, September 2010, Vol. 146, 2, p 201–206

[18]Yoh Kodera et all, *Prog. Polym. Sci.*, 1998, Vol. 23, 1233–1271.

[19]Francesco M. Veronese, Biomaterials, 2001, 22, p 405-417

[20] S. L. Yowell and S. Blackwell, *Cancer Treatment Reviews*, 2002; 28(SUPPL, A): 3-6

[21] M.J. Roberts et all, *Advanced Drug Delivery Reviews*, 2002, 54, 459–476

[22]José González-Valdez et all, *Anal Bioanal Chem*, 2012, 403:2225–2235

[23] H. C. Kolb, M. G. Finn, and K. B. Sharpless. *Angew. Chem. Int. Ed. Engl*. 2001, 40, 2004–2021.

Chapter 2

Click chemistry strategy applied

in low molecular weight range

(from 1000 to 20000 dalton)

2.1 Synthetic strategy description

As already mentioned, the synthetic strategy of this research work is based on click chemistry, in particular on 1-3 Huisgen cicloaddition(HDC) between azide and alkyne groups catalysed by Cu(I) showed in figure 2.1

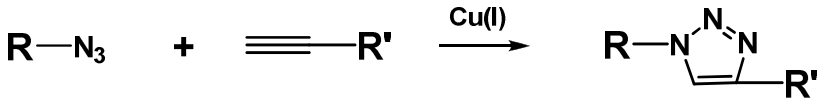

Fig. 2.1:1-3 *Huisgen cicloaddition between azide and alkyne groups catalysed by Cu(I)*

The success of this reaction with respect to others described in Introduction is due to two additional reasons: azides and terminal alkynes are fairly easy installed and they are extremely stable at standard conditions [1,2].They both can tolerate oxygen, water, common organic synthesis conditions, biological molecules, a large range of solvents and pH's, and the reaction conditions of living systems (reducing environment, hydrolysis, etc.). Even though the decomposition of aliphatic azides is thermodynamically favored, a kinetic barrier exists that allows them to be stable in the aforementioned conditions[3]. They will essentially remain "invisible" in solution until a dipolarophile, such as an alkyne, comes into contact. In general, cycloadditions proceed through a concerted mechanism. However, experimental kinetic data[4] and molecular modeling[5] performed on the HDC reaction seem to favour a stepwise reaction pathway. Based on experimental evidence[6,7] and the fact that Cu (I) can readily insert itself into terminal alkynes, it is envisioned that the first step of the reaction involves π-complexation of a Cu(I) dimer to the alkyne (1 in Fig. 2.2). Thereafter, deprotonation of the terminal hydrogen occurs to form a Cu-acetylide. There are actually several different kinds of Cu-acetylide complexes that can form, depending on the reaction conditions utilized; 2 in Fig 2.2 represents just one possibility. The π-complexation of Cu(I) lowers the pKa of the terminal alkyne by

as much as 9.8 pH units, allowing deprotonation to occur in an aqueous solvent. This step is obviously favoured by a base. In organic solvent N,N′-diisopropylethylamine (DIPEA)is widely added[8]. In the following step, N(1) displaces one of the ligands from the second Cu in the Cu-acetylide complex to form 3. In turn, this "activates" the azide for nucleophilic attack C(5)

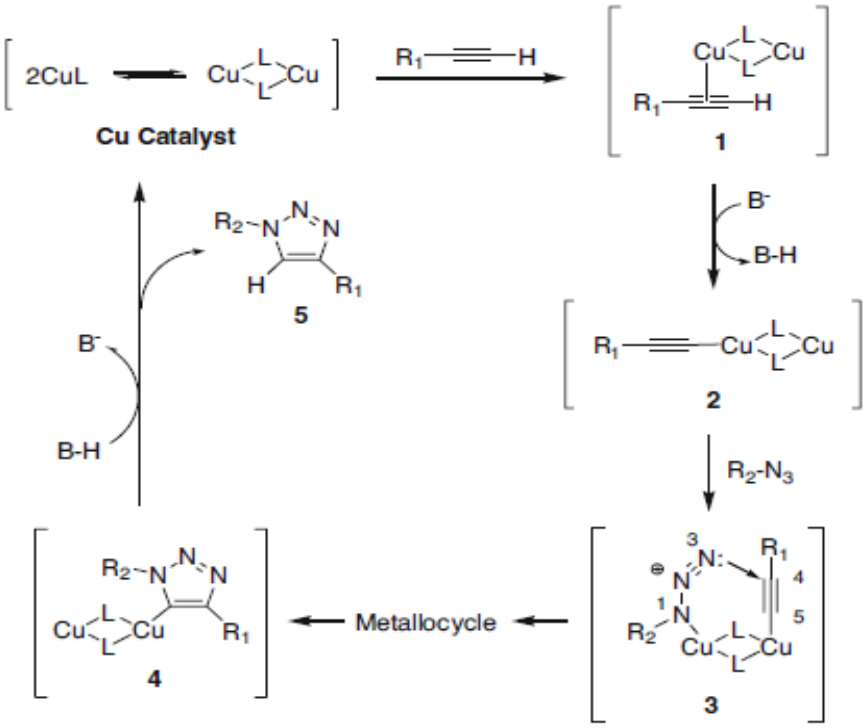

Fig. 2.2*Proposed mechanism for the HDC reaction. Ligands are represented by "L" and symbolize a wide variety of possible compounds, depending on the catalyst used. As an example, if CuBr was used as the catalyst then the ligand would be bromide .Figure adapted from reference 3*

Due to proximity and electronic factors, N(3) can now easily attack C(4) of the alkyne, leading to a metallocycle (not shown for simplicity). The metallocycle then contracts when the lone pair of electrons of N(1) attacks C(5) to form the

respective triazole 4. Once 4 forms, the attached Cu dimer immediately complexes to a second terminal alkyne. However, this second alkyne cannot undergo a cycloaddition due to the unfavorable structure of the complex, and it dissociates upon protonation to reform 4. One final protonation releases the Cu(I) catalyst from the 1,2,3-triazole product 5, to undergo a second catalytic cycle with different substrates. Both of these protonations are most likely the result of interactions with protonated external base and/or solvent, but further studies are needed to conclusively confirm. Recent studies have shown that catalysts are not always required for the cycloaddition to proceed. By using electron deficient alkynes, the reaction can proceed readily at ambient conditions[9]. However, electron deficient alkynes are very reactive toward nucleophiles and can lead to side products , which has kept these types of reactions estranged from the field of click chemistry. Concerning the catalyst, there are a number of methods to achieve the active copper for the HDC reaction. Recently, Cu(I)-modified zeolites were reported as catalysts for the HDC reaction[10]. “Zeolites” refers to a family of aluminosilicate minerals that are highly porous and therefore have large surface areas. Pending more research, this approach could prove to be very valuable. Oxidizing copper metal with an amine salt is another way to generate the catalyst. There are a considerable number of disadvantages with this strategy. Longer reaction times are needed, as well as larger amounts of copper, it is more expensive, and requires a slightly acidic environment to dissolve the metal, which could be damaging to any acidic sensitive functional groups present in the reactants. One of the most common techniques is to reduce Cu(II) salts, such as $CuSO_4 \cdot 5H_2O$, in situ to form Cu(I) salts. Sodium ascorbate is typically used as the reducing agent in a 3- to 10-fold excess, but other reducing agents, including hydrazine[11] and tris(2-carboxyethyl)phosphine (TCEP)[12], have been used with reasonable success. The advantages of this strategy are: it is cheap, can be performed in water, does not require deoxygenated atmosphere[13]. Not only does an aqueous solvent remove the need for a base, as previously explained, but it also eliminates the need for

protecting groups (O–H and N–H functional groups essentially remain “invisible” in aqueous solutions) and it is environmentally safe. The main disadvantage is that the reducing agent might reduce Cu(II) down to Cu(0). This can generally be prevented, though, by using a proper ratio of reducing agent to catalyst and/or adding a copper-stabilizing agent, such as tris-(hydroxypropyltriazolylmethyl) amine (THPTA). A second way to create the catalyst is to directly add Cu(I)salts. Many such compounds have been utilized over the past few years, including CuBr, CuI, $CuOTf{\cdot}C_6H_6$ (OTf= trifluoromethanesulfonate), $[Cu(NCCH_3)_4][PF_6]$, $BrCu(P(Ph)_3)_3$[14].This last catalyst is adopted in synthetic strategy because does not require a reducing agent, but it has to be react in a deoxygenated environment and in an organic solvent (or a mixed solvent) even if posphine ligands mildly protect copper by oxydation.

It is quite usual to find an hydroxyl or amine as terminal group or in side chain of polymers and obtain a quantitative method to turn them in azides or alkyne became critical in preliminary synthesis set up. In fact, the separation of unreacted byproducts in polymer chemistry results extremely hard because of significant similarity of the products that must be separated. The changing in only one monomeric unit negligibly contributes to the properties of the whole macromolecule in terms of polarity, density or other physical-chemical properties useful in most common separation, as for example the chromatography.

Azidation is another distinctive feature of the strategy used in this research work. Frequently is convenient to carry on the azidation on the polymer having hydroxyl groups. Azides can be prepared from alcohols in a two-step process involving first the conversion to ulfonate or halide groups with subsequent azide ion displacement, or by direct conversions. Tertiary alcohols can be converted directly to azides by using hydrazoic acid and boron trifluoride as catalyst[15].Other Lewis acids can be utilized and it was shown that $HN_3/TiC1_4$smoothly converts benzylic, allylic, or tertiary alcohols to the corresponding azides in good yield[16].

Primary alcohols are unaffected and stereochemistry is not maintained, indicative of a carbocation intermediate. The modified Mitsunobu reaction (Ph_3P, diethylazocarboxylate, HN_3 benzene, 2 h, 20°C) converts alcohols to azides with inversion of configuration. Thus, azido benzoate and epoxides and were prepared from the appropriate alcohols[1718].Activation of the alcohol function by formation of a phosphonium salt has also been reported. Thus, protected sugars with a free anomeric OH can be directly converted to the glycosylazides (with inversion of configuration) under extremely mild conditions[19]. The azidation route adopted consists of a two step process with azide displacement from methanesulfonate (mesylate) alcohols obtained by mesyl chloride reaction (Fig 2.3)

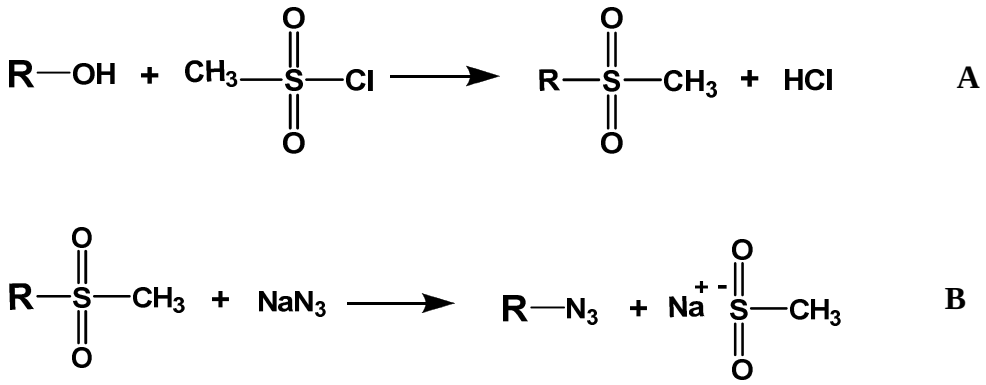

Fig. 2.3Two step process azidation: A) Hydroxyl activation by mesyl chloride B) Nucleophilic substitution by sodium azide

Main advantages respect to halide process are to be found in milder reaction condition, almost quantitative conversion and selectivity because mesyl is an excellent leaving group, avoiding byproduct problem separation, and simplicity of characterization. Methyl group of mesyl adduct, in fact, shows a clear singlet signal in ^{1}H-NMR at around 3 ppm that is an area usually not crowded by other signals, so it is possible to evaluate the azidation reaction degree while subsequent quantitative displacement of azide groups is easily detected by FTIR following the

characteristic azide stretching band around 2100 cm^{-1}. Crossing two evidences, complete disappearing of 3 ppm ^{1}H-NMR singlet and appearing of 2100 cm^{-1} FTIR stretching signal, can be minimized the error in the characterization.

On the other hand, is less complicated to obtain a quantitative conversion degree in alkyne functionalization, starting from different group such as hydroxyl, amine or carboxylic. Amine groups react with propargylchloroformate, in the presence of a proton acceptor, to give propargylcarbamate[20] as shown in Fig 2.4

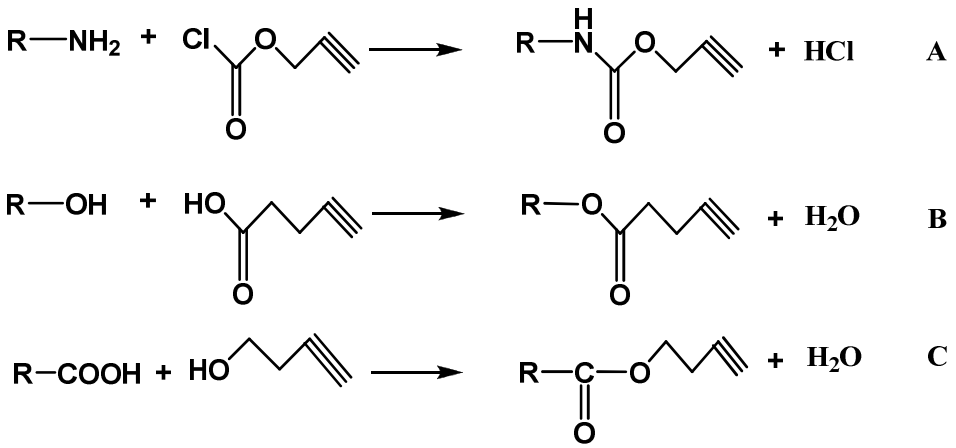

Fig 2.4 Alkyne functionalization A) amine reacts with propargylchloroformate, B) alcohol reacts with 4-pentynoic acid, C) carboxylic acid reacts with 3-butynol

Alcohols react with 4-pentynoic acid using dicyclohexylcarbodiimide (DCC) and dimethyamino-pyridine (DMAP), as a catalyst, to give a propargyl ester[21]. Carboxylic acids give with 3-butynol similar products by the DCC-DMAP system. All these products are easily characterized by ^{1}H-NMR.

2.2 Polymers in drug controlled release

The traditional drugs are low molecular weight compounds that quickly find access to the cells by passage through the cell membranes. For example, in the case of intravenously administration, a high percentage of injected drug is excreted after

few minutes, while the remainder is evenly distributed in body, with little concentration at the site where it is needed the therapeutic action. In the last decade the research is strongly focused on the study of polymeric systems able to ensure the controlled release of biologically active substances[22]. These systems therefore exhibit particular properties for which they can be considered selective carriers for the transport of biologically active substances incorporated in the vector to damaged sites, allowing to improve its efficiency. This is achieved by modifications on the release and absorption of the drug acting on the pharmacokinetic and pharmacodynamic properties or using polymers of different chemical nature. In fact, the physico-chemical properties of the biomaterial and the architecture of the same, may allow a control of the drug release kinetics, optimizing the activity profile as described in introduction. The fundamental requirements of a polymeric biomaterial useful for the preparation of a vector are:

- compatibility between the polymer and the pharmacokinetics of the active principle, intended as physical and chemical characteristics that determine the release;
- mechanical strength to allow for the administration and maintenance of the integrity of the delivery system;
- biocompatibility, that is low toxicity for cells and tissues

It is possible to identify different types of matrices (Introduction 1.5) that constitute an effective vehicle for drug release, such as films, microspheres, nanoparticles (micelles) and hydrogels, each of which is associated with a specific use according to the structural characteristics of bioactive molecule[23]. Research has shown considerable interest in the micellar systems consisting of amphiphilic copolymers[24,25,26] which have proved, for the characteristics set out previously, important use as carriers for the transport of bioactive molecules. When these copolymers are dissolved in a selective solvent, in particular water, good solvent for a block and bad solvent for the other, above a certain concentration, called

Critical Micelle Concentration (CMC), the individual chains ("unimers") self-assembly creating ordered "core-shell" structures of nanoscopic dimensions and, mainly, of spherical shape. The core is formed only by the hydrophobic segment and can be loaded with lipophilic drugs; the shell, in turn, is of hydrophilic nature and has the double duty to protect and ensure solubility of the nanoparticle core in an aqueous environment and, therefore, the drug delivery.

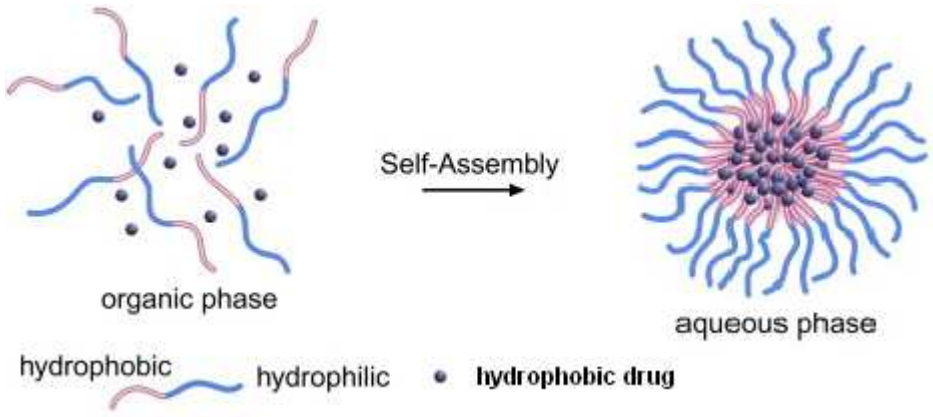

Fig. 2.5 Amphiphilic diblock copolymer self assembly process

The key indicator of the polymeric micelles stability is CMC: typical minimum values of CMC suitable for pharmaceutical applications are in the order of 10^{-6}-10^{-7} M. The high thermodynamic stability of the polymeric micelles, compared to those originated by conventional surfactants, indicates that the former have a low tendency to disassemble even at very low concentrations and, therefore, the dissociation of micelles in unimers is generally slow when the system is diluted into the bloodstream too. One of the major advantages in the formation and then in the use of micelles and nanoparticles is the possibility to administer even in bloodvases of small size thus potentially formulate drugs for direct injection. Furthermore, the residence time of a copolymer in micelles is of the order of hours since these micelles particularly stable [27]. The properties of a micellar system are strongly related to the chemical nature of the constituting polymer blocks and to the

copolymer structure. The obtaining of well-defined structures requires the choice of an appropriate strategy of synthesis with appropriate polymerization reaction (anionic, ring-opening (ROP) or radical).Many efforts have been directed to understanding the dynamics of dissociation to optimize stability and performance of polymeric micelles in vivo. For example, it is shown that in the amphiphilic copolymers stability micellar is well correlated with the length of the hydrophobic segment and higher percentages of hydrophobic component confer more thermodynamic stability. Even the physical state, amorphous or crystalline, of the polymer that forms the hydrophobic core influences the nanostructures kinetic stability[28]. Micelles composed of hydrophobic segments with a glass transition temperature (Tg) above 37 ° C, are said core "frozen", ie that the movements of the molecular chains in the nucleus are forced, this implies as a consequence a greater retention of the drug, decreasing the rate of diffusion of the same from the nucleus. Most amphiphilic copolymers useful to form polymeric micelles employed for drugs delivery, contains a polyester or derivatives of poly (amino acid) (PAA) as a hydrophobic segment. Among the polyesters, poly (lactic acid) (PLA), poly (ε-caprolactone) (PCL), and poly (glycolic acid) (PGA) are widely used as biocompatible and biodegradable materials, approved by the FDA (Food and Drug Administration) for biomedical applications in humans. In particular PCL(Figure 2.6) combines high hydrophobicity, low melting temperatures and glass transition temperature.

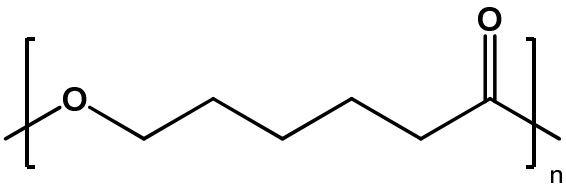

Fig 2.6 PCL repetitive unit

This polyester is usually prepared by ring-opening of ε-caprolactone using an alcohol as mono-, di-or poly-functional initiator[29].The poly (oxyethylene) (PEO)

(Figure 2.6), instead, is commonly used in the majority of amphiphilic micelles, as a hydrophilic segment for the formation of the shell, as it is one of the few synthetic polymers approved by the FDA for internal use for its biocompatibility and lack of toxicity. In fact, when it comes into contact with body tissues or fluids, it does not cause any response of the latter involving a reaction of an inflammatory type or the activation of the coagulation system of the blood that might determine the formation of thrombi. The main feature of the PEO is therefore to make the micelles biomimetic, i.e. invisible ("stealthy") to the immune system. Moreover, thanks to its high solubility in water, high mobility and large volumes of exclusion, the PEO imparts steric stability such as to minimize the interfacial free energy of the core and to hinder the hydrophobic intermicellars attractions avoiding formation of macro-aggregates.

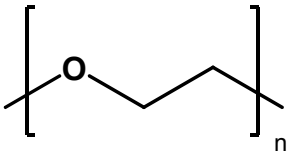

Fig 2.7 PEO repetitive unit

Currently, many drugs, analgesics, cardiovascular agents, antibiotics, tranquilizers, and vitamins are administered by micro and nano scale matrix. The need to encapsulate the drugs, including anticancer agents, (many of which are bulky polycyclic compounds, such as camptothecin, paclitaxel, docetaxel or tamoxifen) arises from their poor solubility in water and high hydrophobicity. In fact it has been estimated that 40% of the active drugs and candidates as potentially useful were rejected already in the screening and have never entered a phase of development due to their poor solubility in water. Polymeric micelles are able to reach a specific target through a passive or active mechanism avoiding biological side effects. Passive targeting depends on the physical or biophysical interactions that take place between particles system and host organism. The particles with sizes

in the range from 0.3 to 2 μm, once taken into the body are recognized as foreign bodies from the immune system and are quickly intercepted by reticulo-endothelial (RES) cells. These occur mainly in liver and can be an advantage if the site of drug action is represented by these cells. The particles location at different target organs can depend both from dimensions and the administration method used. Nanospheres with diameter between 100 and 300 nm tend to localize primarily in the liver, spleen and bone marrow. Administration by intravenous or intra-arterial microspheres with suitable dimensions generally favors orientations of the passive type, given the particular structure of the vascular system in pathological conditions. For example the intra-arterial administration of microspheres of 12μm diameter can lead to the selective localization of the particle to the tumor cell because to grow quickly these cells stimulate the formation of new blood vessels to provide themselves with oxygen and nutrients. These tumor vessels, however, show abnormalities in shape and architecture, as they exhibit the internal endothelial wall with large windows of nanoscopic size (below 200 nm)[30]. Diffusion and accumulation parameters are strongly influenced by size of the cut of the endothelium. This phenomenon is usually associated with a defective lymphatic drainage. As a result, the tumors show a dynamic irregular transport of fluids and molecules. The selective mechanism due to this two factors, fenestrate endothelium and defective lymphatic drainage, has been termed EPR: enhanced permeability and retention effect (Figure 2.8). As regards the active targeting, it is possible to use both the overexpression or exclusive expression of different receptors or epitopes on the tumor cells wall, both of specific physical characteristics. For example antibodies represent one of the most interesting bioconjugates used to obtain a targeted active transport of a therapeutic carrier, while a satisfactory active targeting can also be achieved by exploiting the physical properties of the nanoparticles, for example magnetism[31]. Other targeting approaches are based on the fact that in many pathological processes there is a slight increase of temperature or a decrease in pH. For example, contrary to the normal pH of 7.4 of the blood, the

values of the extracellular pH in tumor tissues were determined around 6.8-7.0. This is mainly attributed to the higher rate of aerobic and anaerobic glycolysis than normal cells. Micelles formed by block copolymers pH-sensitive, able to dissociate in response to a lowering of pH, were studied to release drug molecules incorporated allowing accumulation in tumor sites.

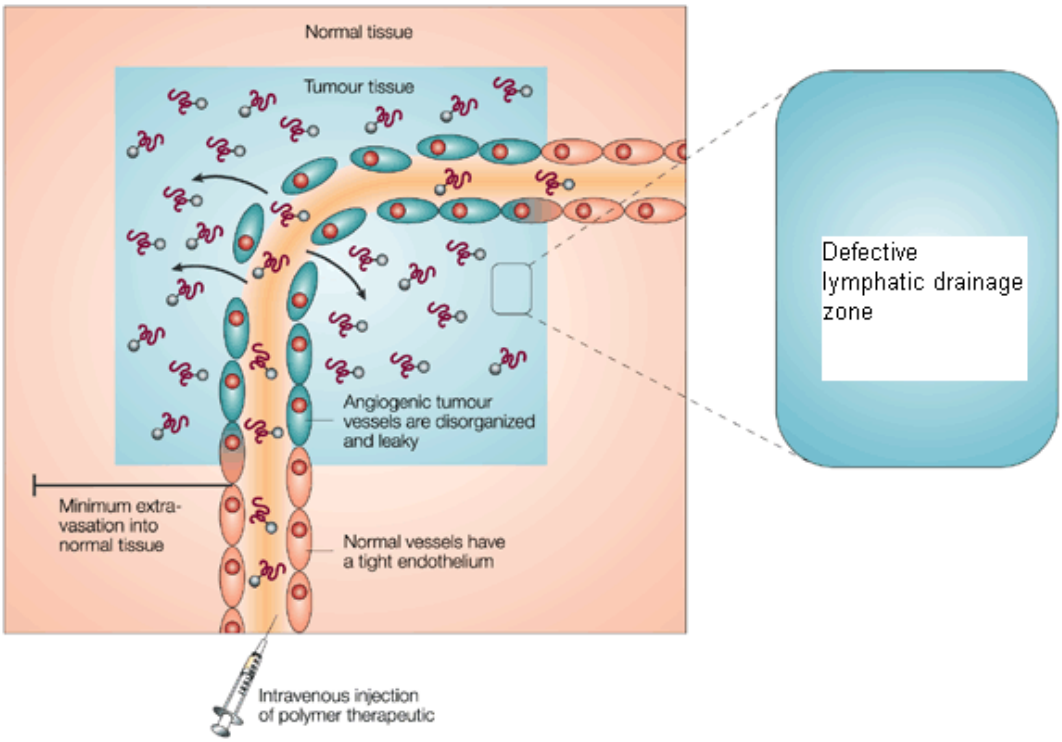

Fig. 2.8 Tumor targeting by EPR effect

2.3 Sate of art and section aim

It well known from the literature that the parameters which can have greatest influence on the micellization processes, the size of nanoparticles and on the CMC, at constant chemical nature of the blocks, are: the composition of the copolymer, the length of the two blocks, hydrophilic and hydrophobic, and the architecture of the copolymer. Furthermore, the study of the relationship between architecture and properties of biomaterials and biopolymers, is currently one of the research topics

of larger interest in the pharmaceutical field. The research team, in which was developed this research work, has devoted significant attention on synthesis and characterization of amphiphilic block copolymers PCL(B)-PEO(A), with a composition richer in hydrophobic segment (≈2/1) to be used as nanocarriers of lipophilic drugs, for the sustained and targeting release of the same[32,33,34]. The linear molecular structures, such as di-block and tri-block, are the most studied as potential nanocarriers. In the case of linear copolymers of-block or tri-block copolymers and of "star-shaped" copolymer, from studies conducted in research work laboratories, has been shown excellent self-aggregation properties in aqueous systems with formation of very regular core-shell structure micelles, of small size (Hydrodinamic Diameter <100 nm) and with low CMC values. In the literature, on the contrary, are reported few works on the preparation of PCL-PEO copolymers with a branched structure and their use as drug nanocarriers.

The research team has also synthesized and characterized star block copolymers (star shaped) with four arms $(PCL\text{-}PEO)_4$, and branched copolymers "miktoarm" (called in this way because from a single center spread blocks of different nature) such as PEO-$(PCL)_2$ and PEO-$(PCL\text{-}PEO)_2$ using innovative procedures based on caprolactone polymerization from appropriate macroinitiators. The aim of this research work section was to develop synthetic strategies for PCL-PEO poly(ether-ester)s, based on click chemistry, to obtain linear diblock PCL-PEO and triblock PEO-PCL-PEO copolymers and branched “miktoarm” architectures: "Y" modified shape, such as $(PEO)_2$-PCL-PEO [A_2BA], and the “H” shape , such as $(PEO)_2$-PCL-$(PEO)_2$ [A_2BA_2]. The ester component is constituted by segments of PCL having molecular weights variables (3.0-12.5.0 KDa), while the ether component consists only of PEO segments with 1.0 kDa molecular weight. In this way it was possible to prepare copolymers with different architecture, maintaining constant the weight ratio PCL/PEO ≈ 3 and PEO block molecular weight. These copolymers were compared with “miktoarm” "Y" shape,$(PEO)_2$-PCL [A_2B] with the same PCL/PEO weight ratio already synthetized

in this research laboratory to analyze the influence of copolymer architecture on bulk and aggregation properties. As can be noted in figure 2.9, in ideal copolymer self-assembly model of copolymers with A_2B, A_2BA and A_2BA_2 architectures, to equal both weight ratio PCL-PEO and of junction points, have two chains of PEO in the hydrophilic shell micelle, making the protective crown for hydrophobic core more compact. This should improve the characteristics of biomimetic nanovector, making it invisible to the immune system of host organism, justifying the interest towards this type of architecture. Furthermore, with the same synthetic strategy were obtained linear diblock and triblock copolymers with terminal amino group on PEO segment. This is very useful point to bind folic acid as active targeting agent for nanovectored antitumoral drug or Rhodamine B a fluorescent probe for nanovectors *in vivo* tracking by confocal microscopy. The molecular and structural characterization of the copolymers was carried out by techniques ^{1}H-NMR, FT-IR, DSC, SEC, and X-ray diffraction It has also been carried out an appropriate evaluation of their potential as biomimetic nanocarriers for targeted and sustained release of bioactive substances by analyzing the characteristics of self-assembly in aqueous systems (in collaboration with research group from the "Dipartimento di ChimicaFarmaceutica e Tossicologica" directed by FabianaQuaglia), determining the size (DLS), the critical micelle concentration (CMC), the morphology (TEM) and the surface properties of the aggregates.

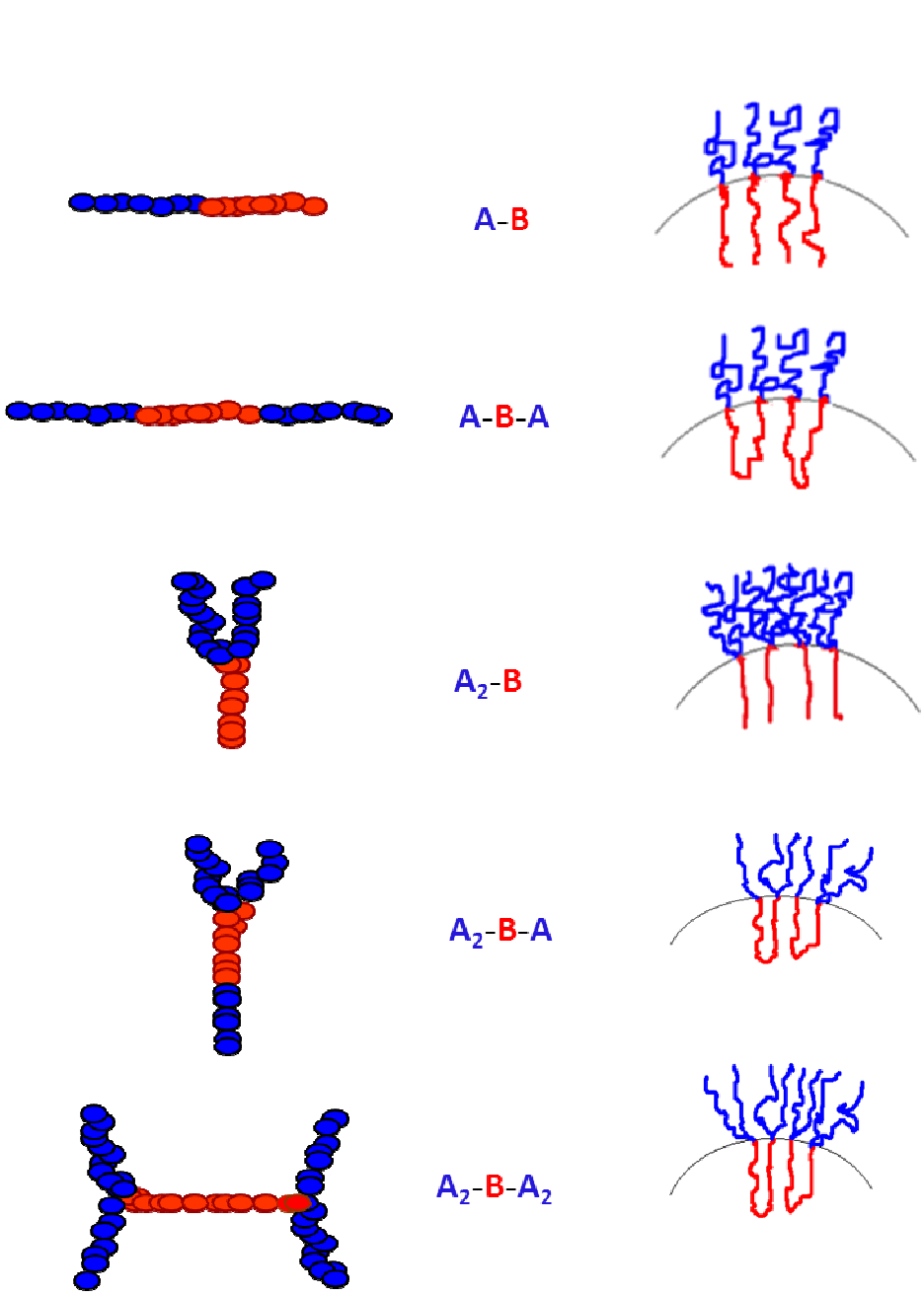

Fig. 2.9:Comparison between designed architecture and relative ideal models of micellization

2.4 Amphiphilic copolymer based on PCL and PEO

The core of synthetic strategy developed in this research work is 1-3 Huisgen cycloaddition catalyzed by Cu(I). For this reason it was necessary to design in very accurately way functionalization steps. As widely reported in literature, the simplest technique used for the synthesis of linear PCL is the ring-opening bulk polymerization (ROP) of CL initiated by an alcohol group in the presence of $Sn(Oct)_2$. The molecular weight of the PCL depends on the amount of monomer introduced compared to initiator[35]. Recent studies agree that the $Sn(Oct)_2$ is not the real catalyst, but that this function is performed by an alkoxide bond formed by the interchange reaction between ethylhexanoate groups and -OH groups of alcohol. The polymerization is carried out through insertion of CL molecules in the metal-oxygen bond and has the typical characteristics of a living polymerization[36,37]. Follows a discussion of details concerning the copolymers synthesis starting from the linear architectures, easier to obtain, and continuing with copolymers of a higher synthesis complexity. Poly-ethylenoxyde(PEO) can be named also poly-ethyleneglycol (PEG). In literature the polymer has the first name above 2.0 kDa, while below this value is named PEG. In the follow synthesis discussion will be bear in mind this distinction

2.4.1 Synthesis of the linear diblock copolymer PEG_{1000}-PCL_{3000}

As already mentioned, molecular weight of PCL obtained by ROP is directly linked to the initiator/monomer molar ratio and the reaction can be initiated by hydroxyl group; so the simplest way to obtain a linear diblock is direct polymerization of ε-CL initiated by mono hydroxyl PEG. The selected initiator was α-metoxy-ω-hydroxyl-PEG-$_{1000}$ (m-PEG_{1000}-OH) (Mn=1000, PI=1.1). Commercial stocks of m-PEG_{1000}-OH contain non negligible tracks of difunctional PEG, α-ω-di-hydroxyl-PEG_{1000} (HO-PEG_{1000}-OH) about 5% in weight. The presence of difunctional PEG can lead to the formation of complex structures and undesirable

where the method of synthesis (coupling and ROP) contemplates the presence of a single alcohol group. In order to remedy these inconveniences, it is developed a purification procedure of m-PEG_{1000}-OH through a silica column chromatography (packed in CH_3Cl with dry loading of the product) eluted with a mixture of CH_3Cl/MeOH gradually increasing the percentage by volume of MeOH (3%, 6%, 9%, 12%). Fractions were analyzed by thin layer chromatography in CH_3Cl/MeOH (1.2/0.8 v/v); the fraction containing purified m-PEG_{1000}-OH shows a value of Rf=0.28 while the fraction containing HO-PEG-OH shows a Rf = 0.16. The product was further purified by precipitation in hexane (yield 80%). As the purified initiator is still a very hygroscopic material, it was necessary to purify it from water by toluene azeotropic distillation before to start polymerization. This reaction is illustrated in the following scheme:

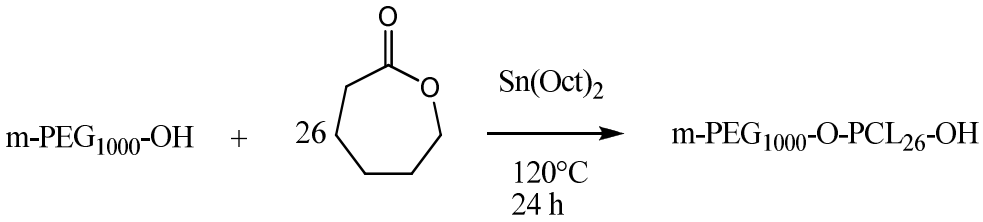

Fig. 2.10 ROP of ε-CL initiated by m-PEG-$_{1000}$-OH

The synthesis was carried out in mass for 24 h at 120 ° C by reacting ε-caprolactone (CL) and m-PEG_{1000}-OH in the presence of $Sn(Oct)_2$ added in a solution of CL ($Sn(Oct)_2$/OH molar ratio of 1:100). The molecular weight of the PCL depends on the molar ratio ε-CL/(m-PEG_{1000}-OH). An excess of CL by 5% compared to the programmed molecular weight was utilized to balance the incomplete conversion of the monomer. The product was purified by precipitation in ether and obtained with a yield of 98%. The ^{1}H-NMR analysis was used to confirm the copolymer chemical structure and to assess the number average molecular weight (Mn) of polyester block. The CL average number units was evaluated comparing the integrations values of the signals related to the PCL

protons-CH_2-O-CO-(d) (δ = 4.0) and-CH_2-CH_2-O-(f) of PEG (δ = 3.6). It has been found that the M_n value of PCL block is almost coincident, within the limits of experimental error, with that designed (figure 2.11).

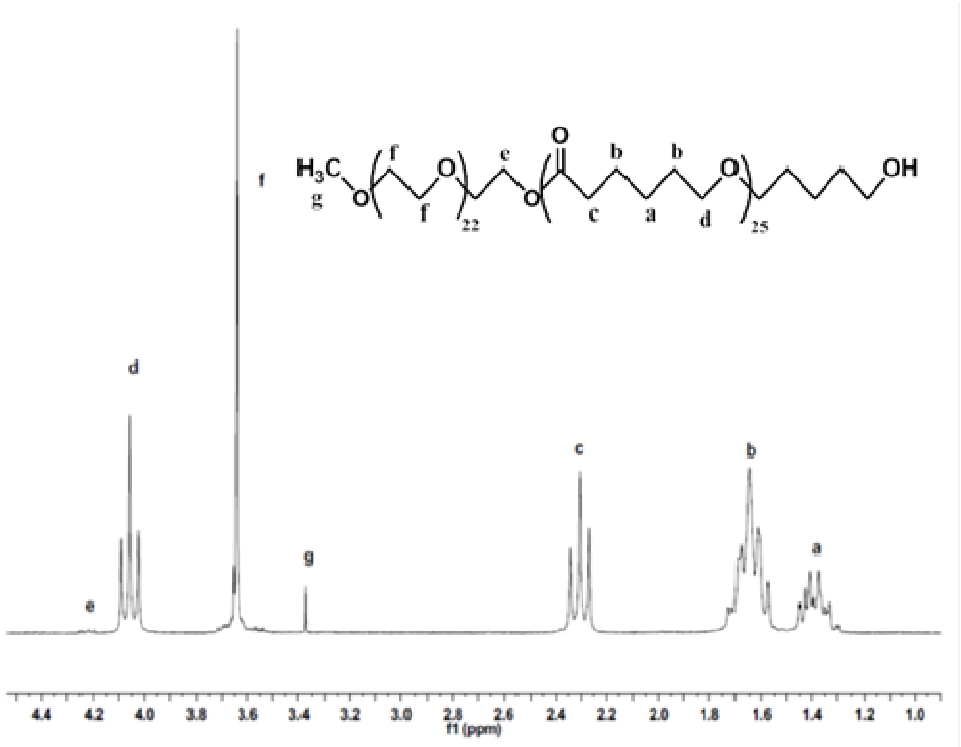

Fig.2.11 ^{1}H-NMR of Diblock copolymer m-PEG-$_{1000}$-PCL_{3000}-OH with proton assignment

2.4.2 Synthesis of linear triblock copolymer PEG_{1000}-PCL_{6000}-PEG_{1000}

The triblock copolymer was obtained from click coupling between two precursors:α-metoxy-ω-alkyne-PEG_{1000} and m-PEG_{1000}-PCL_{6000}-N_3. Synthesis steps of precursors and final click coupling are illustrated in figure 2.12 scheme. In step a) m-PEG_{1000}-OH, purified as described in diblock copolymer synthesis, was reacted with 50% molar excess of 4-pentynoic acid to obtain complete esterification of hydroxyl group catalyzed by DCC and DMAP. The reaction was carried out at room temperature in dry $CHCl_3$ to avoid inactivation of DCC to dicyclohexyl urea. After 48 hours, this latter compound, due to reaction with generated water, was filtered from reaction mixture and the solution containing the

required product, m-PEG_{1000}-alkyne, was concentrated and precipitated in diethyl ether/methanol 5/2 v/v to purify the product from unreacted excess. The ^{1}H-NMR analysis was used to confirm the product chemical structure.Comparing the integrations values of the signals related to the PEG protons CH_3-O-CH_2-CH_2(d) (δ = 3.36) and-CH_2-O-CO (δ =4.26) (figure 2.13) it was evaluated that m-PEG-OH conversion degree is, within the limits of experimental error, higher than 90%. This non quantitative conversion does not represent problem for final triblock purity because both m-PEG_{1000}-OH and m-PEG_{1000}-alkyne are very soluble in methanol while copolymer precipitate in this solvent.

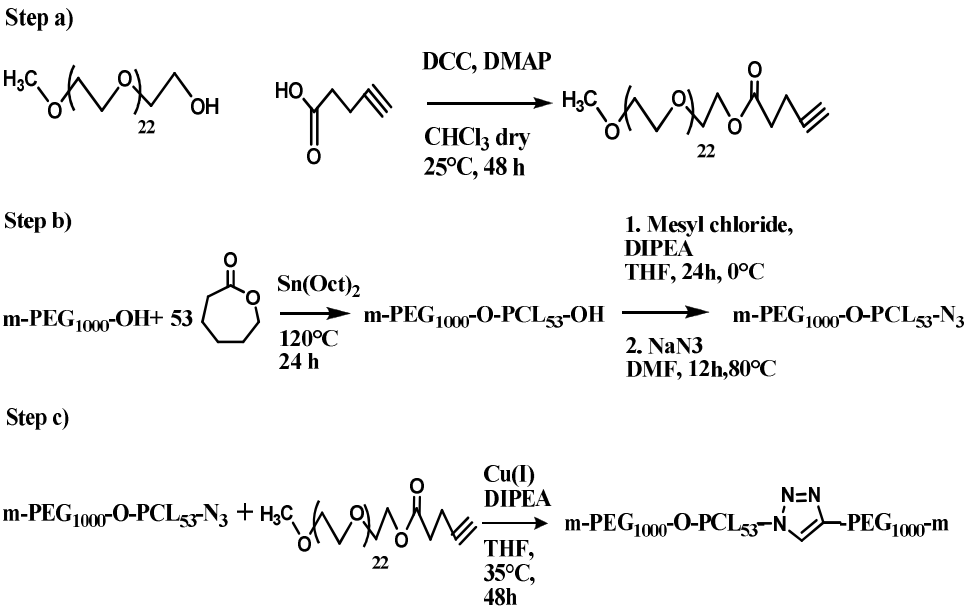

Fig.2.12 Multistep triblock copolymer PEG_{1000}-PCL_{6000}-PEG_{1000} synthesis scheme

Step b) first shows the same polymerization of e-CL initiated from m-PEG_{1000}-OH already described in diblock case, except for initiator/monomer molar ratio. In the second part of step b) is reported the two-steps azidation process. The first reaction of this process concerns m-PEG_{1000}-PCL_{6000}-OH hydroxyl activation by mesyl chloride in presence of DIPEA as HCl acceptor. THE Reaction was carried out in dry THF to avoid mesyl chloride hydrolysis. After diblock

dissolution, reaction batch was dipped in ice bath and a 600% molar excess of mesyl chloride was slowly added. After 12h the reaction mixture, yellow as a result of DIPEA-HCl adduct presence, was concentrated, filtered from DIPEA-HCl adduct and precipitated in a mixture of diethyl ether/methanol 5/2 v/v (yield 96%).

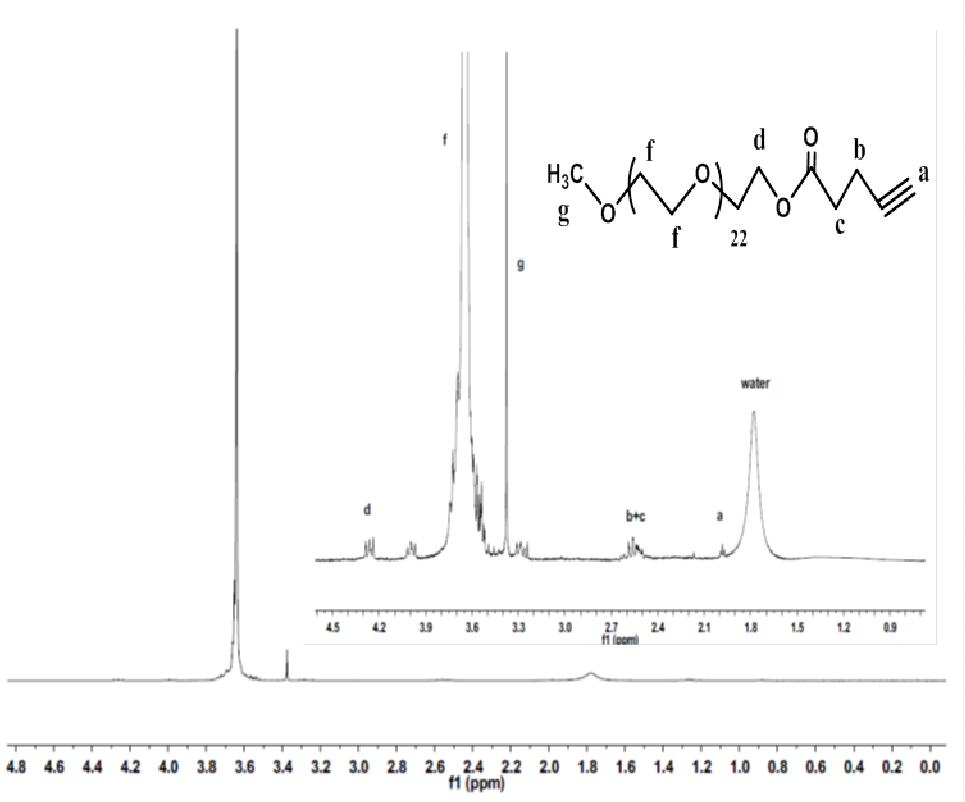

Fig.2.12[1]H-NMR of m-PEG-$_{1000}$-alkyne with proton assignment

[1]H-NMR analysis was used to confirm the product, m-PEG_{1000}-PCL_{6000}-mesyl,chemical structure. Comparing integrations values of the signals related to the PEG protons CH_3-O-CH_2-CH_2 (g) (δ = 3.36) and-CH_3-OSO-CH_2 of mesyl residue (h) (δ =3.01) (figure 2.13) it was evaluated that m-PEG_{1000}-PCL_{6000}-OH conversion degree is, within the limits of experimental error, higher than 95%. The nucleophilic substitution was carried out reacting m-PEG_{1000}-PCL_{6000}-mesyl with a large excess of sodium azide. Mesyl is an excellent leaving group, but reaction needs a good solvent both for sodium azide and mesylated copolymer. Therefore,

chosen refluxing DMF at 80°C. was selected. After 12h the reaction mixture was centrifuged, to eliminate sodium azide excess, dried and redissolved in $CHCl_3$ where residual traces of sodium azide are insoluble. The filtrated chloroform mixture was concentrated and precipitated in diethyl ether. FT-IR analysis confirm the presence of azide group as shown in figure 2.14 by characteristic stretching at 2100 cm^{-1}. Quantitative analysis was carried out by ^{1}H-NMR; the product chemical structure, m-PEG_{1000}-PCL_{6000}-N_3, was evidenced by disappearance of resonances related to the mesyl residue -CH_3-OSO-CH_2 (δ=3.00) and by appearance of –CH_2-N_3 (h) peak (δ =3.27) (figure 2.14). Comparing integrations values of this signals with those related to the PEG protons CH_3-O-CH_2-CH_2(g) (δ = 3.36), it was evaluated that m-PEG_{1000}-PCL_{6000}-mesyl conversion degree is, within the limits of experimental error, higher than 95%.

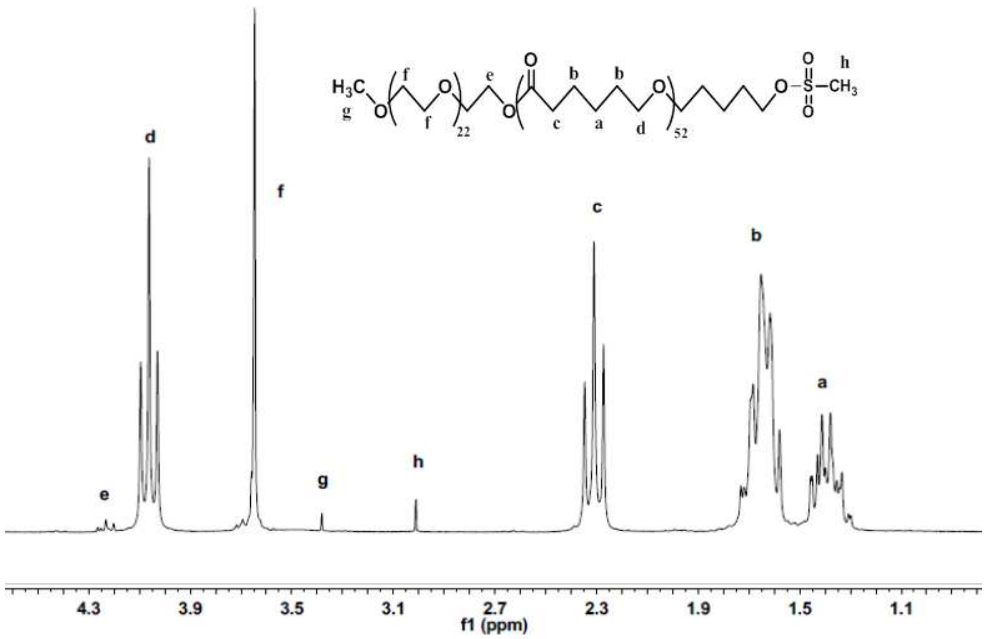

Fig. 2.13 ^{1}H-NMR of Diblock copolymer m-PEG-$_{1000}$-PCL_{6000}-mesy with proton assignment

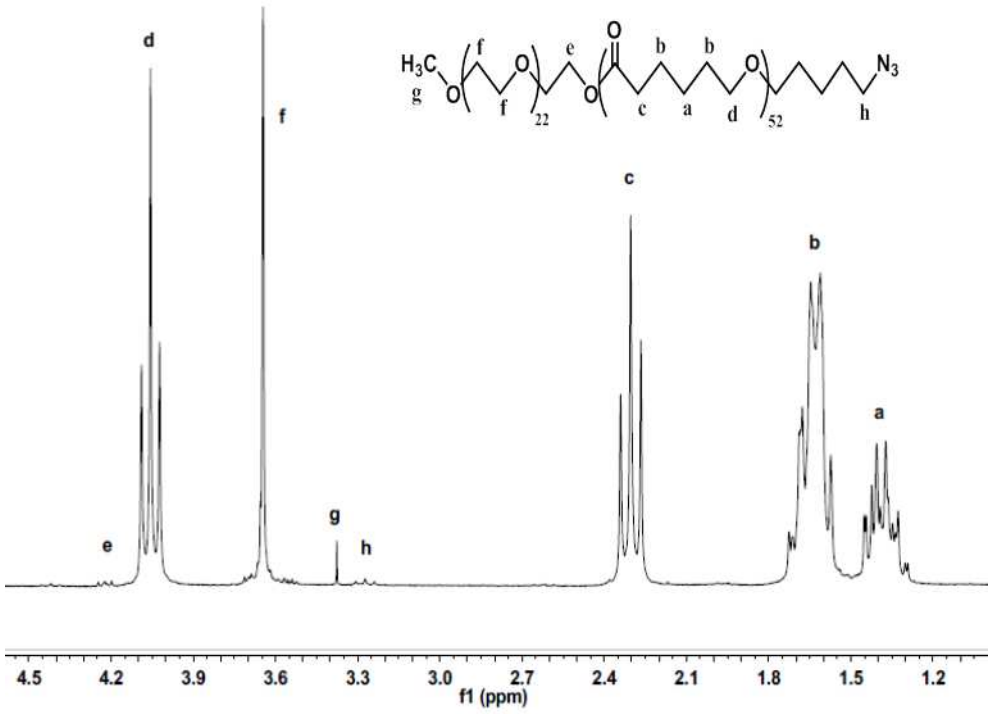

Fig. 2.1 [1]H-NMR of Diblock copolymer m-PEG-$_{1000}$-PCL$_{6000}$-N$_3$ with proton assignment

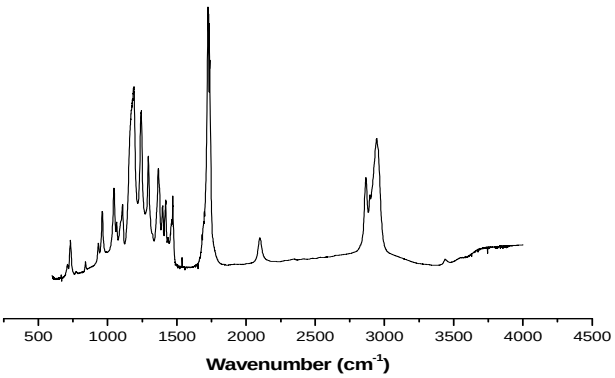

Fig. 2.15 m-PEG$_{1000}$-PCL$_{6000}$-N$_3$FT-IR spectrum. At 2100 cm-1 it can be noted characteristic azide stretching

In the step c) was shown the 1-3 Huisgencycloaddition between m-PEG$_{1000}$-PCL$_{6000}$-N$_3$ and m-PEG$_{1000}$-alkyne catalyzed by Cu(I). Catalyst is quite stable to

oxidation by atmosphere, but to avoid formation of Cu(II), $BrCu(P(Ph)_3)_3$ was stored and manipulated under argon atmosphere in a glovebox in which is not possible introduce organic solvent. For this reason in one bottle apart was measured catalyst while in other one were collocated DIPEA as cocatalyst, m-PEG_{1000}-PCL_{6000}-N_3, m-PEG_{1000}-alkyne in 20% molar excess respect diblock precursor to ensure a complete coupling and dry THF. This batch was submitted to three freeze-thawing cycles in liquid nitrogen. This procedure allows to obtain a degassed reaction mixture which was transferred under argon in batch containing $BrCu(P(Ph)_3)_3$. After 48 hours reaction mixture was purified from copper catalyst by neutral alumina column, concentrated and precipitated in diethyl ether. Triblock copolymer PEG_{1000}-PCL_{6000}-PEG_{1000} was further washed with methanol to solve unreacted m-PEG_{1000}-alkyne or eventual m-PEG_{1000}-OH residue. FT-IR analysis indicates a complete coupling. It can be noted, in fact, the disappearance of azide group characteristic stretching at 2100 cm^{-1}, as shown in figure 2.16

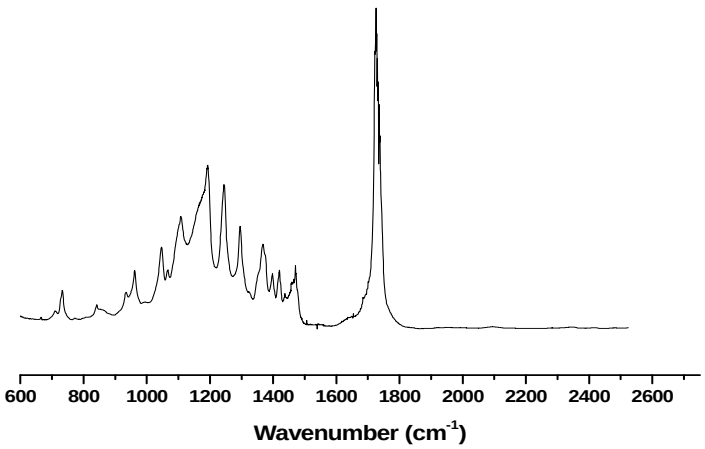

Fig. 2.16 PEG_{1000}-PCL_{6000}-PEG_{1000} FT-IR spectrum. At 2100 cm-1 it can be noted total disappearance of characteristic azide stretching

Also ^{1}H-NMR analysis was used to confirm the product chemical structure. Comparing the integrations values of the signals related to the PEG protons O-CH_2-CH_2(f) (δ= 3.60) and-CH_2-OCO-of PCL(d)(δ =4.05) (figure 2.17) was evaluated that the ratio between PEG and PCL is, within the limits of experimental error, very close to expected value for a triblockPEG_{1000}-PCL_{6000}-PEG_{1000}.

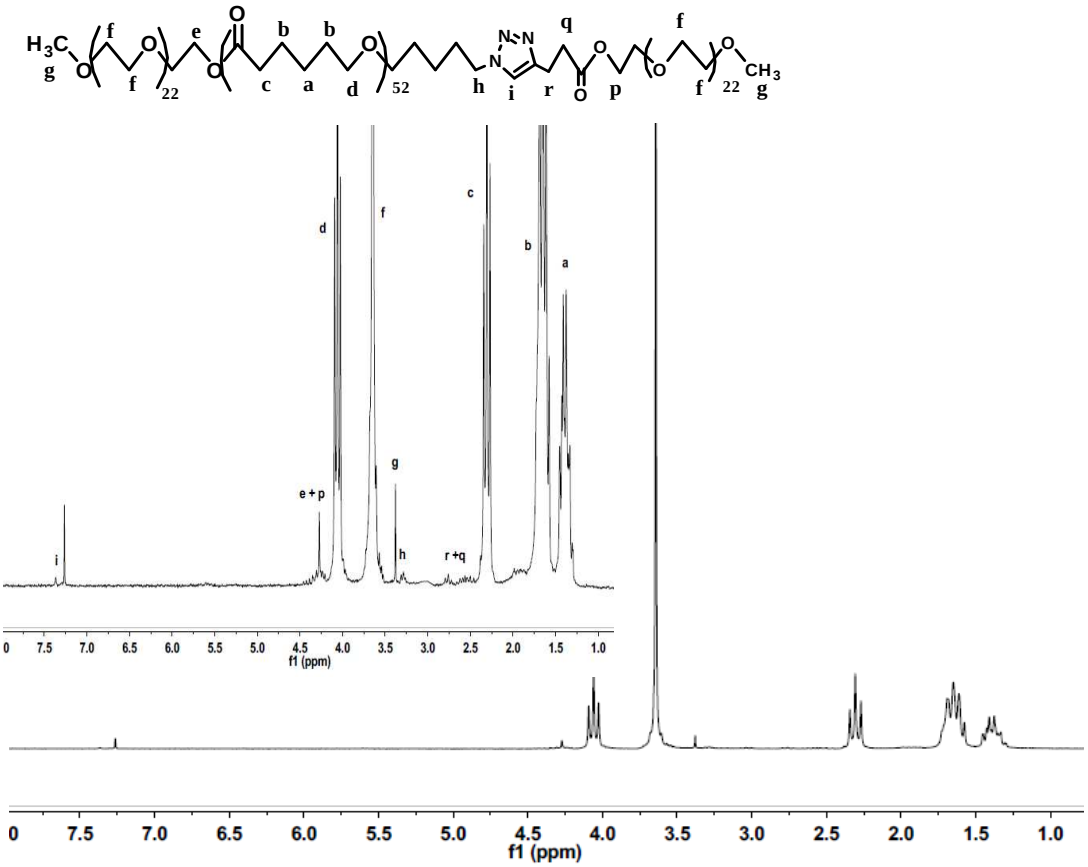

Fig. 2.17 ^{1}H-NMR of Triblock copolymer m-PEG-$_{1000}$-PCL_{6000}-PEG_{1000} with proton assignment

2.4.3 Synthesis of the miktoarm Y-shaped triblock copolymer $(PEG_{1000})_2$-PCL_{6000}

The triblock miktoarm "Y-shaped" copolymer was already synthetized in this research laboratory using the procedure displayed in figure 2.17

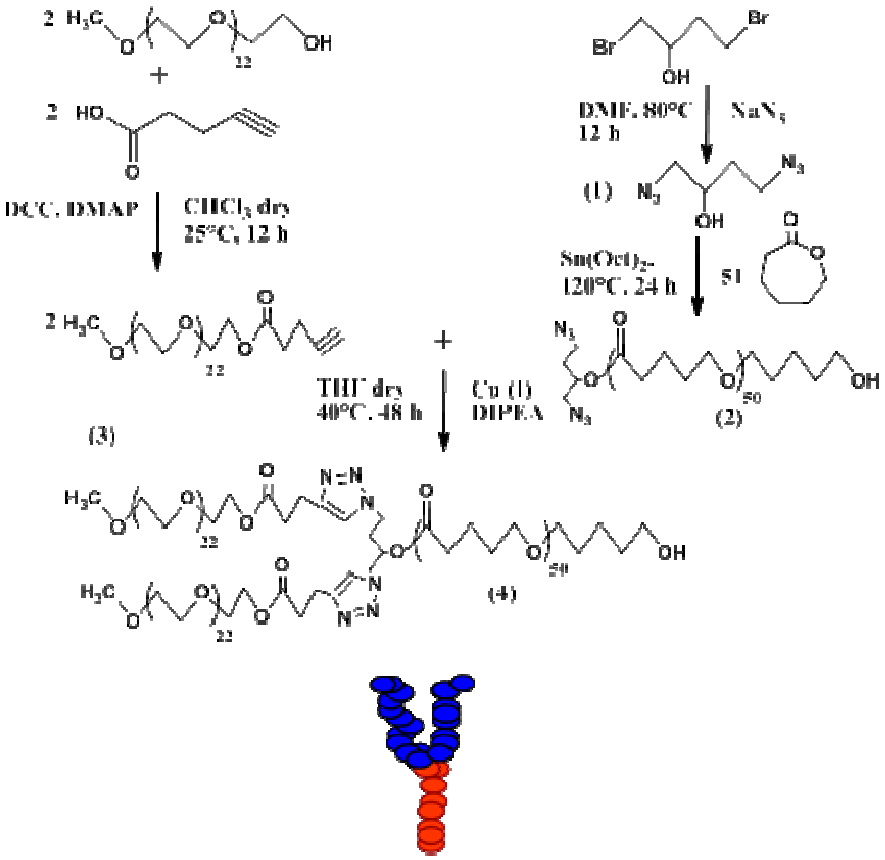

Fig. 2.17 Multistep triblock copolymer$(PEG_{1000})_2$-PCL_{6000}synthesis scheme

In brief:first 1,4(di-azido)-butane-2-ol, obtained by azidation of 1,4(di-bromo)-butane-2-ol, was used as the initiator in the $(Sn(oct)_2$ catalysed ROP of CL yielding a bis-azido functionalized PCL with M_n =5800 Da, $(N_3)_2$-PCL_{5800} , calculated by ^{1}H-NMR from the integration ratio of –CH_2-O-CO- protons in the repeat units at 4.07 ppm and –CH_2-OH methylene protons of the terminal unit at 3.65 ppm. In the

second step, two alkynyl terminated *m*PEG_{1000} segments, obtained reacting. *m*PEG_{1000}.with pentynoic acid, were linked to $(N_3)_2$-PCL_{5800} by means of the Cu(I) catalyzed Huisgen 1,3-cycloaddition leading to the (Y shaped) (PCL_{5800}-)-(-PEG_{1000})$_2$ copolymer. The disappearence in the (Y-shaped) FTIR spectrum of the absorption peak characteristic of the -N_3 stretching at 2100 cm^{-1} suggested that a complete coupling was reached by the "click" reaction as confirmed by ^{1}H-NMR analysis that revealed a PCL:PEG weight ratio of 2.9:1 corresponding to that expected for the (PCL_{5800}-)-(-PEG_{1000})$_2$ structure.

2.4.4 Synthesis of miktoarm copolymer PEG_{1000}-PCL_{7200}-Lys-(PEG_{1000})$_2$

The architecture designed provide two segments of PEG and one PCL segment originate from a single "center" and this is indicated in the literature as "miktoarm star-block". The center point of branching was found in L-Lysine which contains functional groups of different nature which may react in sequence. First two-NH_2 groups of the amino acid were properly functionalized using propargyl chloroformate (PCF), according to the following scheme

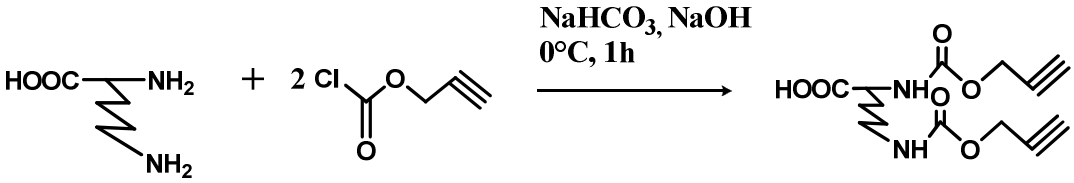

Fig 2.18 Synthesis of Lysine-di-alkyne from L-Lysine and propargyl chloroformate

A simple reaction procedure was employed; the L-Lys was dissolved in an aqueous solution, consisting of $NaHCO_3$ (1N) and NaOH (4N). The solution was cooled to 0°C, PCF was added dropwise and the reaction mixture was stirred for 1h. It was allowed to come to room temperature and was stirred for additional 3 h. Then, the mixture was acidified to pH 2–3 to quench reaction by the slow addition of 1 N KHSO4 and was extracted with ethyl acetate (3 × 25 mL). The organic

layers, containing product of interest, were combined and washed with saturated citric acid solution, water and then with brine. The solvent was removed and the crude product was purified by silica gel (100–200 mesh) column chromatography and eluted with 50–70% ethyl acetate in petroleum ether to get the desired compound Lys-PCF as colorless oil. Yield: 92%. Were collected two fractions, showing the disappearance of the-NH_2 groups of the L-lysine by TLC, (ethyl acetate/hexane 7/3 v/v) and ninhydrin assay. Quantitative analysis was carried out by ^{1}H-NMR to confirm the Lys-di-alkyne chemical structure. Comparing integrations values of OCO-CH-NH (d) (δ =4.34) signals with those of O-CH_2-C≡CH (e) (δ =4.68), the L-Lys conversion degree was evaluated higher than 95%, within the limits of experimental error.

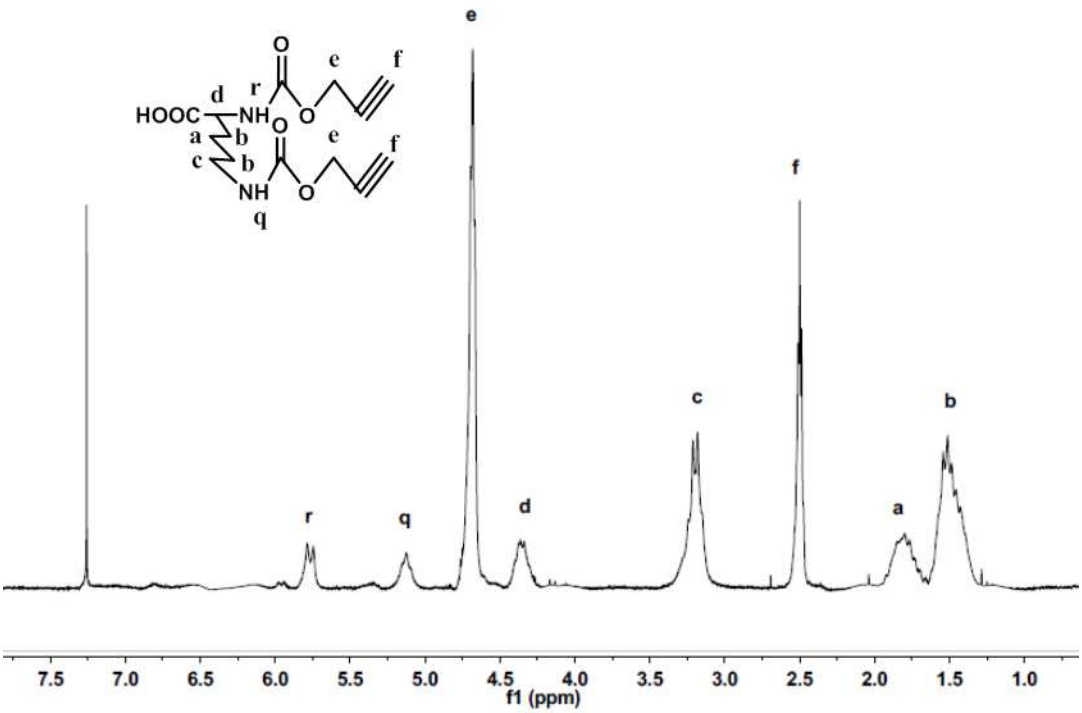

Fig. 2.19 ^{1}H-NMR of Lys-di-alkyne with proton assignment

Lys-di-alkyne was coupled to m-PEG_{1000}-PCL_{7200}-OH, obtained according 2.4.2 synthesis, by DCC and DMAP esterification as illustrated in following scheme:

Fig 2.20 Synthesis of m-PEG-O-$_{PCL7200}$ Lys-di-alkyne

The reaction was carried out with a 30% Lys-di-alkyne molar excess to ensure complete diblock conversion. Unreacted Lys-di-alkyne excess was removed by methanol washing.^{1}H-NMR analysis was used to confirm the product, m-PEG_{1000}-PCL_{7200}-Lys-di-alkyne, chemical structure. Comparing integrations values of the signals related to the PEG protons CH_3-O-CH_2-CH_2 (g) (δ = 3.36) with those of O-CH_2-C≡CH (m) (δ =4.68) (figure 2.20) was evaluated m-PEG_{1000}-PCL_{7200}-OH conversion degree higher than 95%, within the limits of experimental error.

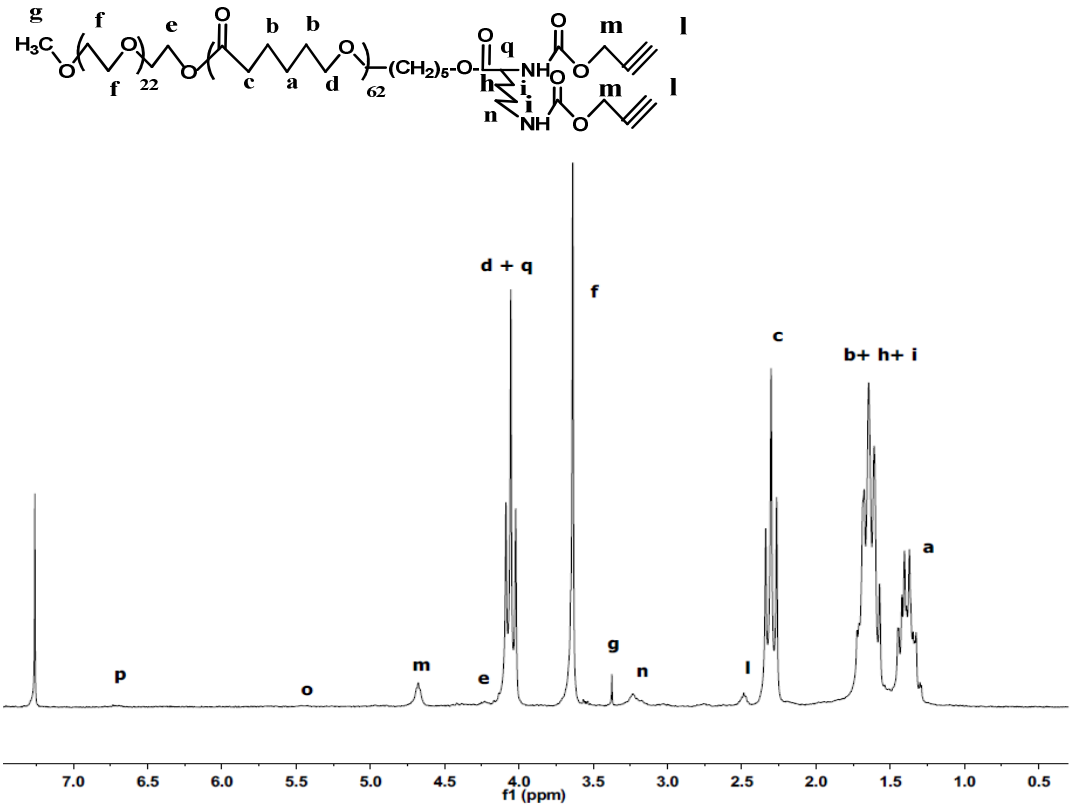

Fig. 2.21 [1]H-NMR of Diblock copolymer m-PEG-$_{1000}$-PCL$_{7200}$-Lys-di-alkyne with proton assignment

Designed architecture can be completed throug 1-3 cycloaddition between m-PEG$_{1000}$-PCL$_{7200}$-Lys-di-alkyne and two m-PEG$_{1000}$-N$_3$ segments. This latter macromer was synthetized by two-step azidation from m-PEG$_{1000}$-OH as shown in following scheme:

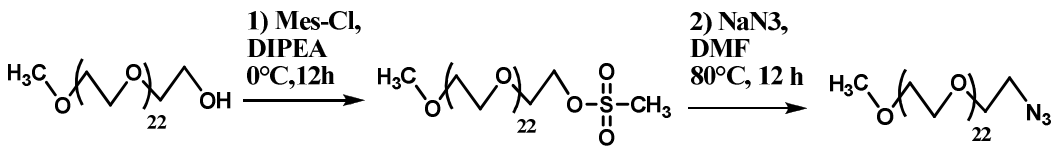

Fig 2.22 Synthesis of m-PEG-N$_3$ by two-step azidation

^{1}H-NMR and FTIR analysis was used to confirm the product, m-PEG_{1000}-N_3, chemical structure. For the first step, comparing integrations values of the signals related to the PEG protons -O-CH_2-CH_2 (b) (δ = 3.60) and- -CH_2-OSO-CH_3 (c) (δ =3.38) (figure 2.21) it was evaluated that m-PEG_{1000}-OH conversion degree was, within the limits of experimental error, higher than 95%.

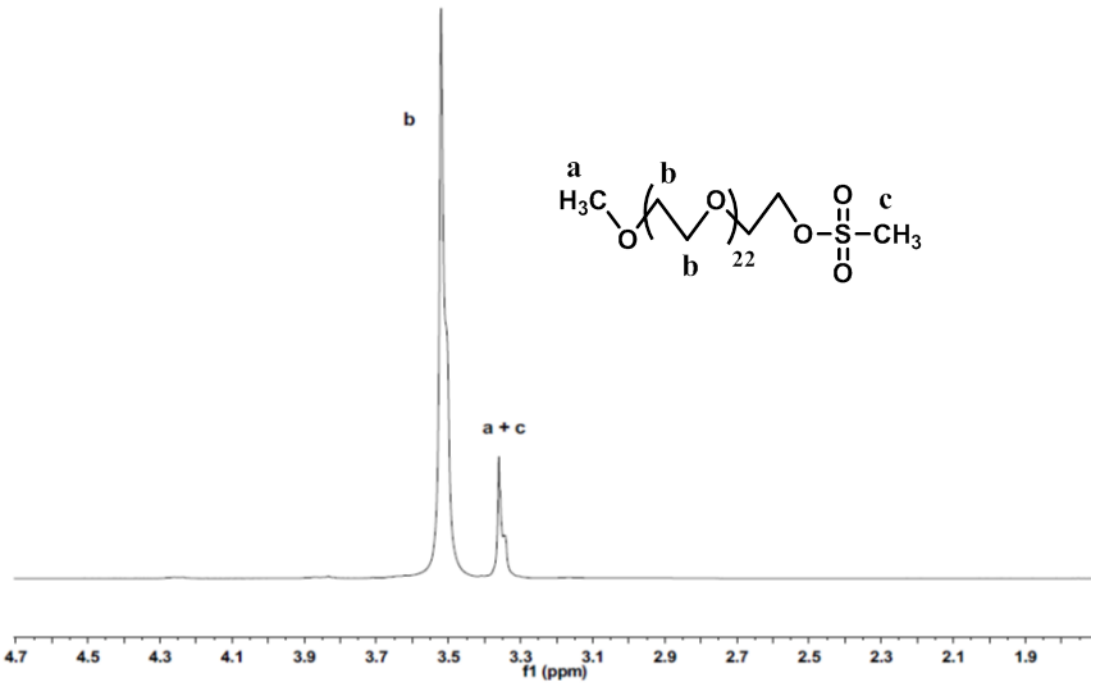

Fig. 2.23 ^{1}H-NMR of m-PEG-$_{1000}$-mesy with proton assignment

For the second step was considered partial disappearing of overlapped PEG signals at (δ =3.38) and comparing integrations values of the signals related to the PEG protons -O-CH_2-CH_2 (b) (δ = 3.60) with those of -CH_2-O-CH_3 (c) (δ =3.38) (figure 2.21) was evaluated that m-PEG_{1000}-mesyl conversion degree was, within the limits of experimental error, higher than 95%.

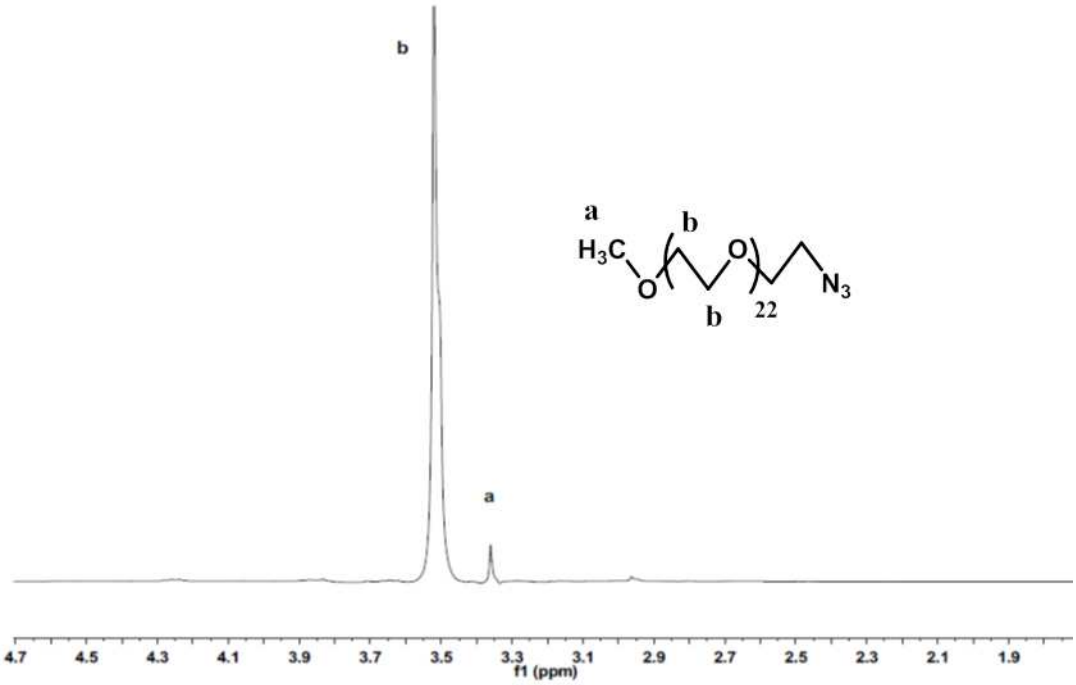

Fig. 2.24 ^{1}H-NMR of m-PEG-$_{1000}$-N_3 with proton assignment

FT-IR analysis (figure 2.25) confirm the presence of azide group. showing, in fact, the characteristic stretching peak at 2100 cm^{-1}. Finally, m-PEG_{1000}-N_3 was reacted, in 220% molar excess, with m-PEG_{1000}-PCL_{7200}-Lys-di-alkyne in the Huisgen cycloaddition catalyzed by Cu(I) according to the protocol used for linear triblock synthesis as illustrated in the figure 2.26 scheme. The miktoarm copolymer m-PEG_{1000}-PCL_{7200}-Lys-$(PEG_{1000})_2$ was washed with methanol to solve unreacted m-PEG_{1000}-N_3. FT-IR analysis confirm complete coupling. It can be noted, in fact, in figure 2.27 a total disappearance of azide group characteristic stretching at 2100 cm-1.

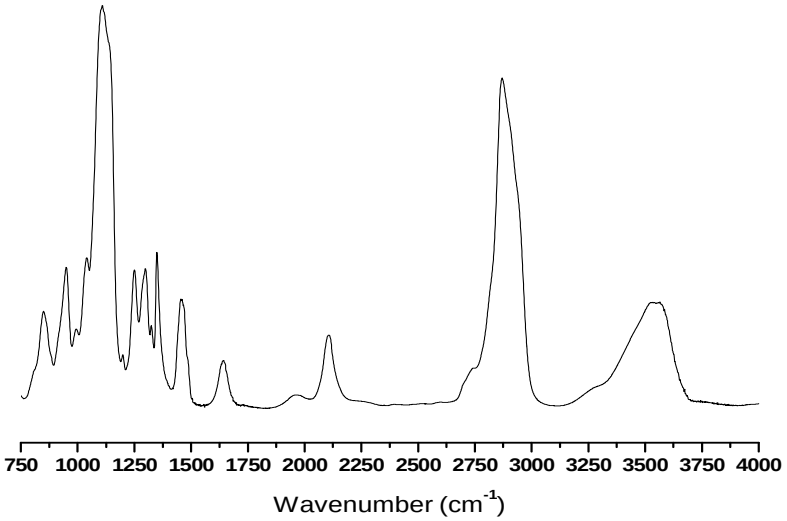

Fig. 2.25 m-PEG$_{1000}$-N$_3$ FT-IR spectrum. At 2100 cm-1 it can be noted characteristic azide stretching

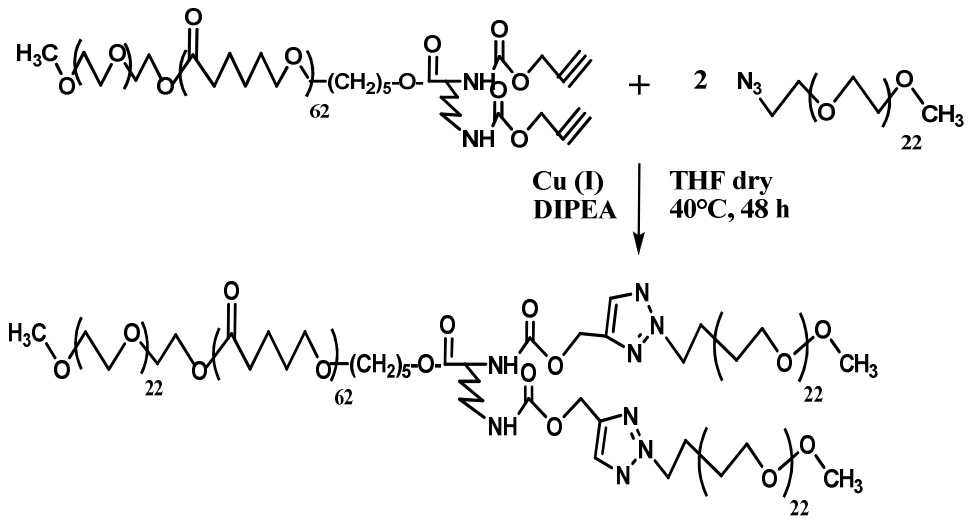

Fig 2.26 1-3Huisgen cycloaddition between m-PEG$_{1000}$-PCL$_{7200}$-Lys-di-alkyne and m-PEG$_{1000}$-N$_3$

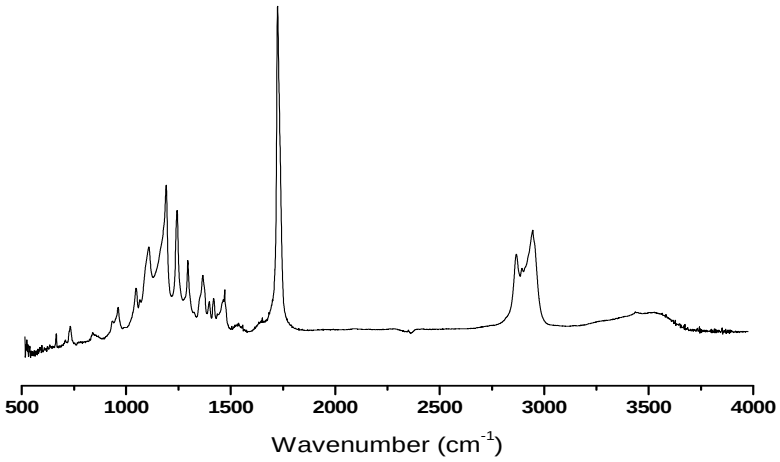

Fig. 2.27 PEG_{1000}-PCL_{6000}-Lys-$(PEG_{1000})_2$ FT-IR spectrum. At 2100 cm-1 it can be noted total disappearance of characteristic azide stretching

Also ^{1}H-NMR analysis was used to confirm the product chemical structure. Comparing the integrations values of the signals related to the protons O-CH_2-CH_2(f) of PEG (δ= 3.60) and-CH_2-OCO-of PCL(d)(δ =4.05) (figure 2.28) the ratio between PEG and PCL was evaluated, within the limits of experimental error, yielding a composition value very close to that for a triblockPEG_{1000}-PCL_{7200}-Lys-$(PEG_{1000})_2$.

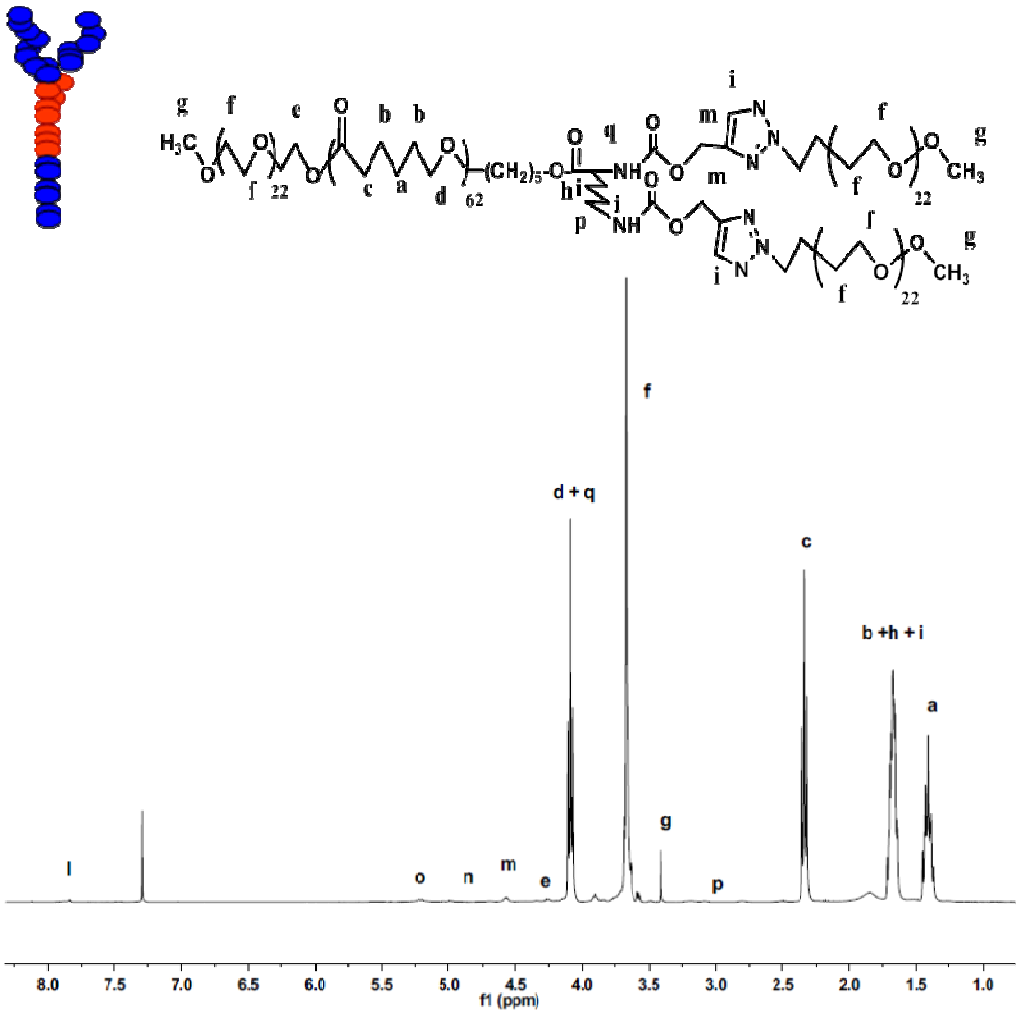

Fig. 2.28 ^{1}H-NMR of miktoarm copolymer m-PEG-$_{1000}$-PCL$_{7200}$-Lys- (PEG-$_{1000}$)$_2$ with proton assignment

2.4.5 Synthesis of the miktoarm copolymer $(PEG_{1000})_2$-Lys-PCL_{11500}-Lys-$(PEG_{1000})_2$

The "H-shaped" miktoarm copolymer was synthetized starting from linear α–ω-di-hydroxyl-PCL_{11500}, HO-PCL_{11500}-OH obtained by ε-CL ROP initiated from 1-4-butanediol $Sn(Oct)_2$ catalyzed (scheme in fig.2.29). This macromer was reacted with two Lys-di-alkyne by the DCC and DMAP protocol to obtain a tetra-alkynyl end-capped PCL, PCL_{11500}-tetra-alkyne.

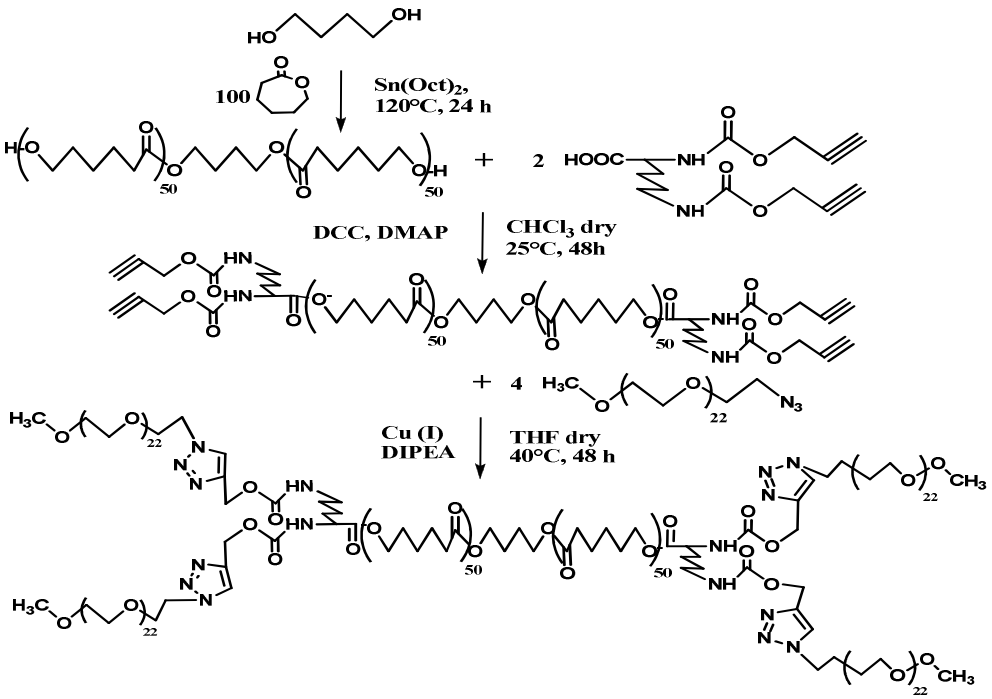

Fig. 2.29 Synthesis scheme for $(PEG_{1000})_2$-Lys-PCL_{11500}-Lys-$(PEG_{1000})_2$

^{1}H-NMR analysis was used to confirm the product chemical structure. Comparing the integrations values of the signals related to the PCL protons O-CH_2-$(CH_2)_2$-CH_2-O (p) (δ= 4.25) and O-CH_2-C≡CH (f) (δ =4.68) (figure 2.30) it was evaluated that HO-PCL-OH conversion degree, within the limits of experimental error, higher than 95%.

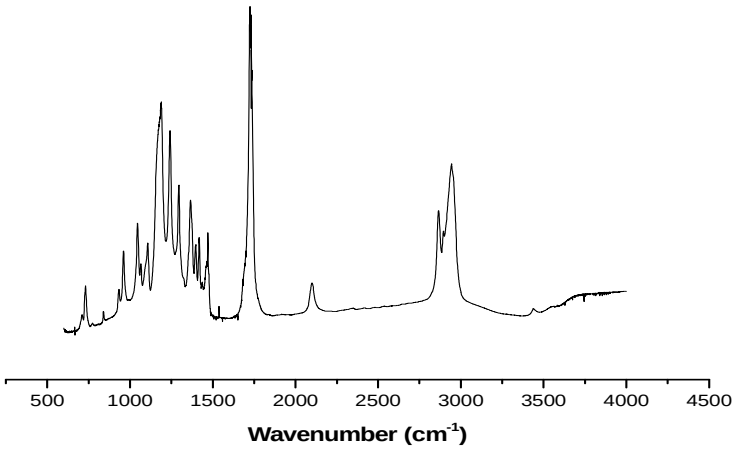

Fig. 2.15 m-PEG$_{1000}$-PCL$_{6000}$-N$_3$FT-IR spectrum. At 2100 cm-1 it can be noted characteristic azide stretching

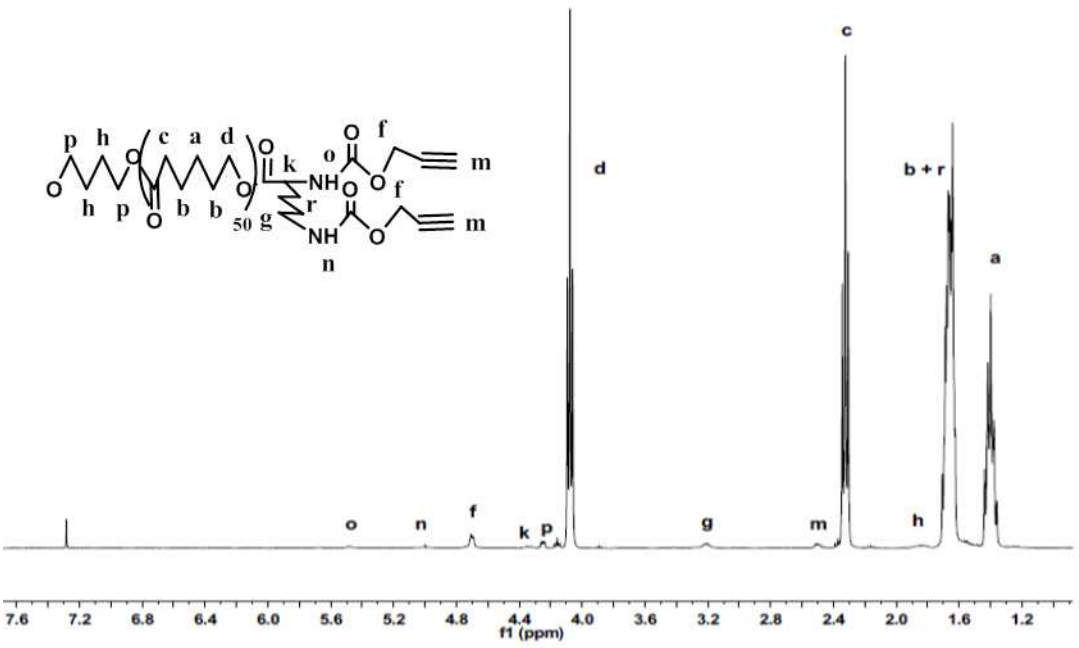

Fig. 2.30 ^{1}H-NMR of PCL-tetra-alkyne with proton assignment

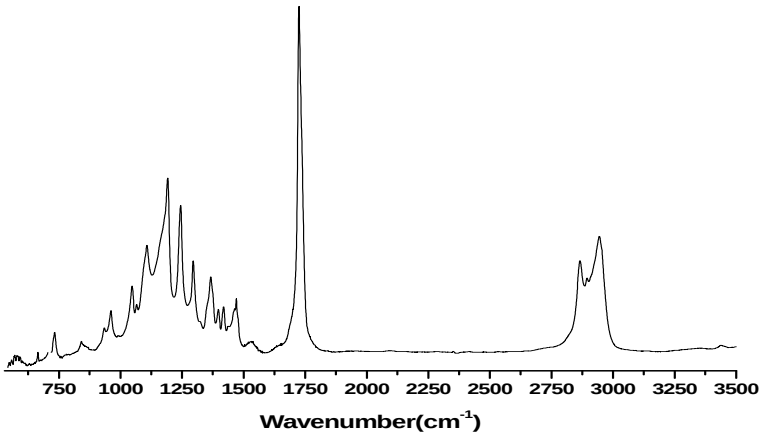

Fig. 2.31 PEG_{1000}-PCL_{6000}-Lys-$(PEG_{1000})_2$ FT-IR spectrum. At 2100 cm-1 it can be noted total disappearance of characteristic azide stretching

After the coupling step of PCL_{11500}-tetra-alkynyl-end capped with four azido terminated methoxy-PEG_{1000} segments, by the described click chemistry method, the structure of the miktoarm copolymer $(PEG_{1000})_2$-Lys-PCL_{11500}-Lys-$(PEG_{1000})_2$ was verified, comparing the integrations values of the signals related to the PEG protons O-CH_2-CH_2(f) (δ= 3.60) and-CH_2-OCO-of PCL(d)(δ =4.05) (figure 2.32), very close to expected value.

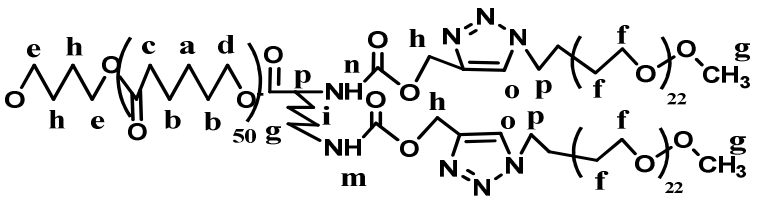

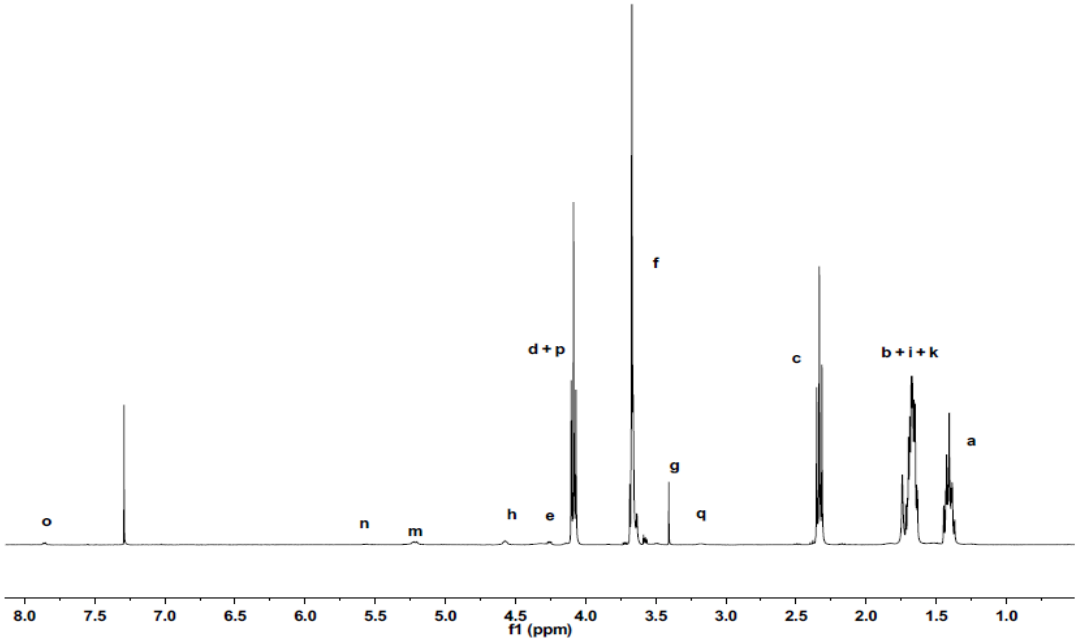

Fig. 2.32 ^{1}H-NMR of $(PEG_{1000})_2$-Lys-PCL_{11500}-Lys-$(PEG_{1000})_2$ with proton assignment

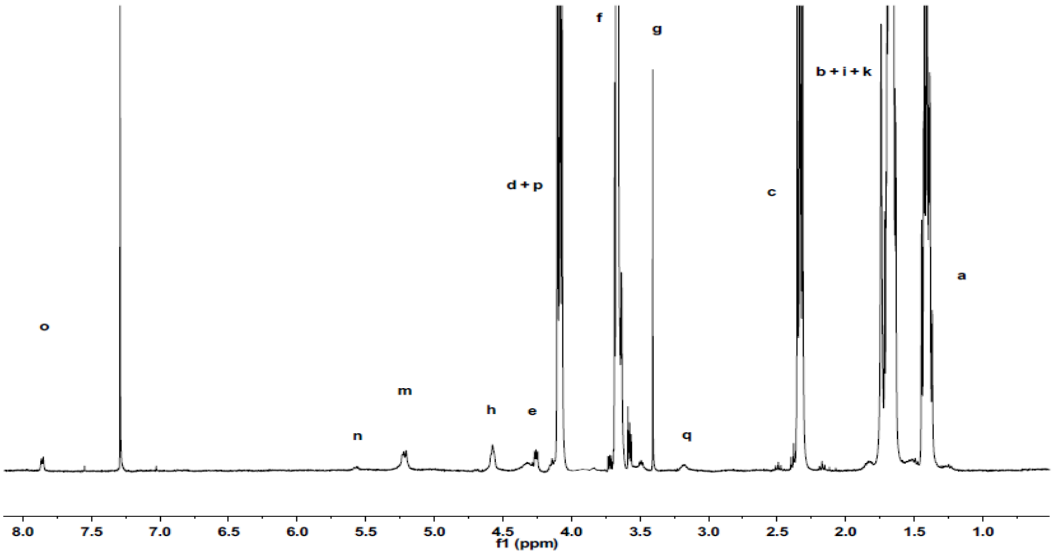

Fig. 2.33 Zoom of ^{1}H-NMR of $(PEG_{1000})_2$-Lys-PCL_{11500}-Lys-$(PEG_{1000})_2$ with proton assignment

2.4.6 Viscometric and molecular characterization

Table 2.1 shows viscosity and molecular characterization data concerning synthesized copolymers, such as the number average molecular weight determined by ^{1}H-NMR and SEC and the polydispersity index. Also noted is the PCL percentage in the copolymers calculated by NMR data.

Table 2.1. Characterization data of star-block Y- and H-shaped and linear diblock and triblock PCL-PEG copolymers. (A = PEG_{1000} , B = PCL).

Copolymer	PCL (wt%)	M_n [a] (kDa)	PDI [b]	η_{inh} [c] ($dL \cdot g^{-1}$)
A-B_{3000}	75.0	4.0	1.18	0.267
A-B_{6000}-A	75.0	8.0	1.29	0.316
(Y-I) $(A)_2$-B_{5800}	74.3	7.8	1.44	0.345
(Y-II) $(A)_2$-B_{7200}-A	70.6	10.2	1.46	0.452
(H-) $(A)_2$-B_{11500}-$(A)_2$	74.2	15.5	1.36	0.475

[a]Number-average molecular weight evaluated by ^{1}H-NMR. [b]Molecular weight polydispersity index determined by SEC. [c]Inherent viscosity at 25 °C in $CHCl_3$, c = 0.50 $g \cdot dL^{-1}$.

The inherent viscosity values, η_{inh}, are compatible with the chemical structure and architecture of the copolymers synthesized. In particular there is a good agreement between increasing trend of molecular weights from AB_{3000} to H-shaped copolymer and viscosity values. The good agreement between the values of molecular weight designed and those determined by ^{1}H-NMR confirmed that the length of segments PCL is almost equal to the predetermined value for the ROP and that the coupling reactions have an almost complete conversion grade. PCL weight percentage is included between 70.6 and 75%. This indicates that the copolymers have very close hydrophobic/hydrophilic block ratio.

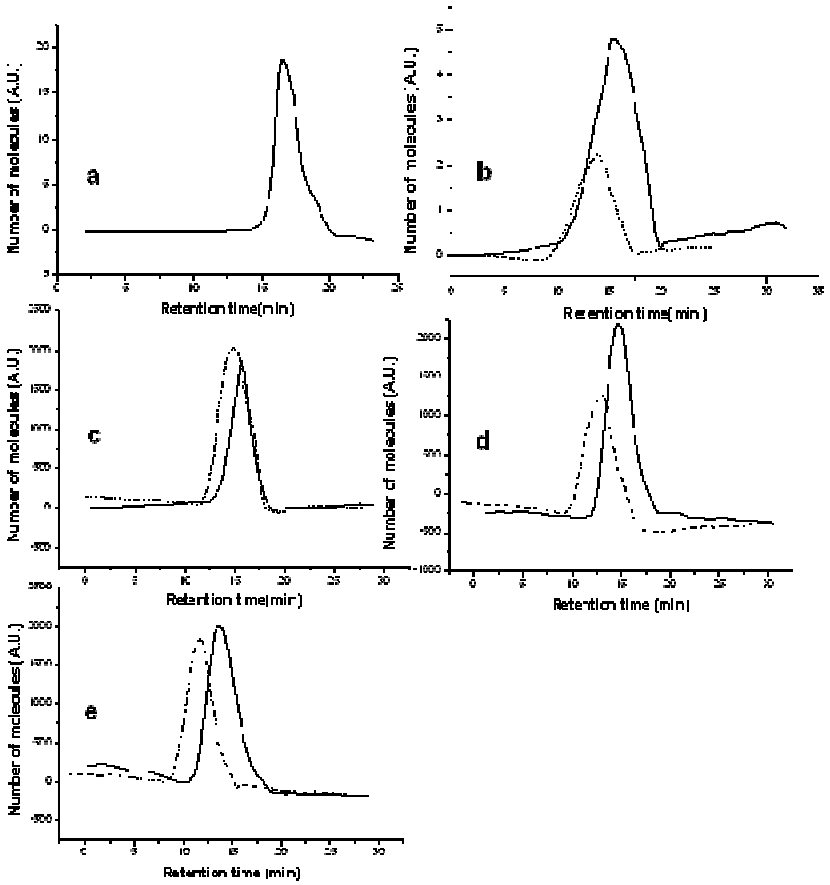

*Fig 2.34 Size exclusion cromatography curves of precursors (solid line) and copolymers (dash line):***a)** *A-B_{3000},* **b)** *A-B_{6000}-OH and A-B_{6000}-A,* **c)** *HO-B_{5800}-$(N_3)_2$ and $(A)_2$-B_{5800},* ***d)*** *A-B_{7200}-OH and A-B_{7200}-$(A)_2$,* ***e)*** *HO-B_{11500}-OH and $(A)_2$-B_{11500}-$(A)_2$*

Solid and dash curves of molecular weight distribution obtained by SEC (figure 2.34) show unimodal distributions, with a maximum at values close to those of designed molecular weight and low polydispersity indices in agreement with a high copolymers structural regularity. Furthermore, there is a shift toward lower retention time (higher molecular weight) of copolymers dash line respect to precursors solid line to confirm the successful coupling of PEG.

2.4.7 Crystallization behaviour

DSC was used to investigate on self-organization and crystallization from the melt, under dynamic conditions, of star and linear block copolymers. After a first melting run, a crystallization-melting cycle was performed with a 80 °C/-20 °C/80 °C route. One or both blocks may crystallize depending on composition and MW of PEO and PCL chains.

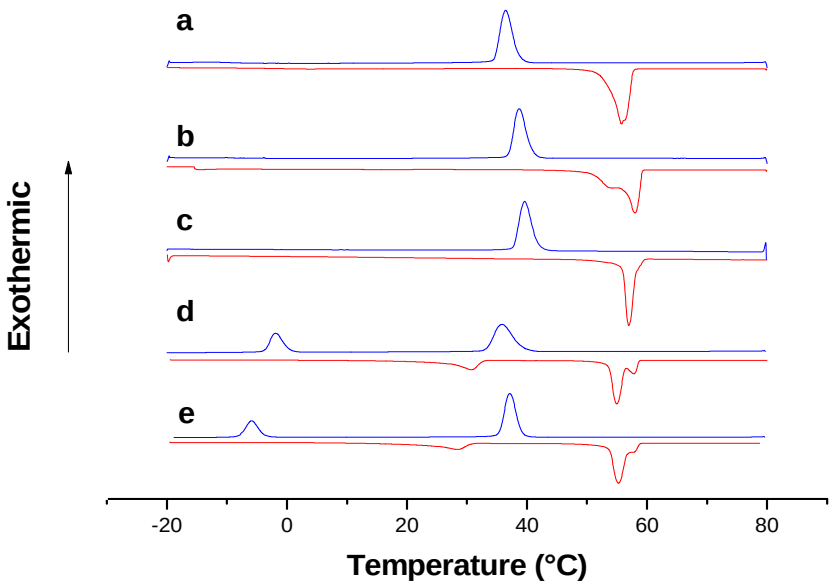

Fig 2.35 DSC curves of copolymers, in red was shown heating, while cooling in blue: **a)** *A-B_{3000},* **b)** *A-B_{6000}-A,* **c)** *$(A)_2$-B_{5800},* ***d)*** *A-B_{7200}-$(A)_2$,* ***e)*** *$(A)_2$-B_{11500}-$(A)_2$*

A low scanning rate (2 °C/min) was selected to promote the microphase separation in the cooling run. The thermograms are reported in figure 2.35 and the results are summarized in Table 2.2. As expected, considering the relevant asymmetry of composition and MW of the different blocks, the PCL crystallize first hindering the crystallization of the low MW PEG segments that in the case of (Y-II) and (H-) copolymers occurs at large overcooling temperatures, while is not observable up to -20°C for (Y-I) and linear copolymers. As all copolymers have

almost coincident compositions, the different behavior can be ascribed to the (Y-II) and (H-) architectures consisting of 2 or 4 PEG segments joined to one or both PCL chain ends, thus favouring the aggregation. of PEG chains in a preformed PCL crystalline environment. All copolymers display a melting temperature and apparent enthalpy of PCL coincident with those of their respective homopolymers, indicating that the PEG segments do not affect the PCL crystallization.

Table 2.2. Thermal behavior and crystallinity of star-block Y- and H-shaped and linear diblock and triblock PCL-PEG copolymers. (A = PEG_{1000} , B = PCL).

Copolymer	T_c (°C) [a]		ΔH_c ($J \cdot g^{-1}$) [a,b]		T_m (°C) [a,b,c]		ΔH_m ($J \cdot g^{-1}$) [a,b,c]		X_{Cr} (%) [d]	
	A	B	A	B	A	B	A	B	A	B
A-B_{3000}	_	36.4	_	88.7	_	54.5	_	91.2	_	65.3
A-B_{6000}-A	_	38.7	_	82.8	_	50.5	_	83.8	_	60.0
(Y-I) $(A)_2$-B_{5800}	_	38.2	_	89.5	_	53.6	_	94.4	_	67.7
(Y-II) $(A)_2$-B_{7200}-A	-1.9	35.5	80.9	76.2	30.8	54.9	75.3	77.9	32.7	55.8
(H-) $(A)_2$-B_{11500}-$(A)_2$	-5.9	37.1	100.6	62.9	28.4	55.3	80.8	63.3	35.1	45.4

[a]Crystallization and melting temperatures determined by DSC. [b]Apparent enthalpies, corrected for the composition. [c]Second heating run. [d] % crystallinity calculated from ΔH_m .

Low temperature melting peaks attributed to PEG, close to that of PEG_{1000} subjected to the same thermal cycle (36,2 °C), are shown in the heating runs of (Y-II) and (H-). Powder WAXS diagrams of all copolymers display diffraction maxima of crystalline PCL at 2θ = 21.5°, 23.9°, whereas evidence of those related to crystalline PEG, shown in figure 2.38, are not observed even in (Y-II) and (H-) diffractogram , shown as example in figure 2.36 and 2.37, because of the very low PEG content and the partial overlapping of PEG and PCL diffraction maxima.

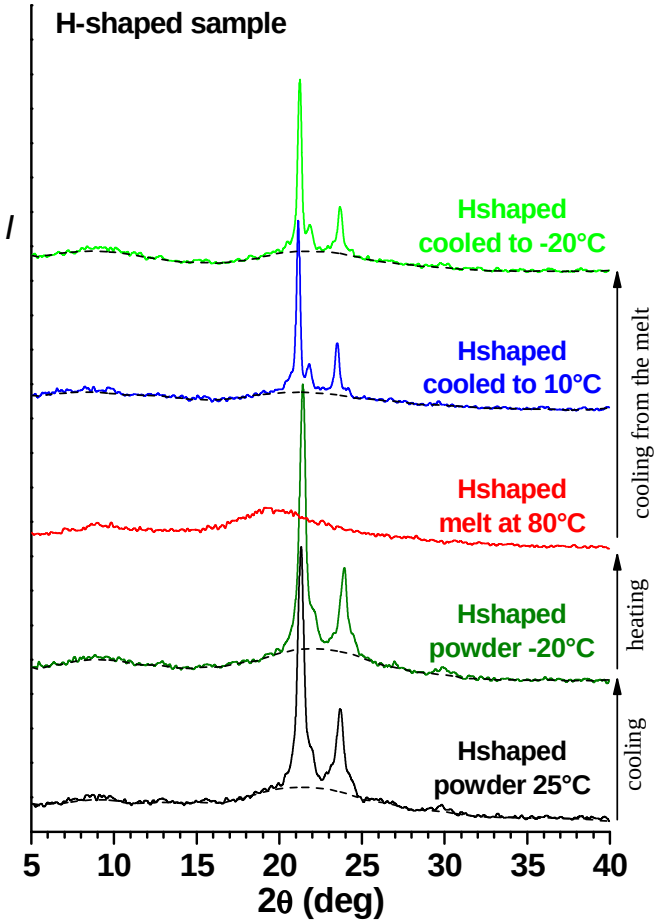

Fig. 2. 36 WAXS diffractogram of H-shaped copolymer $(A)_2$-B_{11500}-$(A)_2$, can be noted absence of maximum relative to crystalline PEG

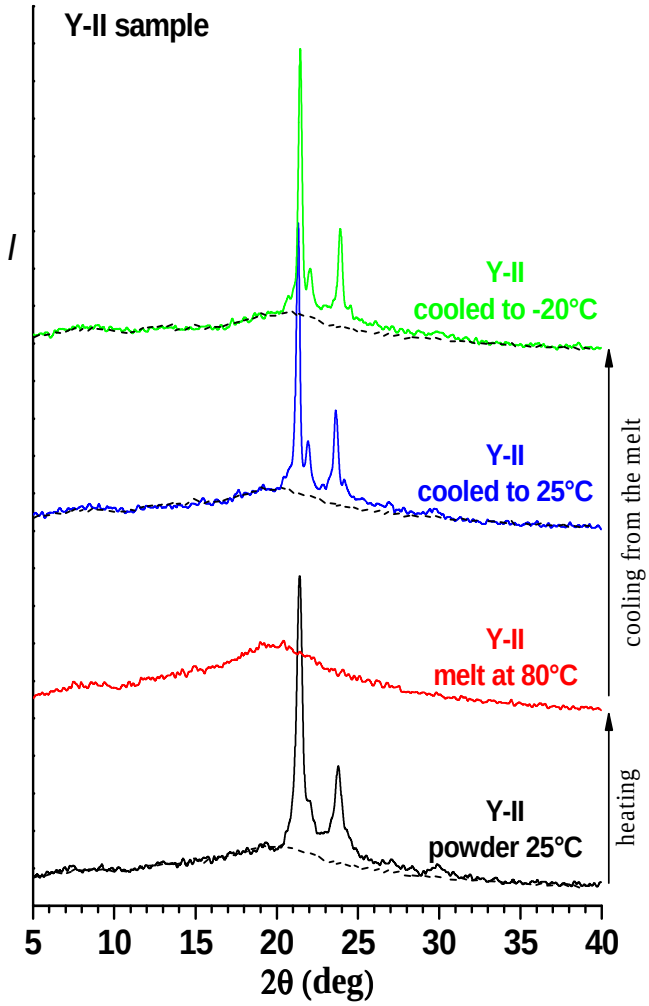

Fig. 2. 37 WAXS diffractogram of H-shaped copolymer $(A)_2$-B_{7200}-A, can be noted absence of maximum relative to crystalline PEG

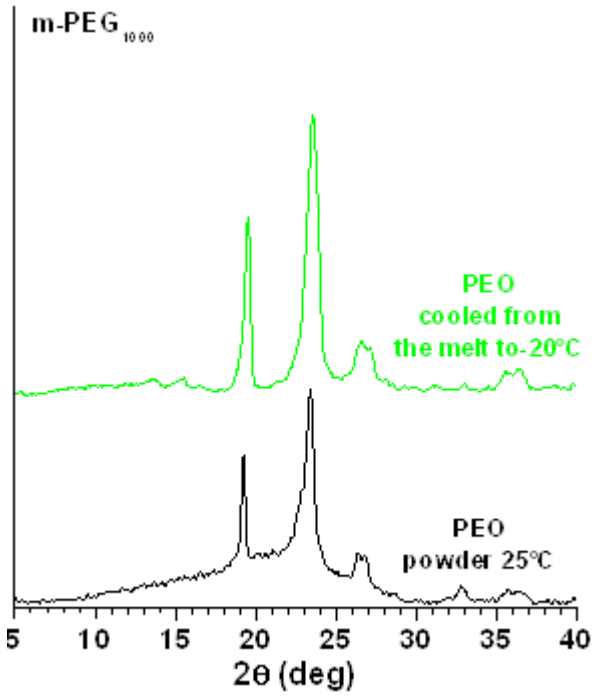

Fig. 2. 38 WAXS diffractogram of crystalline m-PEG$_{1000}$

2.4.8 Self-assembly in aqueous environment.

Core-shell nanoparticles (NP) prepared with the synthetized copolymer were obtained by the dialysis method in collaboration with the research group directed by Fabiana Quaglia at the Dipartimento di Chimica Farmaceutica e Tossicologica and were characterized in terms of dimensions, CAC and Z potential. Self assembly minimizes free energy as descripted in the following equation

$$\Delta G^0 = RT \ln(X_{CAC})$$

where X_{CAC} is the molar fraction of copolymers at the critical aggregation concentration, minimum value of concentration at which it is possible to observe the aggregation of individual macromolecules (unimers) in nanoscopic structures; this is the key indicator of the polymeric nanoaggregate stability. Typical values of

CAC suitable for pharmaceutical applications are in the 10^{-6}-10^{-7} mol·L^{-1} range. The following table 2.3 resumes the properties of obtained nanoparticles.

Table 2.3. Properties of NPs obtained with star-block Y- and H-shaped and linear diblock and triblock PCL-PEG copolymers. (A = PEG_{1000} , B = PCL)

Copolymer	CAC [a] (μg·mL^{-1})	(mol·L^{-1} x 10^{-7})	ΔG^0 [b] (kJ·mol^{-1})	Mean D_H [c] (nm ± SD)	Z potential (mV)	Shell tickness (nm)
(Y-I)	1.82	2.33	- 47.8	142.1 ± 0.48	-33.7	0.37
(Y-II)	1.85	1.81	- 48.4	150.0 ± 0.17	-26.8	0.72
(H)	2.51	1.62	- 48.7	67.8 ± 0.05	-24.3	1.13
A-B_{3000}	0.803	2.001	- 48.1	72±0.52	-26.3	1.20
A-B_{6000}-A	0.63	0.787	- 50.4	86±0.36	-13.4	1.75

[a] Critical aggregation concentration. [b] Gibbs free energy of aggregation. [c] Hydrodynamic diameter obtained by DLS.

The linear triblock copolymer shows the lowest CAC and ΔG^0 while all other copolymer are characterized from very similar values. In general self-assembly tendency is associated with replacement of unfavourable interactions water/hydrophobic block in dispersed state with favourable hydrophobic interactions following core formation. On the other hand the aggregate geometry forces polymer chains to adopt restricted conformations, resulting in a loss of conformational entropy and a higher interfacial energy core-shell. Assuming following ideal aggregation model, the triblock copolymer should be characterized

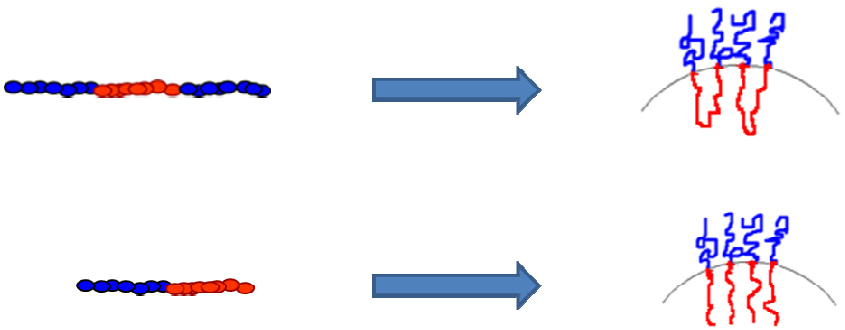

by a lower self assembly tendency and a consequent higher CAC respect to diblock and miktoarm copolymer because is provided of two junction points between PCL and PEO segments for macromolecule, while a single junction points is present in the diblock. In addition, the folding of the hydrophobic segment of PCL, determined by triblock self-assembly, may constitute an unfavourable energy factor. CAC data found could be explained assuming a different aggregation model such as:

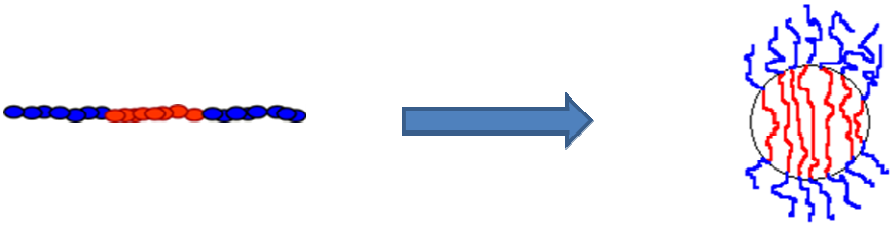

in which PCL segments are stretched and there is only one junction point for macromolecule between hydrophobic and hydrophilic blocks. This hypothesis agrees with a very compact and shielding hydrophilic shell as evidenced by zeta potential data. The zeta potential of a particle is the overall charge that the particle acquires in a particular medium. Knowledge of the zeta potential of nanoparticle preparations can help to predict the fate of nanoaggragates *in vivo*. Measurement of the zeta potential of samples in the Zetasizer Nano was done using the technique of laser Doppler velocimetry. In this technique, a voltage is applied across a pair of electrodes at either end of a cell containing the particle dispersion. Charged particles are attracted to the oppositely charged electrode and their velocity is measured and expressed in unit field strength as their electrophoretic mobility.

The core shell structure of aggregates was investigated by TEM images experiments. H-shaped copolymer aggregates in regular sphere, as shown in figure 2.39, with Hydrodynamic Diameter lower than 100 nm as confirmed by DLS measurement.

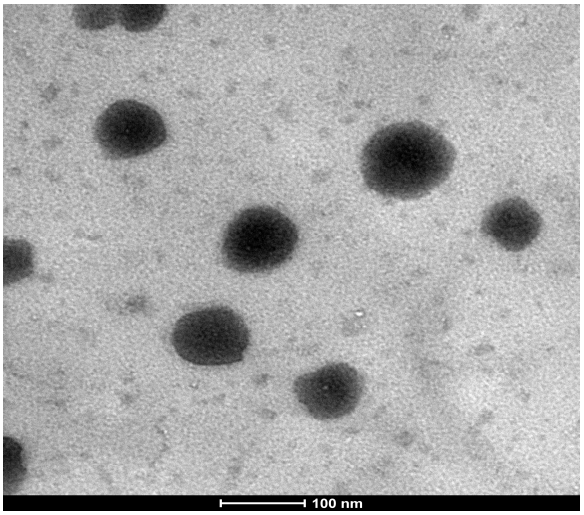

Fig. 2. 39 TEM image of aggregates obtained by dialysis with H-shaped copolymer, $(A)_2$-B_{11500}-$(A)_2$

The regularity of spherical aggregates was evidenced for H-shaped copolymer also by a ^{1}H-NMR experiment carried out in D_2O, reported in figure 2.40, where only protons surrounded by deuterated solvent are observed. It is possible to note only O-CH_2-CH_2-O- PEG signal (δ = 3.60) and no PCL signals, highlighting a compact protective shell around hydrophobic core.

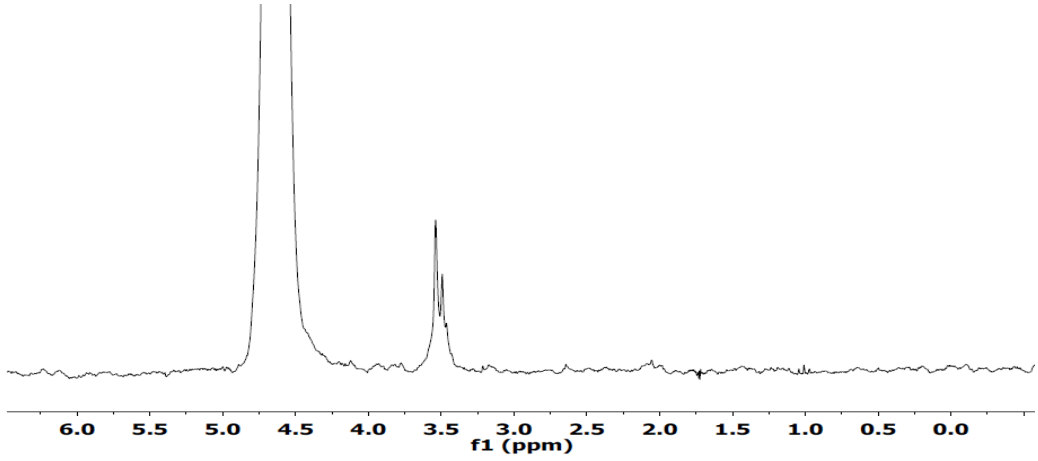

Fig. 2. 40 ^{1}H-NMR in D_2O of aggregates obtained by dialysis with H-shaped copolymer$(A)_2$-B_{11500}-$(A)_2$

The TEM image of Y-II copolymer (figure 2.41) shows heterogeneous nanoaggregates with different hydrodynamic diameter and a prevalent globular morphology,. ^{1}H-NMR experiment in D_2O, reported in figure 2.42, reveals the presence of different PCL broad signals –O-CH_2-$\underline{CH_2}$-$\underline{CH_2}$-$\underline{CH_2}$-CH_2-O-CO (δ = 1-1.5), –O-CH_2-CH_2-CH_2-CH_2-$\underline{CH_2}$-CO (δ = 2.20) and –O-$\underline{CH_2}$-CH_2-CH_2-CH_2-CH_2-O-CO (δ = 4.10) evidencing a less compact shell and an exposed hydrophobic core

.

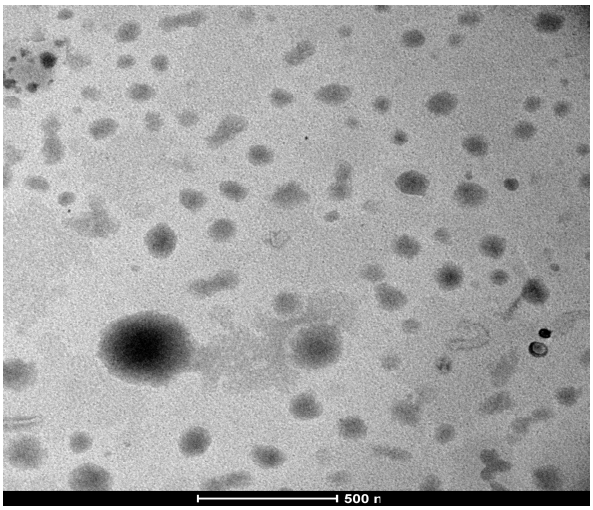

Fig. 2. 41 TEM image of aggregates obtained by dialysis with Y-II copolymer, $(A)_2$-B_{7200}-A

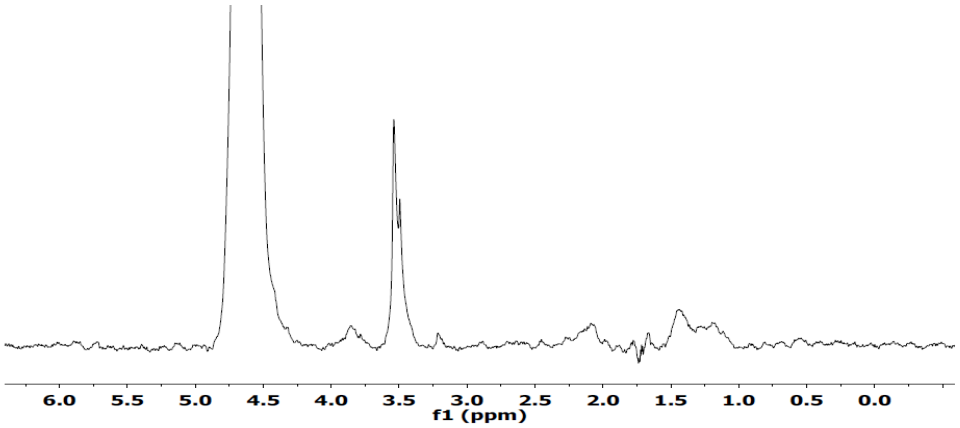

Fig. 2. 42 ^{1}H-NMR in D_2O of aggregates obtained by dialysis with H-shaped copolymer$(A)_2$-B_{7200}-A

Y-I nanoaggregates, reported in figure 2.43, show a “worm like” morphology with a rather compact hydrophilic shell evidenced by ^{1}H-NMR experiment in D_2O (figure 2.44) in which can be noted very weak PCL signals O-CH_2-$\underline{CH_2}$-$\underline{CH_2}$-$\underline{CH_2}$-CH_2-O-CO (δ = 1-1.5)), –O-CH_2-CH_2-CH_2-CH_2-$\underline{CH_2}$-CO (δ = 2.20).

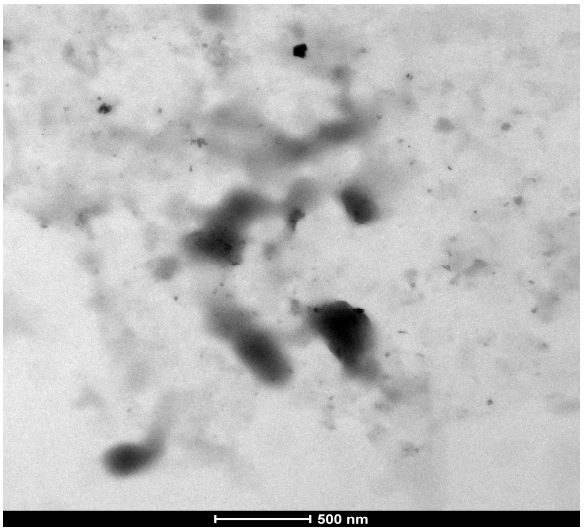

Fig. 2.43 TEM image of aggregates obtained by dialysis with Y-I copolymer, $(A)_2$-B_{5800}

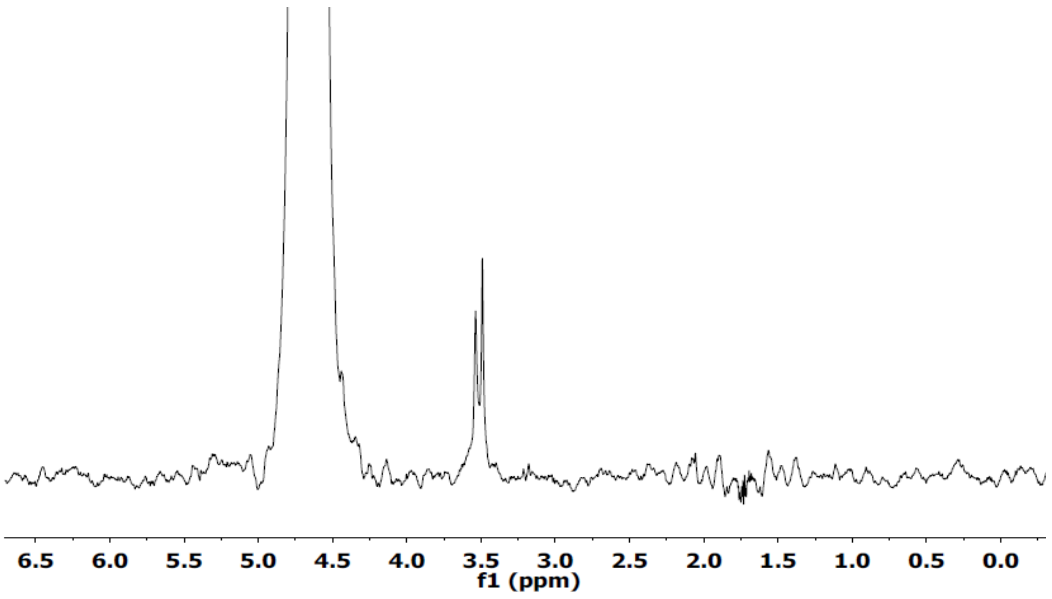

Fig. 2. 44 ^{1}H-NMR in D_2O of aggregates obtained by dialysis with H-shaped copolymer$(A)_2$-B_{5800}

As expected, diblock and triblock copolymer assembly in spherical aggregates with a compact shell (data not shown).

Shell thickness, reported in table 2.3, (Fixed Aqueous Layer Thikness of the outer PEG shell[38],[39]) was determined by measuring the Z-potential as a function of electrolyte molar concentration (c). The hydrophilic PEG moisture shifts the slipping plane away from the surface of the PCL core and this subsequently results in a reduced z-potential. With an increase in ionic strength, Z was found to decrease according to the Gouy-Chapmann theory. A plot of ln(z) against k ($k = 3.3*c^{0.5}$, where k^{-1} is the Debye length, c is molar concentration) gives the thickness of the PEG polymer layer in nm (d_{shell}) as the slope of a linear regression. An example for the diblock copolymer is shown in figure 2.45

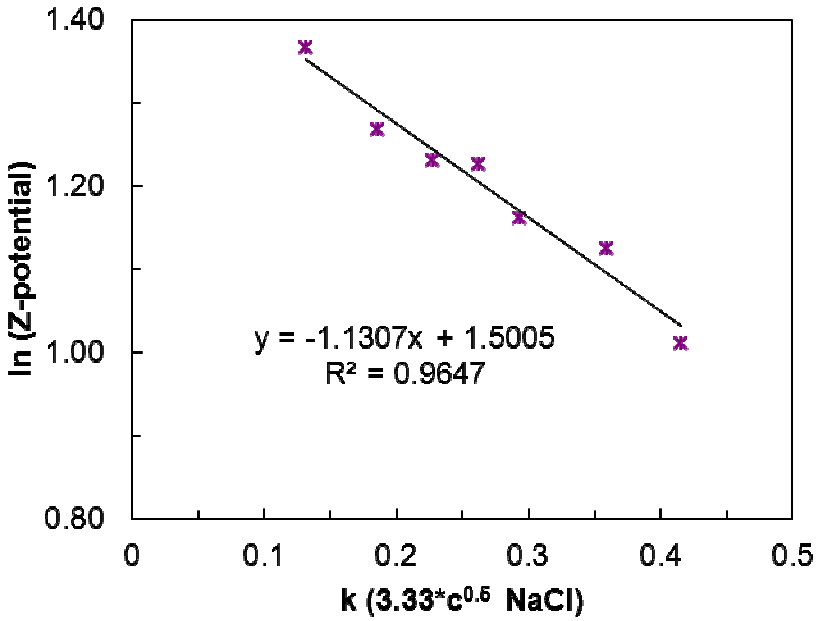

Fig. 2. 45 FALT measurement for diblock copolymer A-B_{3000}

Total length of PEG segment in trans-planar conformation trigonometrically calculated is 4.71 nm, so can be argued that Y-I and Y-II shells are practically

collapsed on hydrophobic core, while diblock and H-shaped show an intermediate conformation and triblock tends to the chain totally stretched as schematically shown in figure 2.44

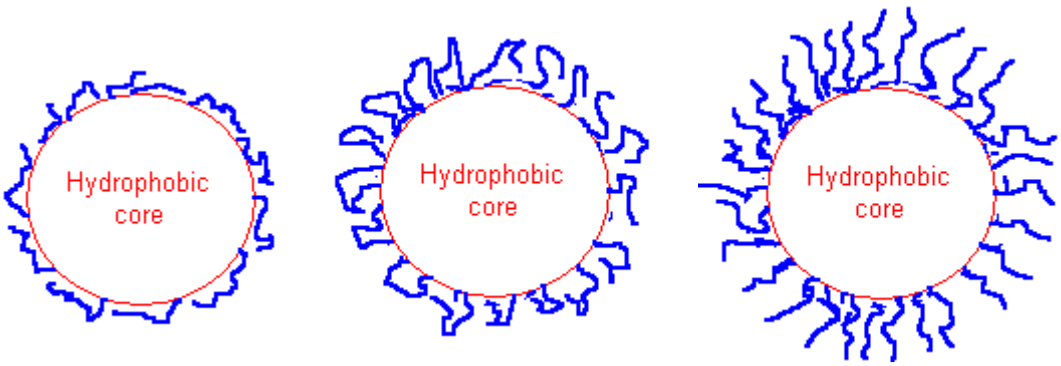

Fig. 2.44 Type of PEG shell: collapsed, intermediate and stretched

Analyzing self-assembly data, influence of copolymer architecture on CAC is, as expected, quite negligible; main factor result to be hydrophobic/hydrophilic block ratio. On the other hand this parameter plays an important role in nanoaggregate morphology and has a critical influence on hydrophilic shell shape and compactness.

2.5 Decorated amphiphilic diblock copolymer

The systems so far described show a high potential in drugs controlled release; block copolymers synthesized form aggregates whose size (<150 nm) and the presence of a hydrophilic shell allow to avoid renal exclusion and recognition by the RES, leading sufficient residence time to reach places such as more permeable. cancer cells Thanks to click chemistry synthetic strategy it is possible to easily concept nanovector with additional features simply “decoring” macromolecules with functional ligands. Field of great interest in anticancer drugs nanovector is active targeting. The main obstacle that nanoassembled systems encountered in clinical applications, and in particular in chemotherapy treatments, is the poorly

selective release of anticancer drugs in tumor tissues with consequent accumulation of the drug in healthy cells. A new approach to improve selectivity toward target cells is the inclusion of molecules on the surface of the nanocarriers specific ligands, capable of being selectively recognized by some tissues[40,41]. Were, then, studied a series of molecules which, chemically linked to release systems, ensure an extremely precise and effective direct drug action (active targeting). As an example can be mentioned folic acid (FOL), also known as vitamin B9 or folacin. Recently it has been discovered that the cellular receptors of many cancer cells specific for this acid are overexpressed compared to healthy cells and this phenomenon is accentuated in some types of cancer such as cancer of the kidney[42]. This means that the cancer cells tend to engulf and metabolize a larger amount of folic acid compared to the surrounding cells. This feature can be exploited to hit preferably tumor cells functionalizing external coating of anticancer drug release devices with folic acid. Other approach provide to functionalize nanocarriers core with molecule able to bind magnetic targeting agents, such as catechol derivatives, giving nanovector the ability to be directed through an external magnetic field suitably made. Functionalised catechol-derived (CAT) ligands have enjoyed success as agents for the masking of superparamagnetic iron-oxide particles, often so as to render them biocompatible with medium to long-term colloidal stability in the complex chemical environments of biological milieux. Catechol-derivative anchor groups possess irreversible binding affinity to iron oxide and thus can optimally disperse super paramagnetic nanoparticles under physiologic conditions. This not only leads to ultrastable iron oxide nanoparticles but also allows close control over the hydrodynamic diameter and interfacial chemistry. The latter is a crucial breakthrough to assemble functionalized magnetic nanoparticles, e.g., as targeted magnetic resonance contrast agents[43].

Effective delivery of bioactive agents within cells is expected to have an enormous impact in the future development of new therapeutic and/or diagnostic strategies based on single-cell–bioactive-agent interactions. Polymeric nanovector should be

able to enter cells, escape from the complex endocytic pathway, and efficiently deliver actives within clinically relevant cells without perturbing their metabolic activity. To monitoring *in vivo* or *in vitro* nanovector track is widely used to label it with some probe or dye. Rhodamine are normally used as a dye and as a dye laser gain medium;are often used as a tracer dye within water to determine the rate and direction of flow and transport. In particular, Rhodamine B (RHOD) is used extensively in biotechnology applications because it is a fluorescent dyes and can thus be detected easily and inexpensively by fluorometers. fluorescence microscopy, flow cytometry, fluorescence correlation spectroscopy and ELISA[44,45]. On these bases, was developed click chemistry synthethic strategy applied in synthesis of diblock an triblock PCL-PEO copolymer with hydrophobic/hydrophilic ratio ≈ 2 useful to be decorated onto PEO segment with folic acid or rhodamine B while onto PCL segment with catechol derivatives. Copolymers were characterized by NMR, FTIR and viscosimetry and were analyzed self-assembly characteristics in aqueous systems (in collaboration with research group from the "Dipartimento di ChimicaFarmaceutica e Tossicologica" directed by FabianaQuaglia), determining the size (DLS), the critical micelle concentration (CMC) and zeta potential.

2.5.1 Synthesis of diblock copolymer FOL-NH-PEO_{2000}-PCL_{4000}

Main drawback in the synthesis of this kind of copolymer is to obtain a PEO segment with two different reactive terminal: -NH_2 useful for folic acid bounding and other functional group to PCL coupling. The problem has been removed reacting di-amine-PEO_{2000} with propargyl chloroformate to achieve α-amino-ω-alkyne-PEO_{2000}, NH_2-PEO_{2000}-alkyne as shown in following scheme:

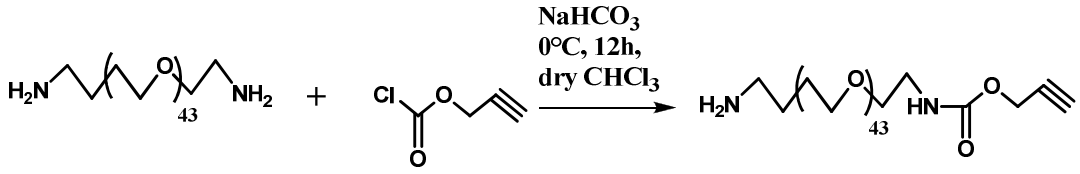

Fig. 2.45 synthesis of α-amino-ω-alkyne-PEO$_{2000}$, NH$_2$-PEO$_{2000}$-alkyne

The reaction was carried out with di amine-PEO$_{2000}$ in 150% molar excess and propargyl chloroformate was dropwise added to ensure partial conversion of amino groups. After 12 h the reaction mixture was filtered from bicarbonate and concentred. In solution were unreacted di-amine-PEO$_{2000}$, NH$_2$-PEO$_{2000}$-alkyne and di-alkyne-PEO$_{2000}$. To remove undesiderated product, PEO solution was purified by silica gel flash cromatography using as eluent methanol in $CHCl_3$ from 5 to 20% in vol. ^{1}H-NMR analysis was used to confirm the product, NH$_2$-PEO$_{2000}$-alkyne, chemical structure. Comparing integrations values of the signals related to the PEO protons O-CH_2-CH_2 (c) (δ = 3.60) and- O-CH_2-C≡CH (d) (δ =4.68) (figure 2.46) was evaluated, within the limits of experimental error, a purity degree higher than 95%. Ninhydrin assay was used to confirm presence of free -NH_2 group

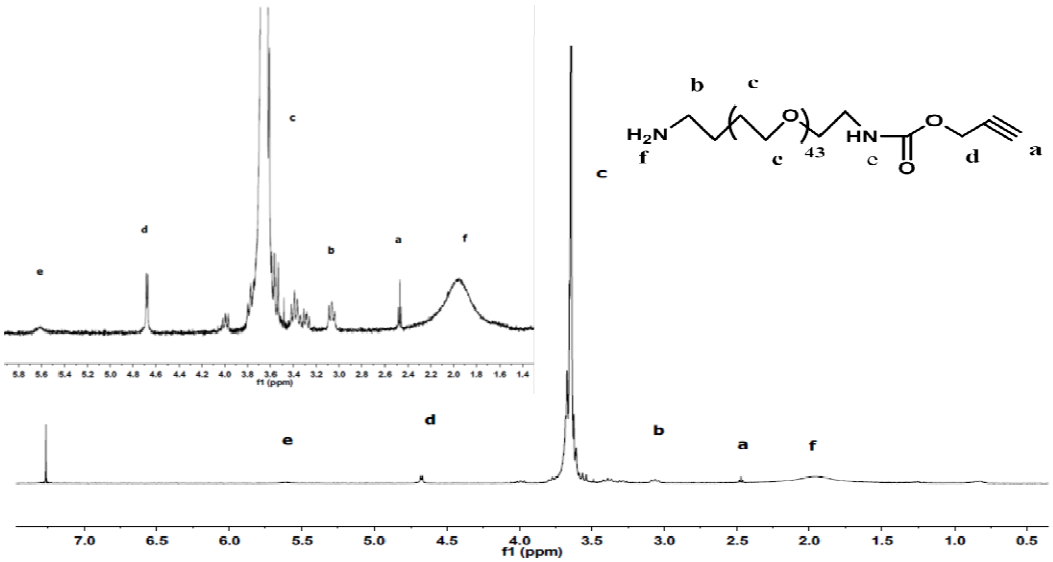

Fig.2.46 ^{1}H-NMR of NH$_2$-PEO$_{2000}$-alkyne with proton assignment

The PCL segment was obtained by ε-CL ROP initiated from hexanol catalyzed by $Sn(Oct)_2$. The terminal hydroxyl group was changed into azide by two-step azidation with mesyl chloride activation to obtain α-hexan-ω-azido-PCL_{4000}, PCL_{4000}-N_3, as reported in figure 2.47.

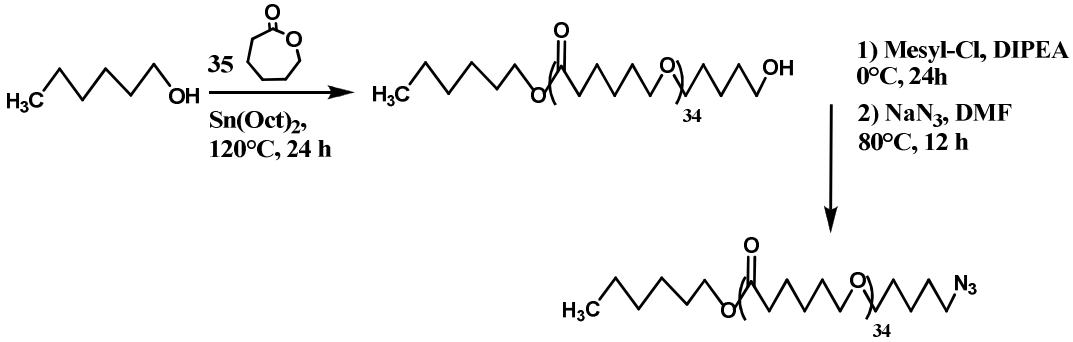

Fig. 2.47 Synthesis of α-hexan-ω-azido-PCL_{4000}.

^{1}H-NMR analysis was used to confirm M_n of PCL segment, comparing integrations values of the signals related to the PCL inner protons CO-CH_2-CH_2 (d) (δ = 2.29) and terminal CH_3-CH_2-CH_2 (a) (δ = 0.88) (figure 2.48). The evaluated number average molecular weight was, within the limits of experimental error, very close to that expected; then was used to confirm chemical structure of PCL_{4000}-N_3, comparing integrations values of the signals related to the PCL terminal CH_3-CH_2-CH_2 (d) (δ = 0.88) and -CH_2-N_3 (f) (δ = 3.27) (figure 2.50), taking in account the complete disappearance of mesyl signal related to intermediate (figure 2.49). The evaluated conversion degree of α-hexan-ω-mesyl-PCL_{4000} was, within the limits of experimental error, higher than 95% . FT-IR analysis confirm presence of azide group; can be noted, in fact, in figure 2.51 the characteristic stretching at 2100 cm^{-1}. Finally, NH_2-PEO_{2000}-alkyne was reacted in 20% molar excess with PCL_{4000}-N_3 with Huisgen cycloaddition catalyzed by Cu(I) according to the protocol used for linear triblock synthesis as illustrated in figure 2.52a scheme. Diblock resulting copolymer PCL_{4000}-PEO_{2000}-NH_2 was washed with methanol to solve unreacted NH_2-PEO_{2000}-alkyne

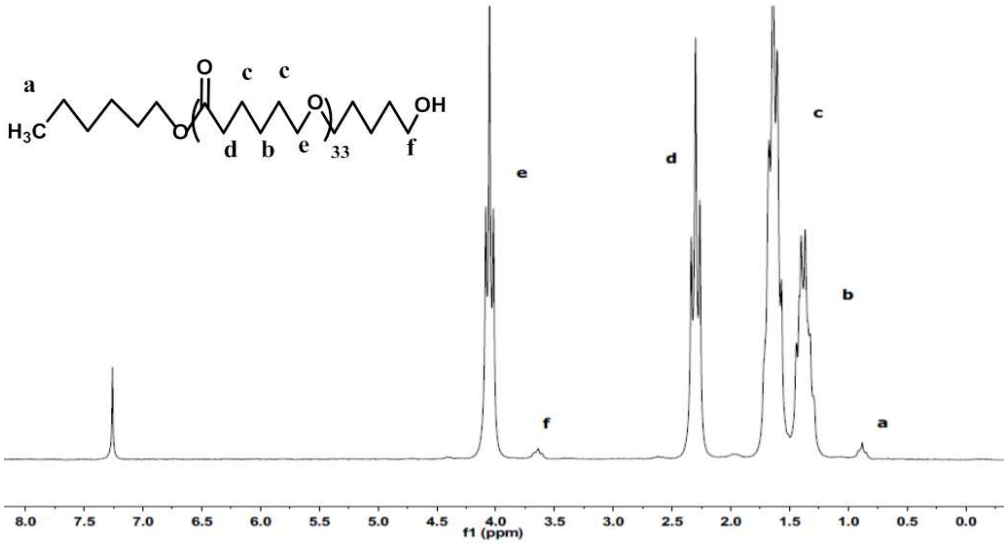

Fig.2.48 [1]H-NMR of PCL_{4000}-OH with proton assignment

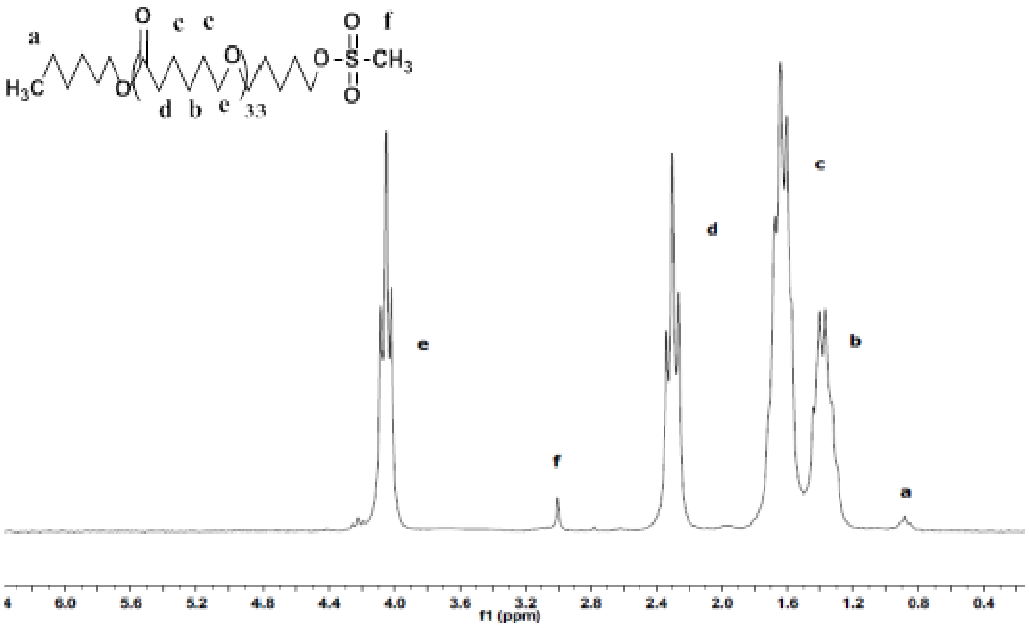

Fig.2.49 [1]H-NMR of PCL_{4000}-mesy with proton assignment

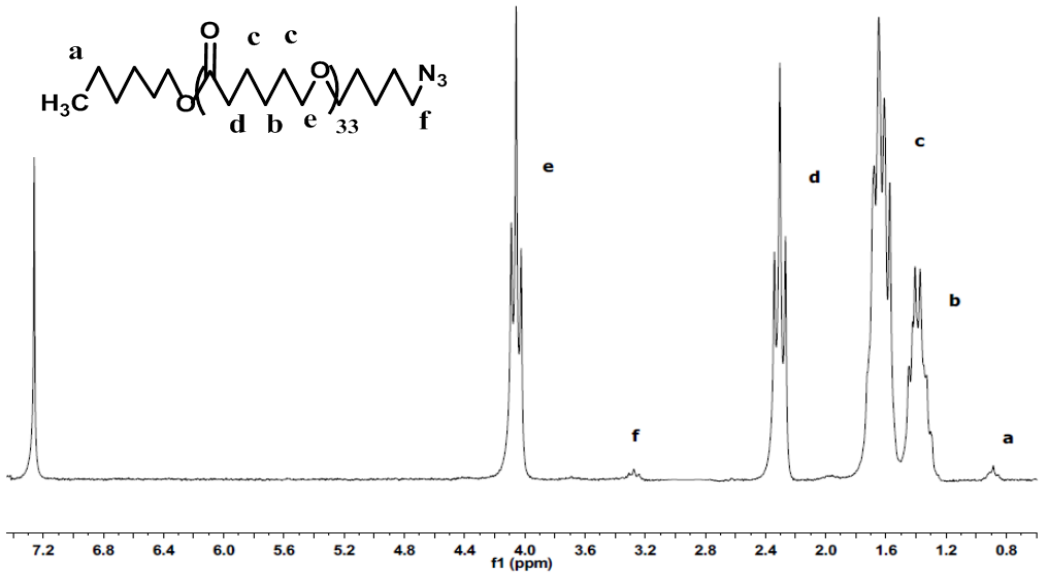

Fig.2.50 ^{1}H-NMR of PCL_{4000}-azido with proton assignment

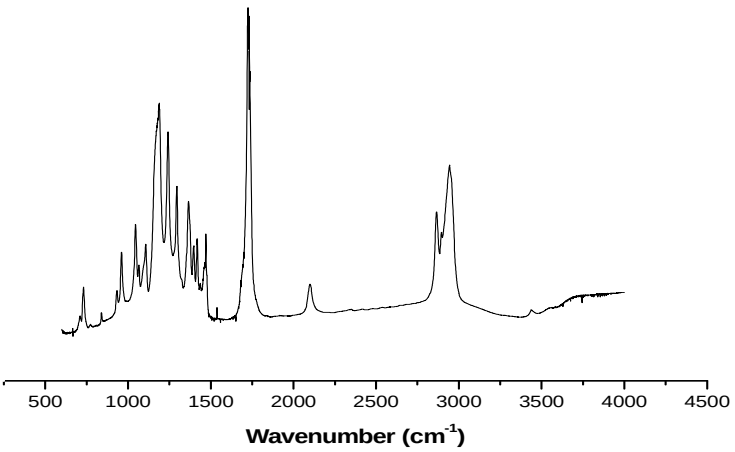

Fig. 2.51 PCL_{4000}-N_3 FT-IR spectrum. At 2100 cm-^{1} can be noted characteristic azide stretching

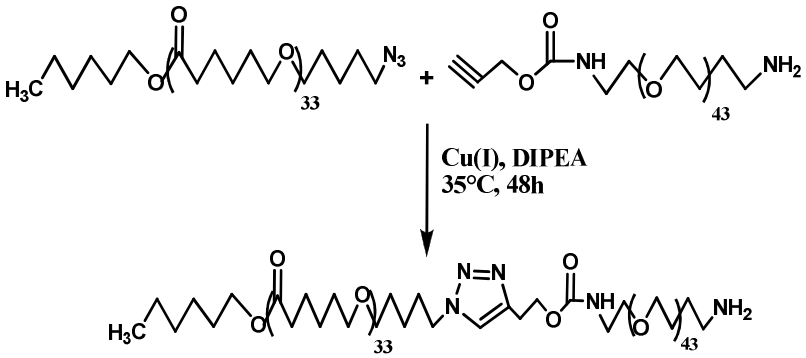

Fig 2.52 a Synthesis of α-hexan-PCL$_{4000}$-PEO$_{2000}$-NH$_2$ by click coupling

FT-IR analysis confirm complete coupling. It can be noted, in fact, in figure 2.52 b total disappearance of azide group characteristic stretching at 2100 cm-1.

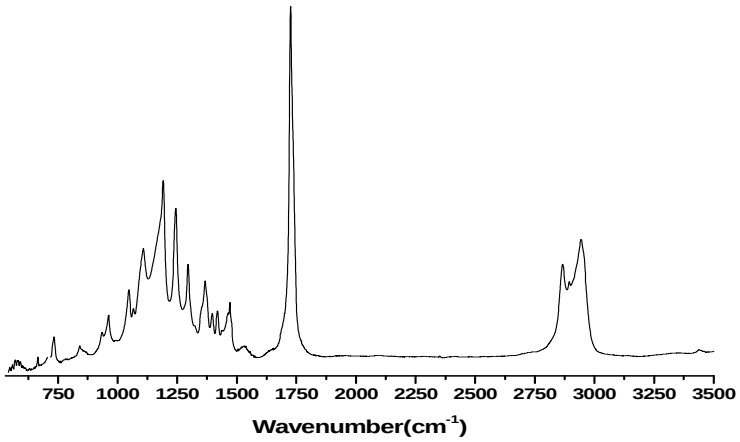

Fig. 2.52 b PCL4$_{000}$-PEO$_{2000}$-NH$_2$ FT-IR spectrum. At 2100 cm-1 it can be noted total disappearance of characteristic azide stretching

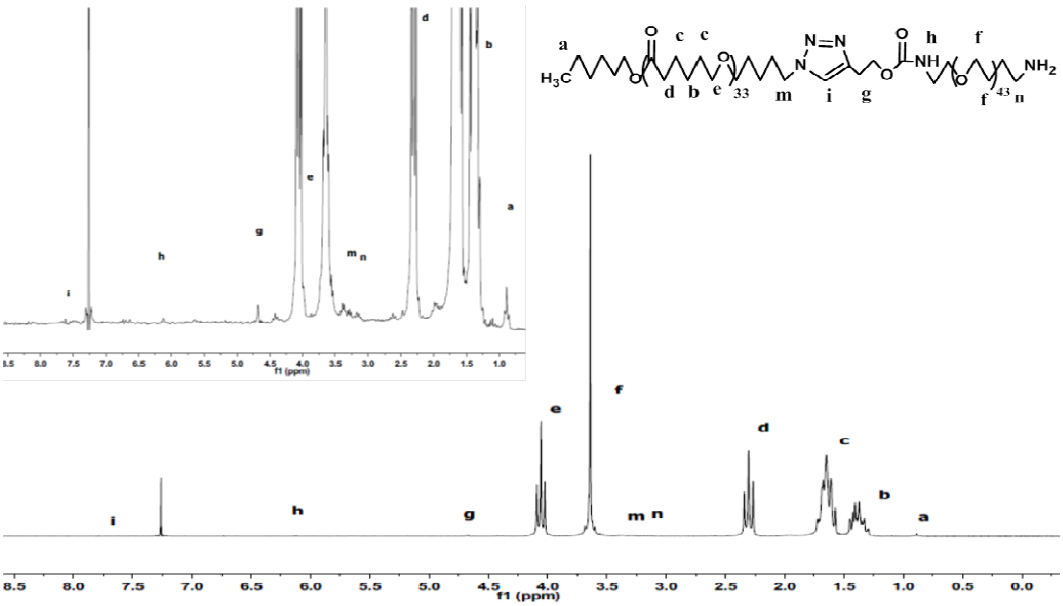

Fig.2.53 ^{1}H-NMR of PCL4$_{000}$-PEO$_{2000}$-NH$_2$ with proton assignment

^{1}H-NMR analysis was used to confirm the chemical structure of product, comparing integrations values of the signals related to the PCL protons CO-CH_2-CH_2 (d) (δ = 2.29) and PEO O-CH_2-CH_2 (f) (δ = 3.60) (figure 2.53). The evaluated ratio between PCL and PEO is, within the limits of experimental error, very close to that expected. Ninhydrin assay was used to confirm free amino group presence. To complete the designed copolymer, folic acid was before activated with N-hydroxysuccinimide by DCC and DMAP reaction and then linked to PCL4$_{000}$-PEO$_{2000}$-NH_2, as reported in figure 2.54

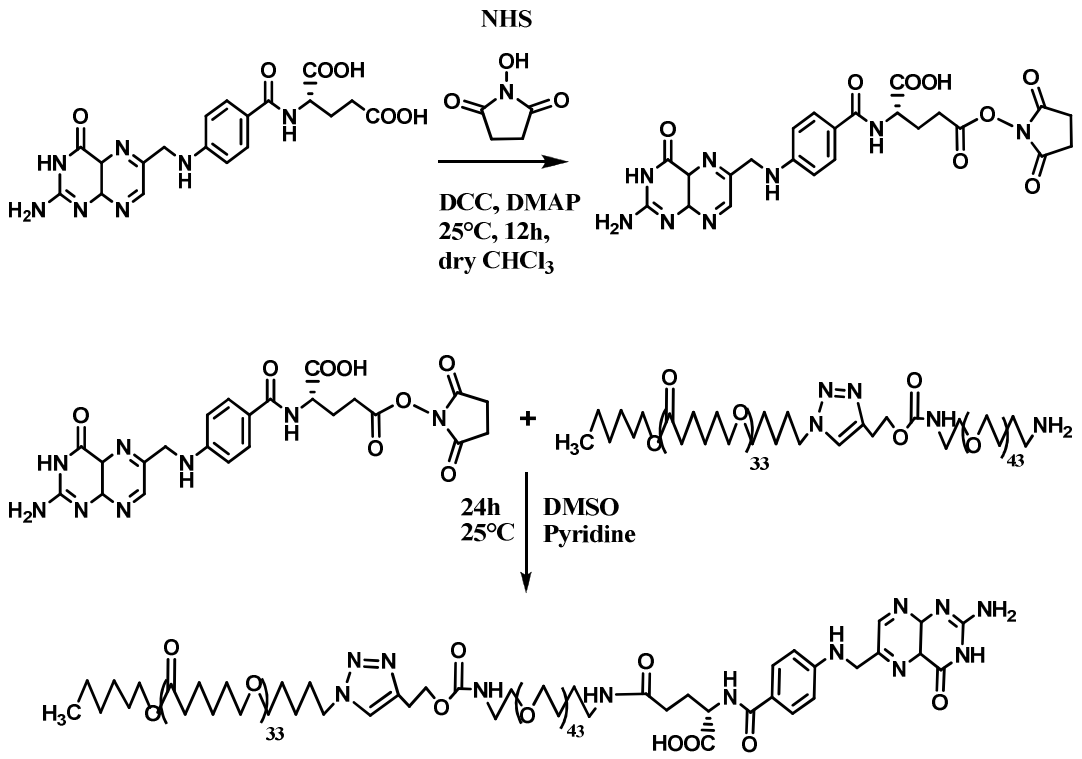

Fig. 2.54 folic acid activation with N-hydroxysuccinimide and subsequent coupling with PCL4$_{000}$-PEO$_{2000}$-NH$_2$

As can be noted from figure 2.54 folic acid present two carboxylic groups, but reactivity of α group is negligible respect to the γ one, thus only γ-group is engaged in coupling with PCL4$_{000}$-PEO$_{2000}$-NH$_2$. Coupling reaction was carried out in 20% activated folic acid molar excess. Traces of unreacted folic acid were removed by dialysis in H_2O of the reaction product dissolved in DMSO. ^{1}H-NMR analysis was used to confirm chemical structure of product, comparing integrations values of the signals related to the terminal PCL protons CH_3-CH_2-CH_2 (a) (δ = 0.88) and O-NH-CO (m) (δ = 7.67) (figure 2.55). It was evaluated that PCL$_{4000}$-PEO$_{2000}$-NH$_2$ conversion degree to the folate derivative was around 80%, within the limits of experimental error.

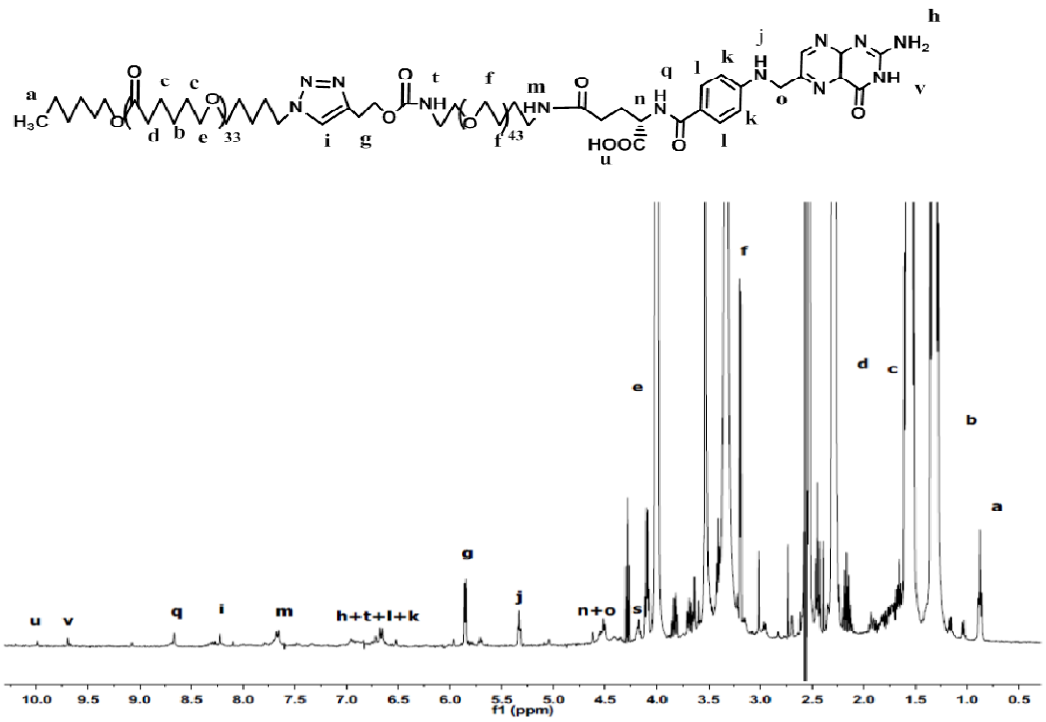

Fig.2.55 Zoom of ^{1}H-NMR of PCL4$_{000}$-PEO$_{2000}$-NH-Folate with proton assignment

The percentages of folic acid are acceptable for diagnostic purposes, since it is not required a total coating of micelles hydrophilic corona in order to be effective the recognition folate-target cell.

2.5.2 Synthesis of triblock copolymer RHOD-NH-PEO$_{2000}$-PCL$_{7000}$-PEO$_{2000}$

The synthesis of this copolymer followed almost the same protocol applied in PCL$_{4000}$-PEO$_{2000}$-NH-Folate, except for the initiator in ε-CL polymerization, in which was used as initiator α-metoxy-ω-hydroxyl-PEO$_{2000}$, m-PEO$_{2000}$-OH and

was changed the initiator/monomer molar ratio, obtaining a m-PEO_{2000}-PCL_{7000}-OH diblock copolymer as illustrated in figure 2.56:

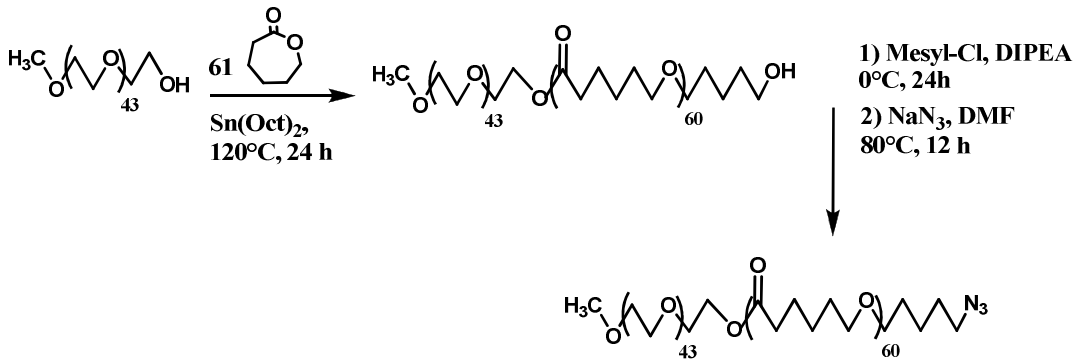

Fig.2.56 Synthesis of diblock copolymer m-PEO_{2000}-PCL_{7000}-OH

^{1}H-NMR analysis was first used to confirm the M_n of PCL segment in diblock m-PEO_{2000}-PCL_{7000}-OH, comparing integrations values of the signals related to the PCL protons CO-CH_2-CH_2 (c) (δ = 2.29) and terminal PEO CH_3-O-CH_2-CH_2 (g) (δ = 3.36) (figure 2.57). It was evaluated that the number average molecular weight was, within the limits of experimental error, very close to that expected; then, was used to confirm the chemical structure of m-PEO_{2000}-PCL_{7000}-N_3, comparing integrations values of the signals related to the PEO terminal CH_3-O-CH_2 (g) (δ = 3.36) and -CH_2-N_3 (h) (δ = 3.27) (figure 2.59), taking in account the complete disappearance of mesyl related peaks observed in figure 2.58. The evaluated conversion degree of m-PEO_{2000}-PCL_{7000}-OH was, within the limits of experimental error, higher than 95%.

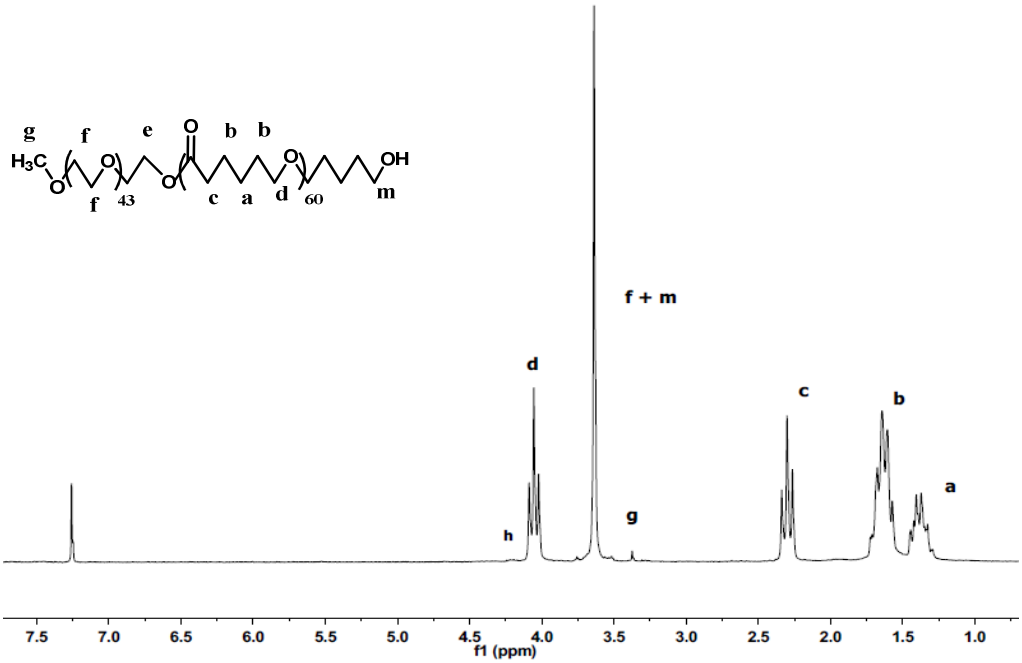

Fig.2.57 ^{1}H-NMR of m-PEO$_{2000}$- PCL$_{7000}$ with proton assignment

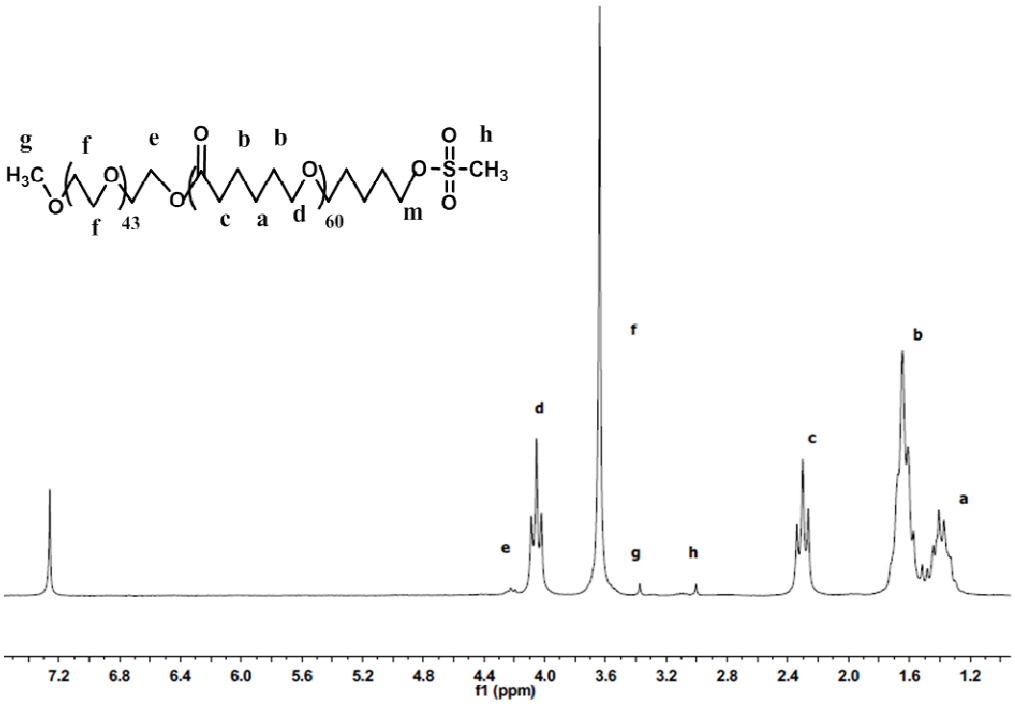

Fig.2.58 ^{1}H-NMR of m-PEO$_{2000}$- PCL$_{7000}$-mesy with proton assignment

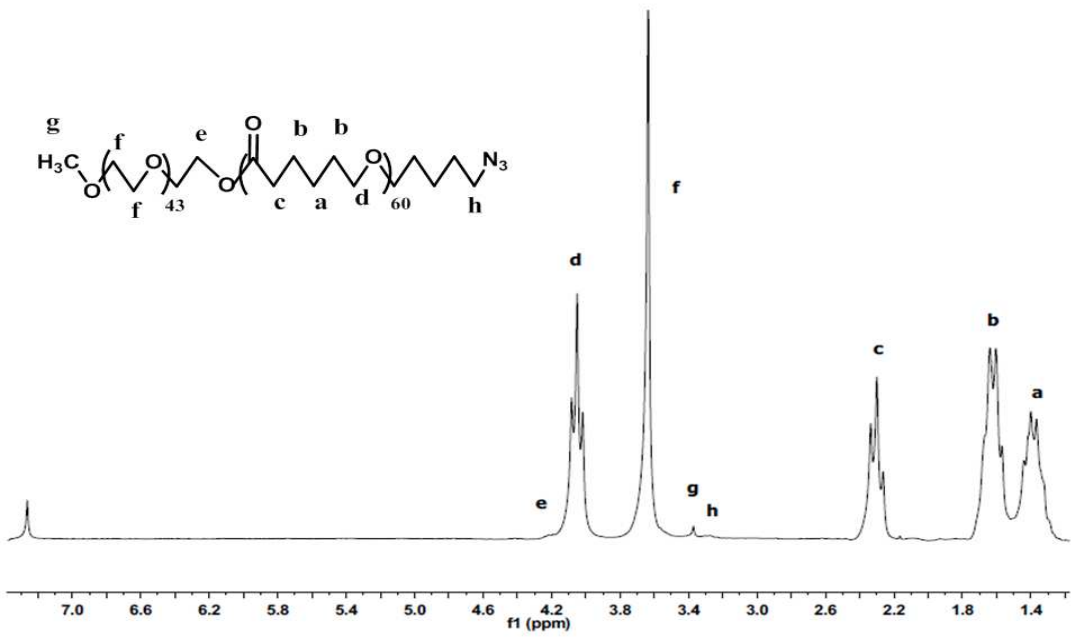

Fig.2.59 [1]H-NMR of m-PEO$_{2000}$- PCL$_{7000}$-azido with proton assignment

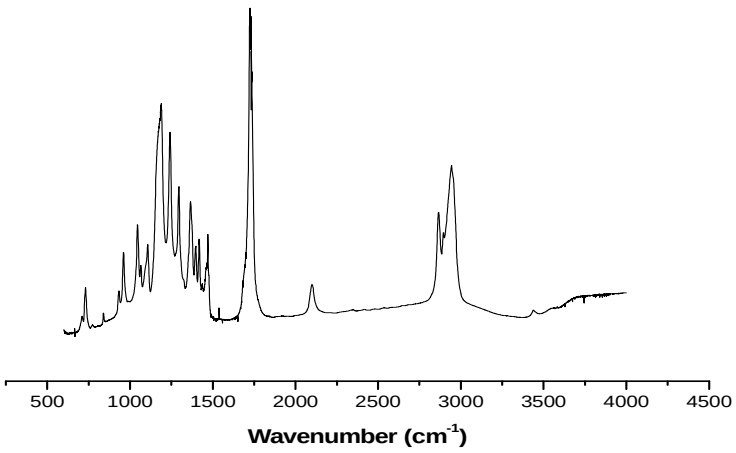

Fig. 2.60 m-PEO$_{2000}$- PCL$_{7000}$-azido FT-IR spectrum. At 2100 cm-[1] can be noted characteristic azide stretching

FT-IR analysis confirms the presence of azide groups; showing in the spectrum reported in figure 2.60 the characteristic stretching at 2100 cm^{-1}. Finally NH_2-PEO_{2000}-alkyne was reacted in 20% molar excess with m-PEO_{2000}-PCL_{7000}-OH in Huisgen cycloaddition catalyzed by Cu(I) according to the protocol used for linear triblock synthesis as illustrated in figure 2.61 scheme. Triblock resulting copolymer m-PEO_{2000}-PCL_{7000}-PEO_{2000}-NH_2 was washed with methanol to solve unreacted NH_2-PEO_{2000}-alkyne

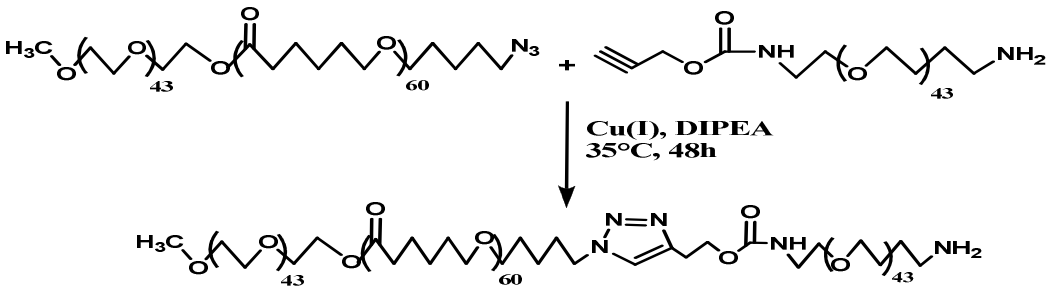

Fig 2.61 Synthesis of m-PEO_{2000}-PCL_{7000}-PEO_{2000}-NH_2 by click coupling

FT-IR analysis confirm complete coupling. It can be noted, in fact, in figure 2.62 the total disappearance of azide group characteristic stretching at 2100 cm-1.

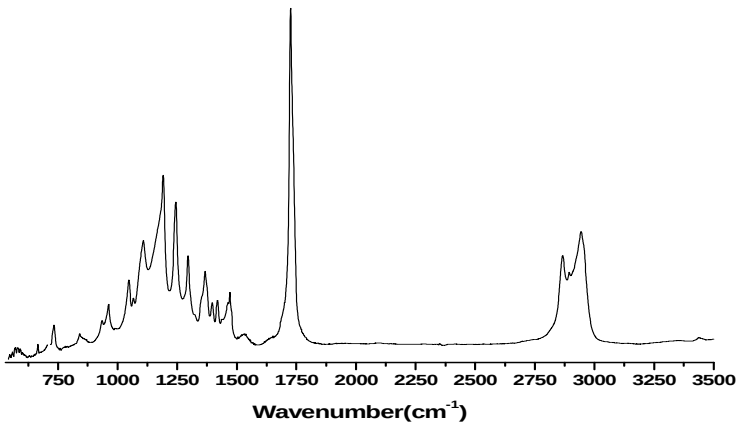

Fig. 2.62 m-PEO_{2000}-PCL_{7000}-PEO_{2000}-NH_2 FT-IR spectrum. At 2100 cm^{-1} can be noted total disappearance of characteristic azide stretching

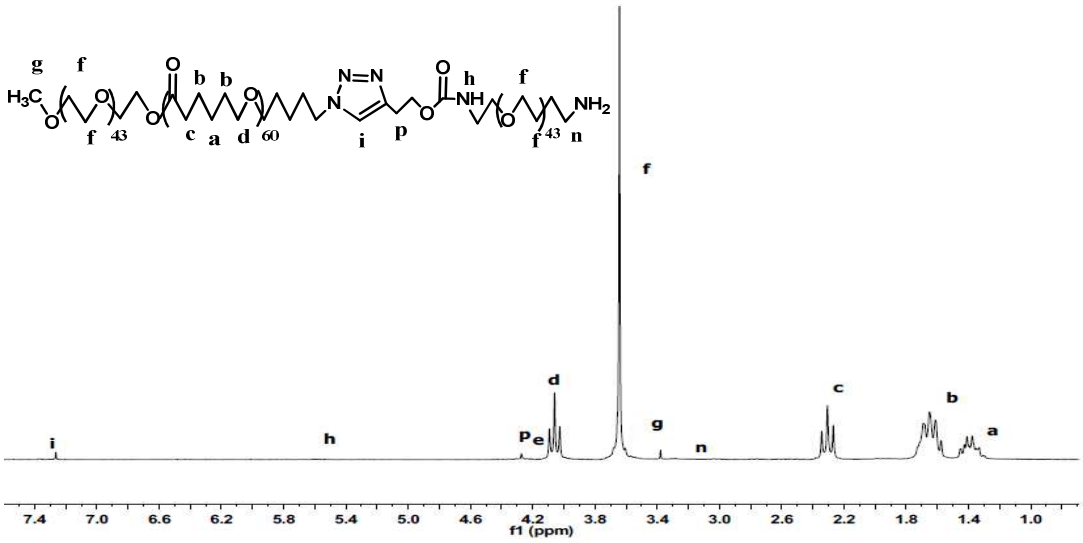

Fig.2.63 [1]H-NMR of m-PEO_{2000}- PCL_{7000}-PEO_{2000}-NH_2 with proton assignment

Rhodamine B was coupled with m-PEO_{2000}-PCL_{7000}-PEO_{2000}-NH_2 by DCC and DMAP reaction without carboxylic group activation as illustrated in figure 2.64

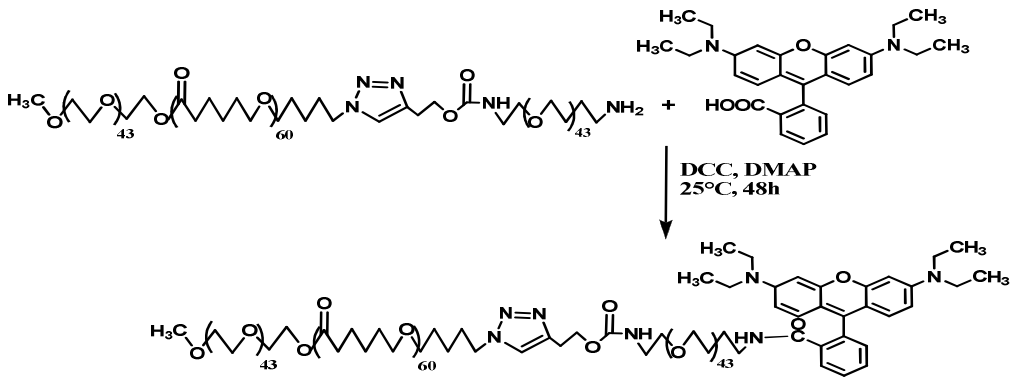

Fig 2.64 coupling between rhodamine B and m-PEO_{2000}-PCL_{7000}-PEO_{2000}-NH_2

[1]H-NMR analysis was used to confirm the chemical structure of m-PEO_{2000}-PCL_{7000}-PEO_{2000}-NH-ROD. Comparing integrations values of the signals related to the terminal PEO protons CH_3-O-CH_2 (9) (δ = 3.36) and O-NH-CO (k) (δ = 5.23) (figure 2.65) it was evaluated that m-PEO_{2000}-PCL_{7000}-PEO_{2000}-NH_2 conversion degree was, within the limits of experimental error, around 80%.

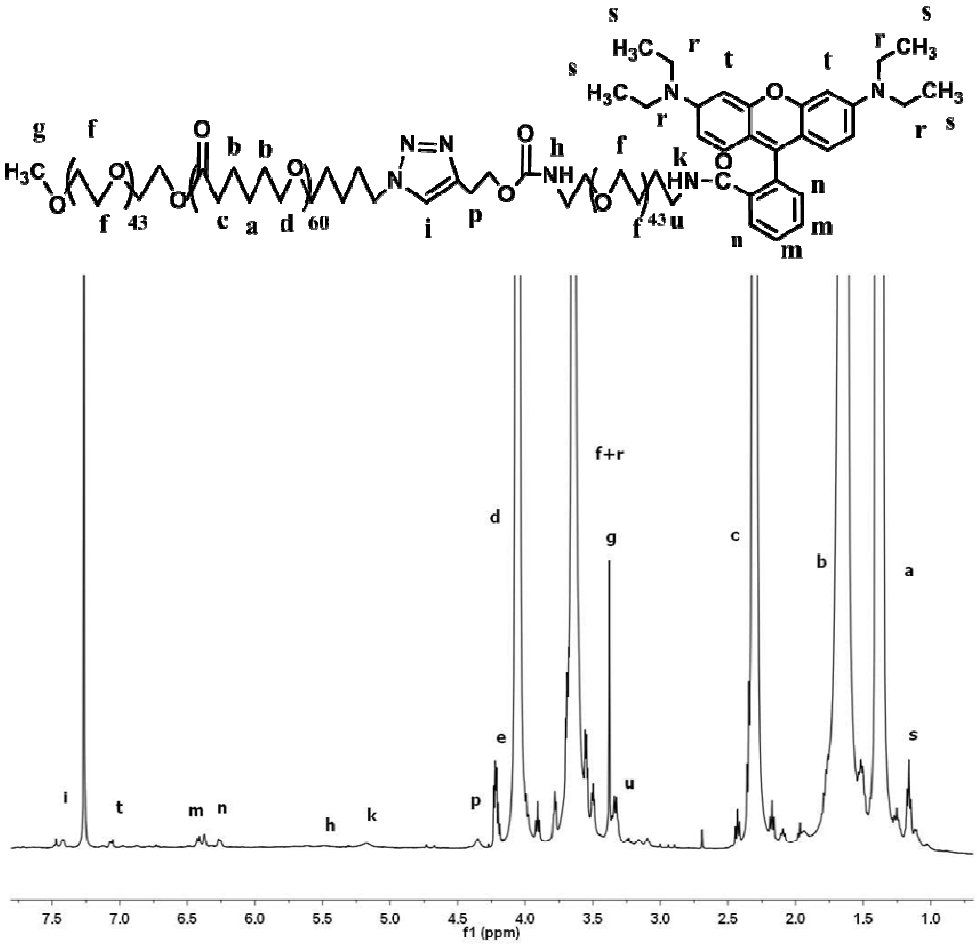

Fig.2.65 ^{1}H-NMR of m-PEO_{2000}- PCL_{7000}-PEO_{2000}-NH_2 with proton assignment

2.5.3 Synthesis of diblock copolymer m-PEO_{2000}-PCL_{4000}-CAT

The Cathehol derivative chosen for diblock functionalization was 3-hydroxy-tyramine hydrobromide, well known as dopamine. Due to the amino group, this compound was reacted with propargyl chloroformate to obtain a catechol-alkyne as illustrated in figure 2.66.

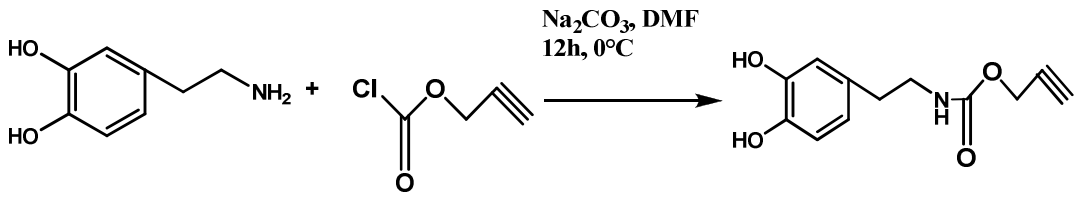

Fig 2.66 Reaction of dopamine with propargyl chloroformate for catechol-alkyne, CAT-alkyne

The reaction was carried out in DMF with sodium bicarbonate as heterogeneous proton acceptor. After 48 h reaction mixture was dried, redissolved in chloroform, filtered from bicarbonate, purified by flash silica gel cromatography with a methanol/chloroform mixture 9/1 v/v as eluent. After drying, a sticky brown solid was recovered with a quantitative yield. ^{1}H-NMR analysis was used to confirm chemical structure of product, CAT-alkyne, comparing integrations values of the signals related to the terminal PEO protons CH_3-O-CH_2 (9) (δ = 3.36) and O-NH-CO (k) (δ = 5.23) (figure 2.67). The m-PEO_{2000}-PCL_{7000}-PEO_{2000}-NH_2 conversion degree was, within the limits of experimental error, higher than 95%. Ninhydrin assay confirmed total functionalization of the amino group.

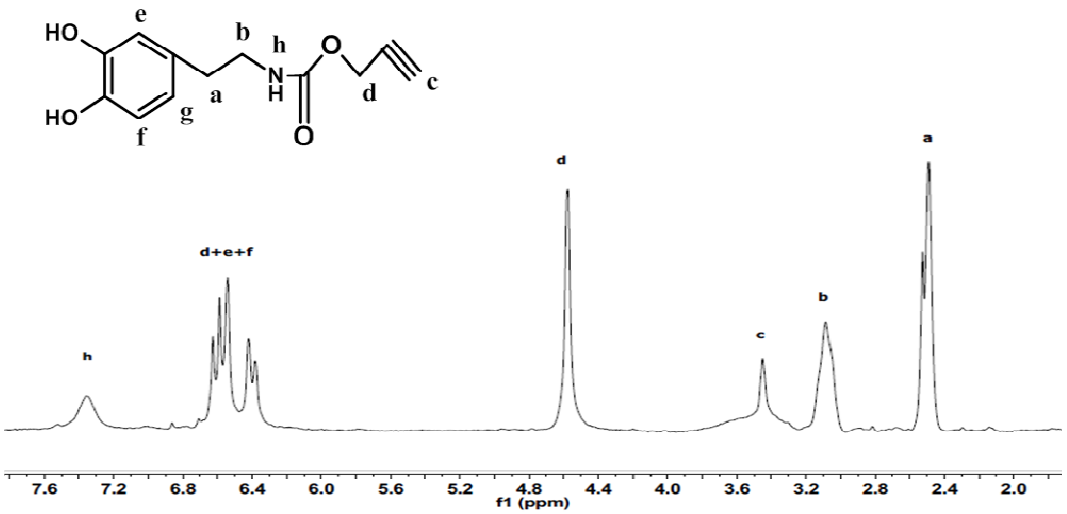

Fig.2.67 ^{1}H-NMR of CAT-alkyne with proton assignment

The azided diblock was obtained as described in paragraph 2.5.2 from m-PEO_{2000}-PCL_{4000}-OH deriving from e-CL ROP initiated from m-PEO_{2000}-OH. ^{1}H-NMR confirmed Mn of PCL segment and quantitative conversion of m-PEO_{2000}-PCL_{4000}-OH into azided product FT-IR analysis confirmed the presence of azide group; as shown in figure 2.68 by the characteristic stretching at 2100 cm^{-1}

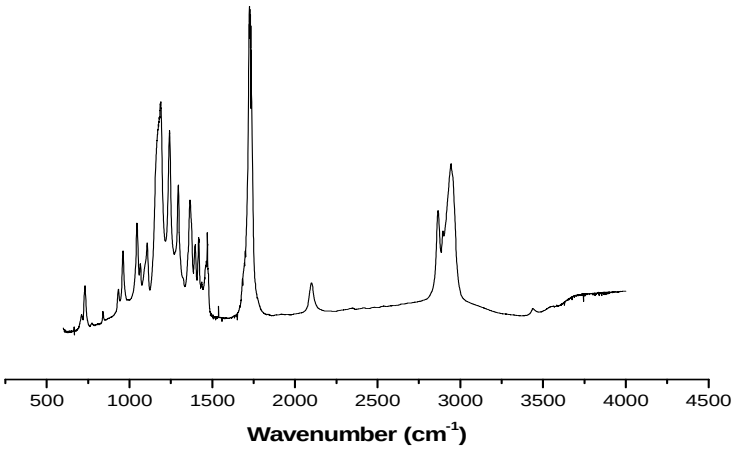

Fig. 2.68 m-PEO_{2000}-PCL_{4000}-azido FT-IR spectrum. At 2100 cm-^{1} can be noted characteristic azide stretching

Diblock m-PEO_{2000}-PCL_{4000}-N_3 was reacted with CAT-alkyne in 20% molar excess by the 1,3 Huisgen cycloaddition, as illustrated in figure 2 following the descripted protocol. Unreacted CAT-alkyne was removed by diethyl ether washing.

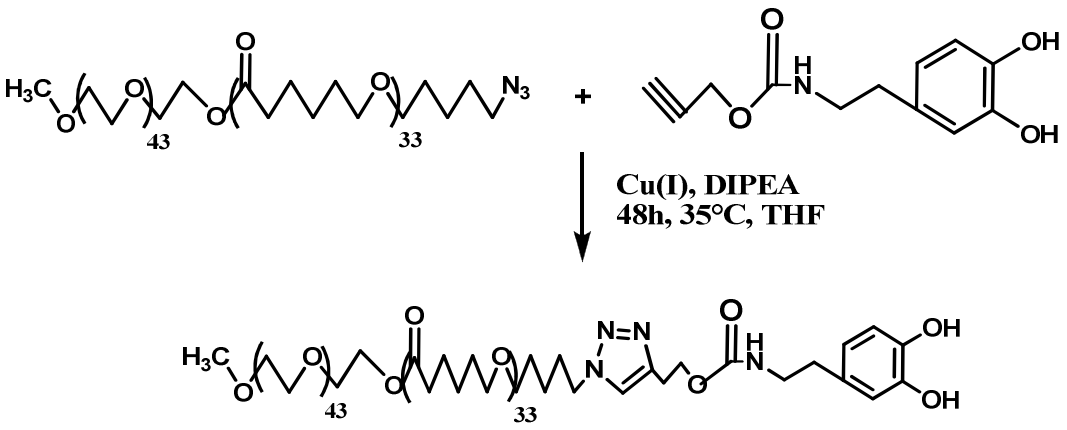

Fig 2.69 1,3 Huisgen cycloaddition between m-PEO_{2000}-PCL_{4000}-N_3 and CAT-alkyne

FT-IR analysis confirm complete coupling. It can be noted, in fact, in figure 2.62 total disappearance of azide group characteristic stretching at 2100 cm-1.

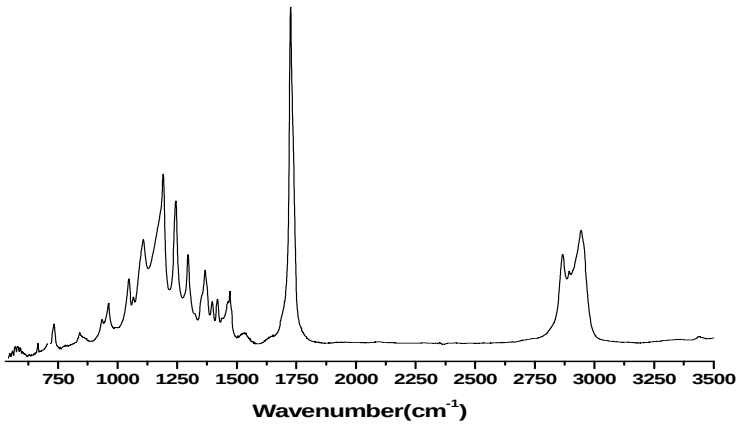

Fig. 2. m-PEO_{2000}-PCL_{4000}-CAT FT-IR spectrum. At 2100 cm^{-1} can be noted total disappearance of characteristic azide stretching

^{1}H-NMR analysis was used to confirm the chemical structure of product, m-PEO_{2000}-PCL_{4000}-CAT, comparing integrations values of the signals related to the terminal PEO protons CH_3-O-CH_2 (g) (δ = 3.36) and O-NH-CO (k) (δ = 5.23)

(figure 2.65). It was evaluated that m-PEO_{2000}-PCL_{4000}-N_3 conversion degree was, within the limits of experimental error, higher than 95%

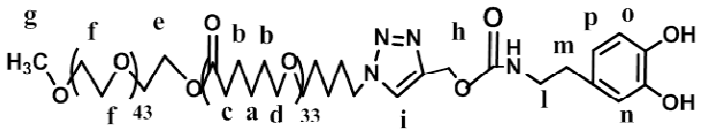

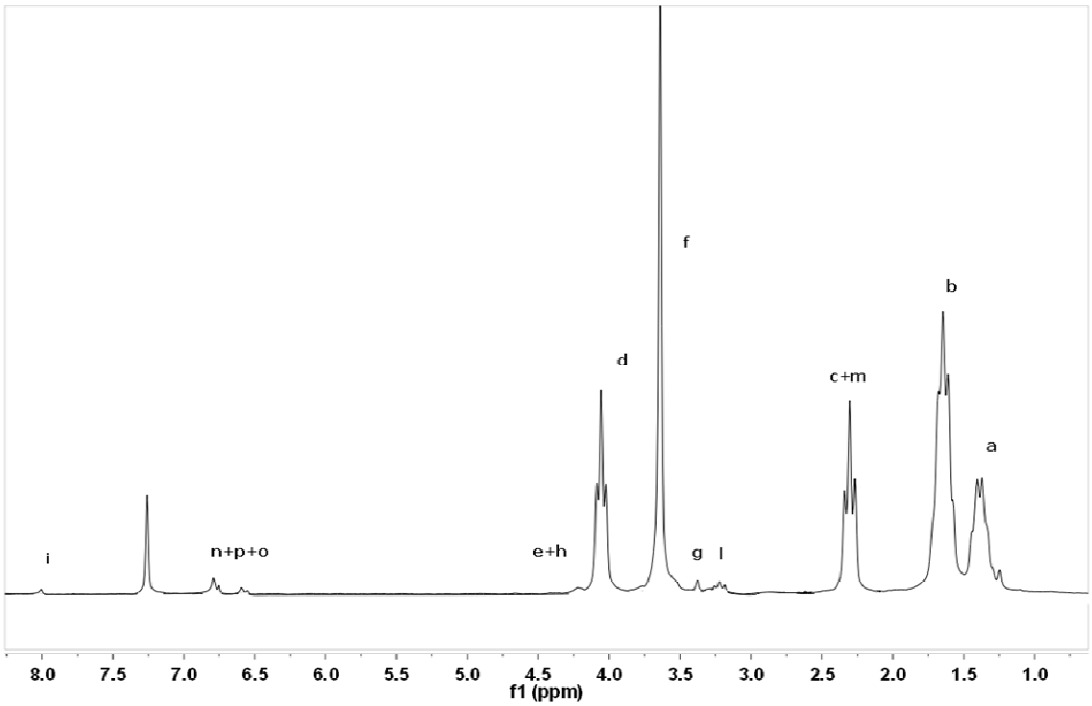

Fig.2.71 ^{1}H-NMR of m-PEO_{2000}- PCL_{4000}-CAT with proton assignment

References

[1]R. Huisgen. 1,3-Dipolar cycloadditions. *Angew. Chem*, 1963. 75:604–637

[2]F. Himo, T. Lovell, R. Hilgraf, V. V. Rostovtsev, L. Noodleman, K. B. Sharpless, and V. V. Fokin. Copper(I)-catalyzed synthesis of azoles. DFT study predicts unprecedented reactivity intermediates. *J. Am. Chem. Soc*., 2005, 127:210–216

[3]V. D. Bock, H. Hiemstra, and J. H.-V. Maarseveen. CuICatalyzedalkyne-azide "click" cycloadditions from a mechanistic and synthetic perspective. *Eur. J. Org. Chem*., 2006:51–68 (2006).

[4]R. Chinchilla, and C. Najera. The sonogashira reaction: a booming methodology in synthetic organic chemistry. *Chem. Rev*. 2007, 107:874–922 .

[5]F. Himo, T. Lovell, R. Hilgraf, V. V. Rostovtsev, L. Noodleman, K. B. Sharpless, and V. V. Fokin. Copper(I)-catalyzed synthesis of azoles. DFT study predicts unprecedented reactivity intermediates. *J. Am. Chem. Soc*. 2005, 127:210–216

[6]V. V. Rostovtsev, L. G. Green, V. V. Fokin, and K. B. Sharpless. A stepwise huisgencycloaddition process: copper(I)-catalyzedregioselective "ligation" of azides and terminal alkynes. *Angew. Chem., Int. Ed. Engl*. 2002, 41:2596–2599

[7]V. O. Rodionov, V. V. Fokin, and M. G. Finn. Mechanism of the ligand-free CuI-catalyzedazide-alkyne cycloaddition reaction. *Angew. Chem., Int. Ed. Engl*. 2005, 44:2210–2215

[8]W. S. Horne, C. D. Stout, and M. R. Ghadiri. A heterocyclicpolymer nanotube. *J. Am. Chem. Soc*. 2003, 125:9372–9376

[9]Z. Li, T. S. Seo, and J. Ju. 1,3-Dipolar cycloaddition of azides with electron-deficient alkynes under mild condition in water. *Tetrahedron Lett*. 2004, 45:3143–3146

[10]S. Chassaing, M. Kumarraja, A. S.-S. Sido, P. Pale, and J. Sommer. Click chemistry in CuI-zeolites: the huisgen [3 + 2]- cycloaddition. *Org. Lett*. 2007, 9:883–886

[11]P. L. Golas, N. V. Tsarevsky, B. S. Sumerlin, and K. Matyjaszewski. Catalyst performance in "click" coupling reactions of polymers prepared by ARTP: ligand and metal effects. *Macromolecules.*2006, 39:6451–6457

[12]W. H. Zhan, H. N. Barnhill, K. Sivakumar, H. Tian, and Q. Wang. Synthesis of hemicyanine dyes for 'click' bioconjugation. *TetrahedronLett*. 2005, 46:1691–1695

[13]H. A. Orgueria, D. Fokas, Y. Isome, P. C.-M. Chane, and C. M. Baldino. Regioselective synthesis of [1,2,3]-triazolescatalyzesby Cu(I) generated in situ from Cu(0) nanosize activated powder and amine hydrochloride salts. *Tetrahedron Lett*. 2005, 46:2911–2914

[14]W. H. Binder, C. Kluger, M. Josipovic, C.J. Straif, *Macromolecules*, 2006, 39, 8092

[15]Adam, G.; Andrieux, J.; Plat, M. *Tetrahedron* 1985,41, 399.

[16]Hassner. A.; Fibiger, R.: Andisik. D. *J. Org. Chem*. 1984, 49, 42337

[17]Loibner. H.: Zbiral. E. *Helu. Chim. Acta* 1976. 59. 2100

[18]Bessodes, M.; Abushanab, E.; Antonakis, K. *Tetrahedron Lett*. 1984, 25, 5899

[19](a) Chretien, F.; Gross, B.; Castro, B. *Synthesis* 1979,937. (b) Chretien. F.: Gross. B. J. *Heterocvcl. Chem*. 1982. 19. 263

[20]R. Ramesh et al., *Tetrahedron* 2007, 63, 9153–9162

[21]Bernhard Neises and Wolfgang Steglich, *Angew. Chem. Int. Ed. Engl*., 1978, 17, 7, p. 522-524

[22]R.M. Gardener, C.M. Buchman, R. Komark, D. Dorschel, C. Boggs and A.W. White, *J. Appl. Polymer Sci*., 1994, 52, 1477.

[23] Kwon G.S., *Crit Rev Ther Drug Carrier Syst*.2003, v. 20, 357.

[24]Rosler A., Vandermeulen G.W., Klok H.A., *Adv Drug Deliv Rev*., 2001, v.53, 95.

[25]R.E. Stratford, L.W. Carson, S.Dodda-Kashi, V.H. Lee, *J. Pharm. Sci*., 77, 883, 1988

[26]Greish K., Fang J., Inutsuka T., Nagamitsu A., Maeda H., *ClinPharmacokinet*., 2003, v. 42,1089.

[27]Soo-Hong Lee, Soo Hyun Kim, Yang-Kyoo Han, Ha Kim, *J. Polym. Chem*., 2002, 40, 2545-2555,

[28]V.P. Torchilin, MicellarNanocarriers: Pharmaceutical Perspective, *Pharmaceutical Research*, January 2007, Vol. 24, No. 1,

[29]J. K. Wegrzyn, T. Stephan, R. Low, R. B. Grubbs *J. Polym. Sci*, 2005, 43 2977.

[30]Duncan, R. and Sat Y.-N. (1998). "Tumour targeting by enhanced permeability and retention (EPR) effect". *Ann. Oncol. 9* (Suppl.2): 39.

[31]S. H. Hobbs et al. 'Regulation of tran sport pathways in tumor vessels: role of tumor type and microenvironment', *Proceedings of the National Academy of Sciences of United States of America* vol. 95, pp. 4607-4612.

[32]Crisci L., Della Volpe C., Maglio G., Nese G., Palumbo R., Rachiero G.P., Vignola M.C., *Macromol. Biosci*., 2003, v.3, 749.

[33]F. Quaglia, L. Ostacolo, G. De Rosa, M. La Rotonda, G. Nese, G.Maglio, R. Palumbo, *International Journal of Pharmaceutics*, 2006, 324, 56-66.

[34] G. Maglio, G. Nese, M. Nuzzo, R. Palumbo, *Macromol. Rapid. Commun*., 2004, 25, 1139-1144

[35]Quaglia F., Vignola M.C., De Rosa G., La Rotonda M.I., Maglio G., Palumbo R. *Journal Of Controlled Release*. vol. 83 pp. 263-71

[36]J. K. Wegrzyn, T. Stephan, R. Low, R. B. Grubbs *J. Polym. Sci*, 2005, 43 2977,.

[37]A. Kowalski, A. Duda, S. Penczek, *Macromol*., 2000, 33, 7359-7370,

[38]Shimada K, Miyagishima A, Sadzuka Y, Nozawa Y, Mochizuki Y, Ohshima H, et al. Determination of the thickness of the fixed aqueous layer around polyethyleneglycol-coated liposomes. *J Drug Target* 1995;3(4):283-9…..

[39]T.K. Endres et al., *Biomaterials* 32 (2011) 7721-7731

[40]Hallahan D., Geng L., et al., *Cancer Cell*, 3, 63-74, 2003

[41]Garnett M.C:, *Adv. Drug Deliv., Rev*.53, 171-216, 2001

[42]Garin-Chesa, P. Campbell, I. Saigo, P.E.Lewis, J.L.Jr.Old, L.J. and Rettig ed. *Am.J.Pathol*. 142, 557-567, 1993.

[43]Esther Amstad , Torben Gillich , Idalia Bilecka , Marcus Textor and Erik Reimhult, *Nano Lett*., 2009, 9 (12), pp 4042–4048

[44]Qi-Ying Jianga, Li-Hua Laic, Jie Shena, Qing-Qing Wang, Fu-Jian Xub, Gu-Ping Tang *Biomaterials* ,Volume 32, Issue 29, October 2011, Pages 7253–7262

[45]Patricia Urbána Joan Estelrichd, Alfred Cortése, Xavier Fernàndez-Busquets, *Journal of Controlled Release* Volume 151, Issue 2, 30 April 2011, Pages 202–211

Chapter 3

Click chemistry stategy applied

in Medium molecular weight range

(from 20000 to 50000 daltons)

3.1 Different block copolymer aggregation

As seen also in the course of Chapter 2, block copolymers (BCPs) show a marked tendency to aggregation both in bulk and in solution because chemical incompatibility between the blocks induces microphase separation (self-assembly) with formation of chemically distinct nanodomains (figure 3.1)

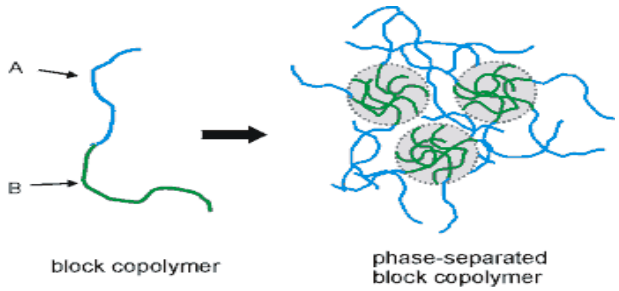

Fig. 3.1: Scheme of self-assembly in AB diblock copolymers.

The broad variety of self-organizing structures of block copolymers is shown in Figure 3.2.

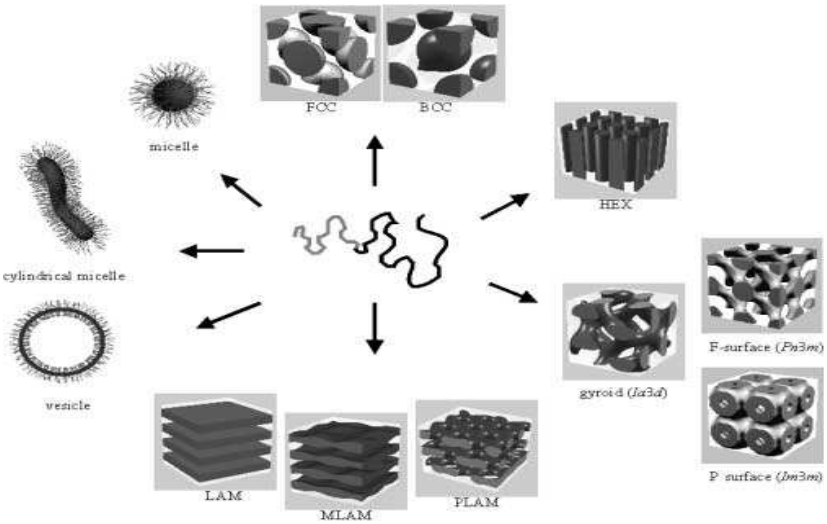

Fig. 3.2: Self-organization structures of block copolymers: spherical micelles, cylindrical micelles, vesicles, fcc- and bcc-packed spheres (FCC, BCC), hexagonally packed cylinders (HEX), various minimal surfaces (gyroid, F surface, P surface), simple lamellae (LAM), as well as modulated and perforated lamellae (MLAM, PLAM).

The morphology of these self-organizing structures can be specifically adjusted through the choice of block lengths and polymer concentration[1]. Thus, it is possible to prepare a large number of tailor-made nanostructured materials.

Micelle formation, as already described, is a simple and well-known example of the self-assembly of polymers. Not only PCL-PEO, but a lot of block copolymers were studied in formation of micelles with defined size and shape in dilute solutions[2,3,4,5,6,7]. As a consequence of the chemical structure of the blocks, BCPs form micelles not only in polar solutions, such as water, but also in very nonpolar media, such as fluorinated hydrocarbons or supercritical CO_2. The well-defined micelles have a core consisting of the insoluble A blocks and a shell or corona of the soluble B blocks (Figure 3.3).

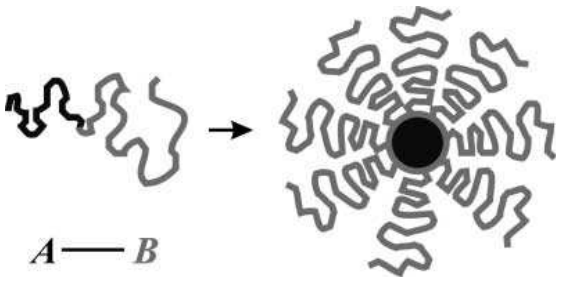

Fig. 3.3: Formation of a micelle of AB block copolymers as the simplest form of self-organization.

The size of the micelle depends on the length of the polymer blocks. Some organization of micelles into a core/shell structure can be well observed in the electron micrograph in Figure 3.4a[8]; the micelles have a total diameter of 30 nm, with the core diameter being 10 nm. Block copolymers with large soluble B blocks form spherical micelles preferably (Fig 3.4a), whereas cylindrical micelles or vesicles result from smaller soluble blocks. Cylindrical micelles, for example, of poly(butadiene-*b*-ethylenoxide (PB-*b*-PEO; Figure 3.4b) may have lengths of several micrometers[9]. Block copolymer vesicles were observed with diameters

from 100 nm up to several micrometers. Polymer vesicles (polymersomes) are mechanically and thermodynamically much more stable[10] than the well investigated lipid vesicles, and, as already discussed, are well suited for the encapsulation and the release of substances. Figure 4c shows vesicles of poly(2-vinylpyridine-*b*-ethylene oxide) (P2VP-*b*-PEO) with diameters of more than 10 µm (giant vesicles).

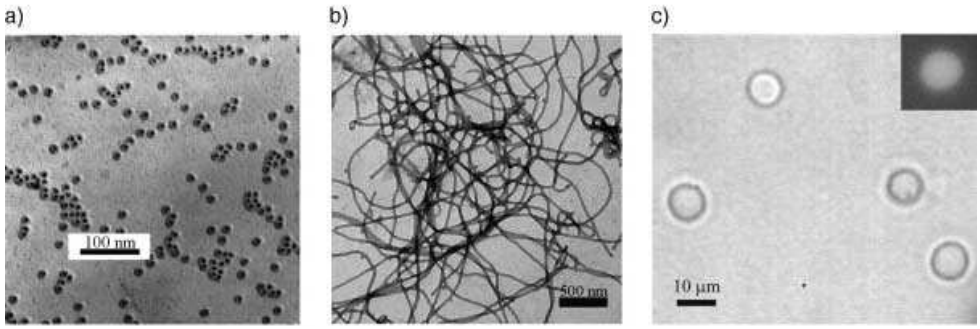

Fig. 3.4: Electron micrographs (a, b) and optical micrographs (c) of the three most frequent forms of self organization of block copolymers: a) spherical micelles (PS-b-PI/DMF) b) cylindrical micelles (PB-b-PEO/water) and c) vesicles (P2VP-b-PEO/water). Figure c shows top right a single vesicle in which the solution of a fluorescent dye was encapsulated.

Block copolymers in a microphase-separated state are also present in bulk and in high concentrations solutions. A variety of copolymer morphologies such as lamellae (LAM), hexagonally ordered cylinders (HEX), arrays of spherical microdomains (BCC, FCC), modulated (MLAM) and perforated layers (PLAM), ordered bicontinuous structures such as the gyroid, as well as the related inverse structures have been documented (see figure 3.2). The stability ranges of the different structures can be represented in a phase diagram as shown in Figure 3.5 for the system poly-(styrene-*b*-isoprene) (PS-*b*-PI)[11],[12]. By using the phase diagrams one can specifically adjust the morphology of these structures through the choice of molecular mass and relative block lengths.

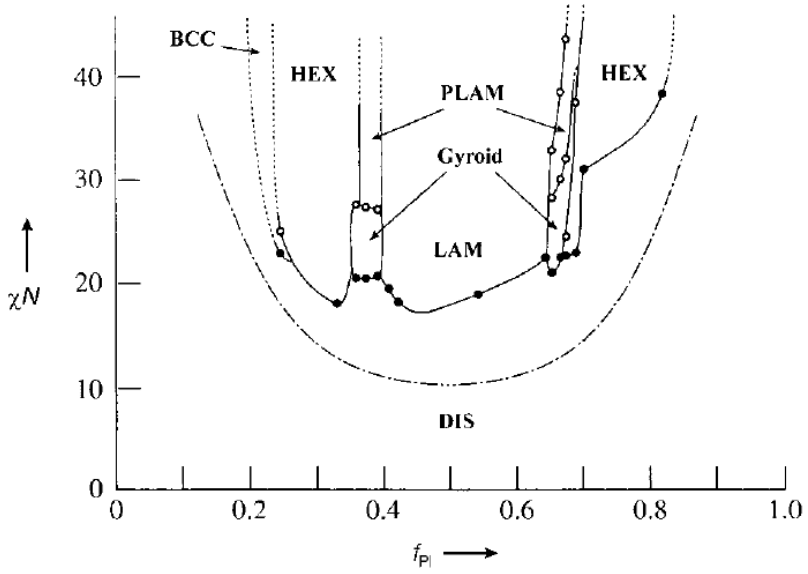

Fig. 3.5. Experimentally determined phase diagram of PS-b-PI. The individual morphologies can be specifically prepared by adjusting the volume ratio fPI of the block copolymers, the total degree of polymerization N, and the temperature (χ ~1/T). χ is the Flory-Huggins interaction parameter and represents the strength of interaction between the blocks. The structures of the individual phases are depicted in Figure 2.

The morphology mainly depends on the relative block length, parameterized as the volume fraction of one of the constituent blocks. For the simplest class of block copolymers, linear AB diblocks, the following structures are known to be stable, as confirmed by theory[13]and experiment[14],[15]: close-packed spherical, hexagonal-packed cylinder, continuous network structures and lamellar. Examples of these nanostructures are shown in Figure 3.6; the typical periodicity is in the range 10-200 nm and, depending on the relative volume fraction of blocks, different morphologies can be obtained. If, for example, there is one minority block with a volume fraction of 21-33% a cylindrical morphology is obtained. If the blocks are of very similar length (volume fraction 37-50%) lamellar structures are formed.

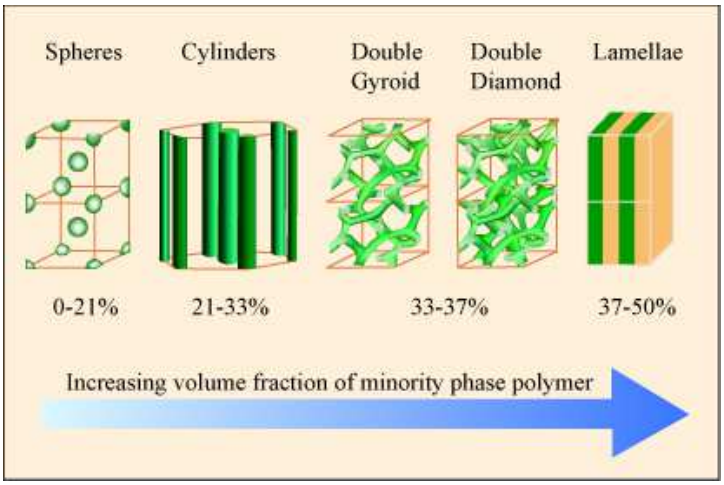

Fig. 3.6: Nanostructures formed by self-assembly in di-block copolymers. The minority component is segregated in spheres, cylinders, continuous network or lamellae, depending on the relative volume fraction.

The block copolymers ability to form a rich variety of nanoscale periodic patterns offers the potential to fabricate materials that have utility in a wide variety of applications. The majority of applications proposed to date rely on the use of BCPs thin film. In thin films, in addition to composition and molecular weight, the domain structure is also dependent on the surface energies of the blocks and on geometrical constraints introduced by confinement in a thin film[16]. Block copolymer films are usually prepared by the spin-coating technique, where drops of a solution of the polymer in a volatile organic solvent are deposited on a spinning solid substrate. The polymer film spreads by centrifugal forces, and the volatile solvent is rapidly driven off. With care, the method can give films with a low surface roughness over areas of square millimetres. The film thickness can be controlled through spin speed, concentration of the block copolymer solution or the volatility of the solvent, which also influences the surface roughness[17]. In figure 3.7 are reported examples of phase separated BCPs thin films prepared by spin-coating[18],[19].

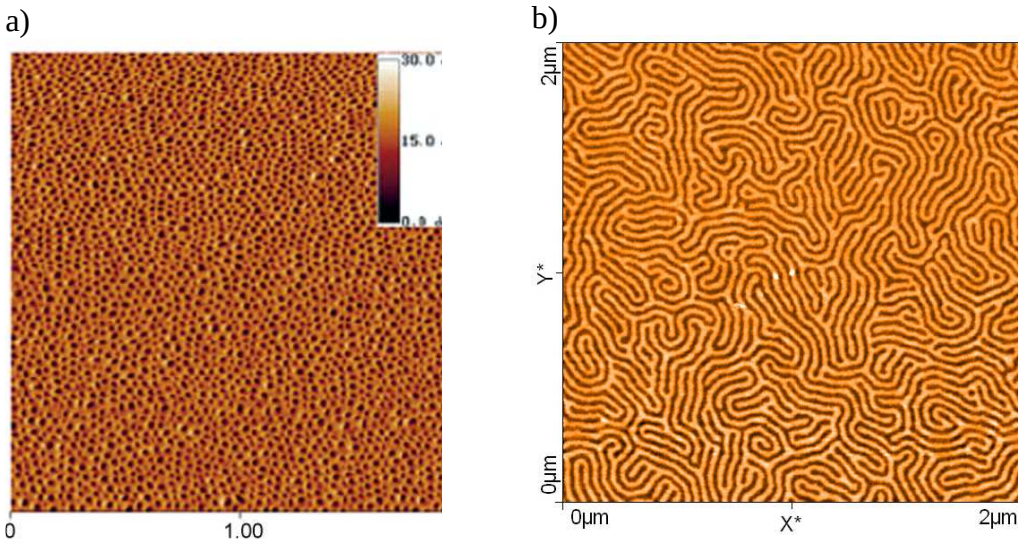

Fig. 3.7: AFM phase contrast images of a cylinder (a) and a lamellar forming (b) block copolymer thin films. The cylinder forming BCP is a PS-b-PEO (PEO cylinders); the lamellar forming BCP is a PS-b-PMMA. Two distinct phases can be identified on the samples surfaces corresponding to the two phase separated blocks of the copolymer.

During the last decade more and more advanced techniques of "living" or controlled polymerization, such as ROP in the case of ε-CL, to prepare block copolymers have become available. The different synthetic routes to block copolymers comprise living anionic, living cationic, and living radical polymerization. Combining different polymerization techniques provides a larger variety of block copolymers[20]. It has become possible to prepare block copolymers of various architectures, solubility, and functionality[21]. The solubilities vary from polar solvents such as water to media with very low cohesion energies such as silicon oil or fluorinated solvents. Control of BCPs functionality has become important, motivated by the necessity to stabilize metallic, semiconductor, ceramic, or biological systems; so block copolymers can be further modified by subsequent chemical reaction. The two most important demands on a BCP functionalization reaction are to maintain the block copolymer architecture and to achieve a selective reaction, which should be as complete as possible. To reach the first goal, the reaction conditions must be such that the chains will neither be degraded nor cross-

linked. To reach the second goal, reactive and selective reagents are necessary to allow the reaction to be determined by their molar ratio. This is important because, as remembered in Introduction chapter, polymers are often hard to purify after such reactions. A number of polymer-analogue reactions have so far been carried out with block copolymers. These comprise hydrogenation [22],[23],[24],[25], epoxidation with subsequent ring opening by nucleophiles and acid chlorides[26], hydroboration/oxidation with subsequent esterification of the OH group[27,28], quaternization[29], hydrolysis of tert-butylmethacrylates[30], sulfonation[31], fluorocarbene addition[32] and the reaction of olefinic double bonds with N-chlorosulfonyl isocyanate for the preparation of blood-compatible heparin analogues[33]. By means of functionalization reactions the polymer blocks can be transformed into blocks of desired solubility, flexibility, and chemical functionality. A chemical functionalization of one block can be used to selectively introduce inorganic, organic, and biological molecules into BCPs. In particular, if the chemical functionalization does not destroy the BCP ability to generate nanostructures by self-assembly, functional nanomaterials very useful in biomaterial science can be obtained. Most important potential application can be found in material for protein and nucleic acid adsorption and biosensors realization. So precise control over the functionalities is a fundamental prerequisite to obtain useful BCPs based nanomaterials that exhibit unparalleled versatility.

3.2 Biodegradable random copolymer in drug controlled release: PLA and PLGA

The possibility of developing new pharmaceutical forms based on biocompatible polymers, able to protect and release the active ingredient in prolonged times, has dramatically increased the interest in biodegradable particles such carriers for therapeutic peptides and proteins[34],[35],[36]. Among the more biodegradable materials used in the preparation of Controlled Release System

(CRS) for proteins and peptides, the polyesters based on lactic acid (PLA) and their copolymers with glycolic acid (PLGA) (figure 3.8) play a central role in virtue of their proved biocompatibility and use safety[37],[38]. Food and Drug Administration (FDA) approved these polymers for clinical applications in humans, whose main advantage is related to their complete biodegradation in vivo. The bioerosion, in fact, causes the polymer backbone demolition by chemical means, with water-soluble derivatives formation of low molecular weight engaged in normal metabolic organism pathways, in particular the Krebs cycle.

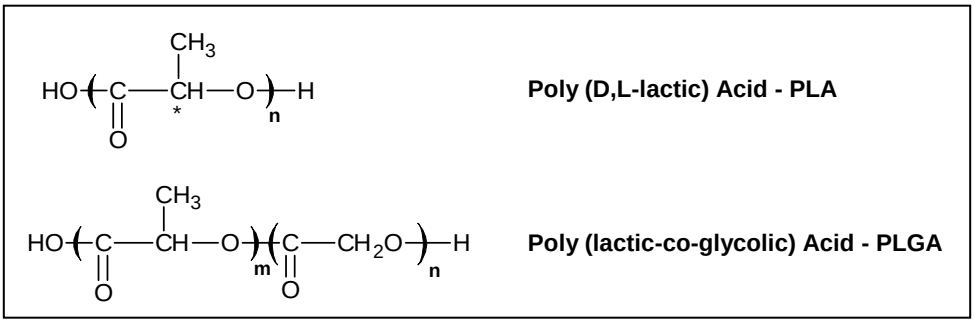

Fig. 3.8 PLA and PLGA chemical structure

Among the biodegradable polymers, therefore, PLGAs, have been the subject of numerous studies due to their high versatility of use. The vehiculated drug rate of release, in fact, can be easily modulated by varying the composition of the polymer (ie ratio lactic acid/glycolic acid), molecular weight and chemical structure (ie carboxy-terminal capped or uncapped), with particular reference to biodegradation and hydrolysis rate[39]. The physico-chemical properties of the polymer, as the molecular weight and the polydispersity index, influence polymer stability and the potential use in CRS formulation[40]. The PLA presents more pronounced hydrophobicity compared to PLGA, and a progressive increase of the hydrophilic component (ie, a reduction ratio of lactic/glycolic) determines a most attractive of water and a reduction in the degradation times[41]. For this reason,

PLGAs characterized by *in vivo* degradation time from three weeks to reach a maximum of one year, are currently commercially available.

The importance of PLA and PLGA copolymers is greatly increased as a result of their use as building block for particle systems in drug delivery. The advantages of use of particle systems already discussed in Introduction chapter include, in fact, the possibility to administer the drug directly to the site of action where the system forms a deposit from which the active ingredient can be released and act for a prolonged period of time [42],[43].

PLGA particle systems can be classified into two main categories which differ in size: nanoparticle and microparticle systems. Usually, has been defined microparticulate systems, particles with dimensions between 1 and 1000 μm, even if size of the most interesting microparticles are generally in the range 1-200 μm. The bioactive molecule encapsulated in a microparticulate system can be located in cavities within the system (ie, microcapsules), or finely dispersed in the polymer matrix (eg microspheres), depending on the technique of production and/or the starting formulation (Figure 3.9) .

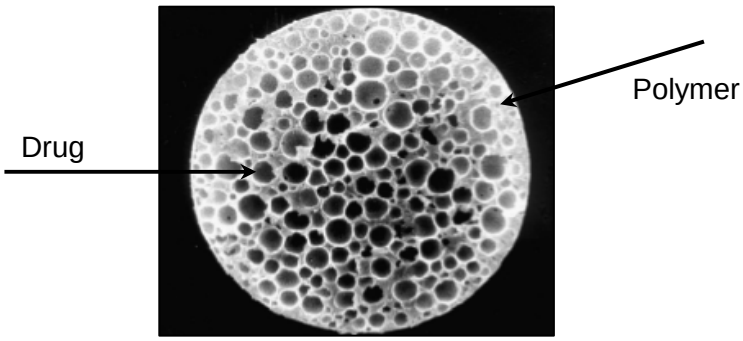

Fig 3.9 Biodegradable drug loaded microsphere

The active principle release from biodegradable polymers microspheres is primarily regulated by the diffusion of the encapsulated active ingredient through the polymer matrix and the biodegradation of the polymer[44]. In the mechanism

coupled diffusion-erosion an important role is played the activity of water in the environment of release. Microsphere, in contact with the aqueous environment, is hydrated (hydration phase) and penetrating water solubilizes the drug, which begins to spread through the PLGA micropores with dimensions comprised between angstroms or nanometers, and through the macroporous structure of the particles, which is a consequence of the preparation process (ie, multiple emulsion technique). Employing different preparation techniques, the PLGA can also be used for nanometric systems production, characterized by different properties compared to microparticles[45]. Nanoparticles generally have dimensions between 10 and 1000 nm. Depending on preparation technique used, it is possible to obtain nanoparticle systems with different structures (ie; nanocapsules, nanospheres, nanoparticles). In particular, nanocapsules are characterized by an inner core consisting of the drug surrounded by a polymer layer, while has been defined nanoparticles and nanospheres systems matrix in which the drug is more or less finely dispersed (Figure 3.10).

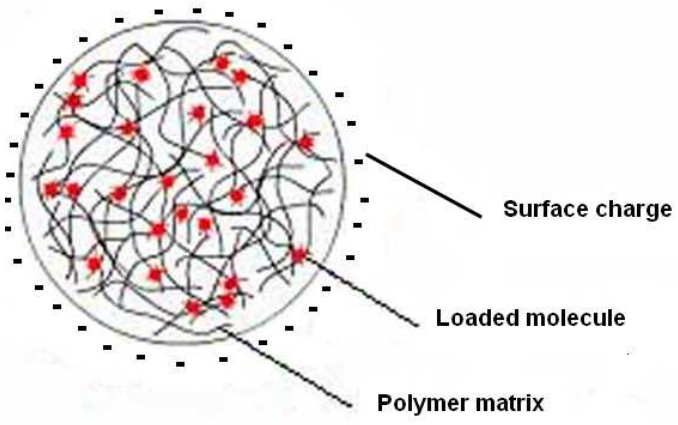

Fig. 3.10 Biodegradable nanoparticle typical structure

As described above for the microparticles, also the rate of release of polymeric nanoparticles encapsulated drug depends on two fundamental processes: diffusion through the polymer matrix and its bioerosion.[4647]

A considerable interest parameter in nanoparticles characterization is the surface charge, deductible by Z-potential measure. In the case of PLGA polymeric

nanoparticles surface charge will be negative due to presence of the acid carboxylic groups. A huge non neutral value surface charge causes strong interactions with biological fluids components, in particular plasma proteins. Such molecules adsorbed on the nano particles surface can, by interacting with cellular proteins, promote phagocytosis by cells such as macrophages, phenomenon well note as opsonization[48]. On the other hand it is possible to apply changes to the particle surface such as to minimize the phagocytosis by cells or, on the contrary, direct the carrier action targeted to a particular cellular species[49].

Taking in account their many advantages systems based on PLGA, both micro and nanoparticles, have been widely used for development of carriers for unstable macromolecules, especially proteins and peptides. In particular, PLGA microspheres for proteic molecules controlled release are now a reality in pharmaceutical market (eg Lupron Depot ®, Nutropin Depot ®, Sandostatin LAR ®). On the other hand, PLGA nanoparticles for peptides and proteins delivery have been the subject of numerous studies, because of their ability to overcome organism physical barriers, as demonstrated in studies about mucosal, oral and nasal vaccination[50];[51]. These studies suggest the possibility of encapsulating peptides and proteins in nanoparticle systems without compromising the structural integrity, which is closely related to biological activity of these macromolecules. In addition, the nanometer size of the nanoparticles can represent a fundamental parameter for the delivery of drugs within cells[52];[53], or in gene therapy[54]. Several techniques are developed to monitor nanocarrier track *in vitro* and *in vivo*. A widely used approach, already seen in chapter 2, concerns nanocarrriers labelling with fluorescent probe such as rhodamine B encapsulated together with bioactive molecule. Main drawback found, using this approach, is related to rhodamine diffusion during nanovector route.

3.3 Section aim

In this section of research work the synthetic strategy developed has been adapted in PS-*b*-PEO block copolymers and PLGA random copolymer functionalization. Both copolymer are characterized by Mn higher than 40000 Dalton with only two terminal group for macromolecular chain. These features increase synthesis difficult in terms of a complete grade of reaction and in characterization of final product. Moreover it is of paramount importance that reaction pathway does not negatively influence self assembly copolymer features. In PS-*b*-PEO case was set a method to functionalize PEO ends with an azide terminal group, in order to prepare BCPs to be used as substrates in coupling reactions with different molecules and/or polymers containing a CC triple bond, exploiting the potential of azide-alkine Huisgen cycloaddition reactions. Indeed, such kind of reactions can turn out useful in a large variety of nano-technological pharmaceutical applications as for instance in coupling reactions with a different polymer to prepare tri-block copolymers or a different BCP for drug controlled release, or even with bioactive proteins and nucleic acids. As concern PLGA case was set a method to change hydroxyl terminal into azide and by this link rhodamine-alkyne molecule through 1-3 Huisgen cycloaddition. PLGA-rhodamine was used in microparticles preparation and was investigated their morphology by confocal microscopy. Triazole bond fixes fluorescent probe onto nanocarriers and avoid diffusion problem, allowing a more accurate route monitoring. It is possible, in fact, administer microparticulete preparation to the test animal and follow fluorescence.

3.4 Polystyrene-PEO block copolymer functionalization

Diblock copolymer chosen for functionalization is a commercial sample. Molecular characterization carried out by SEC evidenced a Mn for polystyrene

block of 22.0 kDa and 21.5 kDa for PEO, a Polydispersity index of 1.09. chemical structure was illustrated in figure 3.11

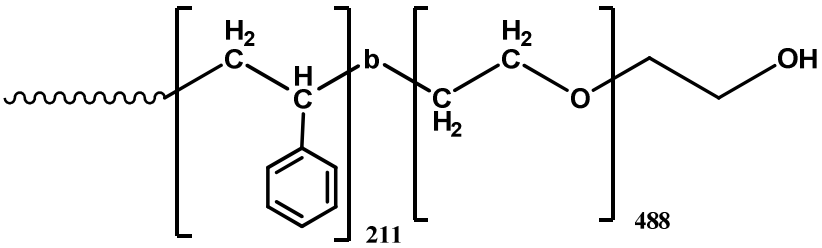

Fig. 3.11 Commercial Polystyrene-b-PEO-OH chemical structure

^{1}H-NMR analysis does not evidences PEO terminal because chemical shift is the same of macromolecular backbone as illustrated in figure 3.12

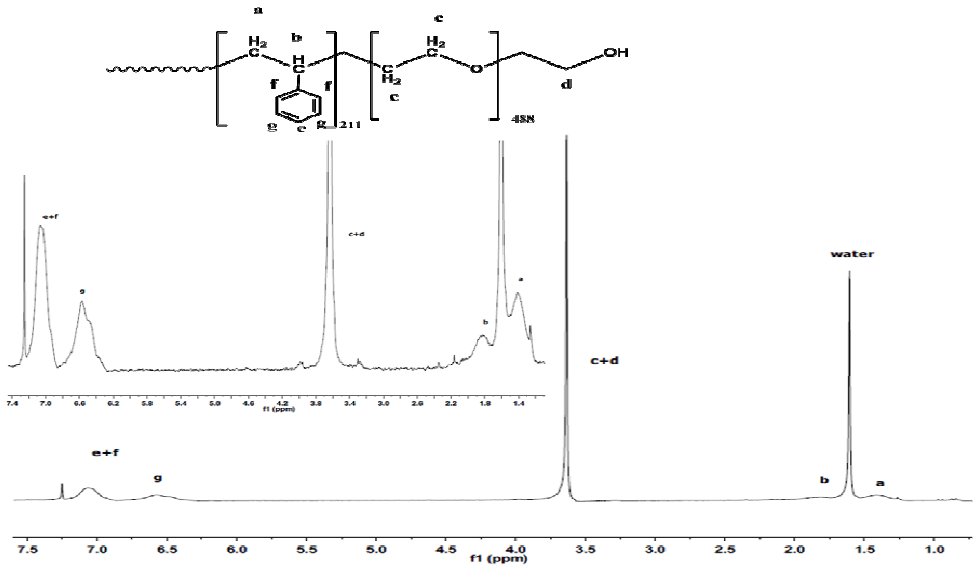

Fig. 3.12 ^{1}H-NMR of commercial PS-b-PEO-OH with proton assignment

To point out terminal α-hydroxyl methylene, (d) in figure 3.12, copolymer was reacted with trifluoroacetic anhydride directly in NMR tube. In particular, trifluoroacetic anhydride (TFAA) is the perfluorinated derivative of acetic anhydride. Like many acid anhydrides, it may be used to introduce the

corresponding trifluoroacetyl group. The corresponding trifluoroacetyl chloride, is a gas, making it inconvenient to work with. Therefore reaction between copolymer and TFAA (figure 3.13) gives as result trifluoroacetic ester, changing chemical shift of terminal methylene from 3.6 to 5.20 (figure 3.14)

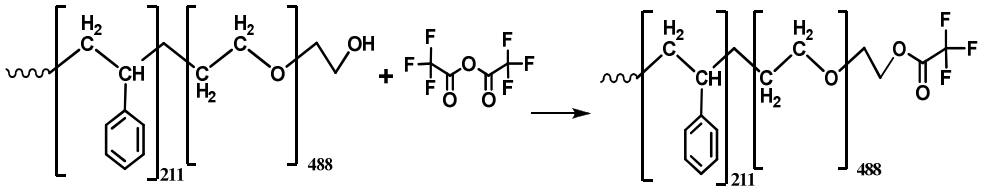

Fig. 3.13 PS-b-PEO-OH reaction with trifluoroacetic anhydride in NMR tube

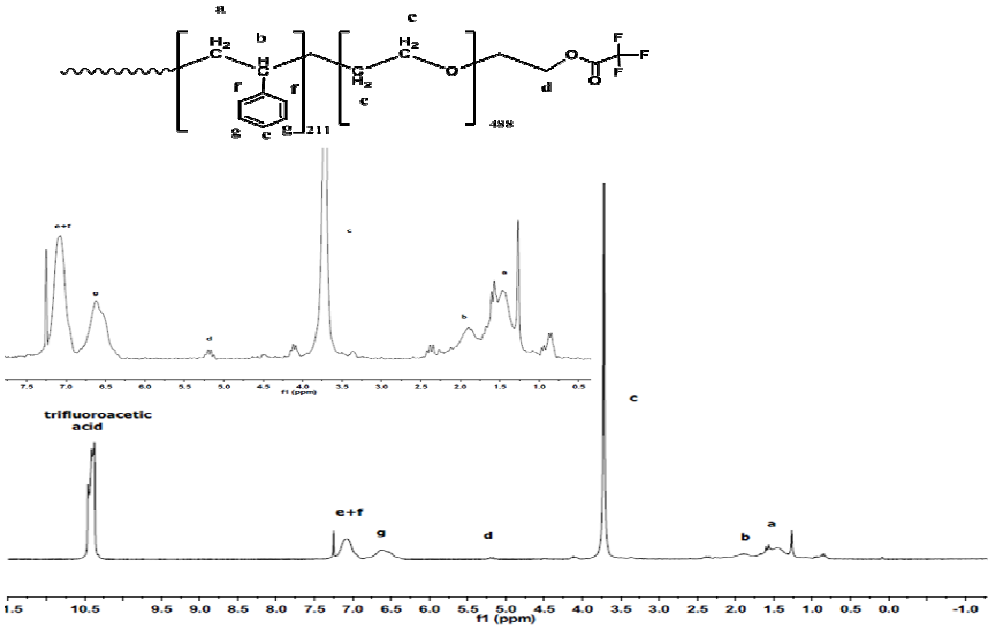

Fig. 3.14 ^{1}H-NMR PS-b-PEO-TFFA with proton assignment

Reaction was carried out in large TFAA molar excess: 200 µL (1.4 mmol) was added in 700 µL of 1 mg/100µL copolymer in $CDCl_3$solution to ensure terminal complete conversion. Once characterized starting material, it was possible

to proceed with hydroxyl activation by mesyl chloride. This compound is subject of inactivation in water presence. For this reason PS-b-PEO-OH diblock copolymer was dried at 50°C under vacuum and P_2O_5 overnight. After water purification copolymer was reacted with a large mesyl chloride molar excess as illustrated in figure 3.15

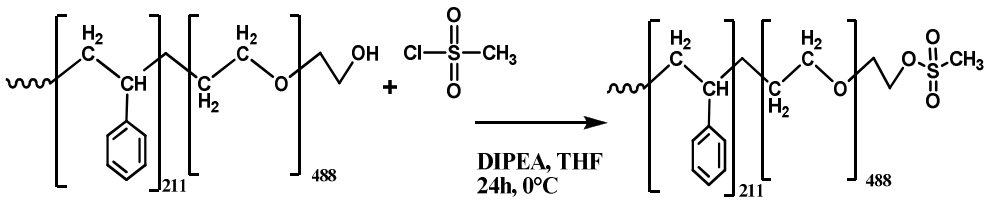

Fig.3.15 PS-b-PEO-OH hydroxyl activation by mesyl chloride

Unreacted mesyl chloride was removed from PS-b-PEO-mesyl thanks to precipitation in diethyl ether methanol 1/1 v/v solution and subsequent washing with methanol. ^{1}H-NMR analysis was used to confirm product chemical structure, comparing integrations values of the signals related to the PEO protons O-CH_2-CH_2 (c) (δ = 3.60) and terminal CH_3-OSO-CH_2 (d) (δ = 3.00) (figure 3.16) was evaluated that PS-b-PEO-OH conversion grade is, within the limits of experimental error, higher than 95%. An evidence of complete conversion was non appearance of trifluoroacetate ester-methylene after addition of 200 µL of TFAA in NMR tube containing PS-b-PEO-mesyl dissolved in $CDCl_3$ (700µL 1mg/100µL). In fact, can be noted in figure 3.16, the strong signal due to trifluoroacetic acid at 10.0 ppm while there are no signal in the zone between 4.0 and 5.0, so there are no residual hydroxyl terminal group able to react with TFAA.

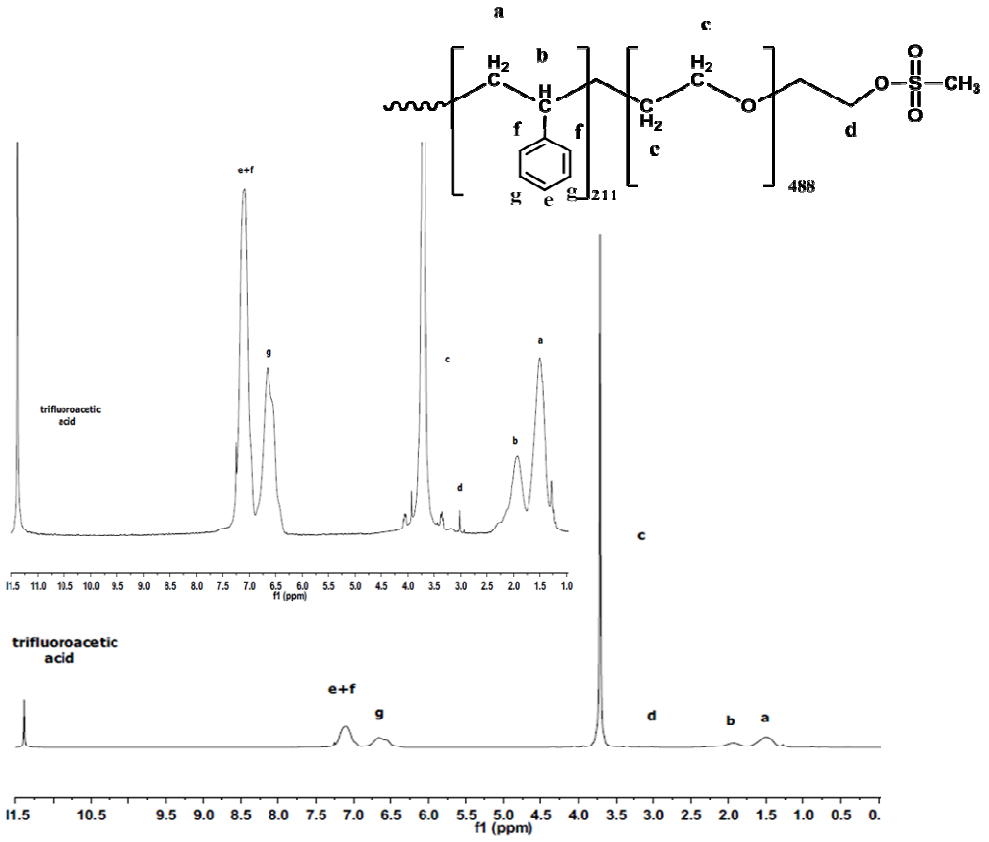

Fig. 3.16 [1]H-NMR PS-b-PEO-mesyl after TFAA addition with proton assignment

Verified conversion grade for hydroxyl activation step, it was possible to achieve nuclueophilic substitution with sodium azide. This reaction was carried out as usual in large NaN_3 molar excess. Both copolymer and sodium azide were dissolved in a mixture of DMF and water (20/1 v/v) and stirred under reflux at 80°C. Water helps partial sodium azide dissolution, forcing thermodynamic equilibrium to substitution. After 24 hours reaction mixture, become darker, was dried, redissolved in $CHCl_3$ filtered from insoluble sodium azide excess and precipitated in diethyl ether methanol mixture 1/1 v/v to purify desired product from eventual byproduct. ^{1}H-NMR analysis was used to confirm product chemical structure, PS-b-PEO-N_3 comparing integrations values of the signals related to the PEO protons O-CH_2-CH_2 (c) (δ = 3.60) and terminal CH_2-N_3 (d) (δ = 3.57) (figure

3.17) was evaluated that PS-b-PEO-mesyl conversion grade is, within the limits of experimental error, higher than 95%.

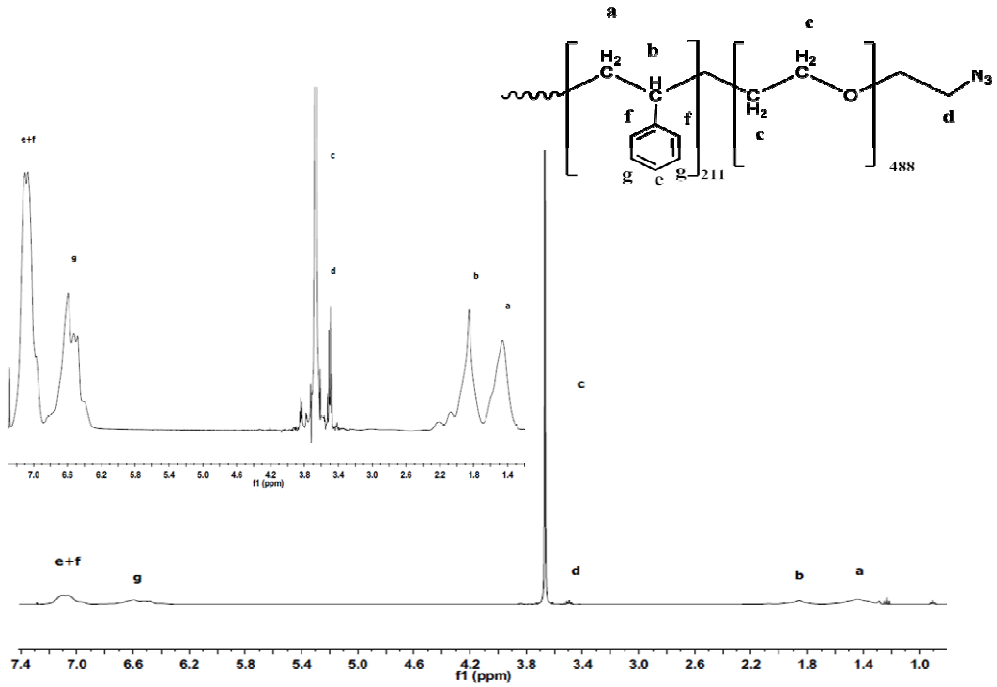

Fig. 3.16 ^{1}H-NMR PS-b-PEO-N_3 with proton assignment

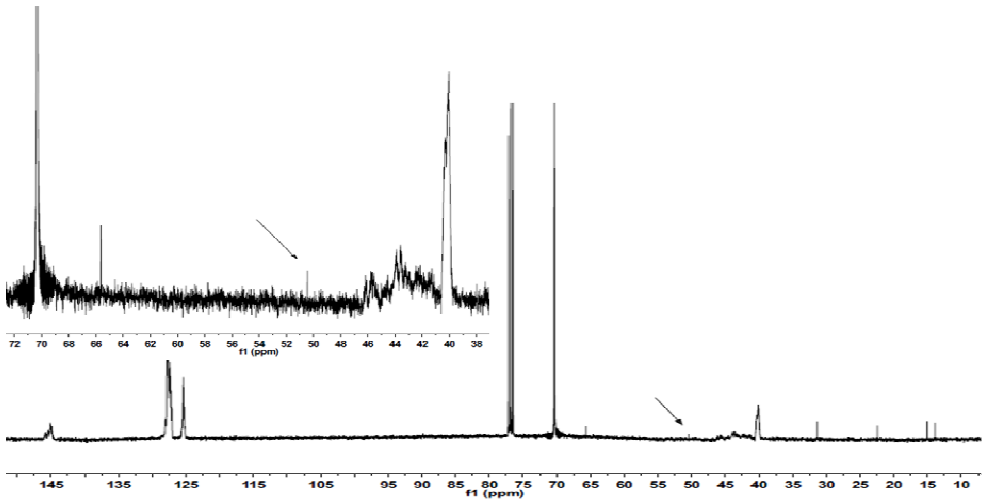

Fig. 3.17 ^{13}C-NMR PS-b-PEO-N_3 arrow indicates $\underline{C}H_2$-N_3 at 50 ppm

To further confirm chemical structure was registered also ^{13}C-NMR;can be noted, in fact, in figure3.17 α-azide terminal carbon at 50 ppm

3.4 PLGA-Rhodamine B labeled random copolymer microparticles

3.4.1 Synthesis of PLGA-Rhodamine labeled

PLGA or poly(lactic-co-glycolic acid) is a copolymer which is used in a host of Food and Drug Administration (FDA) approved therapeutic devices, owing to its biodegradability and biocompatibility; is synthesized by means of random ring-opening co-polymerization of two different monomers, the cyclic dimers (1,4-dioxane-2,5-diones) of glycolic acid and lactic acid (figure 3.18). Common catalysts used in the preparation of this polymer include tin(II) 2-ethylhexanoate, tin(II) alkoxides, or aluminum isopropoxide. During polymerization, such as PCL "living" reaction, successive monomeric units (of glycolic or lactic acid) are linked together in PLGA by ester linkages, thus yielding a linear, aliphatic polyester as a product.

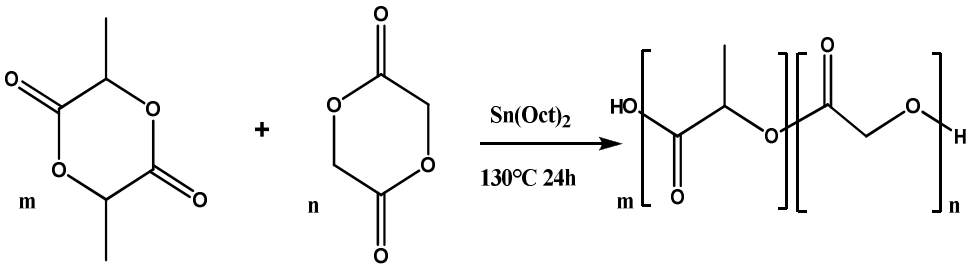

Fig. 3.18 Random ROP copolymerization of lactide and glycolide

Depending on the ratio of lactide to glycolide used for the polymerization, different forms of PLGA can be obtained: these are usually identified in regard to the monomers' ratio used (e.g. PLGA 75:25 identifies a copolymer whose

composition is 75% lactic acid and 25% glycolic acid). All PLGAs are amorphous rather than crystalline and show a glass transition temperature in the range of 40-60 °C. Unlike the homopolymers of lactic acid (polylactide) and glycolic acid (polyglycolide) which show poor solubilities, PLGA can be dissolved by a wide range of common solvents, including chlorinated solvents, tetrahydrofuran, acetone or ethyl acetate. PLGA degrades by hydrolysis of its ester linkages in the presence of water. It has been shown that the time required for degradation of PLGA is related to the monomers' ratio used in production: the higher the content of glycolide units, the lower the time required for degradation. An exception to this rule is the copolymer with 50:50 monomers' ratio which exhibits the faster degradation (about two months).PLGA has been successful as a biodegradable polymer because it undergoes hydrolysis in the body to produce the original monomers, lactic acid and glycolic acid. These two monomers under normal physiological conditions, are by-products of various metabolic pathways in the body. Since the body effectively deals with the two monomers, there is minimal systemic toxicity associated with using PLGA for drug delivery or biomaterial applications. As described above, the possibility to tailor the polymer degradation time by altering the ratio of the monomers used during synthesis has made PLGA a common choice in the production of a variety of biomedical devices such as: grafts, sutures, implants, prosthetic devices, micro and nanoparticles. Copolymer chosen for synthesis is a α-hydroxyl-ω-carboxyl-50:50 $PLGA_{30000}$ (c-$PLGA_{30000}$-OH) commercial available with Mn of 30 kDA and Mw of 50 kDa illustrated in figure 3.19

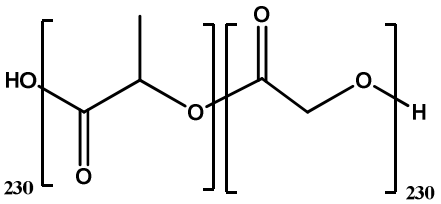

Fig. 3.19 α-hydroxyl-ω-carboxyl-50:50$PLGA_{30000}$

The most suitable part for copolymer functionalization is the hydroxyl terminal which can be changed into azide group by two-step protocol already described. Therefore c-PLGA$_{30000}$-OH was characterized by ^{1}H-NMR analysis to point out terminal signal. As illustrated in figure 3.20, α-hydroxyl methylene (d) is quite visible at 4.31 ppm and is possible adopt this signal as diagnostic standard for further reaction. Thus c-PLGA$_{30000}$-OH was reacted with mesyl chloride to activate hydroxyl group as illustrated in fig. 3.21

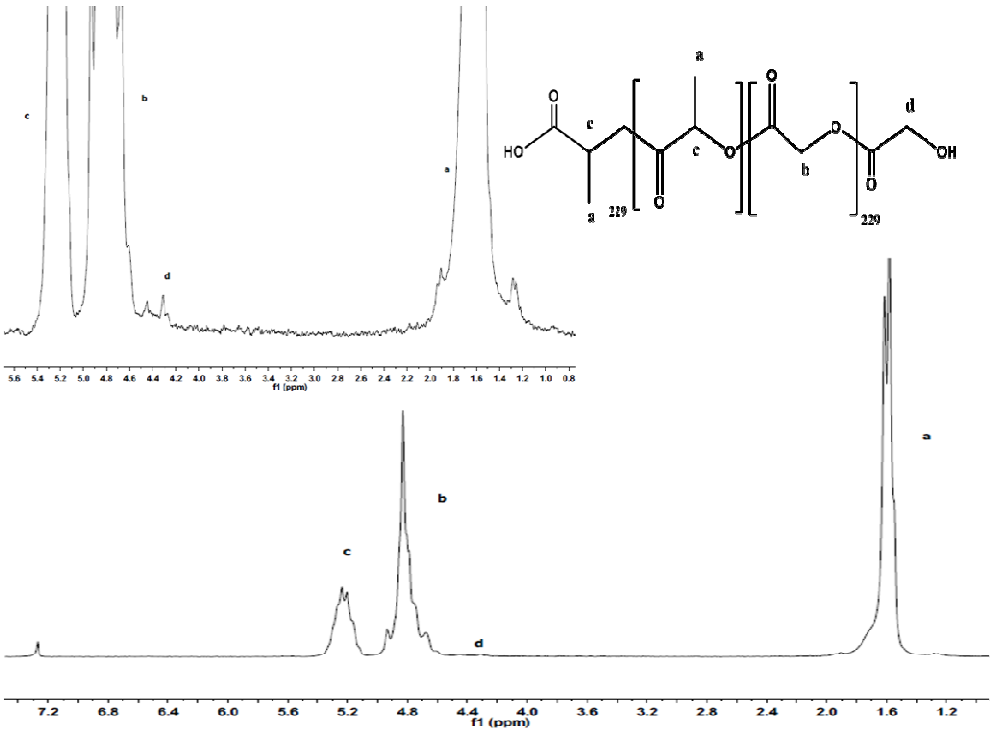

Fig.3.20 ^{1}H-NMR of α-hydroxyl-ω-carboxyl-50:50 PLGA$_{30000}$ (c-PLGA$_{30000}$-OH) with proton assignment

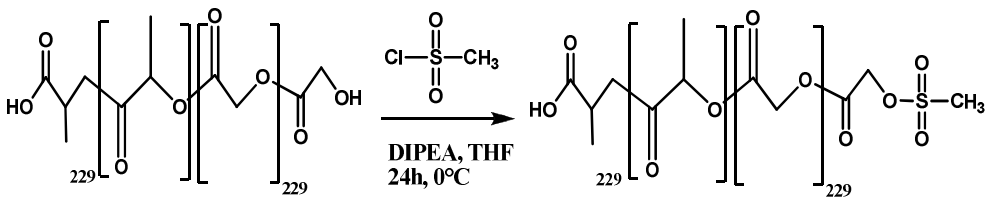

Fig.3.21 c-PLGA$_{30000}$-OH hydroxyl activation with mesyl chloride

After 24 hours reaction mixture was simply concentrated and precipitated in diethyl ether methanol solution 1/1 v/v obtaining a sponge like solid. ^{1}H-NMR analysis was used to confirm product chemical structure, c-PLGA$_{30000}$-mesyl, comparing integrations values of the signals related to the protons CH_3-CH- (a) (δ = 1.60) and terminal CH_3-OSO (e) (δ = 3.21) (figure 3.22) was evaluated that c-PLGA$_{30000}$-OH conversion grade is, within the limits of experimental error, higher than 95%. Other evidence of quantitative reaction is total disappearance of signal at 4.31 ppm related to α-hydroxyl methylene

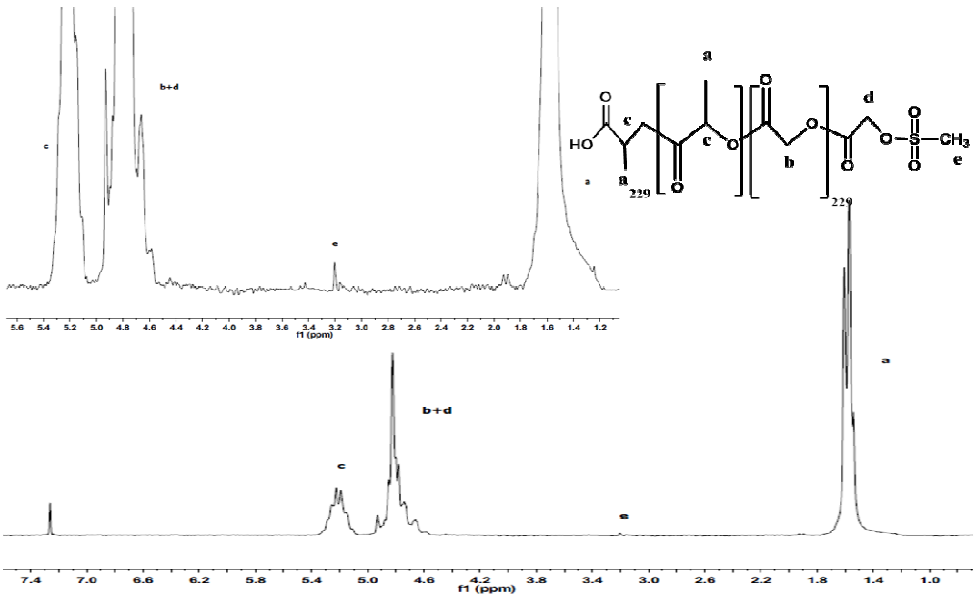

Fig.3.22 ^{1}H-NMR of c-PLGA$_{30000}$-mesyl with proton assignment

Nucleophilic substitution with sodium azide was carried out in DMF and water solution (20/1 v/v) as described above, but temperature was set at 38°C. PLGA, in fact, is amorphous copolymer and temperature of glass transition is within 40-60°C. Once it reaches that temperature, presence of water induces a rapid hydrolysis completely and irreversibly degrading polyesteric chain. Thus temperature must be high enough to help sodium azide dissolution, but must not exceed the Tg. Reaction mixture was dried, redissolved in $CHCl_3$ and precipitated in diethyl ether methanol solution 1/1 v/v obtaining a sponge like solid. ^{1}H-NMR analysis was used to confirm product chemical structure, c-$PLGA_{30000}$-N_3, comparing integrations values of the signals related to the protons CH_3-CH- (a) (δ = 1.60) and terminal CH_2-N_3 (d) (δ = 4.30) (figure 3.23) was evaluated that c-$PLGA_{30000}$-mesyl conversion grade is, within the limits of experimental error, higher than 95%. Other evidence of quantitative reaction is total disappearance of signal at 3.21 ppm related to mesyl

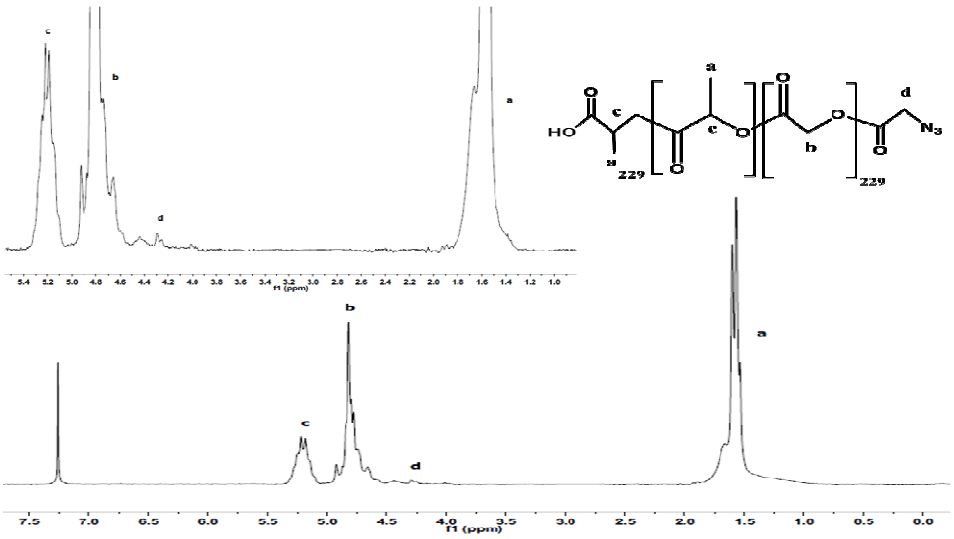

Fig.3.23 ^{1}H-NMR of c-$PLGA_{30000}$-N_3 with proton assignment

Also FTIR analysis shows clearly diagnostic stretching signal of azide at 2100 cm^{-1} (Figure 3.24).

Rhodamine B, already treated in chapter 2, was reacted with 3-Butynol in presence of DCC and DMAP to give alkyne ester useful for Huysgen cycloaddition together with c-PLGA$_{30000}$-N$_3$ as illustrated in figure 3.25

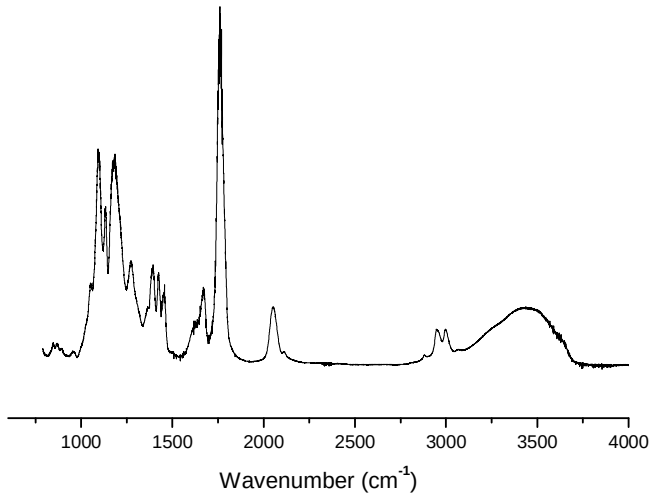

Fig.3.24 FTIR spectrum of c-PLGA$_{30000}$-N$_3$, can be noted characteristic azide stretching at 2100 cm^{-1}

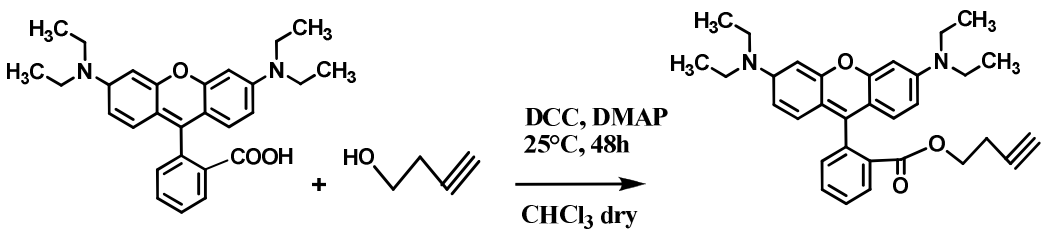

3.25 reaction between Rhodamine B and 3-Butynol to give Rhodamone-alkyne

After 48 hours reaction mixture was filtered from dicyclohexylurea, concentrated and purified by silica gel chromatography with $CHCl_3$/Methanol 9/1 v/v as eluent. ^{1}H-NMR analysis was used to confirm product chemical structure, Rhodamine-alkyne, comparing integrations values of the signals related to the protons CH_3-CH- (a) (δ = 1.60) and terminal CH_2-N_3 (d) (δ = 4.30) (figure 3.23)

was evaluated that c-PLGA$_{30000}$-mesyl conversion grade is, within the limits of experimental error, higher than 95%

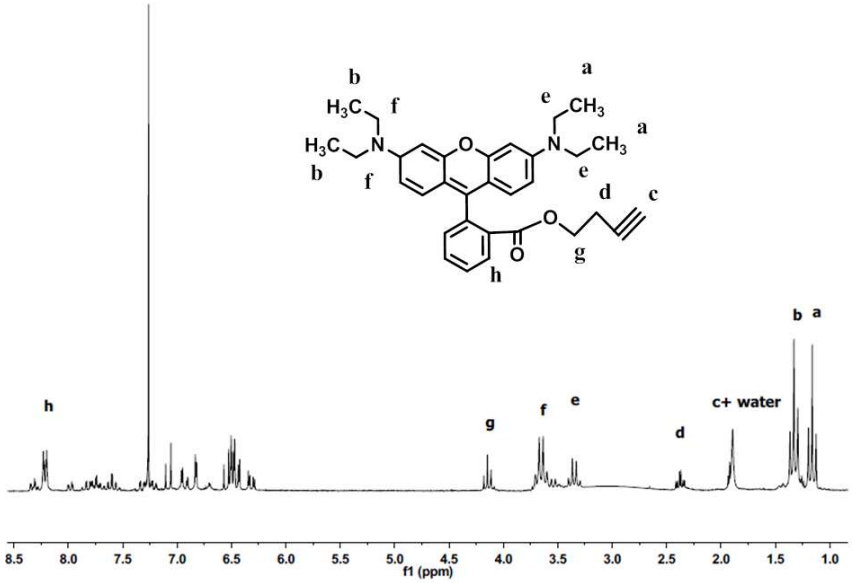

Fig.3.26 ^{1}H-NMR of Rhodamine-alkyne with proton assignment

Huysgen cycloaddition between Rhodamine-alkyne and c-PLGA$_{30000}$-N_3 was illustrated in figure 3.27. This reaction was carried out in 30% Rhodamine-alkyne molar excess. After 48 hours reaction mixture was concentrated, purified by Cu(I) catalyst by neutral alumina column and precipitated in diethyl ether methanol solution 1/1 v/v according to developed protocol. FTIR confirm quantitative coupling; can be noted, in fact, complete disappearance of diagnostic stretching signal of azide at 2100 cm^{-1} (Figure 3.28). ^{1}H-NMR analysis was used to confirm product chemical structure, c-PLGA$_{30000}$-Rhodamine, comparing integrations values of the signals related to the protons CH_3-CH- (a) (δ = 1.60) and terminal CH_2-N_3 (d) (δ = 4.30) (figure 3.23) was evaluated that c-PLGA$_{30000}$-mesyl conversion grade is, within the limits of experimental error, higher than 95%

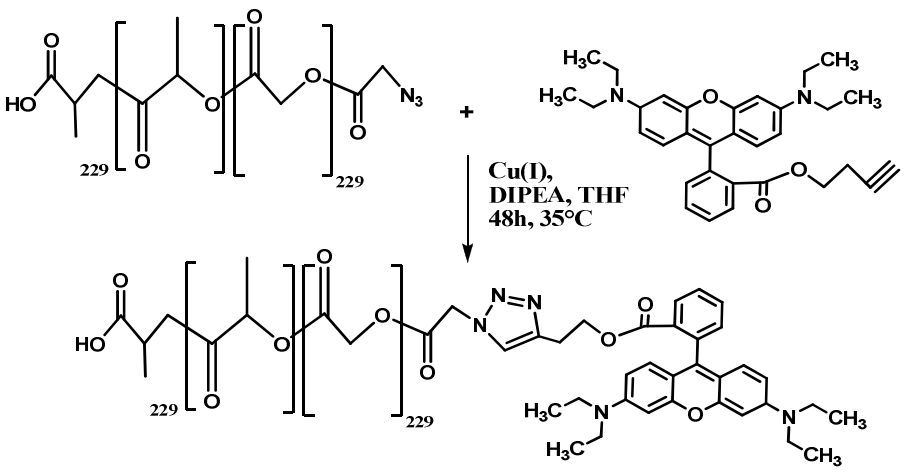

Fig. 3.27 Huysgen cycloaddition between Rhodamine-alkyne and c-PLGA$_{30000}$-N$_3$

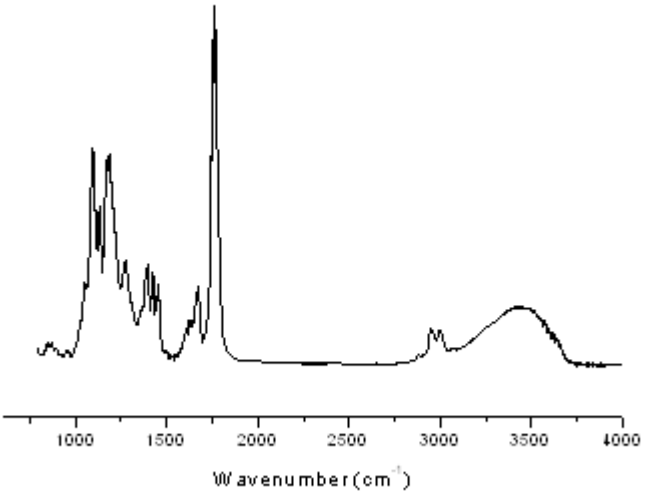

Fig.3.28 FTIR spectrum of c-PLGA$_{30000}$-Rhodamine, can be noted complete disappearance of characteristic azide stretching at 2100 cm^{-1}

3.4.2 PLGA-Rhodamine mcroparticles

Starting PLGA c-PLGA$_{30000}$-OH without functionalization has already successfully used with a lipid helper excipient, namely 1,2-dipalmitoyl-sn-glycero-3-phosphocholine (DPPC) in development of large porous particles (LPP) for local and prolonged delivery of a decoy oligonucleotide to nuclear factor-kB in the lung

(dec-ODN). Among molecular targets, the nuclear factor-kB (NF-kB) transcriptionally regulates the expression of several inflammatory mediators, such as cytokines and chemokines (e.g., IL-6 and IL-8)[55]. In particular, persistent NFkB activation has been reported both in the presence and absence of pathogens in the airways of cystic fibrosis patients and in vitro[56]. In addition, inflammatory mediators contribute to the overproduction of mucins/mucus, responsible for airway obstruction and mucociliary function failure in cystic fibrosis patients[57,58]. Thus, NF-kB blockade by decoy ONs has recently been proposed as a strategy to limit the progression of chronic lung inflammation in cystic fibrosis[59]. Biodegradable PLGA-based LPP containing dec-ODN were prepared with good yields by the double emulsion technique employing ammonium bicarbonate as porogen. SEM analysis performed on a representative LPP sample showed that the adopted formulation conditions allowed the achievement of a homogeneous population of spherical and porous particles (Figure 3.28). As can be seen in figure 3.28A, surface pores appear small, regular, and uniformly distributed throughout the polymeric matrix. Confocal Laser Scanning Microscopy (CLSM) analysis of fluorescent LPP confirmed the internal macroporous structure of the developed formulations, as illustrated in figure 3.28B

A B

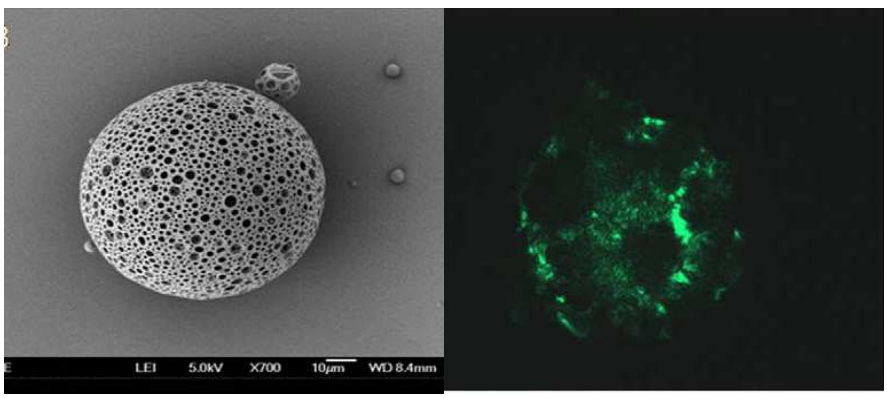

Fig. 3.28 PLGA-based LPP containing dec-ODN: A) SEM image B)Confocal Laser Scanning Microscopy PLGA treated with green fluorescent dye

Thus, to evaluate effect of Rhodamine functionalization on the PLGA template ability, porous microparticles were prepared using the same protocol described above and characterized by CLSM analysis. As can be noted in figure 3.29, PLGA-Rhodamine is characterized by a good quality image without other dye treatment and internal macroporous structure is conserved to highlight the goodness of synthetic strategy adopted

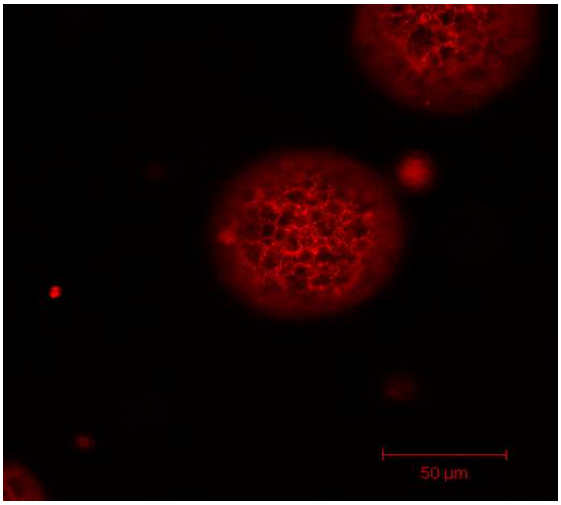

Fig. 3.28 PLGA-Rhodamine Confocal Laser Scanning Microscopy. without fluorescent dye treatment

References

[1] Stephan Forster, T. Plantenberg, *Angew. Chem. Int*. Ed. 2002, 41, 688 -714

[2] Z. Tuzar, P. Kratochvil in Surface and Colloid Science (Ed.: E. Matijevic), Plenum, New York, 1993.

[3] A. Gast, NATO ASI Ser. Ser. E 1998, 303, 311

[4] B. Chu, Langmuir 1995, 11, 414

[5] P. Alexandridis, Curr. Opin. Colloid Interface Sci. 1996, 1, 490

[6] J. Selb, Y. Gallot in Developments in Block Copolymers, Vol. 2 (Ed.:I. Goodman), Elsevier, Amsterdam, 1985, p. 27

[7] M. Moffitt, K. Khougaz, A. Eisenberg, Acc. Chem. Res. 1996, 29, 95.

[8] H.-G. Elias, Makromolek¸le, Vol. 1, H¸thig & Wepf, Basel, 1990

[9] S. Forster, B. Berton, H.-P. Hentze, E. Kramer, M. Antonietti, P. Lindner, Macromolecules 2001, 34, 4610.

[10] B. Discher, Y.-Y. Won, D. Ege, J. Lee, F. S. Bates, D. Discher, D. Hammer, Science 1999, 284, 113

[11] S. Forster, A. K. Khandpur, J. Zhao, F. S. Bates, I. W. Hamley, A. J. Ryan, W. Bras, Macrom olecules 1994, 27, 6922

[12] A. K. Khandpur, S. Forster, F. S. Bates, I. W. Hamley, A. J. Ryan, W.Bras, K. Almdal, K. Mortensen, Macromolecules 1995, 28, 8796

[13] Matsen M W 2001 J. Phys.: Condens. Matter 14 R21

[14] Hamley I W 1998 The Physics of Block Copolymers (Oxford:Oxford University Press

[15] Hamley I W 2001 J. Phys.: Condens. Matter 13 R643

[16] Fasolka M J and Mayes A M 2001 Annu. Rev. Mater. Res. 31 323

[17] Strawhecker KE, Kumar SK, Douglas JF, Karim A. The critical role of solvent evaporation on the roughness of spin-cast polymer films. Macromolecules 2001;34:4669–72

[18]Kim SH, Misner MJ, Xu T, KimuraM, Russell TP. Adv Mater 2004;16:226–31.

[19]V. Kapaklis, S. Grammatikopoulos, R. Sordan, A. Miranda, F. Traversi, Hans von Känel3, D. Trachylis, P. Poulopoulos, C. Politis, J. Nanosc. & nanotech. 10, 6056 (2010)

[20] Y. Yagci, M. K. Mishra in The Polymeric Materials Encyclopedia, CRC, Boca Raton, 1996

[21] R. Jerome, J. D. Tong, Curr. Opin. Solid State Mater. Sci. 1998, 3, 573.

[22] L. A. Mango, R. W. Lenz, Makromol. Chem. 1973, 163, 13

[23] N. A. Mohammadi, G. L. Rempel, Macromolecules 1987, 20, 2362

[24] J. H. Rosedale, F. S. Bates, J. Am. Chem. Soc. 1988, 110, 3542

[25] M. D. Gehlsen, F. S. Bates, Macromolecules 1993, 26, 4122

[26] M. Antonietti, S. Forster, J. Hartmann, S. Oestreich, Macromolecules 1996, 29, 3800

[27] D. R. Invengar, S. M. Perutz, C. A. Dai, C. K. Ober, E. J. Kramer, Macromolecules 1996, 29, 1229

[28] M. Antonietti, S. Forster, M. A. Micha, S. Oestreich, Acta Polym. 1997, 48, 262

[29] J. Selb, Y. Gallot in Developments in Block Copolymers, Vol. 2 (Ed.:I. Goodman), Elsevier, Amsterdam, 1985, p. 27

[30] C. Ramireddy, Z. Tuzar, K. Prochazka, S. E. Webber, P. Munk, Macromolecules 1992, 25, 2541

[31] H. Vink, Makromol. Chem. 1970, 131, 133. W. A. Thaler, Macromolecules 1983, 16, 623.

[32] Y. Ren, T. P. Lodge, M. A. Hillmyer, J. Am. Chem. Soc. 1998, 120, 6830.

[33] C. G. Gebelein, D. Murphy in Advances in Biomedical Polymers (Ed.: C. G. Gebelein), Plenum, New York, 1987.

[34] Couvreur P., Prieto M.J., Puisieux F., Raques B., Fattal E. Multiple emulsion technology for the design of microspheres containing peptides and oligopeptides Adv. Drug Del 28 (1997) 85-96.

[35] Crotts G. and Park T.G. Protein delivery from poly(lactic-co-glycolic acid) biodegradable microspheres: release kinetics and stability issues. J. Microencapsul. 15 (1998) 699-713.

[36] Walter E., Dreher D., Kok M., Thiele L., Kiama S.G., Gehr P., Merkle H.P. Hydrophilic poly(DL-lactide-co-glycolide) microspheres for delivery of DNA to human-derived macrophages and dendritic cells. J. Contr. Rel. 76 (2001) 149-168.

[37] Kissel T. and Koneberg R. Injectable biodegradable microspheres for vaccine delivery. In S. Cohen and H. Bernstein (Eds.), Microparticulate Systems for the delivery of proteins and vaccines. Marcel Dekker, New York, 1996, pp. 51-58.

[38] Blanco D., Alonso M.J., Protein encapsulation and release from poly(lactide-co-glycolide) microspheres : effect of the protein and polymer properties and of the co-encapsulation of surfactants Eur. J. Pharm. Biopharm 45 (1998) 285-294

[39] Park T.G., Lu W., Crotts G. Importance of in vitro experimental condition on protein release kinetics, stability and polymer degradation in protein encapsulated poly(D,L-lactide-co-glycolide) microspheres. J. Contr. Rel. 33 (1995) 211-222.

[40] Yang Y.Y., Chung T.S., Ping Ng N. Morphology, drug distribution and in vitro release profiles of biodegradable polymeric microspheres containing protein fabricated by double emulsion solvent extraction/evaporation method. *Biomaterials* 22 (2001) 231-241.

[41] Park T.G., Lu W., Crotts G. Importance of in vitro experimental condition on protein release kinetics, stability and polymer degradation in protein encapsulated poly(D,L-lactide-co-glycolide) microspheres. J. Contr. Rel. 33 (1995) 211-222.

[42] Ravi Kumar M.N.V. Nano and microparticles as controlled drug delivery devices. *J. Pharm. Pharmaceut. Sci*. 3 (2000) 234-258.

[43] Davis S.S., Illum L. Polymeric microspheres as drug carriers. Biomaterials. 9 (1988) 111-115.

[44] Washington C. Drug release from microparticulate systems. In S. Benita (Eds.), Microencapsulation. Marcel Dekker, New York, 1996, pp. 155-182

[45] Benoit J.P, Marchais H., Rolland H., Vande Velde V. Biodegradable Microspheres: Advances in Production Technology. In S. Benita (Eds.), Microencapsulation. Marcel Dekker, New York, 1996, pp. 36-62.

[46] Kumaresh S. Soppimatha, Tejraj M. Aminabhavia,*, Anandrao R. Kulkarnia, Walter E. Rudzinskib Biodegradable polymeric nanoparticles as drug delivery devices Journal of Controlled Release 70 (2001) 1–20

[47] Kumar M, Bakowsky U, Lehr CM: Preparation and characterization of cationic PLGA nano-spheres as DNA carriers. Biomaterials 2004a;25:1771–1777.

[48] Panyam J, Dali MA, Sahoo SK, Ma WX, Chakra- varthi SS, Amidon GL, Levy RJ, Labhasetwar V: Polymer degradation and in vitro release of a model protein from poly(D,L-lactide-co-gly-colide) nano- and microparticles. J Control Release 2003;92:173–187.

[49] C Perez, A Sanchez, D Putnam, D Ting, R Langer, M.J Alonso Poly(lactic acid)-poly(ethylene glycol) nanoparticles as new carriers for the delivery of plasmid DNA Journal of Controlled Release Volume 75, Issues 1–2, 10 July 2001, Pages 211–224

[50] Ana Vilaa, Howard Gillb, Orla McCallionb, María José Alonso, Transport of PLA-PEG particles across the nasal mucosa: effect of particle size and PEG coating density, *Journal of Controlled Release*, Volume 98, Issue 2, 11 August 2004, Pages 231–244

[51] Galindo-Rodriguez SA, Allemann E, Fessi H, Doelker E. Polymeric nanoparticles for oral delivery of drugs and vaccines: a critical evaluation of in vivo studies *Critical Reviews in Therapeutic Drug Carrier Systems* [2005, 22(5):419-464]

[52] C.N. Grama, D.D. Ankola, M.N.V. Ravi Kumar, Poly(lactide-co-glycolide) nanoparticles for peroral delivery of bioactives Review Article, *Current Opinion in Colloid & Interface Science*, Volume 16, Issue 3, June 2011, Pages 238-245

[53] D.S.W. Benoit, W. Gray, N. Murthy, H. Li, C.L. DuvallpH-Responsive Polymers for the Intracellular Delivery of Biomolecular Drugs, Comprehensive Biomaterials, Volume 4, 2011, Pages 357-375

[54] Jayanth Panyama, Vinod Labhasetwar Biodegradable nanoparticles for drug and gene delivery to cells and tissue *Advanced Drug Delivery Reviews* Volume 64, Supplement, December 2012, Pages 61–71

[55] Courtois G, Gilmore TD (2006) Mutations in the NF-kappaB signaling pathway: implications for human disease. *Oncogene* 25: 6831–6843.

[56] DiMango E, Ratner AJ, Bryan R, Tabibi S, Prince A (1998) Activation of NfkappaB by adherent Pseudomonas aeruginosa in normal and cystic fibrosis respiratory epithelial cells. *J Clin Invest* 101: 2598–2605.

[57] Li JD, Dohrman AF, Gallup M, Miyata S, Gum JR, et al. (1997) Transcriptional activation of mucin by Pseudomonas aeruginosa lipopolysaccharide in the pathogenesis of cystic fibrosis lung disease. *Proc Natl Acad Sci U S A* 94: 967–972.

[58] Hauber HP, Foley SC, Hamid Q (2006) Mucin overproduction in chronic inflammatory lung disease. *Can Respir J* 13: 327–335

[59] Francesca Ungaro, Daniela De Stefano, Concetta Giovino, Alessia Masuccio, Agnese Miro, Raffaella Sorrentino, Rosa Carnuccio, Fabiana Quaglia, PEI-Engineered Respirable Particles Delivering a Decoy Oligonucleotide to NF-kB: Inhibiting MUC2 Expression in LPS-Stimulated Airway Epithelial Cells, *PLOS ONE*, October 2012 | Volume 7 | Issue 10 |

Chapter 4

Click chemistry stategy applied

In High molecular weight range

(from 50000 to 200000 daltons)

4.1 Chitosan-PEO based biomaterials

Chitosan is a linear polysaccharide composed of randomly distributed β-(1-4)-linked D-glucosamine (deacetylated unit) and N-acetyl-D-glucosamine (acetylated unit) (figure 4.1).

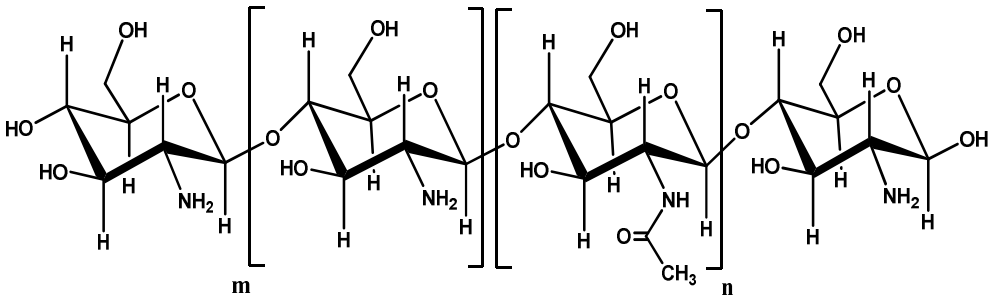

Fig.4.1 Chitosan chemical structure

Chitosan is produced commercially by deacetylation of chitin, which is the structural element in the exoskeleton of crustaceans (such as crabs and shrimp) and cell walls of fungi and second most abundant biopolymer after cellulose. The degree of deacetylation (%DD) can be determined by NMR spectroscopy, and the %DD in commercial chitosans ranges from 60 to 100%. On average, the molecular weight of commercially produced chitosan is between 3800 and 250,000 Daltons. A common method for the synthesis of chitosan is the deacetylation of chitin using sodium hydroxide in excess as a reagent and water as a solvent. It can be used in agriculture as a seed treatment and biopesticide, helping plants to fight off fungal infections[1].. In winemaking it can be used as a fining agent, also helping to prevent spoilage[2], In industry, it can be used in water treatment[3,4] catalysis[5] and biofabrication[6] applications . More controversially, chitosan has been asserted to have use in limiting fat absorption, which would make it useful for dieting, but there is evidence against this. Other uses of chitosan that have been researched include use as a soluble dietary fiber. As regard biomedical use, thanks to its biocompatibility and biodegradability finds a wide range of applications from

bandages to reduce bleeding and as an antibacterial agent to use in controlled drug delivery and transdermal formulations enhancing the transport of polar drugs across epithelial surfaces. The amino group in chitosan has a pKa value of ~6.5, which leads to a protonation in acidic to neutral solution with a charge density dependent on pH and the %DA-value. This makes chitosan water soluble and a bioadhesive which readily binds to negatively charged surfaces such as mucosal membranes Lack of a positive charge means chitosan is insoluble in neutral and basic environments. However, in acidic environments, protonation of the amino groups leads to an increase in solubility. The implications of this are very important to biomedical applications. This molecule will maintain its structure in a neutral environment, but will solubilize and degrade in an acidic environment. This means chitosan can be used to transport a drug to an acidic environment, where the chitosan packaging will then degrade, releasing the drug to the desired environment. One example of this drug delivery has been the transport of insulin[7]. Chitosan and its derivatives, such as trimethylchitosan (where the amino group has been trimethylated), have been used in nonviral gene delivery. Trimethylchitosan, or quaternised chitosan, has been shown to transfect breast cancer cells, with increased degree of trimethylation increasing the cytotoxicity; at approximately 50% trimethylation, the derivative is the most efficient at gene delivery. Oligomeric derivatives (3-6 kDa) are relatively nontoxic and have good gene delivery properties[8]. Chitosan is hypoallergenic and has natural antibacterial properties, which further support its use in field bandages, allowing it to rapidly clot blood, and has recently gained approval in the United States and Europe for use in bandages and other hemostatic agents. These work by an interaction between the cell membrane of erythrocytes (negative charge) and the protonated chitosan (positive charge) leading to involvement of platelets and rapid thrombus formation. Chitosan hemostatic products have been shown in testing by the U.S. Marine Corps to quickly stop bleeding and to reduce blood loss, and result in 100% survival of otherwise lethal arterial wounds in swine[9] Chitosan hemostatic products reduce

blood loss in comparison to gauze dressings and increase patient survival[10]. Chemical modification of native polysaccharides, a prerequisite for access to polysaccharide-based functional materials, is still troublesome. The hydroxyl groups of chitosan have similar reactivity toward electrophiles, making regioselective and quantitative reactions difficult. Much research effort has been devoted to exploit chemical/enzymatic strategies to obtain polysaccharide derivatives having various functionalities at desired positions. For example, enzymatic polymerization of chemically modified monosaccharides to afford the corresponding polysaccharides (bottom-up approach) has high potential'[11,12] but tedious synthetic routes for the modified monosaccharides and their lowered affinity (especially, those having large substituents) toward synthase enzymes hinder their wide application. Convenient, general, quantitative, and regioselective methods useful for direct modifications of native polysaccharides are, therefore, sought for obtaining suitable polysaccharide-based materials. The numerous reactions that were employed to obtain derivatives with well-defined structures and functionalities[13,14] and complex macromolecular architectures, such as networks[15] or graft copolymers[16] have played a key role in increasing the number of chitosan and chitin application. Chitosan-based hydrogels in particular are used in widespread application such as devices for the controlled release of drugs and proteins[17], scaffolds for tissue engineering[18,19] and in materials for wastewater treatment[20,21]. Moreover, N-Phthaloyl- Chitosan is regarded as one of the most useful precursors for subsequent modification due to its solubility in common aprotic polar solvents (DMSO, DMF, NMP) and it also allows the simple deprotection of the amino groups by hydrazine monohydrate[22]. It has therefore been extensively used for the regioselective functionalization and graft copolymerization onto chitosan[23,24.] The covalent crosslinking of chitosan has been largely performed with dialdehydes such as glyoxal[25,26] and in particularglutaraldehyde[27,28,29] by reaction with the amino groups of chitosan to form covalent imine bonds[30]. Other compounds, generally used for polysaccharide

crosslinking, such as epichlorohydrin (EPI)[31,32] ethylene glycol diglycidyl ether[33,34] isocyanates, or the less toxic diethyl squarate[35], oxalic acid[36] or genipin[37] can also be used with chitosan. Crosslinking improves chitosan stability against solubilization and leaching but can reduce its swellability, and absorption capacity. EPI and genipin crosslinking are more advantageous than other methods because they do not eliminate the cationic amine functionality, which may interact specifically with dyes, metals and plasmids so to enhance absorption efficiency[38]. The swellability of crosslinked chitosan is inversely proportional to the crosslinking degree and rigidity of chain segments between crosslinking points[39]. The latter depends on the flexibility of the crosslinking bridges formed and the carbon atom of chitosan involved in the bonding. Indeed, if the reaction involves the C-6 rather than C-2 or C-3, the resulting network is less rigid because of its larger conformational freedom. Selective and regioregular methods must be implemented so as to define structure properties relations of crosslinked chitosan, more accurately. In this context, efficient and high yielding ‘‘click type” reactions[40,41] are useful and versatile tools. In particular, the Cu(I)-catalyzed 1,3-dipolar cycloaddition of terminal alkynes with azides to give 1,4-regioselectively substituted triazoles[42,43] has attracted much attention for the synthesis and post-polymerization modification of polymers. Indeed synthesis of block and graft copolymers, dendrimer synthesis/functionalization, bioconjugation, surface immobilization/modification, and orthogonal functionalization of polymers were successfully performed[44,45,46] In recent literature the interest has been shown in this cycloaddition for the modification of polysaccharides. It was used for the functionalization of curdlan[47,48] cellulose[49,50] dextran[51] and starch[52]. This was further used to prepare hydrogels from hyaluronic acid (HA)[53], for the functionalization of chitosan-grafted-PEO nanostructures[54], to obtain microparticles and block copolymers from dextran[55,56] and to synthesizes graft copolymers and crosslinked products from functionalized poly(ethylene oxyde)

(PEO) and guar gum[57]or others dilkyne moieties[58]. Click cycloaddition was recently applied to the grafting of PEO onto N-azidated chitosan also[59].

4.2 Protein stabilizing strategies: protein-PEG conjugates

Conjugate is an hybrid system polymer-protein which aims to hold together the unique catalytic and functional properties of proteins and enzymes and structural properties of synthetic molecules and macromolecules. By far, the desire to overcome the intrinsic limitations of protein therapeutic agents has been the driving force for the developments in this field, given that approximately 25% of all new medicines approved by the American Food and Drug Administration are protein-based.1 Initially, the philosophy for overcoming the immunogenicity of therapeutic proteins, their renal elimination, and their proteolysis while maintaining therapeutic activity has been to modulate the number, the length, and to a certain extent the architecture (i.e., linear versus branched) of the polymer segments used for preparing the conjugate. As result the physicochemical properties of the polymer is conveyed to the protein, thereby modifying the biodistribution and solubility. A first approach in this sense can be considered the ”pharmacologically active polymer” in which a bioactive molecule was linked to a polymer backbone decorated with a solubilizer group and transport system[60,61.] To accomplish this role, polymer carrier can be metabolized or hydrolyzed and ultimately is eliminated from the body, so should be quite hydrophilic and of low molecular weight while linkers should be biodegradable to release the protein from the polymer in a time controlled manner or in response to certain physiological conditions. Chemical linkage that cleave hydrolytically are amide linkers or based on thiol conjugation chemistry. Otherwise chemical linkages that cleave enzymatically has to be designed in relation of specific protease activity in specific parts of the body. The conjugation studies for attaching polymers to the ε-group of lysine or carboxylic

acid side chains of proteins sometimes leads to the alteration in bioactivity. In antibody conjugation, carbohydrate in the hinge region, a site distant from the antigen binding domain is utilized. Most used synthetic routes provide “Grafting onto”, in which the polymers are covalently attached to the amino acid side chains and ligand binding sites of the protein or “Grafting from” where the protein itself acts as an initiator for the synthesis of the polymer.

Grafting onto can be divided in three subcategories: direct functionalization, in which polymer properly functionalized binds protein directly, indirect functionalization in which there is a binding spacer between protein and polymer and, finally, functionalization via cofactor o ligands, in which polymer interact with protein via opportune ligand[62]. Very common direct functionalization concerns NHS-activated carboxylic acid as illustrated in figure 4.2 and aldehyde addition in figure 4.3

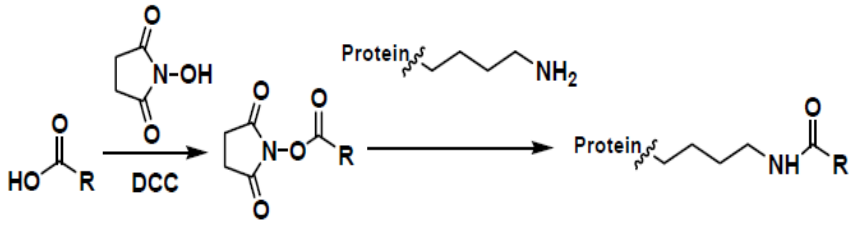

Fig.4.2 grafting onto route by NHS carboxylic acid activation

Selectivity of the first reaction is low due to the presence of many Lysine residues on the protein surface in addition to often exposed α-N terminus. Difference in reactivity towards activated carboxylic acids is related to pKa of different amino groups; for ε-amine group on Lysine pKa= 10, for α-N terminus pKa= 7.8, resulting in practice however difficult. In mains advantages regard aldehyde addition can be included an overall charge of protein preservation and a good selectivity toward α-terminus which react at pH 5. Disadvantage can be resumed in a more challenging two-step procedure and aldehyde synthesis.

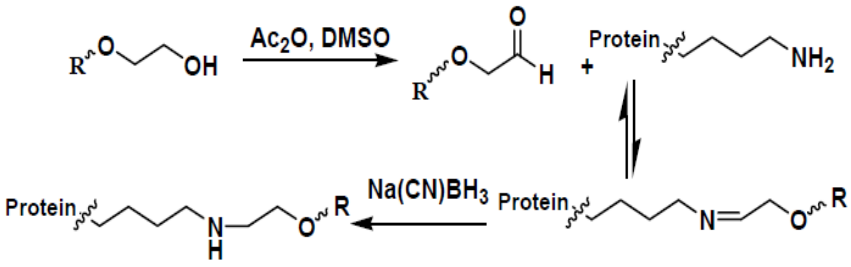

Fig.4.3 grafting onto route by aldehyde addition

Monochlorotriazine was employed to functionalize protein amino groups also: 2,4-bis(methoxy-poly(ethylene glycol)-6-chloro-s-triazine was conjugated to asparaginase by direct reaction[63]. Thiols amino acid side chain represent an excellent alternative for the functionalization. Maleimide end functional polystyrene[64] as illustrated in figure 4.4, Vinyl sulfone-end functional polymer[65]

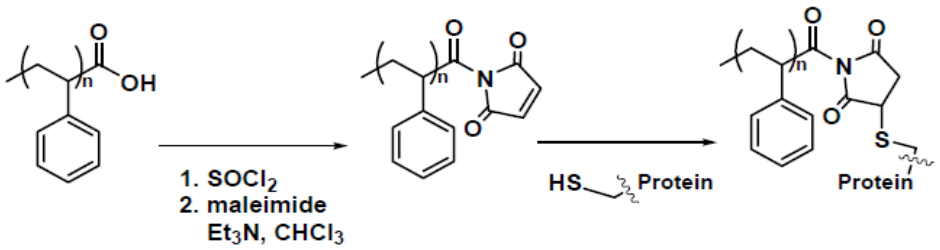

Fig.4.4 grafting onto route by thiols maleimide addition

and α, ω-Pyridyl disulfide activated Pluronic were successful attached[66]. More challenging is tyrosine residue functionalization by diazonium salt, Mannich reaction[67] or p-allyl palladium complex[68]. The methods discussed above for direct specific functionalization of proteins can also be used for indirect functionalization. In this case the protein does not react directly with the polymer but rather gets linked via a secondary non-natural functionality that is introduced into the protein structure named spacer. The heterobifunctional spacers helps in circumventing problems associated with lack of reactivity when two large molecules are brought together. Careful consideration of the type of spacer should be taken to avoid intra-

or intermolecular cross-linking. Trough this route it is possible to introduce alkyne or azide groups for Huisgen cicloaddition or Staudinger ligation[69,70]. Co-factors and ligands for polymer functionalization should have reactive terminus modifiable without any effect on the binding properties toward proteins such as biotin, heme, NAD and FAD. Aminoethyl-appended NAD has been successfully modified with both PEG and dextran without significant loss of activity with yeast dehydrogenase[71]. Modification with the low molecular weight cofactors and ligands can be done using traditional synthetic and purification techniques: the reconstituted bioconjugate is purified by dialysis or size exclusion chromatography.

As already mentioned, in "Grafting from" approach polymers are generated from defined initiation sites on the protein. The protein is first modified with an initiator for a Control Radical Polymerization[72], Atom Transfer Radical Polymerization (ATRP)[73] or Reversible Addition Fragmentation Transfer (RAFT), to form the protein macroinitiator and polymerization occurs from defined sites on the protein. 2-Bromoisobutyrylbromide was successful used in macroinitiator protein preparation with Lysozyme[74], Bovin serum albumin[75], streptavidine[76], α-chimotrypsin. In comparison with Grafting onto, in Grafting from approach is possible a pre-determination of precise number of polymer chains and their placements and a simple purification of final conjugate, on the contrary became very challenging post-polymerization modifications and protein-polymer couplings. Early on, many natural polymers as well as synthetic polymers such as poly(ethylene glycol) (PEG) have been evaluated for protein-polymer preparation. Possibly due to the fact that PEG was one of the first non-immunogenic, well-defined (hetero) telechelic polymers capable of conveying ''stealth'' properties to proteins, it is not surprising that the PEGylation (i.e., the covalent attachment of PEG chains) of therapeutic proteins has dominated this field for many years[77,78] and that several therapeutic PEGylated proteins have reached the market.[79,80] More recently, the philosophy for overcoming the shortcomings of therapeutic proteins

with minimal detrimental effect on protein biological activity has changed to controlling the site at which the polymer is attached to the protein.[81,82] This has become a possibility with the development of a veritable (bio)chemical toolbox of orthogonal coupling strategies for residue- or site-specific protein modification.[83,84,85] Concurrently, access to well-defined (hetero)telechelic polymers other than PEG has become possible due to advances in the field of controlled/‘‘living’’ polymerization.[86]. These combined developments in addition to already consolidated click chemistry techniques have lead to a boom in the number of studies implicating protein–polymer conjugates, whether for therapeutic purposes or not[87]. With these advances, many new possibilities are available for adjusting the properties of the final conjugate. One aspect which is of prime importance in the field is that while proteins are used to prepare many functional constructs, they are sensitive biomolecules and their bioactivity can be either positively or negatively influenced by many different aspects of polymer modification.

4.3 Section aim

In this section of research work click chemistry strategy developed was applied in Chitosan chemical modification in order to study the possible exploitation of click cycloaddition to the regioselective crosslinking of chitosan with PEO di-alkyne. Has been used the following strategy: (a) NH_2 protection by phthaloylation, (b) regioselective C-6 functionalization with N_3 groups, (c) crosslinking by cycloaddition with di-alkyne PEO, and (d) NH_2 deprotection. In particular, N-Phthaloyl-Chitosan was first selectively functionalized with azide groups. The crosslinking of the azide-functionalized chitosan was then obtained by Cu(I)-catalyzed azide–dialkynes [3+2] dipolar cycloaddition with α-ω-dialkyne-PEO_{6000}. The obtained biomaterial crosslinked with dialkyne PEO was

characterized by swellability tests to explore the possibility of its application as hydrogel for pharmaceutical application. Last part of section regards 1-3 Huisgen cycloaddition in aqueous environment. In particular was developed, in collaboration with ETHZ research group directed by professor Jean Cristophe Leroux, a synthetic strategy to obtain charged conjugates α-chymotrypsin-PEG methacrylate using Grafting from approach by Control Radical Copolymerization of azided monomer and different PEG methacrylate initiated from α-chymotrypsin macroinitiator. Azide groups present in polymer moieties were then coupled by 1-3 Huisgen cycloaddition catalysed by Cu(I) and DIPEA with different alkyne ionisable molecules such as propargyl alcohol, propargyl amine and propiolic acid. To evaluate influence of charged polymer coating on α-chymotrypsin activity, were carried out activity test with protein and amino acid substrates.

4.4 Synthesis of PEO crosslinked Chitosan

4.4.1 Synthesis of azided Chitosan

Chitosan chosen for synthetic pathway is commercial available with viscosity molecular weight of 110-150 kDa and degree of deacetylation estimated by ^{1}H-NMR around 90% (figure 4.5), for this reason in all figure concerning synthesis will be showed only deacetylated unit.

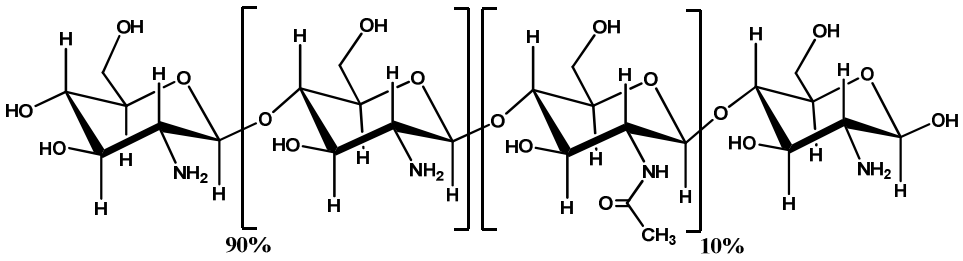

Fig.4.5 Chitosan chosen for synthesis chemical structure

First step of strategy regarded amino group protection by reaction with phtalic anhydride as illustrated in figure 4.5

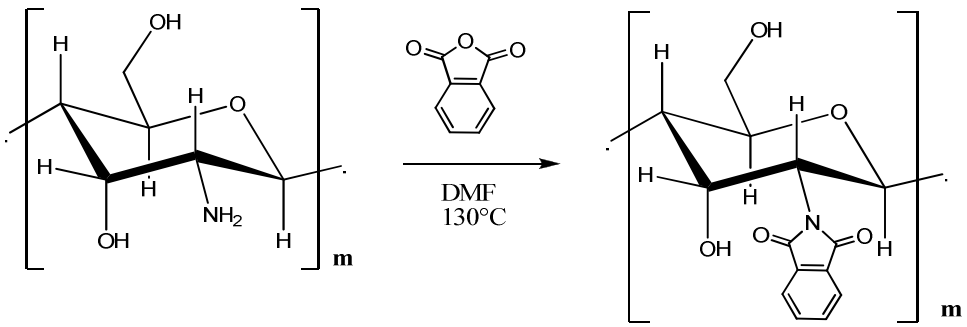

Fig. 4.6 Chitosan amino group protection by phtalic anhydride reaction

Protection increases chitosan solubility in polar aprotic solvent such as DMF and DMSO, avoids amino group interferences with further reaction and aromatic ring protons are a good internal standard for N-Phthaloyl-Chitosan ^{1}H-NMR characterization because their signals can be found between 7-8 ppm a zone not crowded from others protons signals. N-Phthaloyl-Chitosan was obtained by reacting chitosan with phthalic anhydride under conventional conditions[88] in absence of moisture. To achieve this condition Chitosan was dried under P_2O_5 vacuum at 100°C overnight. Reaction was carried out under magnetic agitation for 6 hours then reaction mixture was precipitated in ice water bath. Filtered product was washed with ethanol and dried. ^{1}H-NMR analysis was used to confirm product chemical structure, N-Phthaloyl-Chitosan, comparing integrations values of the signals related to the phtalimide aromatic protons (f+g) (δ = 7.39-7.78) and C1 proton (e) (δ = 5.20) (figure 4.7) was evaluated that Chitosan conversion degree is, within the limits of experimental error, around 90%. As already mentioned, N-Phthaloyl-Chitosan is more soluble in DMF respect starting Chitosan. This feature helps two-steps azidation process. First step provide, as usual, hydroxyl group

activation by mesyl chloride. Was observed that this reaction is extremely selective toward primary hydroxyl group as illustrated in figure 4.8.

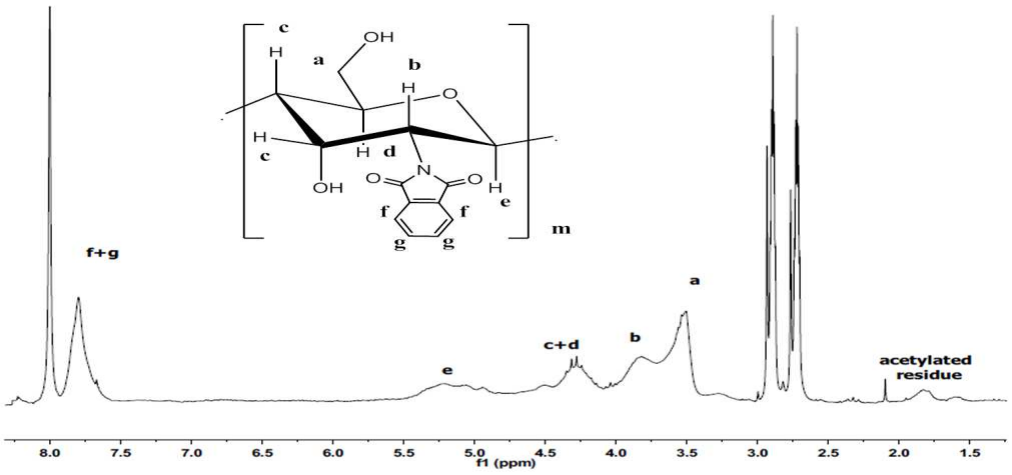

Fig. 4.7 ^{1}H-NMR spectrum of N-phtaloil Chitosan with proton assignment

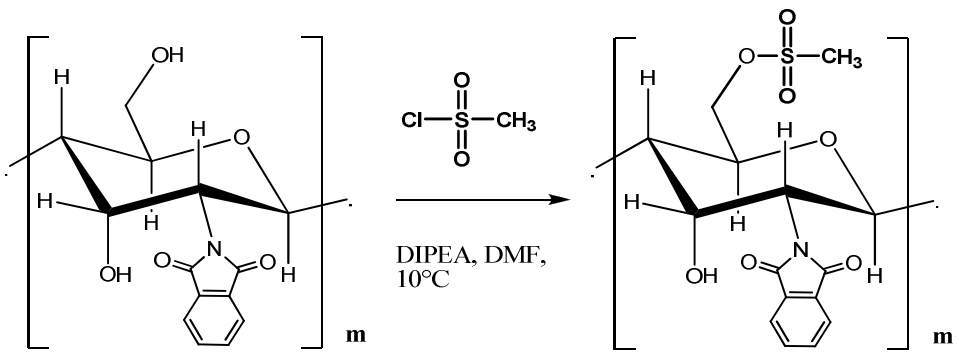

Fig.4.8 activation of chitosan primary hidroxyl group by mesyl chloride reaction

N-Phthaloyl-Chitosan was before solved in dry DMF at 80°C then cooled under nitrogen at room temperature, observing an homogeneous solution. Temperature was set to 10°C by thermostatic bath to avoid eventual Chitosan precipitation and to dissipate heat of reaction. Under magnetic stirring were added

DIPEA and dropwise mesyl chloride. After five minutes reaction mixture viscosity increase up to a gel formation. This phenomenon was probably due to ionic an hydrogen interactions between charged Chitosan and DMF[89]. Reaction gelled mixture was transferred in methanol, obtaining an heterogeneous powder. This powder showed poor solubility in deuterated DMF at room temperature, but was very soluble in basic D_2O. In this solvent was carried out ^{1}H-NMR analysis to define powder chemical structure which resulted to be (figure 4.9). mesylated N-Phthaloyl-Chitosan (N-Pht-Chitosan-mesy). Comparing integrations values of the signals related to the phtalimide aromatic protons (f+g) (δ = 7.39-7.78) and mesyl protons, CH_3-OSO (k) (δ = 3.20) (figure 4.9) was evaluated that N-Phthaloyl-Chitosan conversion degree is, within the limits of experimental error, around 10%

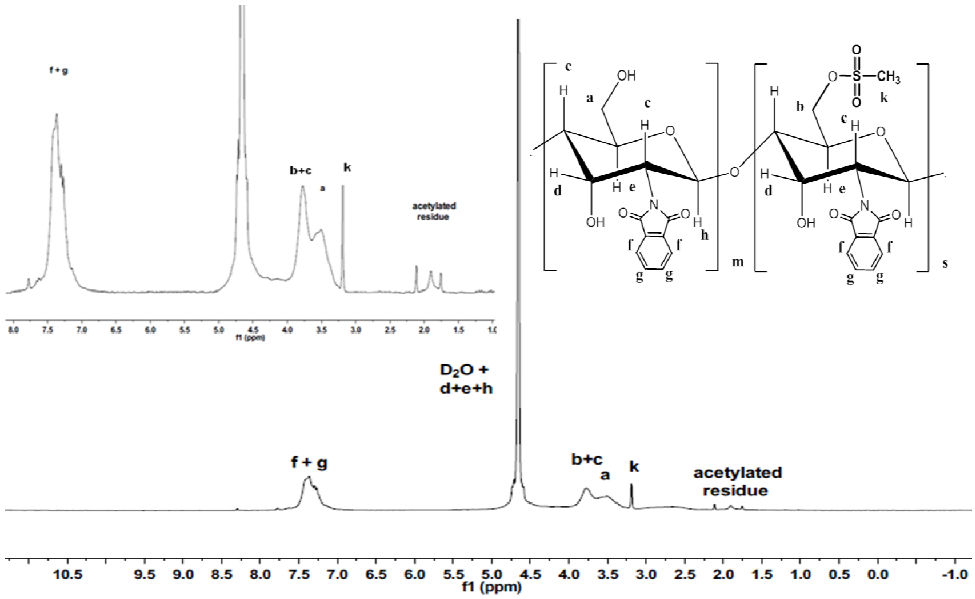

Fig. 4.9 ^{1}H-NMR spectrum of N-phtaloil Chitosan- mesy with proton assignment

N-Pht-Chitosan-mesy powder was dried under vacuum at 80°C to remove any methanol trace and redissolved in dry DMF. Reaction with mesyl chloride and subsequent purification was repeated according to the same procedure described

above. ^{1}H-NMR in basic D_2O showed an increase of N-Phthaloyl-Chitosan conversion degree

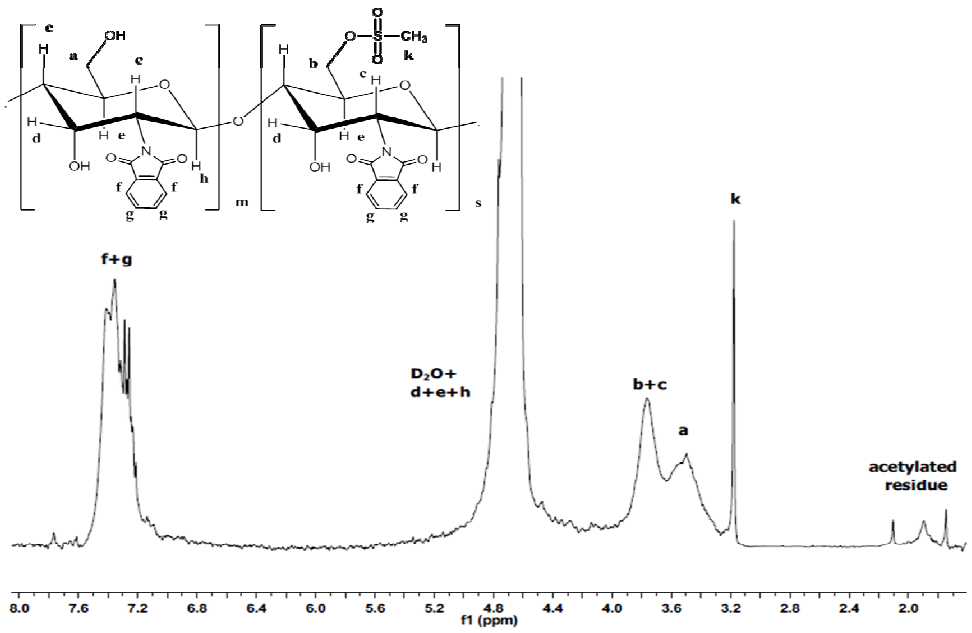

Fig. 4.10 ^{1}H-NMR spectrum of N-phtaloil Chitosan- mesy after second reaction with mesyl chloride with proton assignment

Comparing integrations values of the signals related to the phtalimide aromatic protons (f+g) (δ = 7.39-7.78) and mesyl protons, CH_3-OSO (k) (δ = 3.20) (figure 4.9) was evaluated that N-Phthaloyl-Chitosan conversion degree is, within the limits of experimental error, around 25%. The limiting step of the hydroxyl activation with Mesyl chloride seems to be DMF gel formation. Therefore repeating reaction and methanol washing cycle it is possible to suitably tune functionalization degree. Nucleophilic substitution was carried out as usual in large excess of sodium azide in a refluxing mixture of DMF an water 20/1 v/v at 80°C for 24 hours as illustrated in figure 4.11. Reaction mixture was concentrated, precipitated in cool water, filtered and washed with ethanol

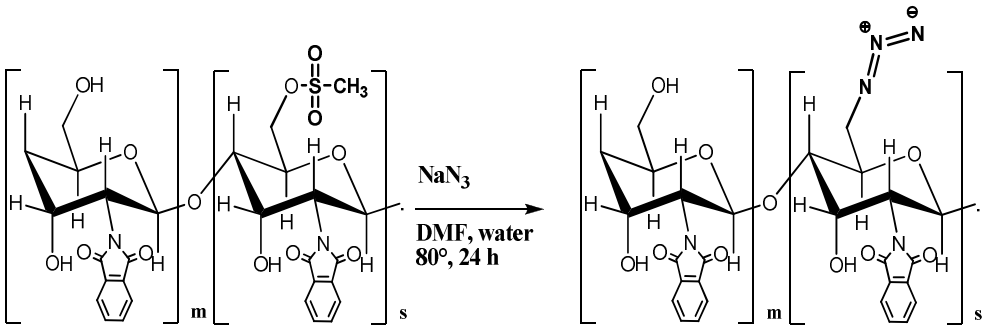

Fig. 4.11 Nucleophilic substitution of N-phtaloil Chitosan- mesy with sodium azide

^{1}H-NMR and FTIR analysis were used to confirm N-Phthaloyl-Chitosan-N_3 chemical structure; in spectrum showed in figure 4.12 can be noted complete disappearance of signal related to mesyl group CH_3-OSO protons (k) (δ = 3.20). FTIR spectrum shows azide characteristic stretching band at 2100 cm^{-}1 (figure 4.13)

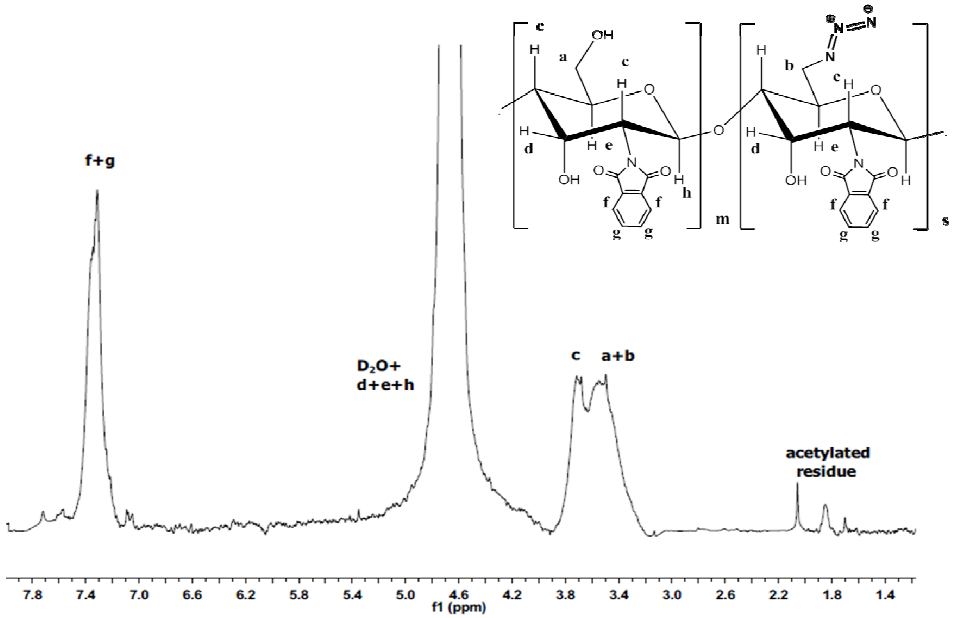

Fig. 4.12 ^{1}H-NMR spectrum of N-phtaloil Chitosan-N_3 with proton assignment

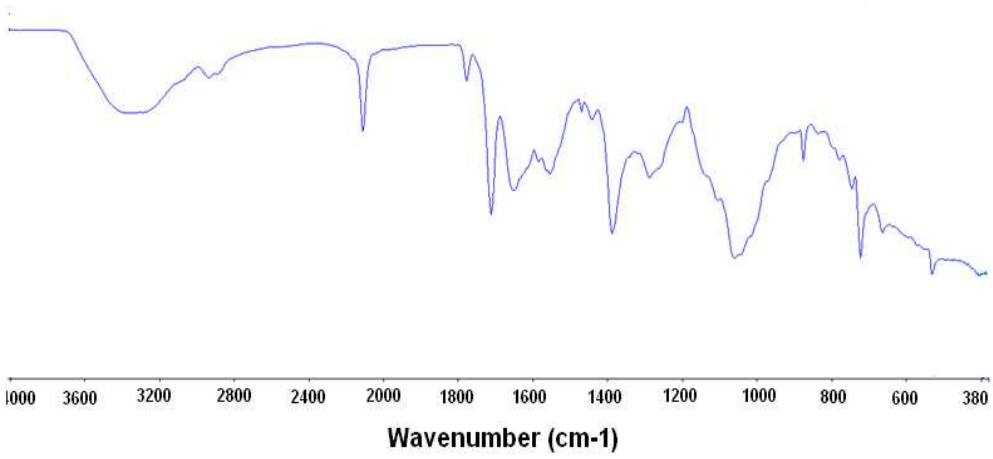

Fig.4.13 FTIR spectrum of N-phtaloil Chitosan-N_3 can be noted characteristic azide stretching band at 2100 cm-[1]

On these bases was estimated a quantitative conversion of N-Phthaloyl-Chitosan-mesy toward azided product.

4.4.2 Synthesis of α-ω-dialkyne-PEO_{6000}

Synthetic pathway to achieve α-ω-dialkyne-PEO_{6000}, illustrated in figure 4.13, started from α-ω-dihydroxyl-PEO_{6000}. Terminal hydroxyl group were changed into azide through two step process via mesyl activation and azide groups were in their turn changed into amine groups through H_2/Pd reduction. This reaction was carried out in hydrogen flux bubbling the gas through capillary immersed in chloroform/ methanol solution containing palladium on carbon and α-ω-di-azide-PEO_{6000}. Was not tried esterification of 4-pentynoic acid catalysed by DCC and DMAP onto α-ω-dihydroxyl-PEO_{6000} to avoid drawbacks deriving from incomplete reagent conversion. All steps were characterized from conversion degrees, calculated by ^{1}H-NMR analysis, higher than 95%. In particular, comparing

integrations values of the signals related to PEO protons CH_2-NH-CO (b) (δ = 4.0) and mesyl protons, HC≡C-CH_2-OCO- (c) (δ = 4.65) (figure 4.14) was evaluated a quantitative conversion of α-ω-di-amine-PEO_{6000}.

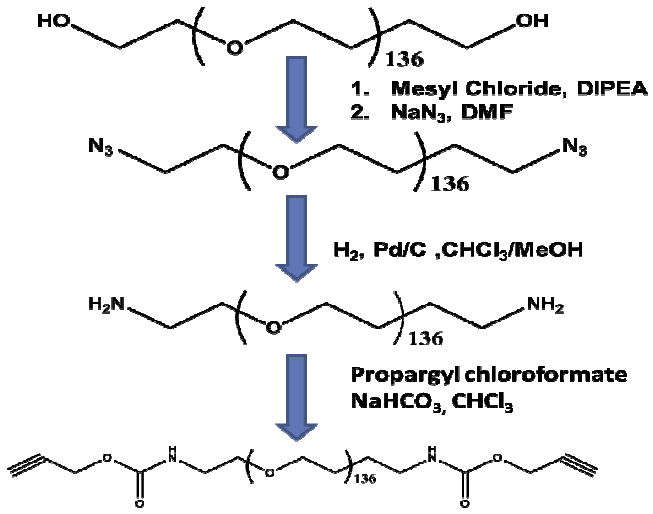

Fig.4.13 Synthetic pathway for α-ω-dialkyne-PEO_{6000} preparation

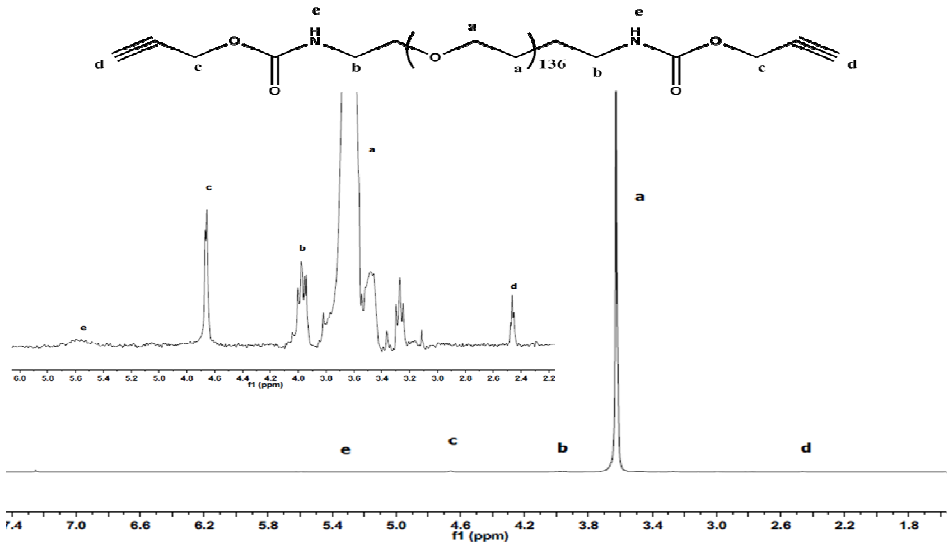

Fig. 4.14 ^{1}H-NMR spectrum of α-ω-dialkyne-PEO_{6000} with proton assignment

Ninhydrin assay confirmed quantitative coupling revealing no amine groups.

4.4.3 1-3 Huisgen cycloaddition between N-Phthaloyl-Chitosan-N_3 and α-ω-dialkyne-PEO_{6000}

The final coupling between N-Phthaloyl-Chitosan-N_3 and α-ω-dialkyne-PEO_{6000} to obtain cross-linked Chitosan was carried out according to the usual protocol, as illustrated in figure 4.15.

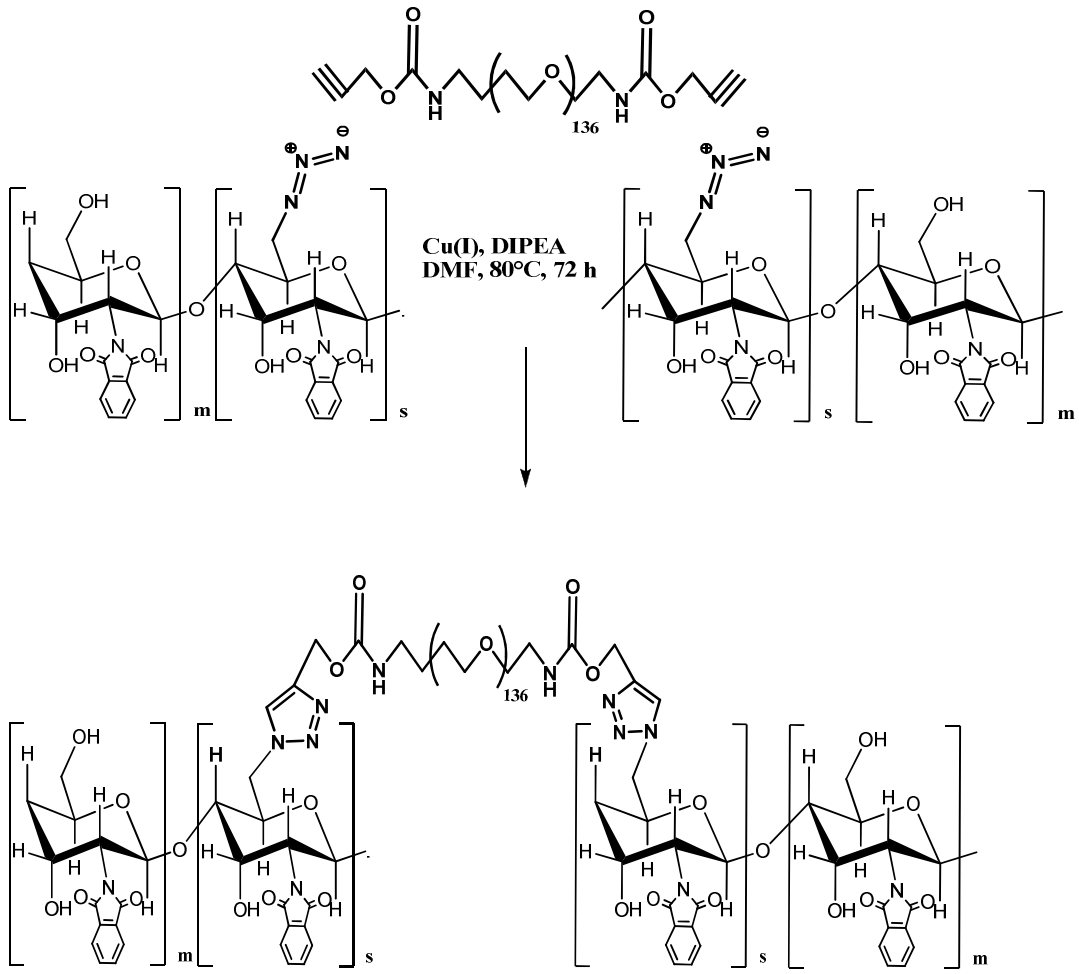

Fig. 4.15 1-3 Huisgen cycloaddition between N-Phthaloyl-Chitosan-N_3 and α-ω-dialkyne-PEO_{6000}

In a first bottle was solved α-ω-dialkyne-PEO_{6000} with a 10% molar excess respect to azided Chitosan and DIPEA in dry DMF. This solution was subjected to three freeze in liquid nitrogen and thawing under vacuum cycle; then was transferred under argon in a second bottle containing N-Phthaloyl-Chitosan-N_3 and $BrCu(P(Ph)_3)_3$. The reaction mixture was stirred for 72 hours at 80°C. During the reaction was observed a gradual chitosan desolvatation. The final reaction dispersion was precipitated in chloroform and filtrated. FT-IR analysis shows the the complete disappearance of the azide characteristic stretching peak at 2100 cm^{-1} (figure 4.16)

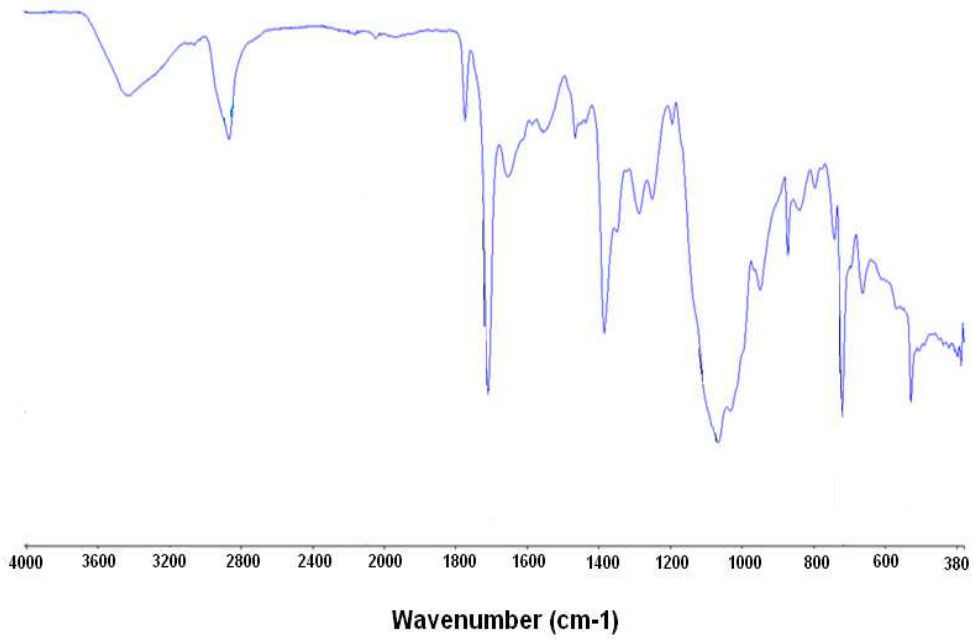

Fig.4.16 FTIR spectrum of PEO-cross-linked-Chitosan can be noted complete disappearance of the characteristic azide stretching band at 2100 cm-[1]

^{1}H-NMR analysis carried out in basic D_2O was used to confirm the chemical structure of PEO-cross-linked-Chitosan. Figure 4.17 shows characteristic signal of

PEO protons O-CH_2-CH_2 (δ = 3.60) and those of phtalimide aromatic protons (δ = 7.30). Can be noted also the signal related to the alkyne proton of α-ω-dialkyne-PEO_{6000} (δ = 2.50),highlighting the presence of not crosslinked PEO chains. This is probably due to 10% PEO molar excess used.

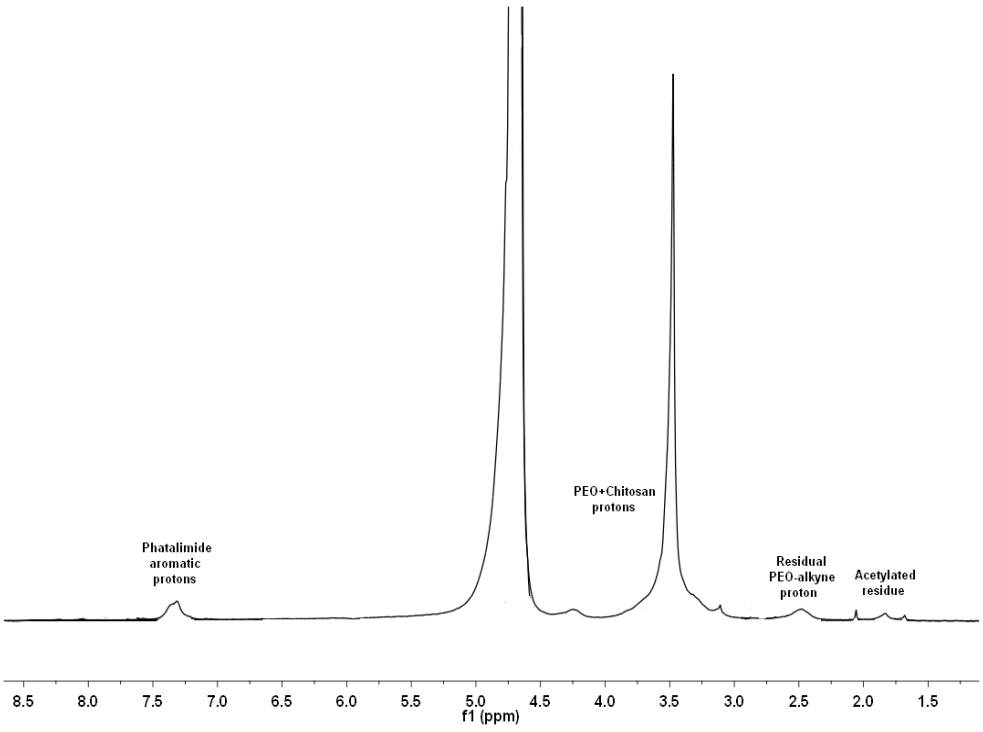

Fig. 4.17 ^{1}H-NMR spectrum of PEO-cross-linked-Chitosan with proton assignment

4.4.4 NH_2 deprotection of PEO-cross-linked-Chitosan

PEO-cross-linked-Chitosan was treated with hydrazine monohydrate in order to restore the free amino groups, as illustrated in figure 4.18. The fine dispersion of PEO-cross-linked-Chitosan was stirred under nitrogen for 15 hours at 80°C. After

cooling, the mixture was diluted with water and evaporated with a rotary evaporator, recovering deprotected PEO-cross-linked-Chitosan as an almost colorless powdery material.

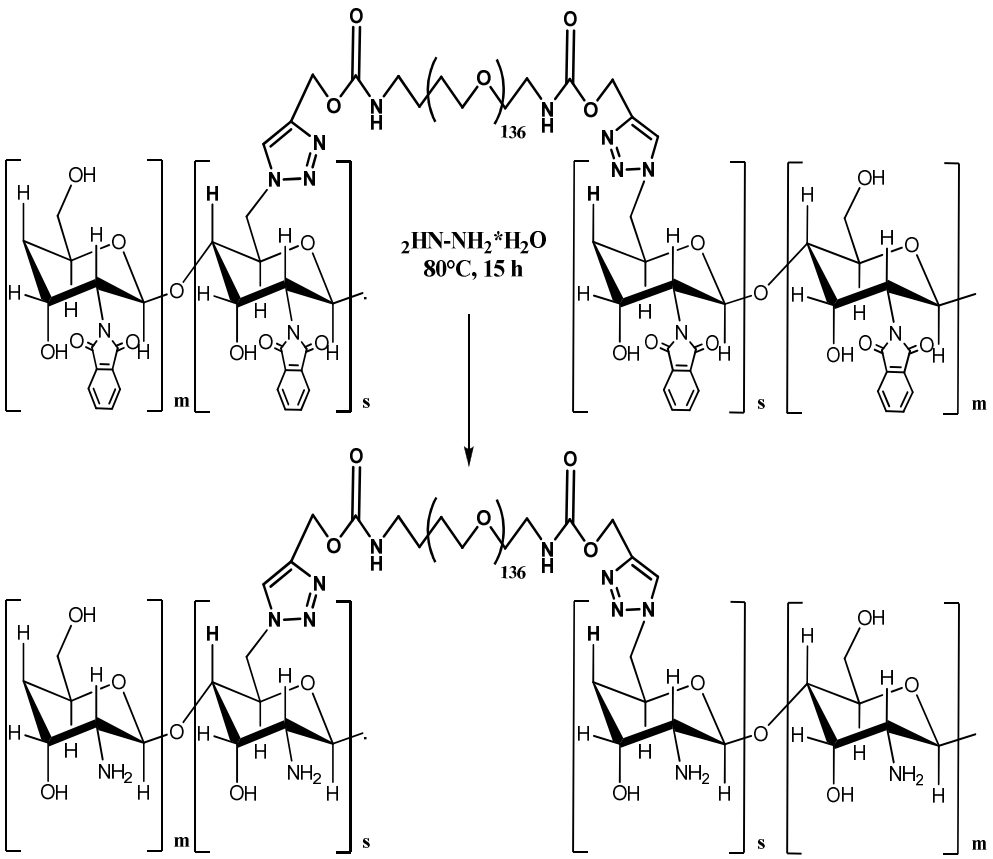

Fig. 4.18 NH_2 deprotection of PEO-cross-linked-Chitosan through hydrazine idrate reaction

^{1}H-NMR analysis carried out in basic D_2O was used to confirm the chemical structure of PEO-cross-linked-Chitosan-NH_2. Figure 4.19 shows the complete disappearance of signal related to phtalimide aromatic protons (δ = 7.30).

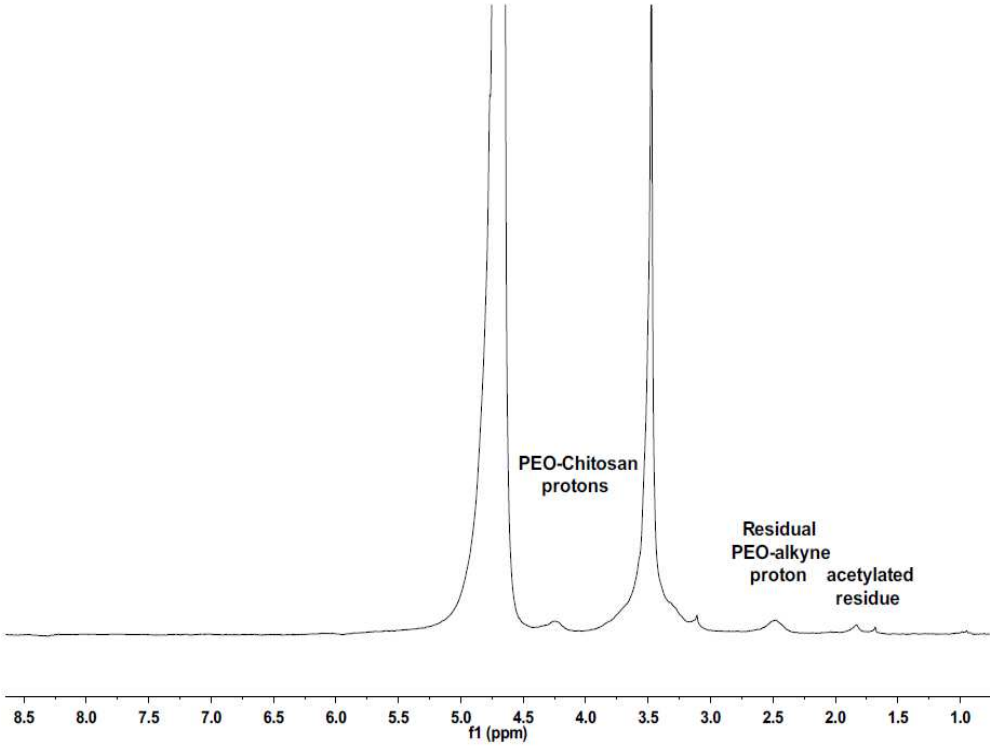

Fig. 4.19 ^{1}H-NMR spectrum of PEO-cross-linked-Chitosan-NH_2 with proton assignment

4.4.5 Swelling behaviour preliminary study

As already described, the NH_2 deprotection product was almost colorless powder. In order to explore possible application in hydrogel preparation the PEO-cross-linked-Chitosan-NH_2 powder was extracted with water/acetic acid mixture 5/1 v/v to purify cross-linked network from residual free chain. No weight decreasing was observed after acidic extraction. Therefore were prepared two tablets using PEO-cross-linked-Chitosan-NH_2. These two tablets were dropwise hydrated, dried with absorbent paper and was monitored their weight during 10 hours. This survey showed a 940% mass average increase, confirming the potentials in hydrogel preparations

4.5 1-3 Huisgen cycloaddition in aqueous environment: charged α-chymotrypsin-PEG methacrylate conjugates

So far have been reported applications of synthetic strategy developed in this research work only for the synthesis of biomaterials in organic solvents. In paragraph 4.2 of this chapter has been described the importance of polymer-protein conjugates in mantaining the protein three-dimensional structure and to avoid any degradation or elimination phenomenon. In this part of research project was developed a click chemistry strategy based on 1-3 Huisgen cycloaddition to modify polymer moieties of conjugates α-chymotrypsin-PEG methacrylate, inserting ionisable groups, and to study the influence of these modification on final conjugates activity. This work was carried out in collaboration with Jean Cristophe Leroux research team, supervised by Dott. Marc Andre Gauthier from ETHZ

In professor Leroux laboratory has been already studied the influence of comb-like PEG chain obtained polymerizing PEG methacrylate (PEG-MA) on conjugates activity, using α-chymotrypsin as ATRP initiator (Atom Transfer Radical Polymerization) and taking in account different parameters like:

• Number of polymer chain in the conjugate

• Different molecular weight monomer (PEG MA 188 u.m.a, 300 u.m.a, 475 u.m.a., 1100 u.m.a.)

• Degree of polymerization

These studies show that the polymer cannot be considered as an inert entity, on the contrary, can strongly influence conjugate activity toward different substrate such as a protein, an amino acid or a peptide[90]. In particular has been found that the polymer moiety gives to conjugate a “molecular sieves” capacity, in fact the activity toward amino acid was found to be also ten times higher than towards

protein substrate and this effect is more pronounced for conjugates with four polymer chains, using PEG_{475}-MA as monomer with a degree of polymerization between 25-40 monomer units. On these bases, it was interesting evaluate the influence of a different parameter such as the presence of charged group on polymer moiety on conjugate activity. In particular α-chymotrypsin-PEG conjugates with azide "clickable" terminal were synthetized. These terminal are useful for coupling of alkyne ionisable groups by 1-3 Huisgen cycloaddition catalyzed by Copper(I). In particular α-chymotrypsin has been functionalized by ATRP initiator to give a macroinitiator for copolymerization of PEG_{475}-MA and Azided triethylenglycol methacrylate properly synthetized. After copolymerization was carried out click coupling in "one pot-two steps" procedure with propargyl alcohol, propargyl amine and propiolic acid simply stopping monomer addition by allyl alcohol, a substrate able to slow dramatically polymerization rate. After purification desired compounds were characterized by NMR, FT-IR, GPC and was evaluated their activity toward amino acid and protein. A synthetic pathway overview was illustrated in figure 4.20

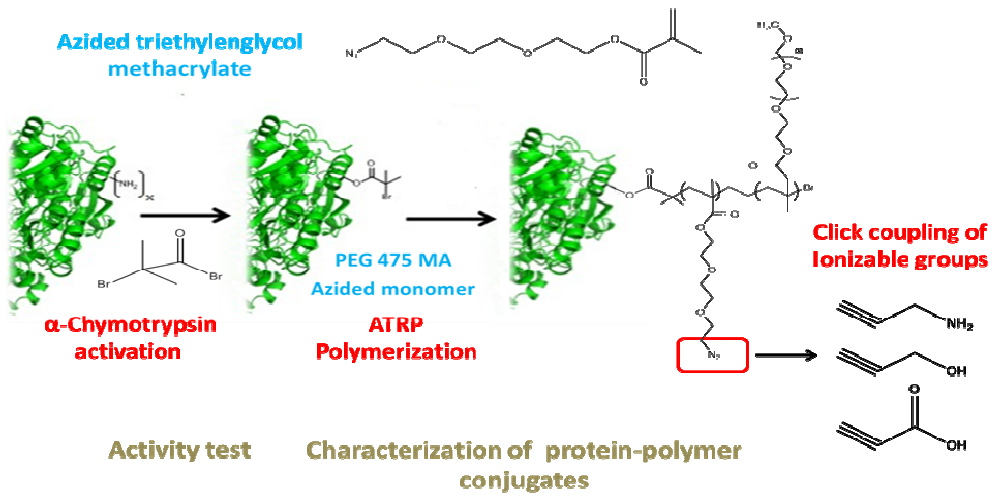

Fig. 4.20 Overview of conjugate synthesis

4.5.1 Synthesis of α-chimotripsin ATRP macroinitiator

Chymotrypsin is a digestive enzyme component of pancreatic juice acting in the duodenum where it performs proteolysis, the breakdown of proteins and polypeptides. Chymotrypsin preferentially cleaves peptide amide bonds where the carboxyl side of the amide bond (the P1 position) is a large hydrophobic amino acid (tyrosine, tryptophan, and phenylalanine).

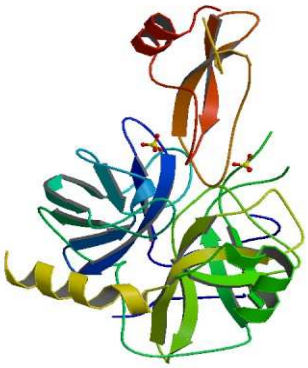

Fig.4.21 Bovine serum α-chymotrypsin crystal structure (RCSB Protein Data Banker)

These amino acids contain an aromatic ring in their sidechain that fits into a 'hydrophobic pocket' (the S1 position) of the enzyme. It is activated in the presence of trypsin. The hydrophobic and shape complementarity between the peptide substrate P1 sidechain and the enzyme S1 binding cavity accounts for the substrate specificity of this enzyme. In vivo, chymotrypsin facilitates the cleavage of peptide bonds by a hydrolysis reaction, which despite being thermodynamically favorable occurs extremely slowly in the absence of a catalyst. The main substrates of chymotrypsin include tryptophan, tyrosine, phenylalanine, leucine, and methionine, which are cleaved at the carboxyl terminal. A secondary hydrolysis will also occur on the C-terminal side of methionine, isoleucine, serine, threonine, valine,

histidine, glycine, and alanine Like many proteases, chymotrypsin will also hydrolyse amide bonds in vitro, a virtue that enabled the use of substrate analogs such as N-acetyl-L-phenylalanine p-nitrophenyl amide for enzyme assays. The synthesis of α-chymotrypsin macroinitiator was carried out starting from native protein and functionalizing Lysine amino groups by 2-Bromo-2 methyl-propionyl bromide according to a protocol already optimized[91]as illustrated in figure 4.22. Have been adopted reaction condition useful to obtain average four initiator points for each protein macroinitiator.

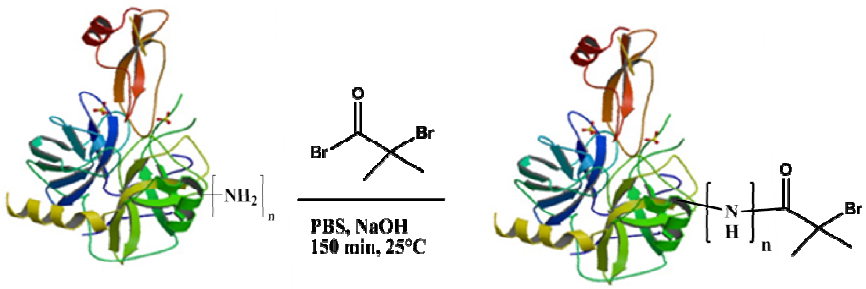

Fig.4.22 Synthesis of α-chymotrypsin macroinitiator

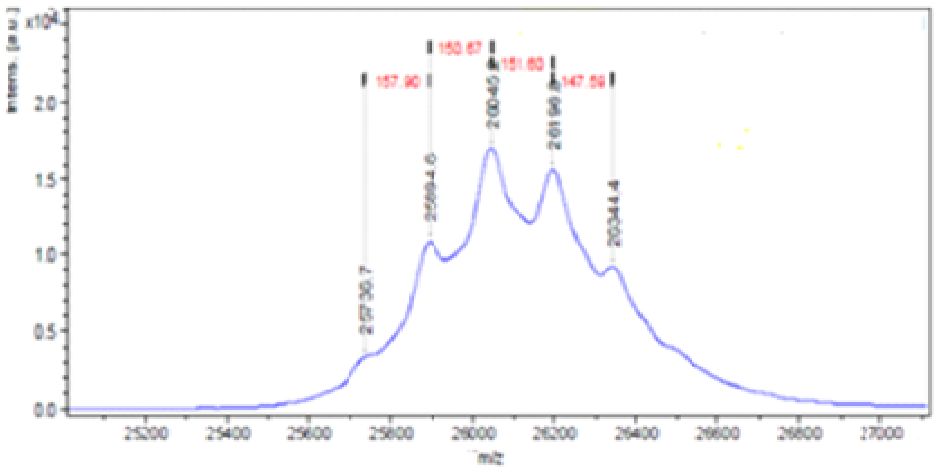

Fig. 4.23 MALDI-TOF analysis of α-chymotrypsin macroinitiator

The average initiators attached to the protein was estimated by MALDI-TOF analysis illustrated in figure 4.23 which evidenced no peak at the native protein m/z (Molecular weight of native protein=25.6 kDa), while five peaks related to functionalized protein. Taking in account that molecular weight of linked initiator group was 150 Da, the distribution of m/z shows a maximum at around 3-4 groups initiators for each protein.

4.5.2 Synthesis of Azided triethylenglycol methacrylate ATRP monomer

The Azided monomer for ATRP copolymerization with commercial PEG_{475}-MA was synthethized starting from Triethylenglycol monochloridine This synthesis provides two steps: the first azidation by Sodium azide followed by the addition of the Methacrylate terminal step by Methacryloyl chloride, as illustrated in figure 4.24

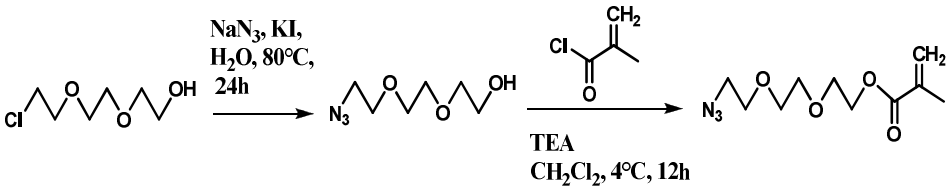

Fig. 4.24 Two step synthesis of azided triethylenglycol methacrylate ATRP monomer

The first step was characterized by a quantitative conversion and yield. After the Methacrylate addition reaction, the crude product was added to a cool (ice bath) 5% $NaCO_3$ solution and the resulting mixture was extracted with ethyl acetate. Organic layer was dried on Sodium Sulphate anhydrous, concentrated and purified by silica gel flash chromatography (ethyl acetate/hexane 50% v/v). The reaction yield was quite low (11%) probably due to liquid extraction from $NaCO_3$ solution of crude product. ^{1}H-NMR analysis was used to confirm the final azided triethylenglycol methacrylate (TEG-MA-azided) purity and chemical structure. In

particular, comparing integrations values of the signals related to the protons CH_2-CH_2-O (d) (δ = 3.70) with those related to -CH_2-OCO protons (e) (δ = 4.20) and with those related to CH_2-N_3(b) (δ = 3.31) (figure 4.25) was evaluated a quantitative conversion of the Triethylenglycol monochloridine

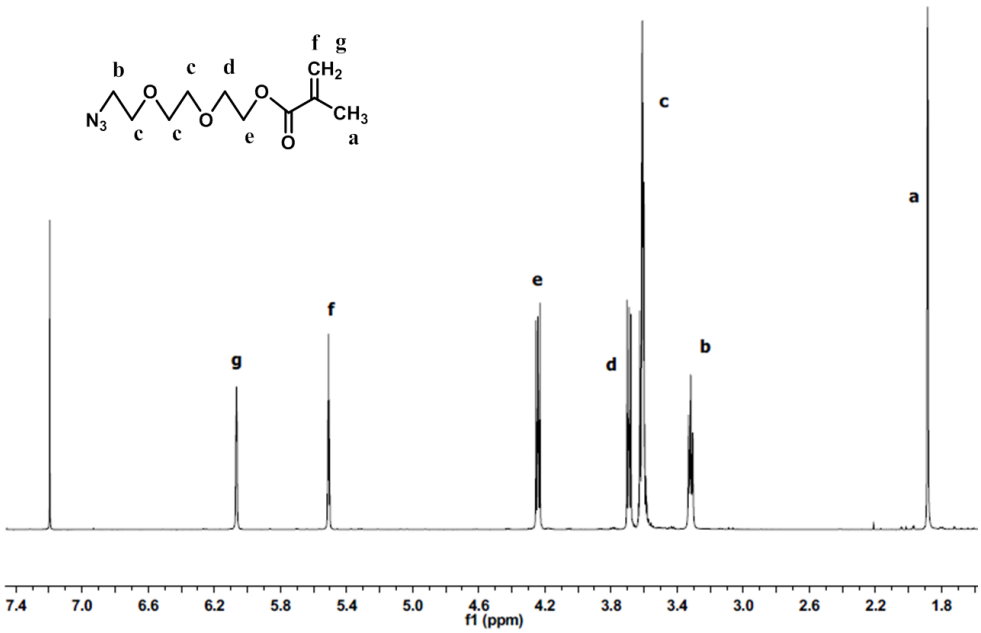

Fig.4.25 1H-NMR of azided triethylenglycol methacrylate ATRP monomer with proton assignment

4.5.3 ATRP Copolymerization and click coupling test

Obtained the azided monomer with a very high grade of purity, it was possible to study copolymerization with PEG_{475}-MA. ATRP has been successfully mediated by a variety of metals, including those from groups 4 (Ti), 6 (Mo), 7 (Re), 8 (Fe, Ru, Os), 9 (Rh, Co), 10 (Ni, Pd) and 11 (Cu)[92]. Complexes of copper have been found to be the most efficient catalysts in the ATRP of a broad range of monomers in diverse media. Similarly to other radical polymerization, a copper(I)

complex is responsible for a homolytic cleavage of an alkyl halide bond (RX) to generate a corresponding copper(II) complex and an organic radical (figure 4.26). The generated radical can then propagate with vinyl monomer (k_p), terminate by either coupling or disproportionation (k_t), or be reversibly deactivated (k_d) by the copper(II) complex to generate halide-capped dormant polymer chain and copper(I) complex. Radical concentration is diminished in ATRP due to persistent radical effect (PRE),18 and the ATRP equilibrium ($K_{ATRP} = k_a/k_d$) is strongly shifted towards dormant species ($k_a << k_d$). As a result, polymers with predictable molecular weights, narrow molecular weight distribution and high functionalities have been synthesized.

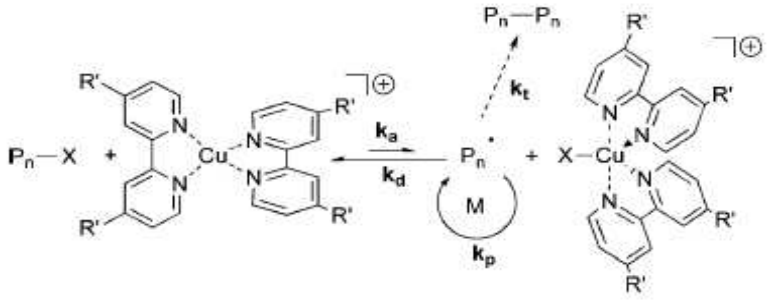

Fig. 4.26 Proposed mechanism for copper/2,2'-bipyridine mediated ATRP.

In order to test feasibility of copolymerization, this reaction was carried out in the same condition used for α-chymotrypsin-PEG-MA conjugates synthetized before in the professor Leroux laboratory, optimizing the amount of catalyst and of monomer to achieve a degree of polymerization between 25-40 monomer units for each initiator group in a reasonable reaction time. Basing on data achieved in a monomer/catalyst screening, it was chosen a 1:200 molar ratio protein initiator groups/monomer and 1:8 molar ratio protein initiator groups/catalyst. The azided monomer is quite hydrophobic and the copolymerization needs of aqueous buffer, for this reason it was decided to add a large amount of PEG_{475}-MA (20% azided monomer 80% PEG-MA on total mol of monomer) to help the dissolution and

avoid phase separation. PEG_{475}-MA, was purified from inhibitor by celite/neutral alumina column then was bubbled with argon and added under argon in 5 mL flask with TEG-MA-azided; α–chymotrypsin macroinitiator was solved in 2 mL of PBS buffer (0.1 M, pH 6.0) bubbled with argon and this solution added to the monomer flask. Solution of monomers and macroinitiator was transferred under argon in catalyst flask containing CuBr, $CuBr_2$, 2-2'-Bipyridil. After 4 hours of stirring in cool room at 4°C, reaction mixture was exposed to air deactivating the catalyst and purified by ultracentrifugation (cutoff tubes membrane≈30 kDa). ^{1}H-NMR in D_2O using the unpurified α-chimotrypsyn-PEG_{475}-TEG-azided conjugate was used to estimate the Degree of polymerization (D.P.). Comparing the decrease of the integrations values related to double bond monomer signals CH_2=C- (f+g) (δ = 5,66 and 6.08) respect those of the PEG terminal methyl CH_3-O-CH_2- (b) (δ = 3.70) in figure 4.28 D.P. ≈40 monomer unit/initiator group was estimated. The presence of azide monomer in polymer chains was verified by FT-IR, monitoring the characteristic azide stretching peaks at 2100 cm^{-1} in conjugate purified by monomer (figure 4.27)

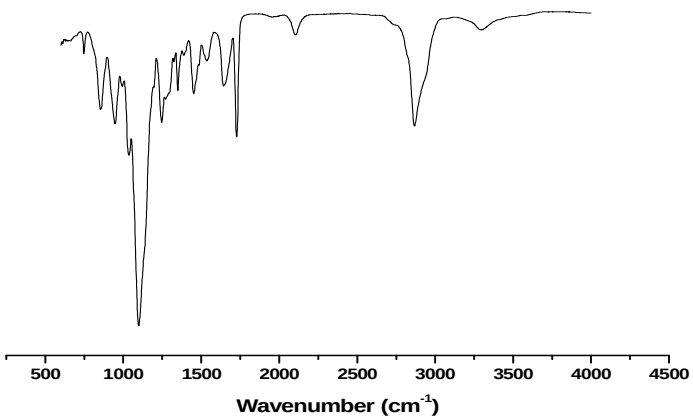

Fig. 4.27 FTIR spectrum of a-chimotrypsyn-PEG_{475}-TEG-azided conjugate

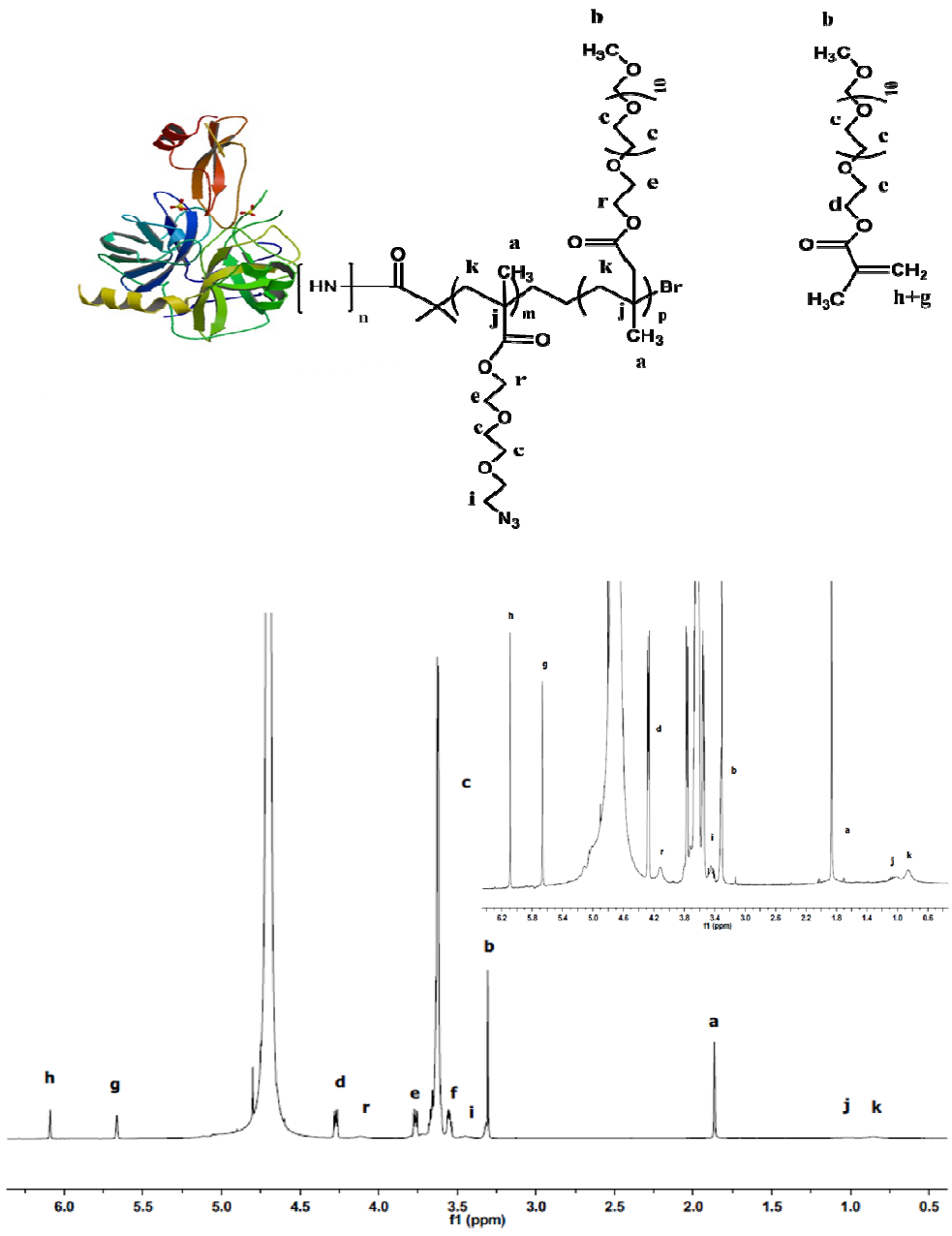

Fig.4.28 [1]H-NMR spectrum of α-chimotrypsyn-PEG$_{475}$-TEG-azided conjugate with proton assignment

A click coupling test was carried out with propargyl alcohol in order to optimize the 1-3 Huisgen cycloaddition reaction conditions. Thus, α-chimotrypsyn-

PEG_{475}-TEG-azided conjugate, propargyl alcohol, Di-isopropyl-ethyl amine (DIPEA), Sodium ascorbate, Copper sulphate, were added under argon in 1.5 mL of aqueous PBS (pH=6, 0.1 M). The mixture was stirred for 12 hours at room temperature and then was purified by ultracentrifugation. Purified product was freeze-dried and analysed by FT-IR. The figure 4.29 shows a complete disappearance of the characteristic azide stretching peaks at 2100 cm^{-1}, evidencing a quantitative coupling.

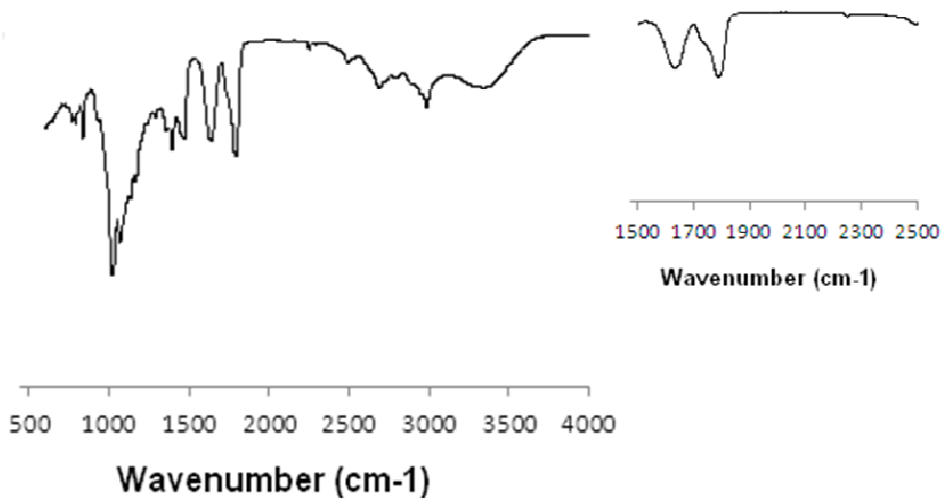

Fig. 4.29 FTIR spectrum of a-chimotrypsyn-PEG_{475}-TEG conjugate after 1-3Huisgen cycloaddition with propargyl alcohol

4.5.4 Smart synthesis of charged conjugates

Verified the successful of the two separated steps, ATRP copolymerization and click coupling, was developed a protocol trying to unify the reactions in one pot two steps synthesis. Both the copolymerization and click coupling, in fact, are catalysed by Cu(I) and other reagent in first reaction do not interfere with coupling. The main problem was stopping the monomer addiction after achieving desired degree of polymerization. To obviate this drawback, was added allyl alcohol as

monomer in polymerization batch. This alcohol can dramatically slow reaction rate closer to total stop[93]. Using this skill, the synthesis was carried out as described in figure 4.30

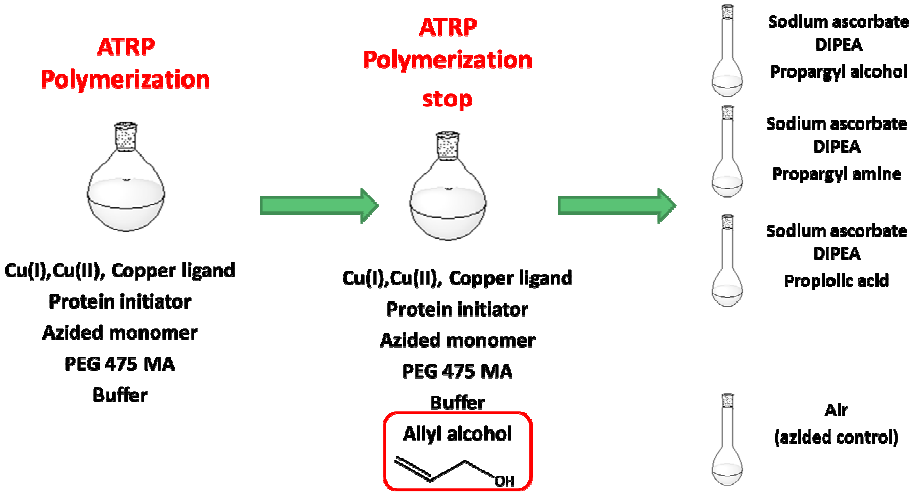

Fig. 4.30 Schematic synthetic protocol for synthesys of charged conjugates

In the first bottle were added all reactive for polymerization, when desired D.P. is achieved polymerization was "stopped" by the allyl alcohol addition. Then reaction mixture was divided in four portions: three for click coupling and another one, exposed to air to deactivate the catalyst, to control the azidation grade. With this smart protocol were synthetized and characterized charged conjugates starting from the protein macroinitiator with four initiator points. After 12 hours of stirring

at room temperature the three click coupling samples and the Azido control were purified by ultracentrifugation (cutoff tubes membrane≈30 kDa). ^{1}H-NMR in D_2O analysis on unpurified conjugate before and after allyl alcohol addition was used to estimate D.P. Comparing the decrease of the integrations values related to double bond monomer signals CH_2=C- (f+g) (δ = 5,66 and 6.08) respect those of the PEG terminal methyl CH_3-O-CH_2- (b) (δ = 3.70) both in the spectrum illustrated in figure 4.31 and in that illustrated in figure 4.32 D.P. ≈14 monomer

unit/initiator group was estimated. The quantitative analysis of the azide group present in polymer chains was obtained from FT-IR and NMR data.

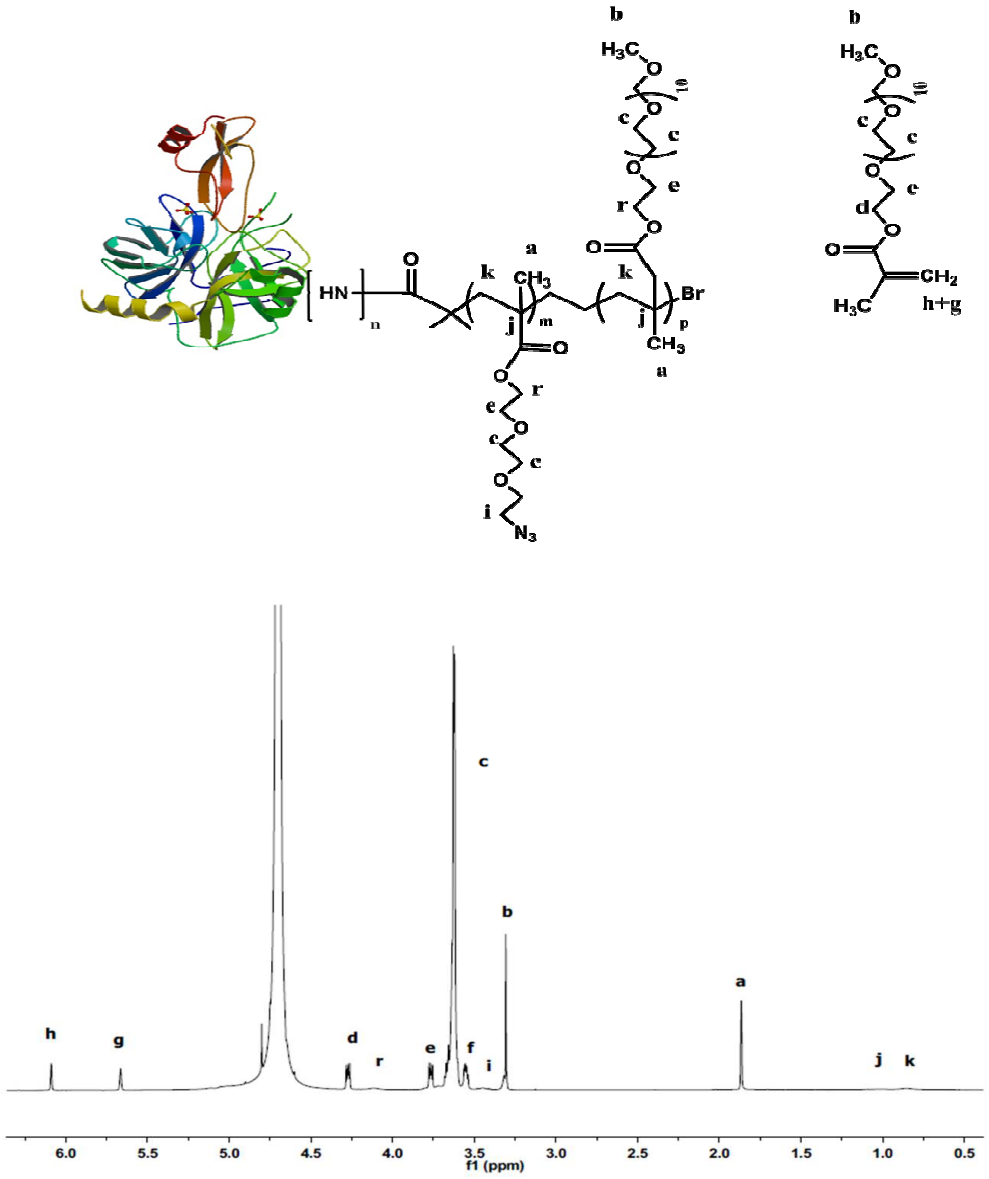

Fig.4.31 ^{1}H-NMR spectrum of α-chimotrypsyn-PEG$_{475}$-TEG-azided conjugate before allyl alcohol addition with proton assignment

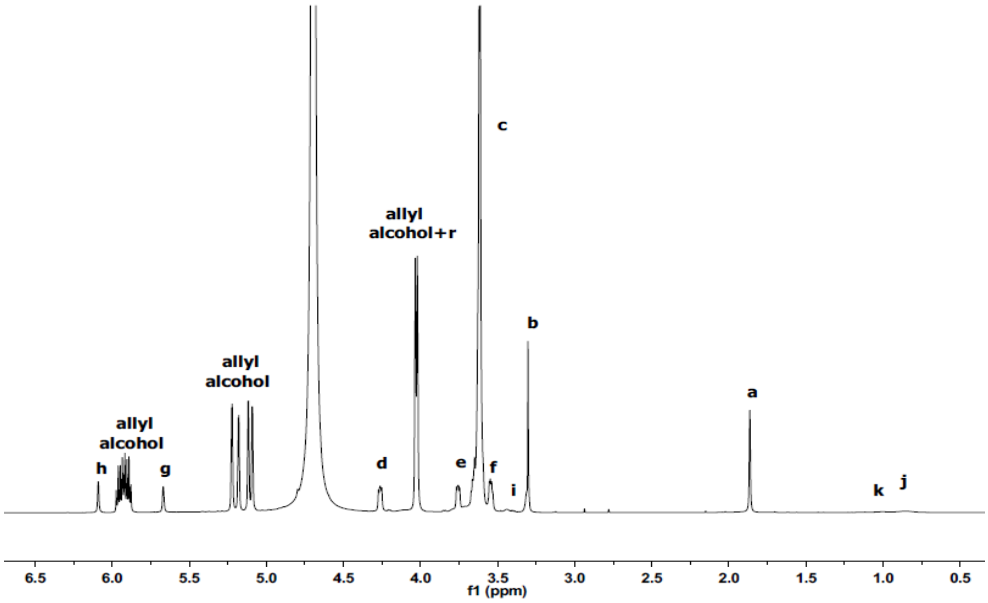

Fig.4.32 ^{1}H-NMR spectrum of α-chimotrypsyn-PEG$_{475}$-TEG-azided conjugate after allyl alcohol addition with proton assignment

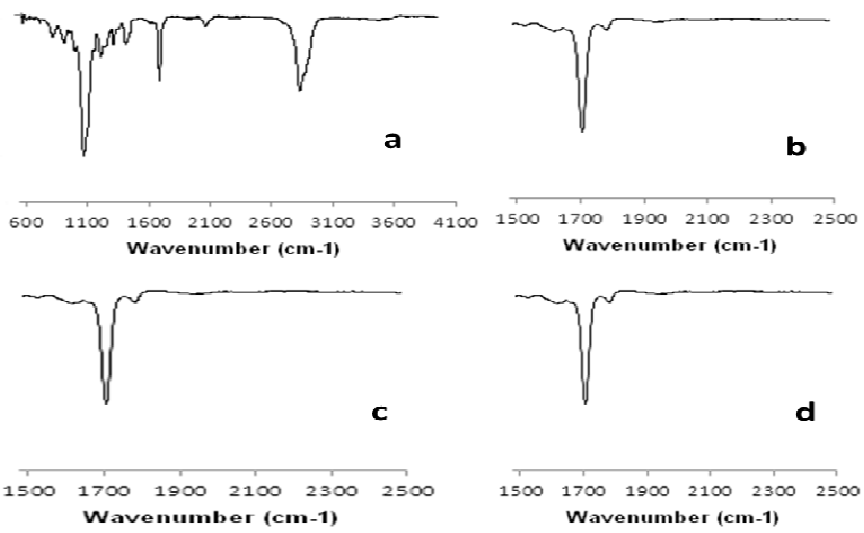

Fig 4.33 FTIR spectra of α-chimotrypsyn-PEG$_{475}$-TEG conjugates synthetized with one pot-two steps protocol after monomers purification: a) azided control, b)propargyl alcohol sample, c)propargyl amine sample, d) propiolic acid sample

FT-IR analysis carried out after monomers purification confirmed the presence of the characteristic azide stretching peaks at 2100 cm^{-1} in the azided control sample and complete disappearance of this signal, evidencing complete conversion, in all three click coupling samples (propargyl alcohol, propargyl amine, propiolic acid) (figure 4.33). Starting from this evidence, more detailed ^{1}H-NMR analysis (512 scans) were carried out to quantitatively define the azided and, consequently after click coupling, charged chains in the conjugates polymer moiety. In particular, were checked integrations of signals related to the α-azide methylene group in the spectra of azided control sample and the propargyl alcohol clicked one before and after monomers purification. After polymerization in unpurified azided control conjugate spectrum the signal related to α-azide methylene group appear as showed in figure 4.34: it is possible to distinguish at δ=3.4-3.45 the triplet signal due to methylene and a shoulder. In purified azided-conjugate (figure 4.35) the triplet and the shoulder become a single collapsed signal. Comparing the integrations related to the single collapsed signal in azided control (δ=-3.47) with those related to same signal in the propargyl alcohol clicked conjugate was found a significant decrease of integration in the last sample. After click coupling reaction in propargyl alcohol clicked conjugate the integration of this single signal decrease because α-azide methylene reacted to give triazole. (the signal at δ= 8.00 in figure 4.36) The resulting decreased integration value can be considered as only contribution of the shoulder to the single collapsed signal, taking in account FTIR data which no evidenced in propargyl alcohol clicked conjugate the characteristic azide stretching signal. Subtracting the contribute of the shoulder to the single collapsed signal was possible to quantify polymer moiety azided chains as 25% of the total. This value represents also the amount of charged groups into conjugates, considering quantitative conversion degree of click coupling reaction

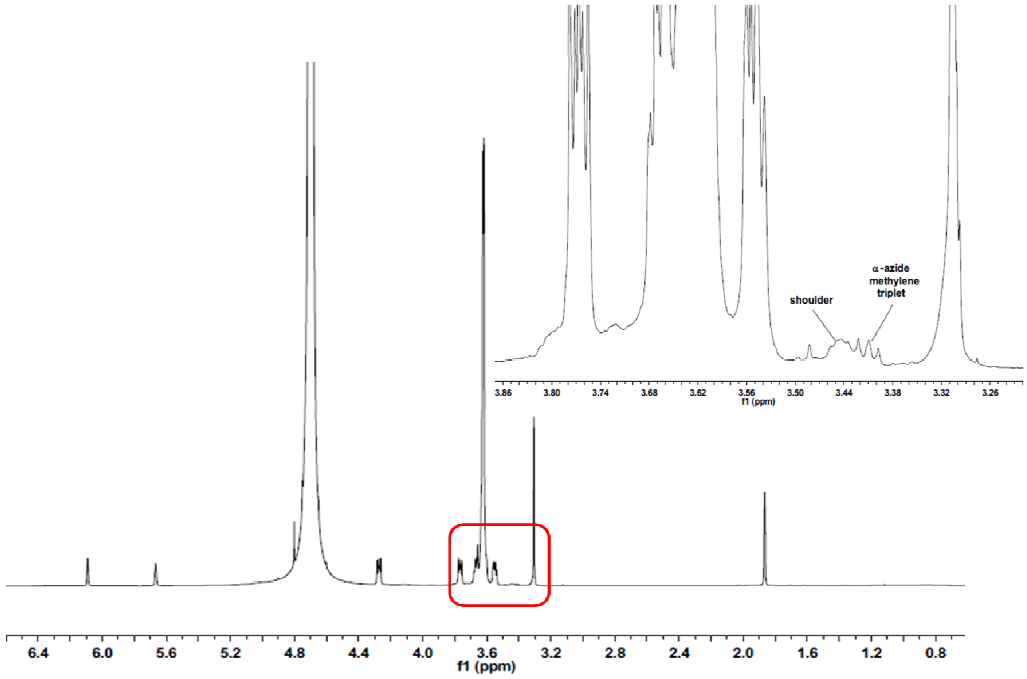

Fig.4.34 ^{1}H-NMR spectrum (512 scans.)of the azided control conjugate before monomers purification

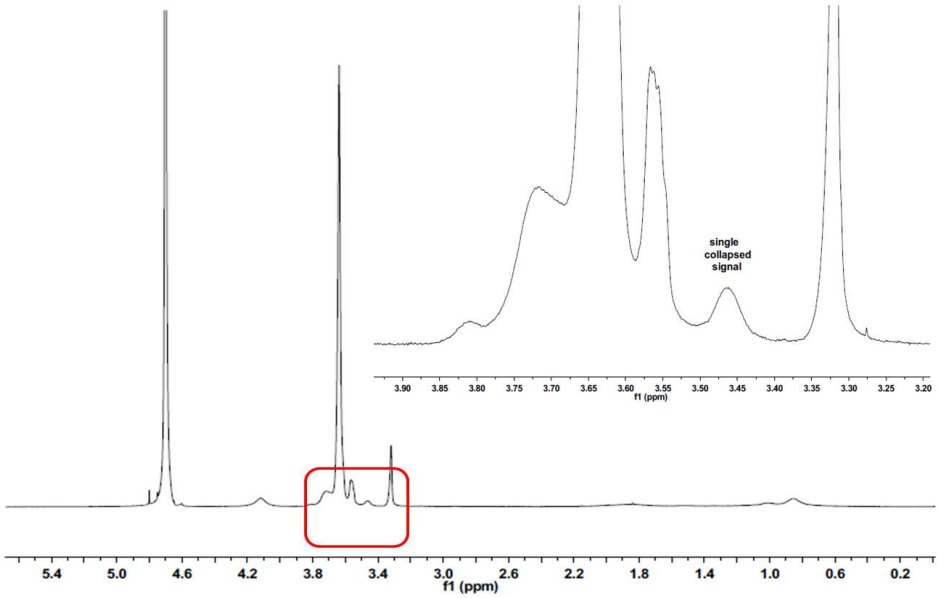

Fig.4.35 ^{1}H-NMR spectrum (512 scans.)of the azided control conjugate after monomers purification

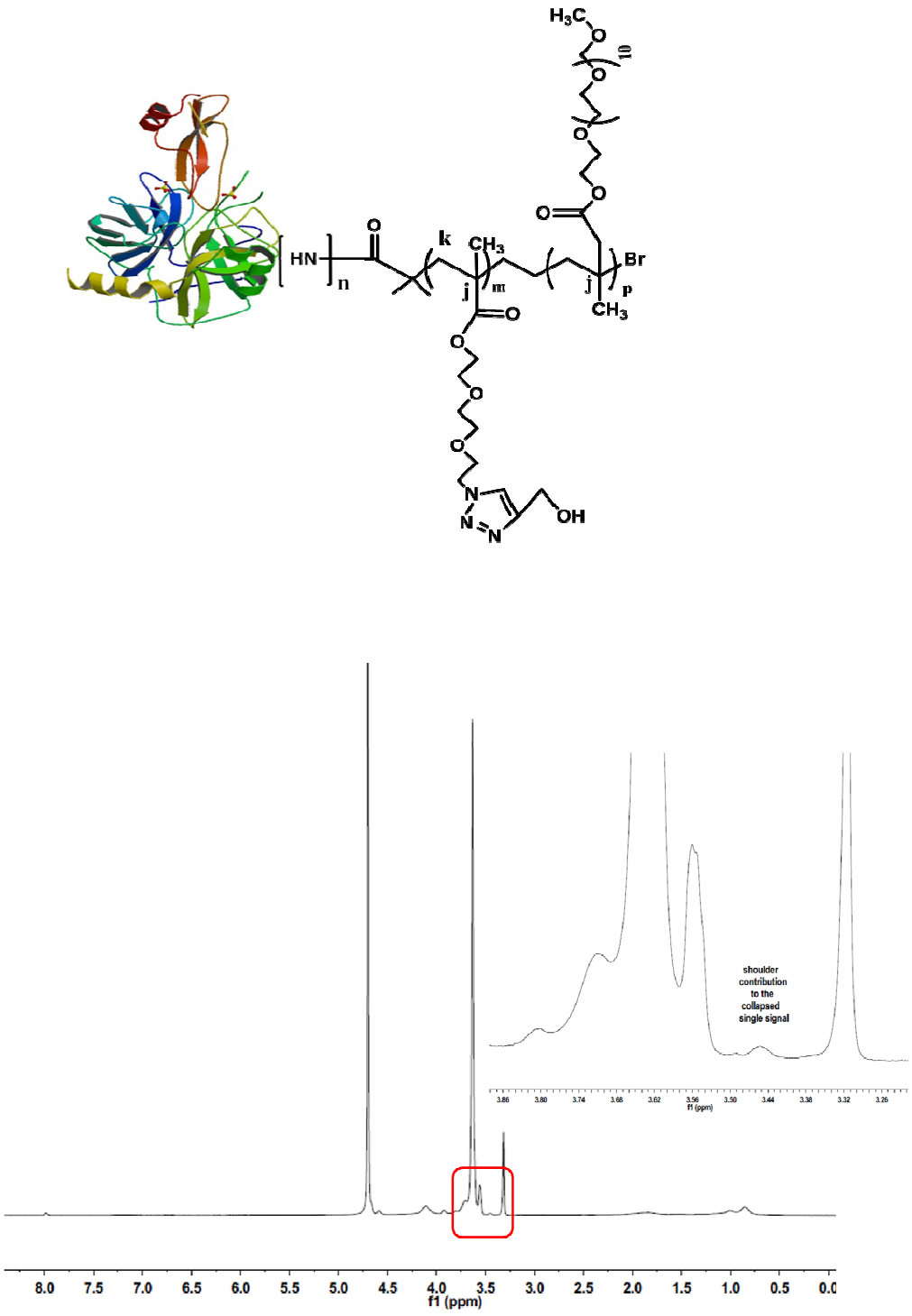

Fig.4.36 [1]H-NMR spectrum (512 scans.)of the propargyl alcohol clicked conjugate after monomers purification; at δ=8.00 can be noted characteristic triazole proton signal

4.5.5 GPC analysis of the synthetized conjugates

All the synthetized conjugates were analysed by GPC (Gel Permeation Cromatography) to check molecular weights distribution of polymer moiety as illustrated in figures 4.37-4.40

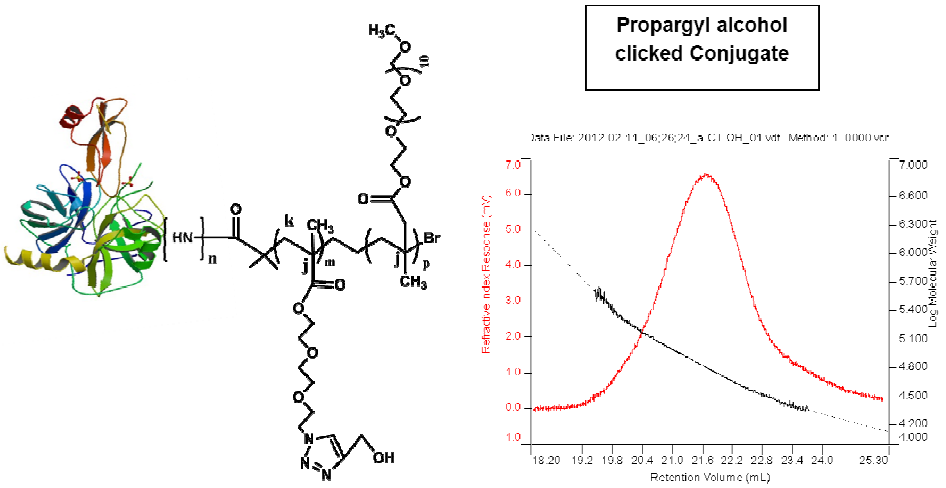

Fig. 4.37 GPC analysis of the propargyl alcohol clicked conjugate

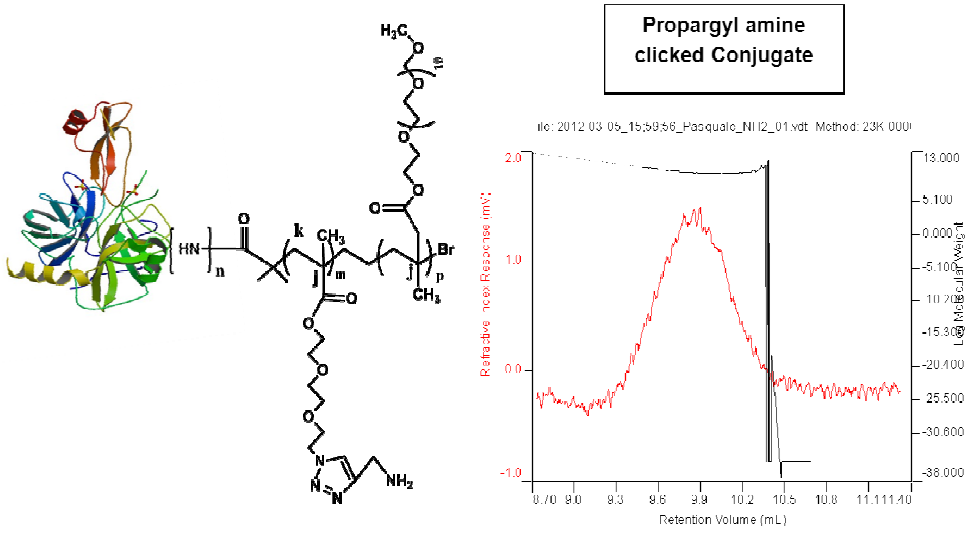

Fig. 4.38 GPC analysis of the propargyl amine clicked conjugate

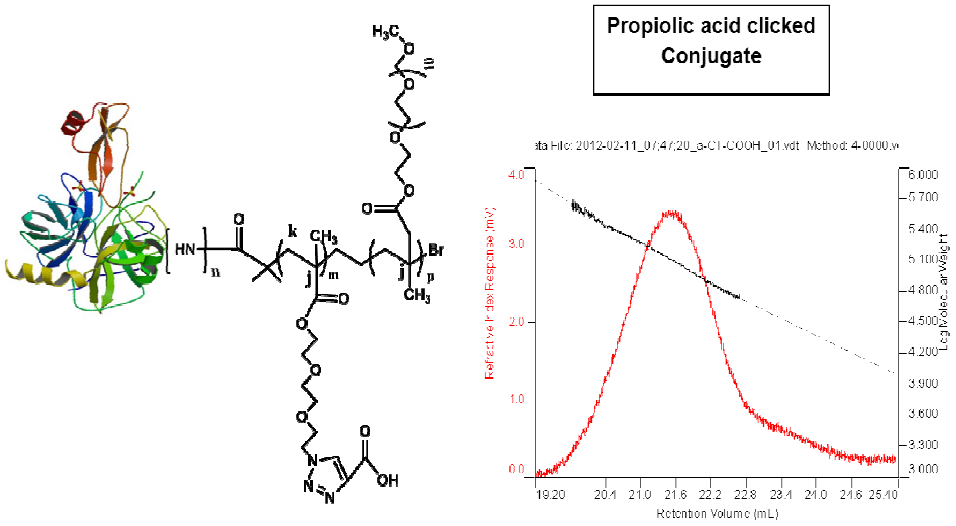

Fig. 4.39 GPC analysis of the propiolic acid clicked conjugate

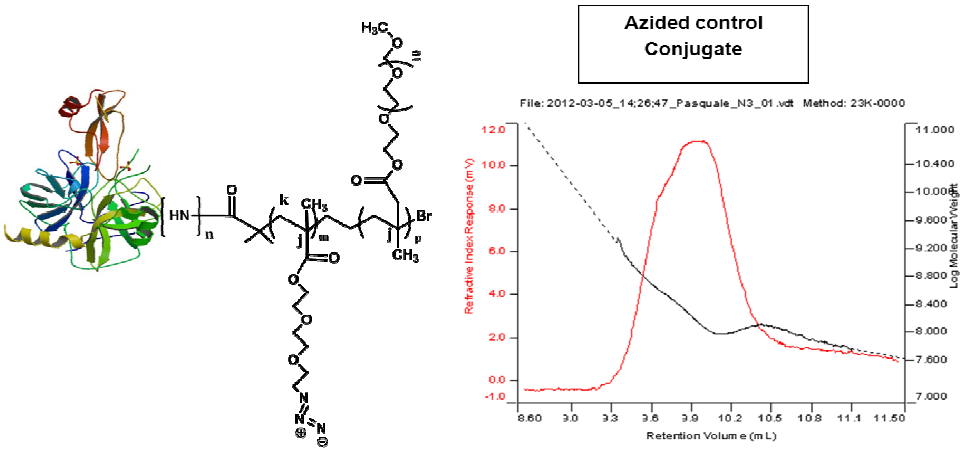

Fig. 4.40 GPC analysis of the azided control conjugate

All synthetized conjugates GPC analysis evidenced a monomodal regular distribution of molecular weights, confirming successful outcome of ATRP copolymerization.

4.5.6 Charged Conjugates activity tests

The activity tests with the synthetized conjugates were carried out by UV measurements following a protocol optimized in prof. Leroux laboratory. Was tested the activity of all conjugates synthetized toward a protein (casein) and amino acid(N-Benzoyl-L-tyrosine p-nitroanilide) and was compared with activity of native protein taken as standard, as illustrated in figures 4.41 and 4.42

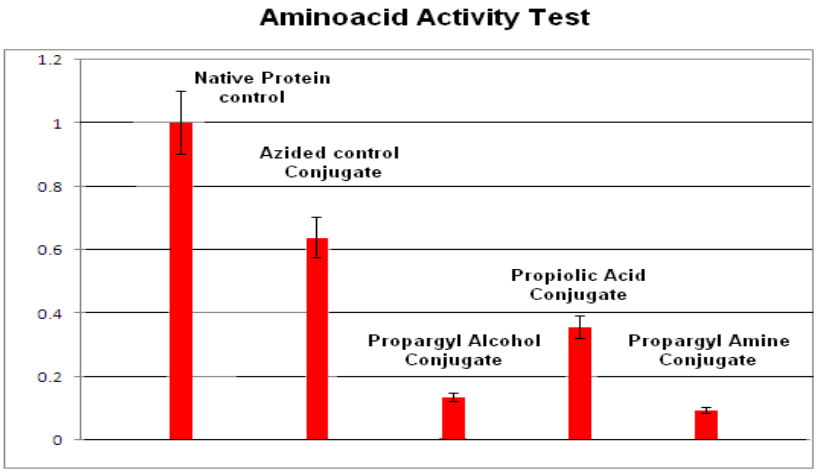

Fig. 4.41 Activity test with amino acid (N-Benzoyl-L-tyrosine p-nitroanilide)

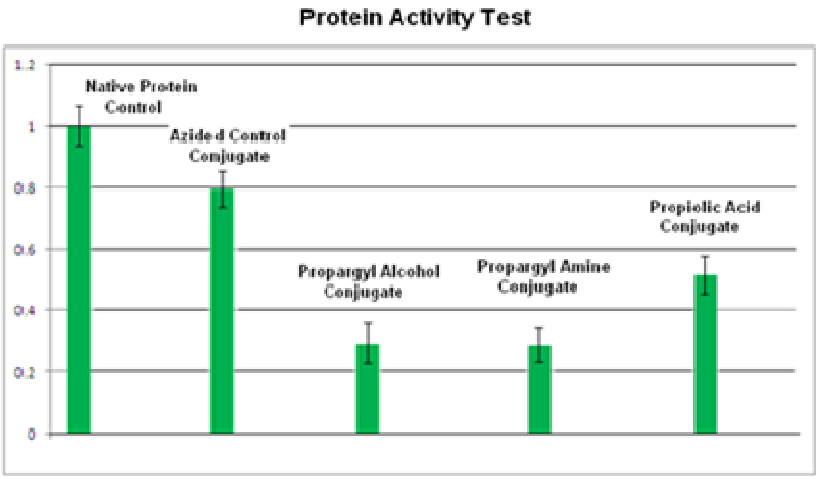

Fig. 4.42 Activity test with protein (casein)

As regard Benzoyl-l-tyrosine *p*-nitroanilide (BT*p*NA) test, to solutions of αCT or αCT–polymer charged conjugates (0.1 mg.mL^{-1} protein) in 200 µL 100 mM Tris buffer (pH 8) in a 96-well plate was added 50 µL of a solution of BT*p*NA (1 mg.mL^{-1}) in DMF at room temperature or 37 ºC. The evolution of absorbance at 412 nm was recorded over 3 minutes and the activity calculated from the initial slope. While in Milk casein test, to solutions of αCT or αCT–polymer charged conjugates (0.1 mg.mL^{-1} protein) in 100 µL 100 mM Tris buffer (pH 8) in Eppendorf vials was added 1 mL of a casein suspension (10 mg.mL^{-1}) and the mixture incubated at room temperature or 37 ºC. After 20 min, the reaction was stopped with 200 µL of 50% trichloroacetic acid in water. The precipitate was removed by centrifugation at 4 ºC and the absorbance of 200 µL of supernatant at 280 nm measured. All the synthetized conjugates show a decreasing of protein catalytic activity both toward amino acid and protein. Loss of activity seems to be less pronounced in the protein test, probably due to lower charge density and consequent ionic repulsion of the protein compared to aminoacid. The azided Control shows an higher catalytic activity respect clicked conjugates both in protein and aminoacid test. This phenomenon could be explained considering tha the polymer moiety intra-chains repulsion due to triazole formation can influence the protein tridimensional structure, disturbing the interaction of the substrate with the catalytic site.

References

[1] K.V. Harish Prashanth, R.N. Tharanathan, *Trends in Food Science & Technology* 18 (2007) 117.

[2] F. Shahidi, J.K.V. Arachchi, Y.-J. Jeon, *Trends in Food Science & Technology* 10 (1999) 37

[3] G. Crini, *Progress in Polymer Science* 30 (2005) 38.

[4] G. Crini, P.-M. Badot, *Progress in Polymer Science* 33 (2008) 399.

[5] D.J. Macquarrie, J.J.E. Hardy, *Industrial & Engineering Chemistry Research* 44 (2005) 8499.

[6] H. Yi, L.-Q. Wu, W.E. Bentley, R. Ghodssi, G.W. Rubloff, J.N. Culver, G.F. Payne, *Biomacromolecules* 6 (2005) 2881

[7] Sunil A. Agnihotri, Nadagouda N. Mallikarjuna and Tejraj M. Aminabhavi (2004). "Recent advances on chitosan-based micro- and nanoparticles in drug delivery" (PDF). Journal of Controlled Release 100 (1): 5–28

[8] Kean T, Roth S, Thanou M (2005). "Trimethylated chitosans as non-viral gene delivery vectors: cytotoxicity and transfection efficiency". J Control Release 103 (3): 643–53.

[9] Journal of Emergency Medicine: 74–81. January 2008.

[10] Pusateri, A. E., S. J. McCarthy, K. W. Gregory, R. A. Harris, L. Cardenas, A. T. McManus & C. W. Goodwin Jr. (2003). "Effect of a chitosan-based hemostatic dressing on blood loss and survival in a model of severe venous hemorrhage and hepatic injury in swine". Journal of Trauma 4 (1): 177–182

[11] Kobayashi, S.; Uyama, H.; Kimura, S. *Chem. Rev*. 2001, 101, 3793–3818

[12] Jahn, M.; Stoll, D.; Warren, R. A. J.; Szabo, L.; Singh, P.; Gilbert, H. J.; Ducros, V. M.-A.; Davis, G. J.; Withers, S. G. *Chem. Commun*. 2003, 1327–1329.

[13] K. Kurita, *Progress in Polymer Science* 26 (2001) 1921.

[14] V.K. Mourya, N.N. Inamdar, *Reactive and Functional Polymers* 68 (2008) 1013

[15] J. Berger, M. Reist, J.M. Mayer, O. Felt, N.A. Peppas, R. Gurny, *European Journal of Pharmaceutics and Biopharmaceutics* 57 (2004) 19

[16] R. Jayakumar, M. Prabaharan, R.L. Reis, J.F. Mano, *Carbohydrate Polymers* 62 (2005) 142

[17] H.T. Ta, C.R. Dass, D.E. Dunstan, *Journal of Controlled Release* 126 (2008) 205

[18] A. Di Martino, M. Sittinger, M.V. Risbuda, *Biomaterials* 26 (2005) 5983

[19] J. Berger, M. Reist, J.M. Mayer, O. Felt, N.A. Peppas, R. Gurny, *European Journal of Pharmaceutics and Biopharmaceutics* 57 (2004) 19.

[20] G. Crini, *Progress in Polymer Science* 30 (2005) 38

[21] G. Crini, P.-M. Badot, *Progress in Polymer Science* 33 (2008) 399.

[22] K. Kurita, H. Ikeda, Y. Yoshida, M. Shimojoh, M. Harata, *Biomacromolecules* 3 (2002) 1.

[23] R. Makuska, N. Gorochovceva, *Carbohydrate Polymers* 64 (2006) 319.

[24] N. Gorochovceva, R. Makuska, *European Polymer Journal* 40 (2004) 685

[25] M.N. Khalid, L. Ho, J.L. Agnely, J.L. Grossiord, G. Couarraze, *STP Pharma Sciences* 9 (1999) 359.

[26] V.R. Patel, M.M. Amiji, *Pharmaceutical Research* 13 (1996) 588

[27] A.S. Aly, *Angewandte Makromolekulare Chemie* 259 (1998) 13

[28] K. Yamada, T.H. Chen, G. Kumar, O. Vesnovsky, L.D.T. Topoleski, G.F. Payne, *Biomacromolecules* 1 (2000) 252

[29] E.B. Denkbas, M. Seyyal, E. Piskin, *Journal of Membrane Science* 172 (2000) 33.

[30] S. Dumitriu, P.F. Vidal, E. Chornet, *Polysaccharides in Medicinal Applications*, vol. 1, Marcel Dekker, New York, 1999.

[31] M.S. Chiou, P.Y. Ho, H.Y. Li, *Dyes Pigments* 60 (2004) 69

[32] W.S. Wan Ngah, C.S. Endud, R. Mayanar, *Reactive & Functional Polymers 50* (2002) 181

[33] M.S. Chiou, H.Y. Li, *Chemosphere* 50 (2003) 1095.

[34] F.L. Mi, S.S. Shyu, C.T. Chen, J.Y. Lai, *Polymer* 43 (2002) 757.

[35] A.A. De Angelis, D. Capitani, V. Crescenzi, *Macromolecules* 31 (1998) 1595.

[36] S. Hirano, R. Yamaguchi, N. Fukui, M. Iwata, *Carbohydrate Research* 201 (1990) 145.

[37] F.L. Mi, H.W. Sung, S.S. Shyu, *Journal of Polymer Science – Polymer Chemistry* 38 (2000) 2804

[38] G. Crini, *Progress in Polymer Science* 30 (2005) 38

[39] G. Crini, P.-M. Badot, Progress in Polymer Science 33 (2008) 399

[40] H.C. Kolb, M.G. Finn, K.B. Sharpless, *Angewandte Chemie International Edition* 40 (2001) 2004

[41] H.C. Kolb, K.B. Sharpless, *Drug Discovery Today* 8 (2003) 1128.

[42] C.W. Tornøe, C. Christensen, M. Meldal, *Journal of Organic Chemistry* 67 (2002) 3057.

[43] V.V. Rostovtsev, L.G. Green, V.V. Fokin, K.B. Sharpless, *Angewandte Chemie International Edition* 41 (2002) 2596

[44] R.A. Evans, *Australian Journal of Chemistry* 60 (2007) 384

[45] W.H. Binder, R. Sachsanhofer, *Macromolecular Rapid Communications* 28 (2007) 15.

[46] W.H. Binder, *Macromolecular Rapid Communications* 29 (2008) 951.

[47] T. Hasegawa, M. Umeda, M. Numata, T. Fujisawa, S. Haraguchi, K. Sakurai, S. Shinkai, *Chemistry Letters* 35 (2006) 82

[48] T. Hasegawa, M. Umeda, M. Numata, C. Li, A.H. Bae, T. Fujisawa, S. Haraguchi, K. Sakuraib, S. Shinkai, *Carbohydrate Research* 341 (2006) 35

[49] M. Pohl, J. Schaller, F. Meister, T. Heinze, *Macromolecular Rapid Communications* 29 (2008) 142

[50] J. Hafrén, W. Zou, A. Córdova, *Macromolecular Rapid Communications* 27 (2006) 1362

[51] J. Bernard, M. Save, B. Arathoon, B.J. Charleux, *Journal of Polymer Science – Polymer Chemistry* 46 (2008) 2845.

[52] P.F. Tankam, R. Müller, P. Mischnick, H. Hopf, *Carbohydrate Research* 342 (2007) 2049.

[53] V. Crescenzi, L. Cornelio, C. Di Meo, S. Nardecchia, R. Lamanna, Biomacromolecules 8 (2007) 1844.

[54] E. Lallana, E. Fernandez-Megia, R. Riguera, *Journal of the American Chemical Society* 131 (2009) 5748

[55] B.G. De Geest, W. Van Camp, F.E. Du Prez, S.C. De Smedt, J. Demeester, W.E. Hennink, *Chemical Communications* (2008) 190.

[56] C. Schatz, S. Louguet, J.-F. Le Meins, S. Lecommandoux, *Angewandte Chemie International Edition* 48 (2009) 2572.

[57] E. Fleury, M. Tizzotti, M. Destarac, M.-P. Labeau, T. Hamaide, E. Drockenmuller, European Patent WO2009063082 A1 (22/05/2009)

[58] G. Zampano et al, *Reactive & Functional Polymers* 70 (2010) 272–281

[59] R. Kulbokaite, G. Ciuta, M. Netopilik, R. Makuska, *Reactive and Functional Polymers* 69 (2009) 771.

[60] Rinsdorf, H.; J. Polym. Sci., 1975, 51, 135

[61] Pettit D. K., Gombotz W. R., Bioconjugate Chem., 1995, 6, 332

[62] Thordarson, P., Droumaguet, B. L., Velonia, K., Appl. Microbiol. Biotechnol., 2006, 73, 243

[63] Matsushima, A., Nishimura, H., Ashihara, Y., Yokota, Y., Inada, Y., *Chem. Lett*., 1980, 773

[64] Velonia, K., Rowan, A. E., Nolte, R. J. M., *JACS*, 2002, 124, 4224

[65] Stayton, P.S., Shimoboji, T., Long, C., Chilkoti, A., Chen, G., Harris, J.M., Hoffman, A.S., *Nature*, 1995, 378, 472

[66] Li, J. T., Carlsson, J., Lin, J. N., Caldwell, K. D., *Bioconjugate Chem*., 1996, 7, 592

[67] Joshi, N. S., Whitake, L. R., Francis, M. B., *JACS*, 2004, 126, 15942

[68] Tilley, S.D., Francis, M.B., *JACS*, 2006, 128, 1080

[69] Saxon E., Armstrong, J.I., Bertozzi, C.R., *Org. Lett*., 2002, 2, 2141

[70] Kiick, K.L., Saxon, E., Tirell, D.A., Bertozzi, C.R., *Proc. Natl. Acad. Sci.* USA, 2002, 99, 19

[71] Buckmann, A.F., Carrea, G., *Adv. Biochem. Eng. Biotechnol*, 1989, 39, 97

[72] In Controlled/Living Radical Polymerization; Matyjaszewski, K.; ACS Symposium Series; American Chemical Society: Washington, DC, 2006

[73] Tomislav Pintauer and Krzysztof Matyjaszewski, Atom transfer radical addition and polymerization reactions catalyzed by ppm amounts of copper complexes *Chem. Soc. Rev*., 2008, 37, 1087–1097 | 1087

[74] Heredia, K.L., Bontempo, D., Ly, T., Byers, J.T., Halstenberg, S., Maynard, H.D., *JACS*, 2005, 16955

[75] Nicolas, J., Miguel, V.S., Mantovani, G., Haddleton, D.M., *Chem. Commun*., 2006, 4697

[76] Bontempo, D., Maynard, H.D., *JACS*, 2005, 127, 6508

[77] G. Pasut and F. M. Veronese, *Prog. Polym. Sci*., 2007, 32, 933–961

[78] F. M. Veronese, *Biomaterials*, 2001, 22, 405–417.

[79] G. Pasut, M. Sergi and F. M. Veronese, *Adv. Drug Delivery Rev*., 2008, 60, 69–78.

[80] G. Pasut and F. M. Veronese, Adv. Drug Delivery Rev., 2009, 61, 1177–1188.

[81] S. Brocchini, A. Godwin, S. Balan, J.-w. Choi, M. Zloh and S. Shaunak, Adv. Drug Delivery Rev., 2008, 60, 3–12.

[82] A. J. de Graaf, M. Kooijman, W. E. Hennink and E. Mastrobattista, *Bioconjugate Chem*., 2009, 20, 1281–1295.

[83] M. A. Gauthier and H.-A. Klok, *Chem. Commun*., 2008, 2591–2611

[84] V. Coessens, T. Pintauer and K. Matyjaszewski, *Prog. Polym. Sci*., 2001, 26, 337–377.

[85] A. J. Link, M. L. Mock and D. A. Tirrell, *Curr. Opin. Biotechnol*., 2003, 14, 603–609.

[86] B. Le Droumaguet and J. Nicolas, *Polym. Chem*., 2010, 1, DOI:

[87] Patricia L. Golas and Krzysztof Matyjaszewski, Click Chemistry and ATRP: A Beneficial Union for the Preparation of Functional Materials, *QSAR Comb. Sci*. 26, 2007, No. 11-12, 1116 – 1134

[88] S. Nishimura, O. Kohgo, L. Kurita, H. Kuzuhara, *Macromolecules* 24 (1991) 4745

[89] Yi Lei , Haoran Li ,* Haihua Pan , and Shijun Han Structures and Hydrogen Bonding Analysis of N,N-Dimethylformamide and N,N Dimethylformamide−Water Mixtures by Molecular Dynamics Simulations *J. Phys. Chem. A*, 2003, 107 (10), pp 1574–1583

[90] Mi Liu, Pasquale Tirino, Milos Radivojevic, Daniel J. Phillips, Matthew I. Gibson, Jean-Christophe Leroux, Marc A. Gauthier, Molecular Sieving on the Surface of a Protein Provides Protection Without Loss of Activity, *Advanced Functional Materials*, published on line 15 NOV 2012

[91] Mi Liu, Pasquale Tirino, Milos Radivojevic, Daniel J. Phillips, Matthew I. Gibson, Jean-Christophe Leroux, Marc A. Gauthier, Molecular Sieving on the Surface of a Protein Provides Protection Without Loss of Activity, *Advanced Functional Materials*, published on line 15 NOV 2012

[92] 17 T. E. Patten and K. Matyjaszewski, *Acc. Chem. Res*., 1999, 32, 895–903

[93] Xinming Tong, Bao-hua Guo and Yanbin Huang, Toward the synthesis of sequence-controlled vinyl copolymers, *Chem. Commun*., 2011, 47, 1455–1457

Chapter 5

Concluding remarks

This research work can be included in the broader context of synthesis and characterization of polymeric biomaterials. In particular, has been developed a synthetic strategy based on click chemistry, in particular on 1-3 Huisgencicloaddition (HDC) between azide and alkyne groups catalysed by Cu(I). The main advantages of this strategy is to be found in the simplicity of the characterization of synthetic intermediates, essentially ^{1}H-NMR and FT-IR, and the possibility to make useful as point of couplig any functional group generally present in polymers such as –OH, -NH_2 or -COOH. The azidation route adopted concern two-step process with azide displacement from methanesulfonate (mesylate) alcohols obtained by mesyl chloride reaction. This process demonstrated to be more performing in macromolecular functionalization regarding milder reaction condition, almost quantitative conversion and selectivity because mesyl is an excellent leaving group, avoiding byproduct problem separation, and simplicity of characterization. Alkyne functionalization was obtained starting from different polymer terminal groups such as hydroxyl, amine or carboxylic. The terminal amine groups were reacted with propargyl chloroformate, in presence of an proton acceptor, to give propargyl carbamate. The terminal hydroxyl were reacted with 4-pentynoic acid by dimethyl amino pyridine (DMAP) and dicyclohexylcarbodiimide (DCC) catalyst to give propargyl ester, while terminal carboxylic groups, by same catalyst, give alkyne-esters with 3-butynol. All these products can be easily characterized by ^{1}H-NMR. The synthetic strategy developed is a very powerful tools employed in different molecular weight range with satisfying results. To simplify the discussion, the results have been summarized in three ranges of molecular weights: low molecular weight from 1000 to 20000 Da, medium from 20000 to 50000 Da and high from 50000 to 200000 Da.

As regard Low molecular weight range were synthetized and characterized amphiphilic diblock copolymer of hydrophobic poly-ε-caprolactone (PCL) and hydrophilic poly(ethylenglycol) (PEG) block with non-linear architecture. Thanks to click coupling strategy has been possible to achieve copolymer with different

architecture and to evaluate the influence of this parameter on copolymer bulk and self-assembly properties. In particular were synthetized diblock PEG_{1000}-PCL_{3000}, triblock PEG_{1000}-PCL_{6000}-PEG_{1000}, miktoarm Y-I-shaped $(PEG_{1000})_2$-PCL_{5800}, miktoarm Y-II-shaped $(PEG_{1000})_2$-PCL_{7200}-PEG_{1000} and miktoarm H-shaped $(PEG_{1000})_2$-PCL_{11000}-$(PEG_{1000})_2$. The molecular and structural characterization of the copolymers were carried out by techniques ^{1}H-NMR, FT-IR, DSC, SEC, and X-ray diffraction It has also been carried out an appropriate evaluation of their potential as biomimetic nanocarriers for targeted and sustained release of bioactive substances by analyzing the characteristics of self-assembly in aqueous systems (in collaboration with research group from the "Dipartimento di ChimicaFarmaceutica e Tossicologica" directed by FabianaQuaglia), determining the size (DLS), the critical aggregation concentration (CAC), the morphology (TEM) and the surface properties of the aggregates. In molecular characterization was observed a very high regularity in structure and composition with monomodal distributions of the products molecular weight. DSC and WAXS showed an huge influence of PCL segments on the PEG segment crystallization in all the copolymers synthetized. In particular was not possible to find crystalline PEG by WAXS analysis. The analysis of water self-assembled nanoaggregates revealed CAC of in the order of 10^{-7} mol L^{-1}, hydrodynamic diameter from 67 to 150 nm and superficial negative Z-potential from 13 to 33 mV. The copolymer architecture has a negligible influence on these nanoaggregates properties, except for hydrodynamic diameter. Was tried an indirect estimation of the PEG shell tickness by Z-potential measurement, evidencing a collapsed PEG shell for Y-shaped copolymers and an intermediate condition between collapsed and fully stretched PEG shell for all other copolymers. The TEM analysis together with ^{1}H-NMR in D_2O on the copolymer nanoaggregates evidenced globular morphology with a very compact PEG shell for the H-shaped copolymer, quite globular but more heterogeneous morphology with quite compact PEG shell for Y-II-shaped copolymer and worm like aggregates for Y-I-shaped with non-compact PEG shell

Furthermore were synthetized folate diblock FOL-PEO_{2000}-PCL_{4000} and rhodamine triblock ROD-PEO_{2000}-PCL_{7000}-PEO_{2000} copolymer with a very high regularity in structure and composition, obtaining a reasonable PEO functionalization degree. A cathechol derivative Diblock PEO_{2000}-PCL_{4000}-CAT was also synthetized with quantitative PCL functionalization degree

Concerning medium molecular weight range, was obtained the quantitative modification of hydroxyl terminal into azide group of a poly(ethyleneoxyde-polystyrene) diblock copolymer used in nano-technological application without modifying the backbone molecular structure of the final product. Was also synthetized poly(lactic-co-glycolic acid)(PLGA) functionalized with rhodamine using hydroxyl terminal of polyester with an high coupling yield. The microspheres obtained with ROD-PLGA were characterized in term of dimension and morphology by Confocal Laser Scanning Microscopy. without fluorescent dye treatment, showing intrinsic fluorescent due to rhodamine moiety and the same properties of microsphere constituted of only PLGA.

In high molecular weight range the developed synthetic strategy was appled in Chitosan chemical modification to obtain a PEO di-alkyne crosslinked chitosan. Has been used the following strategy: NH_2 protection by phthaloylation, regioselective C-6 functionalization with N_3 groups by two-step process via mesyl chloride with 25% of conversion degree, quantitative crosslinking of all azided terminal by cycloaddition with di-alkyne PEO, and hydrazine hydrate final NH_2 deprotection. The obtained crosslinked material with dialkyne PEO was characterized by preliminary swellability tests showing a water weight increase of 940% respect to the starting mass. Last part of high molecular weight section regards 1-3 Huisgen cycloaddition in aqueous environment. In particular was developed, in collaboration with ETHZ research group directed by professor Jean Cristophe Leroux, a smart synthetic strategy one pot-two steps to obtain charged conjugates α-chymotrypsin-PEG methacrylate using “Grafting from” approach by Atom Transfer Radical copolymerization of azided monomer and PEG_{475}-

methacrylate initiated from α-chymotrypsin macroinitiator obtaining a polymerization degree of 14 monomer unit/initiator group estimated by NMR analysis. After stopping copolymerization by allyl alcohol addition, azide groups present in polymer moieties were then coupled by 1-3 Huisgen cycloaddition catalysed by Cu(I) and DIPEA in PBS-water solution using sodium ascorbate as reducing agent with different alkyne ionisable molecules such as propargyl alcohol, propargyl amine and propiolic acid. All the synthetized conjugates was characterized by GPC showing very regular monomodal molecular weight distribution. To evaluate influence of charged polymer coating on α-chymotrypsin activity, were carried out activity test with protein and amino acid substrates. These tests evidenced a sensible loss of catalytic activity of the synthetized conjugates respect to the native protein

The future perspectives related to this research work are linked to a better characterization of material obtained thanks to synthetic strategy developed, such as, for example, more accurate swelling behaviour studies for Chitosan-PEO material or an encapsulation/release hydrophobic drug study for PEO-PCL materials, to implement an operative protocol for pharmaceutical applications.

Chapter 6

Experimental section

6.1 Materials.

Solvents, monomers and chemicals were purchased from Sigma-Aldrich unless otherwise stated. poly(styrene-*b*-ethylenoxide) poly(lactic-co-glycolic) acid, 4-Pentynoic acid, trichloroacetic acid, trifluoroacetic anhydride, 2,2'-bipyridine, methacryloyl chloride, 2-bromoisobutyryl bromide, copper(I) bromide, copper(II) bromide, α-chymotrypsin (αCT) from bovine pancreas, milk casein (sodium salt), *N*-Benzoyl-L-tyrosine *p*-nitroanilide (BT*p*NA), sodium azide (NaN_3), *N*,*N*-diisopropylethylamine (DIPEA), *N*,*N*′-dicyclohexylcarbodiimide (DCC) (1 M solution in methylene chloride), lysine (lys), 4-(dimethylamino) pyridine (DMAP), N,N-dimethylformamide (DMF anhydrous, inhibitor free), tetrahydrofuran (THF, anhydrous, inhibitor free), propargyl chloroformate (PCF) and methane sulfonyl chloride (Mes-Cl), Rhodamine B, Folic acid, 3-hydroxy-tyramine hydrobromide, Triethylenglycol monochloridine were used as received. Tin(II) (2-ethylhexanoate)$_2$ (Sn(oct)$_2$ was distilled under vacuum and stored in inert atmosphere. Bromotris(triphenylphosphine)Cu(I), Br-Cu(P(ph)$_3$)$_3$, was stored under argon in a glove-box. 1,4-Dibromo-2-butanol (85%) was purified by column chromatography on silica gel with chloroform/methanol 95/5 v/v as eluent (98% purity checked by GC-MS). ε-Caprolactone (CL, Fluka) was distilled from CaH_2 under vacuum and stored over molecular sieves in inert atmosphere. α-Metoxy, ω-hydroxy-poly(ethylene glycol) (*m*-PEG$_{1000}$-OH, M_n =1,0 kDa *m*-PEO$_{2000}$-OH M_n =2,0 kDa, from Cleriant), α-ω-di-hydroxy-poly(ethylene-oxyde) (HO-PEO$_{6000}$-OH, M_n =6,0 kDa from Fluka) were dehydrated by azeotropic distillation with dry toluene in a Dean-Stark trap. Chloroform dry (Carlo Erba) was distilled from CaH_2 and stored over molecular sieves in inert atmosphere.

6.2 Characterization.

TLC analyses were performed on silica gel support Merk 60 F254 using UV lamp, iodine and/or ninhydrin as detectors. ^{1}H- and ^{13}C-NMR spectra were

recorded at 25 °C on Varian Gemini VXR-200 (200 MHz) and Bruker DRX (400 MHz) spectrometers using chloroform-*d* ($CDCl_3$) as a solvent and TMS as internal standard. FTIR spectra were obtained using a Jasco FT-IR-430 spectrometer. The samples were analyzed as thin films obtained by solution casting onto a NaCl plate. Wide-angle X-ray diffraction patterns (WAXS) were collected at r.t. using a Bragg-Brentano θ/2θ Philips diffractometer (Cu-Kα source, λ = 1.5418 Å), with a 2θ range 0-90° and a scanning speed Δ2θ/Δt of 0.04 degree/s). Differential Scanning Calorimetry (DSC) analyses were carried out under nitrogen on a Mettler Toledo-30 instrument; two heating runs (-20°C to 80°C) and one cooling run (80°C to -20°C) were performed at a 2 °C/min rate. GC-MS spectra were collected using Agilent 6850 with capillary column Zebron Zb5 (Phenomex) and Mass Selector 5973 N quadrupole as mass analyzer. Size exclusion chromatografy (SEC) measurements were performed at 25 °C on a Shimadzu SCL-10DP system equipped with three Phenogel columns connected in series and with a R.I.-10A detector, using polystyrene standards as reference and THF as the eluent. Critical Aggregation Concentration (CAC) values were determined by fluorescence spectroscopy on a Shimadzu RF-1501 spectrofluorimeter using pyrene as a probe. Inherent viscosity were measured at 25°C in chloroform (c=0,5g/dL) using a Cannon-Ubbelhode viscometer. Transmission Electron Microscopy (TEM) pictures were obtained using Tecnai G2 Spirit Twin with emission source LaB6 placing a drop of a NP suspension on a copper grid coated with a formvar film and dried at r.t. Zeta potential was determined by analyzing a NP dispersion in water on a Zetasizer Nano Z (Malvern Instruments Ltd.). Results are reported as mean of three separate measurements of three different batches (n=9) ± SD. Particle shape and external morphology were analysed by Scanning Electron Microscopy (SEM) (Leica S440, Germany). The internal microstructure of FITC labeled PLGA microparticles was investigated by CLSM analysis carried out on a LSM 510 Zeiss confocal inverted microscope equipped with a Zeiss 63/1.25 oil objective lens (Carl

Zeiss, Germany). An argon laser (excitation =541 nm; emission = 572 nm) was used.

6.3 Methods

Low molecular weight range

6.3.1 Synthesis of the linear diblock copolymer PEG_{1000}-PCL_{3000}

89 µL of a solution $Sn(Oct)_2$ in ε-CL (30mg/1 mL) was added under inert atmosphere, avoiding water contamination, to *m*-PEG_{1000}-OH (1100.60 mg, 1.1 mmol) and ε-CL (3.457 g , 30.33 mmol). The mixture was stirred for 24 hours at 120°C. The viscous liquid obtained was cooled to room temperature, solved in chloroform and precipitated in 300 mL of cold diethyl ether. The obtained solid was filtered on glass porous filter and dried for 24 hours under vacuum at 35°C (yield 96%; 4.378 g; 1.09 mmol). **^{1}H-NMR (200 MHz): (PCL:** δ=1.29-1.78, 158H, m; δ=2.19-2.43, 52H, m; δ=3.92-4.21, 52H, t, δ=4.31,2H, t); (**PEG:** δ=3.38, 3H, s ; δ=3.64, 90H, s)

6.3.2 Synthesis of the linear triblock copolymer PEG_{1000}-PCL_{6000}-PEG_{1000}

Synthesis of α-metoxy-ω-alkyne-PEG_{1000}

DCC 1M solution (4.5 mL, 4.5 mmol) was added to a solution of *m*-PEG_{1000}-OH (3 g, 3 mmol), DMAP (73.2 mg, 0.6 mmol) and 4-pentynoic acid (441,5 mg, 4.5 mmol) in dry chloroform (30 mL) under inert atmosphere. The mixture was stirred at 25°C for 48 hours. The mixture was filtered from solid Dicyclohexylurea, concentrated and precipitated in 300 mL of a diethyl ether/petroleum ether 3/2 (v/v) cold mixture. The obtained solid, m-PEG_{1000}-alkyne was filtered on glass porous filter and dried for 24 hours under vacuum at 35°C (yield 89%; 2.932 g; 2.67 mmol). **^{1}H-NMR (200 MHz):** δ=1.99 (1H, s); δ=2.50-2.60 (4H, m); δ=3.38 (3H,s); δ=3.64 (90H, s); δ=4.27 (2H, t)

Synthesis of m-PEG$_{1000}$-PCL$_{6000}$-OH

89 µL of a solution Sn(Oct)$_2$ in ε-CL (30mg/1 mL) was added under inert atmosphere, avoiding water contamination, to *m*-PEG$_{1000}$-OH (550 mg, 0.55 mmol) and ε-CL (3.457 g , 30.33 mmol). The mixture was stirred for 24 hours at 120°C. The viscous liquid obtained was cooled to room temperature, solved in chloroform and precipitated in 300 mL of cold diethyl ether. The obtained solid was filtered on glass porous filter and dried for 24 hours under vacuum at 35°C (yield 96%; 3.978 g; 0.992 mmol). **^{1}H-NMR (200 MHz): (PCL:** δ=1.29-1.78, 306H, m; δ=2.19-2.43, 104H, m; δ=3.92-4.21, 104H, t, δ=4.31,2H, t); (**PEG:** δ=3.38, 3H, s ; δ=3.64, 90H, s)

Activation of terminal hydroxyl group of m-PEG$_{1000}$-PCL$_{6000}$-OH

Methanesulfonyl-chloride (mes-Cl) (346 mg, 3.04 mmol) was added to a solution of m-PEG$_{1000}$-PCL$_{6000}$-OH (3.0 g, 0.43 mmol) and DIPEA (392 mg, 3.04 mmol) in dry chloroform at 0°C. The mixture was stirred for 4 hours. It was allowed to come to room temperature and was stirred for additional 21 h. The mixture was concentrated and precipitated in 300 mL of a diethyl ether/petroleum ether 3/2 (v/v) cold mixture. The obtained solid, m-PEG$_{1000}$-PCL$_{6000}$-mes, was filtered on glass porous filter and dried for 24 hours under vacuum at 35°C. (2.987 g; 0.42 mmol; yield 97%)**^{1}H-NMR (200 MHz): (PCL:** δ=1.29-1.78, 306H, m; δ=2.19-2.43, 104H, m; δ=3.00, 3H, s; δ=3.92-4.21, 104H, t, δ=4.31,2H, t); (**PEG:** δ=3.38, 3H, s ; δ=3.64, 90H, s)

Nucleophilic substitution with sodium azide of m-PEG$_{1000}$-PCL$_{6000}$-mes

Sodium Azide (800 mg, 12.30 mmol) was added to a solution of m-PEG$_{1000}$-PCL$_{6000}$-mes (1.645 g; 0.235 mmol) in DMF (25 mL). The mixture was heated at 80°C for 12 hours. The mixture was dried and solid residue was solved in chloroform. Organic solution was filtered, concentrated and precipitated in 300 mL

of a diethyl ether/petroleum ether 3/2 (v/v) cold mixture. The obtained solid, m-PEG_{1000}-PCL_{6000}-N_3, was filtered on glass porous filter and dried for 24 hours under vacuum at 35°C. (1.481 g, 0.23 mmol yield 90%). **^{1}H-NMR (200 MHz): (PCL:** δ=1.29-1.78, 306H, m; δ=2.19-2.43, 104H, m; δ=3.20, 2H, t; δ=3.92-4.21, 104H, t, δ=4.31,2H, t); (**PEG:** δ=3.38, 3H, s ; δ=3.64, 90H, s)

1-3 Huisgen cycloaddition between m-PEG_{1000}-PCL_{6000}-N_3 and m-PEG_{1000}-alkyne

In a 50 mL bottle was added DIPEA (65.52 mg, 0.52mmol) to a solution of m-PEG_{1000}-PCL_{6000}-N_3 (1.560 g, 0.26 mmol) and m-PEG_{1000}-alkyne (373.3 mg, 0.34 mmol) in dry THF (18 mL) under inert atmosphere. This mixture was freezed in liquid nitrogen and thawed under vacuum for three times and then transferred under argon in other bottle in which was Bromotris(triphenylphophine)Cu(I) (48.37 mg, 0.052 mmol). After catalyst dissolution, mixture was stirring for 48 hours at 35°C. The mixture was filtered through neutral alumina column to remove copper, then concentrated and precipitated in 300 mL of cold diethyl ether. The obtained solid was filtered on glass porous filter and dried for 24 hours under vacuum at 35°C. To remove unreacted PEO, the solid product was washed for 12 hours under stirring with methanol at room temperature. The dipersion was centrifuged and solid dried for 24 hours under vacuum at 35°C (956 mg, yield 70%).**^{1}H-NMR (200 MHz): (PCL:** δ=1.29-1.78, 306H, m; δ=2.19-2.43, 104H, m;; δ=3.92-4.21, 104H, t, δ=4.31,2H, t; δ=7.37, 1H, s); (**PEG:** δ=2.50-2.60, 4H, m; δ=3.38, 6H,s; δ=3.64, 180H, s; δ=4.27, 2H, t)

6.3.3 Synthesis of miktoarm Y-I-shaped (PEG_{1000})$_2$-PCL_{5800} copolymer (Y-s I), (4). (a) → The ROP initiator 1,4-di-azido-2-butanol **(1)** was prepared adding sodium azide (947 mg, 14.6 mmol) to a solution of purified 1,4-dibromo-2-butanol (1.359 g; 5.60 mmol) in14 mL of DMF and heating the mixture under stirring at 60 °C for 12 h. After drying the mixture, the solid residue was extracted with $CHCl_3$.

After filtration, the solution was dehydrated over Na_2SO_4 and dried under vacuum yielding **(1)** as a yellow oil (810 mg, 99% yield). **^{1}H NMR (200Mhz):** δ=3.50 (2H, t); δ=3.65 (1H, s); δ=1.49-1.53 (6H, m). GC-MS= m/z 115.07. (b) → α-Hydroxy,ω-di-azido-PCL_{5800} **(2)** was obtained adding 138 μL of a $Sn(Oct)_2$ solution in CL (27mg/ mL) to a mixture of **(1)** (143 mg, 0.92 mmol) and CL (5.99 g , 52.54 mmol). After stirring for 24 h at 120 °C, the viscous product was cooled to r.t., dissolved in $CHCl_3$ and precipitated in 300 mL of chilled diethyl ether. The precipitate was dried for 24 h under vacuum at 35°C (3.60 g, 96% yield). **^{1}H NMR (200Mhz):** δ=1.29-1.78 (306H, m); δ=2.19-2.43 (102H, m); δ=3.33-3.39 (2H, t); δ=3.59-3.69 (2H, t); δ=3.92-4.21 (102H, t). (c). → The preparation of α-methoxy-ω-alkyne-PEG_{1000} **(3)** was performed adding a DCC 1 M solution in CH_2Cl_2 (6.0 mL) to a solution of *m*PEG_{1000} (3.98 g, 3.98 mmol), DMAP (147 mg, 1.20 mmol) and 4-pentynoic acid (588 mg, 6.01 mmol) in 31 mL of $CHCl_3$. The mixture was stirred at r. t. for 48 h, filtered twice from solid dicyclohexylurea, then was concentrated and precipitated in 300 mL of a chilled diethyl ether/methanol 5/2 (v/v) mixture. The obtained solid **(3)** was collected and dried under vacuum at 35°C (3.717 g, 97% yield). **^{1}H NMR (200Mhz):** δ=1.99 (1H, s); δ=2.50-2.60 (4H, m); δ=3.38 (3H,s); δ=3.64 (90H, s); δ=4.27 (2H, t). (d) → Synthesis of the **(Y-s I)** block copolymer **(4)** by click coupling: after three freeze-thaw cycles, a solution of DIPEA (112 mg, 0.92mmol), **(3)** (860 mg, 0.86 mmol) and **(2)** (1.97 g, 0.34 mmol) in dry THF (20 mL).was transferred under argon in a bottle containing137 mg of Br-$Cu(P(ph)_3)_3$. After catalyst dissolution, the mixture was stirred for 48 h. at 40 °C, passed through a neutral alumina column to remove copper, then concentrated and precipitated in 300 mL of chilled diethyl ether. The precipitated polymer was recovered by filtration, washed with methanol to remove unreacted PEG and. dried in a vacuum oven at 35 °C to obtain 1.52 g (60% yield) of purified **(Y-s I), (4)**.

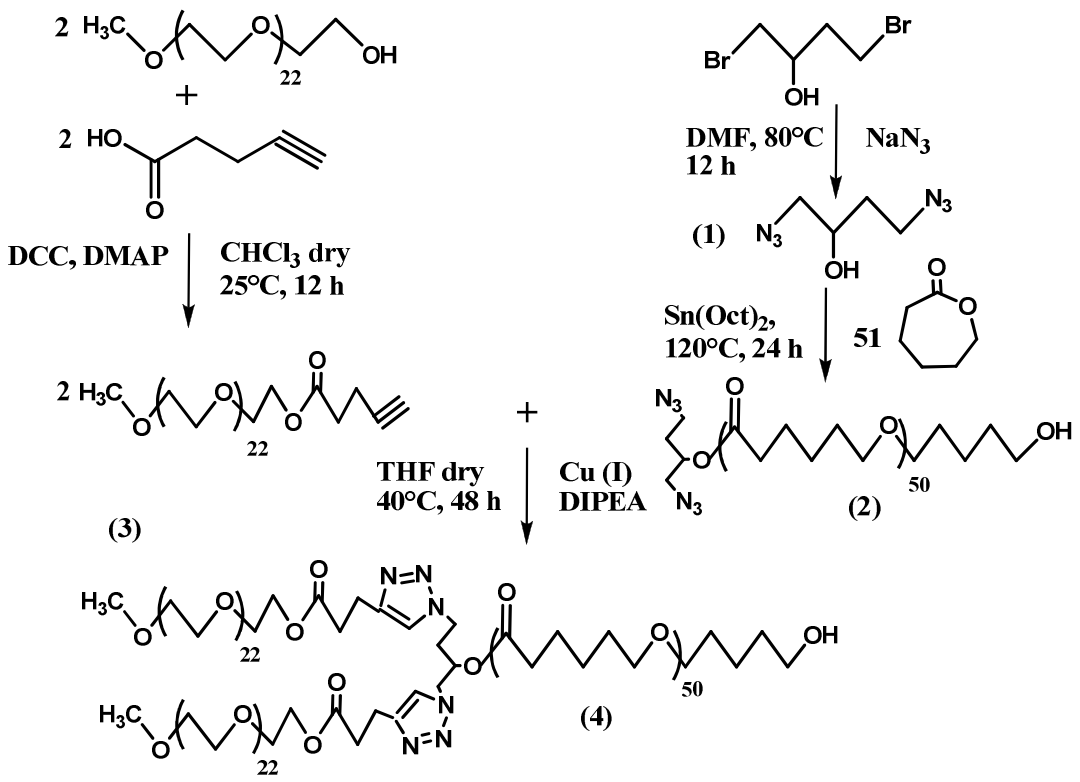

Fig.6.1 Synthetic scheme of miktoarm Y-I-shaped $(PEG_{1000})_2$-PCL_{5800} copolymer (Y-s I)

6.3.4 Synthesis of miktoarm Y-II-shaped $(PEG_{1000})_2$-PCL_{7200}-PEG_{1000} copolymer (Y-s II). (8)

(a) →A diblock copolymer *m*PEG_{1000}-PCL_{7200}-OH was prepared adding 110 µL of a $Sn(Oct)_2$ solution in CL (30mg/ mL) to *m*PEG_{1000}-OH (666.98 mg, 0.67 mmol) and CL (4.030 g , 35.35 mmol). The mixture was stirred for 24 h at 120 °C. The viscous liquid obtained was cooled to r. t., dissolved in chloroform and precipitated in 300 mL of chilled diethyl ether. The recovered solid was dried under vacuum at 35°C (4.61 g; 98% yield). **^{1}H NMR (200 MHz):** (PEG: δ=3.38, 3H, s ; δ=3.64, 90H, s); (PCL: δ=1.29-1.78, 378H, m ; δ=2.19-2.43, 126H, m ; δ=3.59-3.69 (2H, t ; δ=3.92-4.31, 130H, t) (b) → The synthesis of di-alkyne-lys (di-PCF-lys) **(5):**was accomplished adding drop-wise PCF (3.13 mL, 32.14 mmol) to a water solution of

lys (2.136 g; 14.61 mmol), $NaHCO_3$ (1N, 20 mL) and NaOH (4N, 1 mL) at 0°C. After stirring for 1 h and for additional 3 h at r.t., the reaction was quenched adding drop-wise a 1 N water solution of $KHSO_4$. The mixture was extracted with ethyl acetate (3×25 mL) and the organic layers were combined and washed with saturated citric acid solution, water and then with brine. The solvent was removed and the crude product was purified by silica gel (100–200 mesh) column chromatography eluting with 50–70 V% of ethyl acetate-petroleum ether to get **(5)** as a sticky light brown solid (2.947g; 9.49 mmol, 65% yield). The complete disappearance of $–NH_2$ groups was checked by TLC ninhydrin assay.; **^{1}H NMR (200MHz):**. δ=1.30-1.99 (6H, b); δ=2.49 (2H, t); δ;=3.19-3.22 (2H, m) δ=4.37-4.38 (1H, m); δ=4.68 (4H, s); δ=5.02 (1H, b) δ.=5.64-5.68 (1H, b). (c) → Synthesis of the di-block copolymer (di-PCF-lys)-PCL_{7200} PEG_{1000} **(6).** DCC, (1M solution, in CH_2Cl_2, 0.201 mL) was added under inert atmosphere to a solution of **(5),** (62.38 mg, 0.201 mmol), *m*PEG_{1000}-PCL_{7200}-OH (1.01 g, 0.123 mmol) and DMAP (3.27 mg) in dry chloroform (20 mL). The mixture was stirred at 25°C for 48 h, filtered from solid dicyclohexylurea, then concentrated and precipitated in 300 mL of a diethyl ether/petroleum ether 3/2 (v/v) cold mixture. The obtained solid was filtered and dried under vacuum at 35°C. Unreacted di-PCF-lys was removed washing under stirring the product with methanol (3×20mL) at r. t.. The dispersion was centrifuged and the solid dried under vacuum at 35 °C (984 mg, 92% yield). **^{1}H-NMR (200Mhz):** (di-PCF-lys: δ=1.30-1.99, 6H, b ; δ=2.49, 2H, t ; δ=3.19-3.22, 2H, m ; δ=4.37-4.38, 1H, m ; δ=4.37-4.38, 4H, s ; δ=4.68, 1H, b ; δ=5.02, 1H, b ; δ=5.64-5.68, 1H, b); (PEG: δ=2.50-2.60, 4H, m ; δ=3.38, 3H, s ; δ=3.64, 90H, s ; δ=4.27, 2H, t); (PCL: δ=1.29-1.78 378H, m ; δ=2.19-2.43, 126H, m ; δ=3.59-3.69, 2H, t ; δ=3.92-4.31, 126H, t). (d) → Synthesis of α-methoxy-ω-azido-PEG_{1000} **(7).** (Mes-Cl) (334 mg, 1.75 mmol) was added to a solution of *m*PEG_{1000} (1.5 g, 1.5 mmol) in dry pyridine at 0 °C. After stirring at 0°C for 3 h and for additional 21 h. at r. t., the mixture was concentrated and precipitated in 300 mL of a diethyl

ether/petroleum ether 3/2 (V/V) chilled mixture. The obtained solid, m-PEG_{1000}-mes, was filtered and dried for 24 h under vacuum at 35°C. (1.645 g; 95% yield). **^{1}H-NMR (200 MHz):** δ=2.31 (3H, s); δ=3.70 (2H, t); δ=3.38 (3H, s);δ=3.64 (90H, s); δ=7.46-7.75 (4H, m). Sodium Azide (185 mg, 2.85 mmol) was added to a solution of m-PEG_{1000}-mes (1.645 g; 1.425 mmol) in DMF (25 mL). After heating at 80°C for 12 h., the mixture was dried and the residue dissolved in chloroform, filtered, concentrated and precipitated in 300 mL of a diethyl ether/petroleum ether 3/2 (V/V) cold mixture. The obtained solid, **(7)**, was filtered and dried for 24 h under vacuum at 35°C. (1.39 g, 86% yield). FT-IR: 2100 cm^{-1}, stretching C-N_3. **^{13}C-NMR:** δ=50.50 (1C, -$\underline{C}H_2$-N_3), δ=70.4 (21C, -$\underline{C}H_2$-O-CH_2), δ=71.7 (1C, -$\underline{C}H_2$-O-CH_3) δ=58.8 (1C, CH_2-O-$\underline{C}H_3$) **^{1}H-NMR (200 MHz):** δ=3.38 (3H, s); δ=3.64-3.70 (92H, s). (e) → Synthesis of the **(Y-s II)** block copolymer **(8)** by the azide-alkyne cycloaddition click reaction. The coupling of two α-methoxy-ω-azido-PEG_{1000} **(7)** segments (373 mg, 0.37 mmol) to (di-PCF-lys)-PCL_{7200} PEO_{1000} **(6)** (1.56 g, 0.18 mmol) was performed by click reaction (72% yield).as above described in the case of (**Y-s I**)**, (4), ^{1}H-NMR (200 MHz):** (PEG:, δ=1.99, 1H, s ; δ=2.50-2.60, 4H, m ; δ=3.38, 3H, s ; δ=3.64, 90H, s ; δ=4.27, 2H, t) ; (PCL:, δ=1.29-1.78, 378H, m ; δ=2.19-2.43, 126H, m ; δ=3.59-3.69, 2H, t ; δ=3.92-4.31, 126H, t).

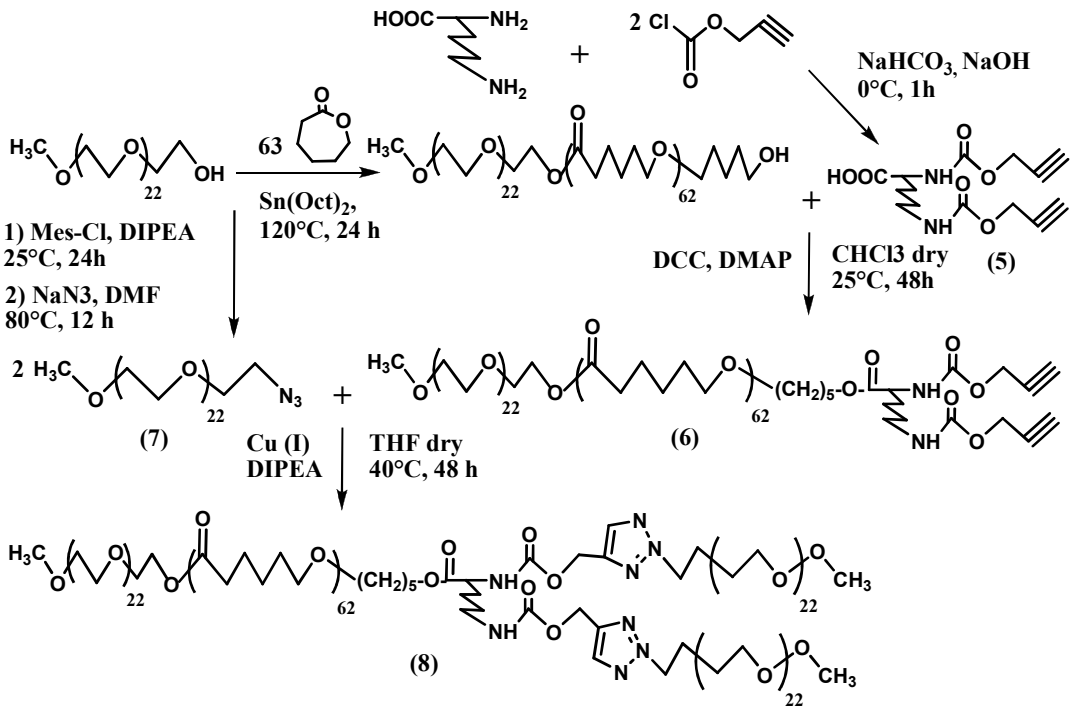

Fig.6.2 Synthetic scheme of miktoarm Y-II-shaped $(PEG_{1000})_2$-PCL_{7200}- PEG_{1000} copolymer (Y-s-II)

6.3.5 Synthesis of miktoarm H-shaped copolymer, $(PEG_{1000})_2$-PCL_{11500}-$(PEG_{1000})_2$, (10)

(a) → Synthesis of α,ω-di-PCF-lys-PCL_{11500} **(9):** DCC, 1 M solution in THF, (0.900 mL) was added to a solution of α,ω-dihydroxy-PCL_{11500} (2.5 g, 0.25 mmol), DMAP (13.56 mg, 0.111 mmol) and di-PCF-lys **(5)**,(259.4 mg, 0.834 mmol) in dry $CHCl_3$ (25 mL) under inert atmosphere. The mixture was stirred at 25 °C for 48 h, then was filtered from solid dicyclohexylurea, concentrated and precipitated in 300 mL of a chilled diethyl ether/petroleum ether 3/2 (v/v) mixture. The recovered solid was dried under vacuum at 35°C, then was washed under stirring with methanol (3×20mL) at r.t. to remove unreacted di-PCF-lys. The dispersion was centrifuged and the solid dried for 24 h. under vacuum at 35°C (2.48 g, 90% yield). **^{1}H NMR(200 MHz)** of **(9):** (di-PCF-lys : δ=1.30-1.99,12H, b; δ=2.49. 4H, t; δ=3.19-3.22,. 4H, m; δ=4.37-4.38, 2H, m; δ=4.68 8H, s; δ=5.02. 2H, b; δ=5.64-5.68, 2H, b)

(PCL : δ=1.29-1.78, 528H, m; δ=2.19-2.43, 176H, m; δ=3.92-4.31, 176H, t.). (b) → Synthesis of the **(H-s)** block copolymer **(10)** by the azide-alkyne cycloaddition click reaction. Four α-methoxy, ω-azido-PEG_{1000} **(7)** segments (471 mg, 0.471 mmol) and one α,ω-di-PCF-lys-PCL (928 mg, 0.096 mmol) **(9)** were "clicked" together as above described in the case of (**Y-s I**)**, (4).** (67% yield) **^{1}H NMR (400 MHz)** of **(10)**: (di-PCF-lys : δ=1.30-1.99, 12H, b, ; δ=2.49, 4H, t; δ=3.19-3.22, 4H, m, ; δ=4.37-4.38, 2H, m, ; δ=4.68, 8H, s, ; δ=5.02, 2H, b, ; δ=5.64-5.68, 2H, b) ; (PEG : δ=2.50-2.60, 8H, m, ; δ=3.38, 12H, s, ; δ=3.64-3.70, 360H, s) ; (PCL : δ=1.29-1.78, 528H, m, ; δ=2.19-2.43, 176H, m, ; δ=3.92-4.31, 176H, t).

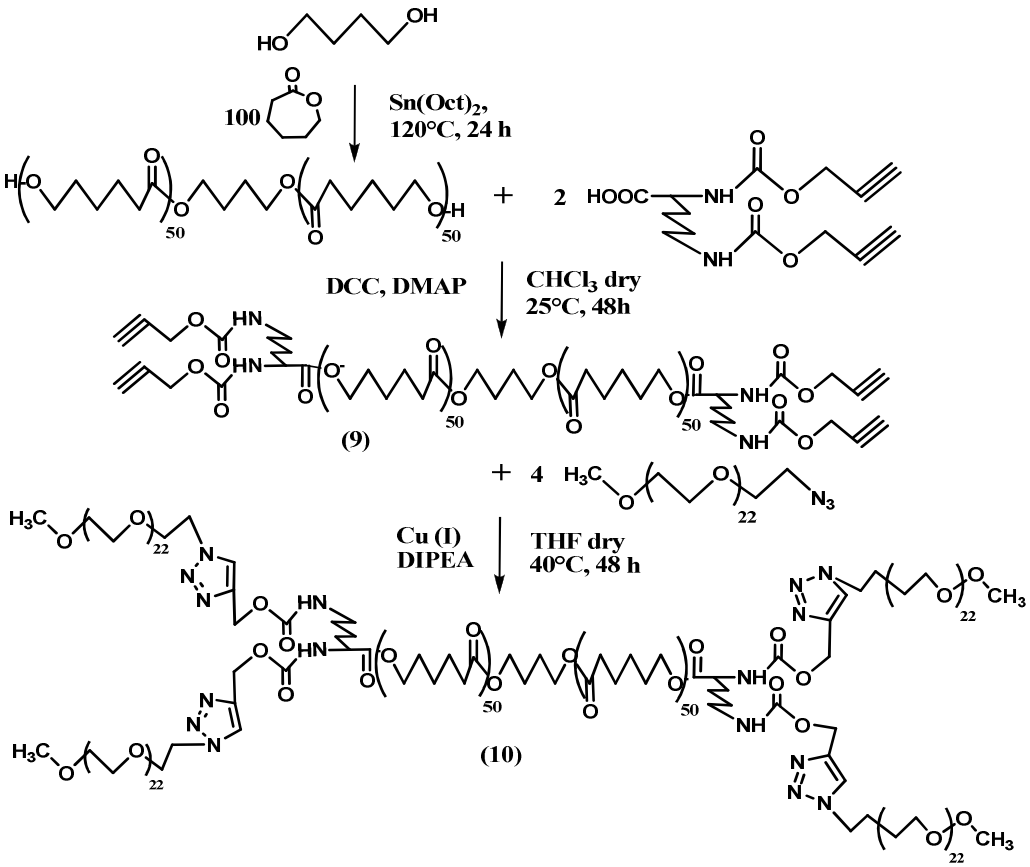

Fig.6.3 Synthetic scheme of miktoarm H-shaped $(PEG_{1000})_2$-PCL_{7200}- PEG_{1000} copolymer (H-s)

6.3.6 Synthesis of triblock copolymer m-PEO_{2000}-PCL_{7000}-PEO_{2000}- NH-ROD

Synthesis of α-amino-ω-alkyne-PEO_{2000}

Propargyl chloroformate (PCF) (165 mg, 1.4 mmol) was added to a solution of di-amine-PEO_{2000} (3.0 g, 1.5 mmol) and anhydrous Na_2CO_3 (3.0 g, 28.30 mmol) in dry chloroform at 0°C. The mixture was stirred for 4 hours. It was allowed to come to room temperature and was stirred for additional 21 h. The reaction mixture was filtered from bicarbonate, concentrated and purified by silica gel flash cromatography using as eluent methanol in $CHCl_3$ from 5 to 20% in vol. The obtained product, NH_2-PEO_{2000}-alkyne, was precipitated in 300 mL of chilled diethyl ether, filtered on glass porous filter and dried for 24 hours under vacuum at 35°C. (2.987 g; 0.49 mmol; yield 97%)**^{1}H-NMR (200 MHz):**; (δ=2.50, 1H, t δ=3.10, 2H, t ; δ=3.64, 180H, s; δ=4.65, 2H, t; δ=5.60, 1H, s)

Synthesis of m-PEG_{2000}-PCL_{7000}-OH

89 µL of a solution $Sn(Oct)_2$ in ε-CL (30mg/1 mL) was added under inert atmosphere, avoiding water contamination, to *m*-PEG_{2000}-OH (1000 mg, 0.50 mmol) and ε-CL (3.591 g , 31.50 mmol). The mixture was stirred for 24 hours at 120°C. The viscous liquid obtained was cooled to room temperature, solved in chloroform and precipitated in 300 mL of cold diethyl ether. The obtained solid was filtered on glass porous filter and dried for 24 hours under vacuum at 35°C (yield 96%; 4.510 g; 0.51 mmol). **^{1}H-NMR (200 MHz): (PCL:** δ=1.29-1.78, 184H, m; δ=2.19-2.43, 122H, m; δ=3.92-4.21, 122H, t, δ=4.31,2H, t); (**PEO:** δ=3.38, 3H, s ; δ=3.64, 180H, s)

Activation of terminal hydroxyl group of m-PEG_{2000}-PCL_{7000}-OH

Methanesulfonyl-chloride (mes-Cl) (346 mg, 3.04 mmol) was added to a solution of m-PEG_{2000}-PCL_{7000}-OH (3.0 g, 0.33 mmol) and DIPEA (392 mg, 3.04 mmol) in dry chloroform at 0°C. The mixture was stirred for 4 hours. It was allowed to come to room temperature and was stirred for additional 21 h. The mixture was

concentrated and precipitated in 300 mL of a diethyl ether/petroleum ether 3/2 (v/v) cold mixture. The obtained solid, m-PEG_{2000}-PCL_{4000}-mes, was filtered on glass porous filter and dried for 24 hours under vacuum at 35°C. (2.987 g; 0.32 mmol; yield 97%)**^{1}H-NMR (200 MHz): (PCL:** δ=1.29-1.78, 184H, m; δ=2.19-2.43, 122H, m; δ=3.00, 3H, s; δ=3.92-4.21, 122H, t, δ=4.31,2H, t); (**PEO:** δ=3.38, 3H, s ; δ=3.64, 180H, s)

Nucleophilic substitution with sodium azide of m-PEG_{2000}-PCL_{7000}-mes

Sodium Azide (800 mg, 12.30 mmol) was added to a solution of m-PEG_{2000}-PCL_{7000}-mes (1.645 g; 0.183 mmol) in DMF (25 mL). The mixture was heated at 80°C for 12 hours. The mixture was dried and solid residue was solved in chloroform. Organic solution was filtered, concentrated and precipitated in 300 mL of a diethyl ether/petroleum ether 3/2 (v/v) cold mixture. The obtained solid, m-PEG_{1000}-PCL_{6000}-N_3, was filtered on glass porous filter and dried for 24 hours under vacuum at 35°C. (1.481 g, 0.164 mmol yield 90%). **^{1}H-NMR (200 MHz): (PCL:** δ=1.29-1.78, 184H, m; δ=2.19-2.43, 122H, m; δ=3.20, 2H, t; δ=3.92-4.21, 122H, t, δ=4.31,2H, t); (**PEO:** δ=3.38, 3H, s ; δ=3.64, 180H, s)

1-3 Huisgen cycloaddition between m-PEG_{2000}-PCL_{7000}-N_3 and NH_2-PEG_{2000}-alkyne

In a 50 mL bottle was added DIPEA (65.52 mg, 0.52mmol) to a solution of m-PEG_{2000}-PCL_{7000}-N_3 (1.560 g, 0.173 mmol) and NH_2-PEG_{2000}-alkyne (373.3 mg, 0.18 mmol) in dry THF (18 mL) under inert atmosphere. This mixture was freezed in liquid nitrogen and thawed under vacuum for three times and then transferred under argon in other bottle in which was Bromotris(triphenylphophine)Cu(I) (48.37 mg, 0.052 mmol). After catalyst dissolution, mixture was stirring for 48 hours at 35°C. The mixture was filtered through neutral alumina column to remove copper, then concentrated and precipitated in 300 mL of cold diethyl ether. The obtained

solid was filtered on glass porous filter and dried for 24 hours under vacuum at 35°C. To remove unreacted PEO, the solid product was washed for 12 hours under stirring with methanol at room temperature. The dipersion was centrifuged and solid dried for 24 hours under vacuum at 35°C (956 mg, yield 70%).**^{1}H-NMR (200 MHz): (PCL:** δ=1.29-1.78, 184H, m; δ=2.19-2.43, 122H, m; δ=3.20, 2H, t; δ=3.92-4.21, 122H, t, δ=4.31,2H, t; δ=7.37, 1H, s); (**PEO**: δ=3.10, 2H, t ; δ=3.64, 360H, s; δ=4.65, 2H, t; δ=5.60, 1H, s)

Coupling between m-PEO$_{2000}$-PCL$_{7000}$-PEO$_{2000}$-NH$_2$ and NHS activated Rhodamine B

DCC 1M solution (4.5 mL, 4.5 mmol) was added to a solution of Rhodamine B (ROD) (500 mg, 1.04 mmol), DMAP (73.2 mg, 0.6 mmol) and N-hydroxysuccinimide (441,5 mg, 3.83 mmol) in dry chloroform (30 mL) under inert atmosphere. The mixture was stirred at 25°C for 24 hours then were added under nitrogen m-PEO$_{2000}$-PCL$_{7000}$-PEO$_{2000}$-NH$_2$ (2.0 g, 0.181 mmol) and DIPEA (65.52 mg, 0.52 mmol). After 48 hours, the mixture was filtered from solid Dicyclohexylurea, concentrated and precipitated in 300 mL of a diethyl ether/petroleum ether 3/2 (v/v) cold mixture. The obtained pink solid, m-PEO$_{2000}$-PCL$_{7000}$-PEO$_{2000}$- NH-ROD was filtered on glass porous filter and dried for 24 hours under vacuum at 35°C (yield 89%; 2.932 g; 2.67 mmol). **^{1}H-NMR (400 MHz): (PCL:** δ=1.29-1.78, 184H, m; δ=2.19-2.43, 122H, m; δ=3.20, 2H, t; δ=3.92-4.21, 122H, t, δ=4.31,2H, t; δ=7.37, 1H, s); (**PEO**: δ=3.10, 2H, t ; δ=3.64, 360H, s; δ=4.65, 2H, t; δ=5.60, 1H, s)(**ROD**: δ=1.20, 12H, t; δ=3.50, 8H, t; δ=6.20-6.50 4H, m; δ=7.10, 2H, d)

6.3.7 Synthesis of diblock copolymer PCL$_{4000}$- PEO$_{2000}$-NH-FOL

Synthesis of α-hexan-ω-hydroxyl-PCL$_{4000}$

89 μL of a solution $Sn(Oct)_2$ in ε-CL (30mg/1 mL) was added under inert atmosphere, avoiding water contamination, to Hexanol (153 mg, 1.5 mmol) and ε-CL (6.156 g , 54.00 mmol). The mixture was stirred for 24 hours at 120°C. The viscous liquid obtained was cooled to room temperature, solved in chloroform and precipitated in 300 mL of cold diethyl ether. The obtained solid, PCL_{4000}-OH, was filtered on glass porous filter and dried for 24 hours under vacuum at 35°C (yield 96%; 4.378 g; 1.09 mmol). **^{1}H-NMR (200 MHz): (PCL:** δ=0.80, 3H, t; δ=1.29-1.78, 115H, m; δ=2.19-2.43, 70H, m; δ=3.92-4.21, 70H, t, δ=4.31,2H, t);

Synthesis of α-hexan-ω-azido-PCL_{4000}

The azided PCL macromer was obtained by two-step process azidation via mesyl chloride, using the same protocol of section 6.3.6. **PCL_{4000}-N_3 ^{1}H-NMR (200 MHz): (PCL:** δ=0.80, 3H, t; δ=1.29-1.78, 115H, m; δ=2.19-2.43, 70H, m; δ=3.20 2H, m; δ=3.92-4.21, 70H, t, δ=4.31,2H, t);

1-3 Huisgen cycloaddition between PCL_{4000}-N_3 and NH_2-PEG_{2000}-alkyne

Click coupling was carried out using the same protocol of section 6.3.6. **PCL_{4000}-PEO_{2000}-NH_2 ^{1}H-NMR (200 MHz): (200 MHz): (PCL:** δ=0.80, 3H, t; δ=1.29-1.78, 115H, m; δ=2.19-2.43, 70H, m; δ=3.20 2H, m; δ=3.92-4.21, 70H, t, δ=4.31,2H, t); (**PEO**: δ=3.10, 2H, t ; δ=3.64, 360H, s; δ=4.65, 2H, t; δ=5.60, 1H, s)

Coupling between PCL_{4000}-PEO_{2000}-NH_2 and NHS activated Folic acid

DCC 1M solution (4.5 mL, 4.5 mmol) was added to a solution of Folic acid (FOL) (500 mg, 1.13 mmol), DMAP (73.2 mg, 0.6 mmol) and N-hydroxysuccinimide (441,5 mg, 3.83 mmol) in dry DMSO (30 mL) under inert atmosphere. The mixture was stirred at 25°C for 24 hours then were added under nitrogen PCL_{4000}-PEO_{2000}-NH_2 (2.0 g, 0.333 mmol) and DIPEA (65.52 mg, 0.52 mmol). After 48 hours, the mixture was filtered from solid Dicyclohexylurea, concentrated and precipitated in

300 mL of a diethyl ether/petroleum ether 3/2 (v/v) cold mixture. The obtained light yellow solid, PCL_{4000}-PEO_{2000}- NH-FOL was filtered on glass porous filter and dried for 24 hours under vacuum at 35°C Traces of unreacted folic acid were removed by dialysis in H_2O of the reaction product dissolved in DMSO (yield 90%; 1.913 g; 0.300 mmol). **^{1}H-NMR (400 MHz): (PCL:** δ=1.29-1.78, 184H, m; δ=2.19-2.43, 122H, m; δ=3.20, 2H, t; δ=3.92-4.21, 122H, t, δ=4.31,2H, t; δ=7.37, 1H, s); (**PEO**: δ=3.10, 2H, t ; δ=3.64, 360H, s; δ=4.65, 2H, t; δ=5.60, 1H, s)(**FOL**: δ=6.50-7.00, 6H, m δ=4.5, 2H, d; δ=8.75 1H, s; δ=9.75, 1H, s; δ=10.01, 1H, s)

6.3.8 Synthesis of diblock copolymer m-PEO_{2000}-PCL_{4000}-CAT

Synthesis of 3-hydroxy-tyramine-alkyne (CAT-alkyne)

Propargyl chloroformate (PCF) (900 mg, 7.89 mmol) was added to a solution of 3-hydroxy-tyramine hydrobromide (702 mg, 3 mmol) and anhydrous Na_2CO_3 (3.0 g, 28.30 mmol) in dry DMF at 0°C. The mixture was stirred for 4 hours. It was allowed to come to room temperature and was stirred for additional 21 h. The reaction mixture was dried, redissolved in chloroform, filtered from bicarbonate, concentrated and purified by silica gel flash cromatography using as eluent methanol in $CHCl_3$ from 5 to 20% in vol. The obtained sticky product, CAT-alkyne, was dried for 24 hours under vacuum at 35°C. (920 mg; 2.64 mmol; yield 88%)**^{1}H-NMR (200 MHz):**; (δ=2.50, 1H, t δ=3.10, 4H, t ; δ=3.64, 180H, s; δ=4.65, 2H, t; δ=6.40-6.70, 5H, m; δ=7.40, 1H, b)

Synthesis of m-PEO_{2000}-PCL_{4000}-N_3

This PEO-PCL macromer was synthetized using m-PEO_{2000}-OH as initiator according to 6.3.1 protocol and was functionalized with terminal azide group according to 6.3.6 protocol. **m-PEO_{2000}-PCL_{4000}-N_3 ^{1}H-NMR (200 MHz): (PCL:** δ=1.29-1.78, 105H, m; δ=2.19-2.43, 70H, m; δ=3.20, 2H, t; δ=3.92-4.21, 70H, t, δ=4.31,2H, t); (**PEO:** δ=3.38, 3H, s ; δ=3.64, 180H, s)

1-3 Huisgen cycloaddition between m-PEO_{2000}-PCL_{4000}-N_3 and CAT-alkyne

Click coupling was carried out using the same protocol of section 6.3.6. **PCL_{4000}-PEO_{2000}-NH_2 ^{1}H-NMR (200 MHz): (200 MHz): (PCL:** δ=0.80, 3H, t; δ=1.29-1.78, 115H, m; δ=2.19-2.43, 70H, m; δ=3.20 2H, m; δ=3.92-4.21, 70H, t, δ=4.31,2H, t); (**PEO**: δ=3.10, 2H, t ; δ=3.64, 360H, s; δ=4.65, 2H, t; δ=5.60, 1H, s) (**CAT:** δ=2.50, 1H, t δ=3.10, 4H, t ; δ=3.64, 180H, s; δ=4.65, 2H, t; δ=6.40-6.70, 5H, m; δ=7.40, 1H, b)

Medium molecular weight range

6.3.9 Synthesis of poly(styrene-*b*-ethylenoxide)-N_3

Activation of terminal hydroxyl group of poly(styrene-*b*-ethylenoxide)-OH

Methanesulfonyl-chloride (mes-Cl) (346 mg, 3.04 mmol) was added to a solution of poly(styrene-*b*-ethylenoxide)-OH (2.0 g, 0.046 mmol) and DIPEA (392 mg, 3.04 mmol) in dry chloroform at 0°C. The mixture was stirred for 4 hours. It was allowed to come to room temperature and was stirred for additional 21 h. The mixture was concentrated and precipitated in 300 mL of a diethyl ether/methanol 3/2 (v/v) cold mixture. The obtained solid, poly(styrene-*b*-ethylenoxide)-mes, was filtered on glass porous filter and dried for 24 hours under vacuum at 35°C. (1.887 g; 0.42 mmol; yield 94%)**^{1}H-NMR (200 MHz): (PS:** δ=1.29-1.78, 633H, b; δ=6.50-7.20, 1055H, b;) (**PEO:** δ=3.30, 3H, s ; δ=3.64, 1952H, s)

Nucleophilic substitution with sodium azide of poly(styrene-*b*-ethylenoxide)-mes

Sodium Azide (800 mg, 12.30 mmol) was added to a solution of poly(styrene-*b*-ethylenoxide)-mes (1.887 g; 0.042 mmol) in DMF (25 mL). The mixture was heated at 80°C for 12 hours. The mixture was dried and solid residue was solved in

chloroform. Organic solution was filtered, concentrated and precipitated in 300 mL of a diethyl ether/petroleum ether 3/2 (v/v) cold mixture. The obtained solid, poly(styrene-*b*-ethylenoxide)-N_3, was filtered on glass porous filter and dried for 24 hours under vacuum at 35°C. (1.481 g, 0.23 mmol yield 90%). **(PS:** δ=1.29-1.78, 633H, b; δ=6.50-7.20, 1055H, b;) (**PEO:** δ=3.50, 2H, s ; δ=3.64, 1952H, s)

6.3.10 Synthesis of poly(lactic-co-glycolic)acid-ROD (PLGA-ROD)

Synthesis of Rhodamine-alkyne

DCC 1M solution (4.5 mL, 4.5 mmol) was added to a solution of Rhodamine B (ROD) (500 mg, 1.04 mmol), DMAP (73.2 mg, 0.6 mmol) and 3-Butynol (210,5 mg, 3.0 mmol) in dry chloroform (30 mL) under inert atmosphere. The mixture was stirred at 25°C for 48 hours, the reaction mixture was filtered from solid Dicyclohexylurea, concentrated and purified by silica gel flash cromatography using as eluent methanol in $CHCl_3$ from 5 to 20% in vol. The obtained sticky pink solid, ROD-alkyne was dried for 24 hours under vacuum at 35°C (yield 79%; 420 mg; 0.82 mmol). **^{1}H-NMR (400 MHz):** (: δ=2.30, 2H, t, δ=4.20, 2H, t; δ=5.60, 1H, s)(: δ=1.20, 12H, t; δ=3.50, 8H, t; δ=6.20-6.50 4H, m; δ=7.10, 2H, d)

Synthesis of poly(lactic-co-glycolic)acid-N_3

This PLGA macromer was functionalized with terminal azide group according to 6.3.9 protocol. **PLGA-N_3 ^{1}H-NMR (200 MHz):** (δ=1.50, 690H, b, δ=3.20, 3H, t; δ=4.80, 460H, b, δ=5.20, 230H, t;)

1-3 Huisgen cycloaddition between PLGA-N_3 and ROD-alkyne

In a 50 mL bottle was added DIPEA (65.52 mg, 0.52mmol) to a solution of m-PLGA-N_3 (1.560 g, 0.052 mmol) and ROD-alkyne (373.3 mg, 0.74 mmol) in dry chloroform (18 mL) under inert atmosphere. This mixture was freezed in liquid nitrogen and thawed under vacuum for three times and then transferred under argon

in other bottle in which was Bromotris(triphenylphophine)Cu(I) (48.37 mg, 0.052 mmol). After catalyst dissolution, mixture was stirring for 48 hours at 35°C. The mixture was filtered through neutral alumina column to remove copper, then concentrated and precipitated in 300 mL of chilled diethyl ether/methanol 1/1 v/v. The obtained pink solid, poly(lactic-co-glycolic)acid-ROD**,** was filtered on glass porous filter and dried for 24 hours under vacuum at 35°C. (1.231 mg, yield 82%).**^{1}H-NMR (200 MHz):** (**PLGA**. δ=1.50, 690H, b,. δ=3.20, 3H, t;. δ=4.80, 460H, b, δ=5.20, 230H, t; δ=7.50, 1H, s;) (**ROD**. δ=2.30, 2H, t,. δ=4.20, 2H, t; . δ=5.60, 1H, s)(: δ=1.20, 12H, t; δ=3.50, 8H, t; δ=6.20-6.50 4H, m; δ=7.10, 2H, d)

High molecular weight range

6.3.11 Synthesis of PEO crosslinked Chitosan

Synthesis of N-phtaloyl-Chitosan

Chitosan (5.0 g, 31 mmol of monomer) was reacted with phthalic anhydride (11.5 g, 78 mmol) in DMF (100 mL) at 130 °C under nitrogen for 6 h. The mixture was then precipitated in ice-water, collected by filtration, washed by Soxhlet extraction with ethanol for 8 h and dried under vacuum for 24 h. **^{1}H-NMR** (DMF-d7): δ = 2.1 (CH_3 acetamide), 3.4–5 (pyranose ring), 7.2–7.9 (phthaloyl group).

Activation of C-6 hydroxyl group of N-phtaloyl-Chitosan

Methanesulfonyl-chloride (mes-Cl) (3.78 g, 33.97 mmol) was added to a solution of N-phtaloyl-Chitosan (3.0 g, 11.0 monomer mmol) and DIPEA (4.38 g, 33.96 mmol) in dry DMF at 10°C. After the mesyl chloride dropwise addition was noted a gel formation. The gel was stirred for 4 hours. It was allowed to come to room temperature and was stirred for additional 21 h. Then reaction gel was transferred in 300 mL of methanol. The obtained solid, N-phtaloyl-Chitosan-mes, was filtered

on glass porous filter and dried for 24 hours under vacuum at 35°C. (2.887 g) **^{1}H-NMR** (DMF-d7): δ = 2.1 (CH_3 acetamide), 3.1 (CH_3 mesyl) 3.4–5 (pyranose ring), 7.2–7.9 (phthaloyl group).

Nucleophilic substitution with sodium azide N-phtaloyl-Chitosan-mes

Sodium Azide (1.3 g, 20.0 mmol) was added to a solution of N-phtaloyl-Chitosan-mesy (1.3 g; 3.8 monomer mmol) in a mixture of DMF (25 mL)and water (1mL). The mixture was heated at 80°C for 12 hours. The mixture was precipitated in water, filtered, and reprecipitated in 300 mL of methanol. The obtained solid, N-phtaloyl-Chitosan-N_3, was filtered on glass porous filter and dried for 24 hours under vacuum at 35°C. (1.203 g). **^{1}H-NMR** (DMF-d7): δ = 2.1 (CH_3 acetamide), 3.4–5 (pyranose ring), 7.2–7.9 (phthaloyl group). **FTIR (cm^{-1})** 3450 (bs, OH), 2110 (N_3), 1776 and 1712 (s, imide C=O), 1290 and 1260 (C–O ester), 1150– 1000 (pyranose ring), 721 (aromatic ring).

Synthesis of di-azidoPEO_{6000}

Starting from α–ω-dihydroxyl-PEO_{6000} was synthetized di-azido-PEO_{6000} with two step azidation process via mesyl chloride according to 6.3.2 protocol. **di-azido-PEO_{6000}.^{1}H-NMR (200 MHz):** δ=3.28 (4H, t); δ=3.64-3.70 (545 H, s). **FTIR (cm^{-1})** 3450 (bs, OH), 2110 (N_3).

Synthesis of di-amino-PEO_{6000}

In a two-necked 100mL flask were placed under a nitrogen atmosphere di-azido-PEO_{6000} (5.336 g 0.89 mmol), 1g of Pd/C and 30mL of a mixture chloroform-methanol 1/1 v/v. The system was placed under hydrogen flow through a capillary for 24 hours at room temperature. The reaction mixture was subsequently centrifuged for 35 minutes at 8000 rpm to remove Pd/C in suspension. The solution was precipitated into a solution of 300mL ethyl ether/hexane 9:1 (v/v). The

precipitate was filtered on a porous septum and dried in a vacuum oven at 35 ° C for 24 hours. The compound, di-amino-$PEO_{6000,}$ is found to be positive to the ninhydrin test. **^{1}H-NMR (200 MHz):** δ=3.10 (4H, t); δ=3.64-3.70 (545 H, s).

Synthesis of di-alkyne-PEO_{6000}

Propargyl chloroformate (PCF) (900 mg, 7.89 mmol) was added to a solution of di-amino-PEO_{6000} (3.0 g, 0.5 mmol) and anhydrous Na_2CO_3 (3.0 g, 28.30 mmol) in dry chloroform at 0°C. The mixture was stirred for 4 hours. It was allowed to come to room temperature and was stirred for additional 21 h. The reaction mixture was concentrated, filtered from bicarbonate and precipitated in 300 mL of chilled diethyl ether. The obtained solid product, di-alkyne-PEO_{6000}, was dried for 24 hours under vacuum at 35°C. (2.8 g; 0.46 mmol; yield 93%)**^{1}H-NMR (200 MHz):** (δ=2.50, 1H, t δ=3.10, 4H, t ; δ=3.64, 545H, s; δ=4.65, 2H, t; δ=7.40, 1H, b)

1-3 Huisgen cycloaddition between N-phtaloyl-Chitosan-N_3 and di-alkyne-PEO_{6000}

In a 50 mL bottle was added DIPEA (65.52 mg, 0.52mmol) to a solution of di-alkyne-PEO_{6000} (1.360 g, 0.23 mmol) in dry DMF (18 mL) under inert atmosphere. This mixture was freezed in liquid nitrogen and thawed under vacuum for three times and then transferred under argon in other bottle in which were N-phtaloyl-Chitosan-N_3 (530 mg, 1.68 monomer mmol) Bromotris (triphenylphophine) Cu(I) (48.37 mg, 0.052 mmol). After catalyst dissolution, mixture was stirring for 48 hours at 35°C. The mixture was filtered through neutral alumina column to remove copper, then concentrated and precipitated in 300 mL of chloroform/methanol 1/1 v/v. The obtained solid was filtered on glass porous filter and dried for 24 hours under vacuum at 35°C. (1.231 mg) **^{1}H-NMR** (basic D_2O): δ = 2.1 (CH_3 acetamide), 2.5 (alkyne proton PEO) 3.4–5 (pyranose ring and PEO), 7.2–7.9 (phthaloyl group).

NH_2 PEO-crosslinked-N-phtaloyl-Chitosan deprotection

A mixture of PEO-crosslinked-N-phtaloyl-Chitosan (3.70 g, 6.93 mmol), hydrazine monohydrate (20 mL), and water (40 mL) was heated withstirring for 15 h at 100°C under a nitrogen atmosphere. After cooling, the mixture was diluted with water (50 mL) and evaporated with a rotary evaporator; this procedure was repeated three times. The residue was resuspended in deionized water, and the white precipitate was filtered. It was washed with ethanol and ether and dried under vacuum at 35°C. **^{1}H-NMR** (basic D_2O): δ = 2.1 (CH_3 acetamide), 2.5 (alkyne proton PEO) 3.4–5 (pyranose ring and PEO).

6.3.12 α-chimotrypsyn-PEG_{475}-charged conjugates

Synthesis of α-chimotrypsyn ATRP macroinitiator

500 mg of α-chymotrypsin (0.02mmol) were dissolved in 50 mL of PBS buffer (pH 8.0, 0.1M). To this mixture was added in 150 min (one portion every 30 min) a chloroform (0.5 mL) solution of 2-bromo-2 methyl-propionyl bromide (30 μL, 0.07 mmol). After every addition pH value was checked and adjusted to 8 by NaOH 0.1 M. The mixture was centrifuged and the precipitation removed. The liquid was purified a first time by ultracentrifugation (cutoff tubes membrane≈10 kDa) then by Sephadex column and at least by a second ultracentrifugation. After freeze-drying were recovered 210 mg of α-chymotrypsin macroinitiator.

Synthesis of Azided triethylenglycol methacrylate monomer

Azidation

Sodium Azide (4 g, 61.53 mmol) and a pinch of Potassium Iodide was added to a solution of 2-[2-(2-Chloroethoxy)ethoxy]ethanol (5 g, 29.65 mmol) in Millipore water (30 mL). The mixture was stirred at 80°C for 12 hours. Reaction mixture was extracted with chloroform three times, organic layers were dried on Sodium

Sulphate anhydrous and evaporated to give a transparent liquid, 2-[2-(2-Azidoethoxy)ethoxy]ethanol (4.97 g, 28.40 mmol; yield 96%). **^{1}H-NMR $CDCl_3$ (400 MHz):** δ=3.74 (2H, t); δ=3.68 (6H, t); δ=3.62 (2H, t); δ=3.41 (2H, s); δ=2.37 (1H, s)

Methacrylate addition

Methacryloyl chloride fresh distilled (9.08 g, 87.36 mmol) was added dropwise to a solution of 2-[2-(2-Azidoethoxy)ethoxy]ethanol (4.0 g, 22.85) and Triethyl amine (8.84 g, 87.36 mmol) in Methylene chloride (30 mL) in ice bath. This mixture is allowed to react under stirring in cool room at 4°C for 12 h, then was filtered from precipitate and concentrate. The crude product was added to a cool (ice bath) 5% $NaCO_3$ solution and the resulting mixture was extracted with ethyl acetate (3*100 mL). Organic layer was dried on Sodium Sulphate anhydrous, concentrated and purified by silica gel flash chromatography (ethyl acetate/hexane 50% v/v). The pure product, 2-[2-(2-Azidoethoxy)ethyl]Methacrylate was a transparent liquid (600 mg, 2.47 mmol yield 11%) **TLC**: RF=0.55; **^{1}H-NMR $CDCl_3$(400 MHz):** δ=6.07 (1H, s); δ=5.52 (1H, s); δ=4.25 (2H, t); δ=3.68 (2H, t); δ=3.61 (8H, t); δ=3.32 (2H, t); δ=1.87 (3H, s)

ATRP Copolymerization

PEG MA 475 (48.64 mg, 0.1024 mmol) was purified from inhibitor by celite/neutral alumina column then was bubbled with argon and added under argon in 5 mL flaṣkwith 2-[2-(2-Azidoethoxy)ethyl]Methacrylate (6.22 mg, 0.0256 mmol); α–chymotrypsin macroinitiator (4 mg, 0.00016 mmol) was solved in 2 mL of PBS buffer (0.1 M, pH 6.0) bubbled with argon and this solution added to the monomer flask. Solution of monomers and macroinitiator was transferred under argon in catalyst flask containing CuBr (0.8 mg, 0.0056 mmol), CuBr2 (1.25 mg, 0.0056 mmol), 2-2'-Bipyridil (1.95 mg, 0.0125 mmol). After 4 hours of stirring in

cool room at 4°C, reaction mixture was exposed to air deactivating the catalyst and purified by ultracentrifugation (cutoff tubes membrane≈30 kDa). Degree of polymerization (D.P.≈40 monomer unit/initiator group) was estimated by ^{1}H-NMR in D2O on unpurified conjugate calculating the decrease of double bond monomer signal respect terminal methyl of PEG. The presence of azide monomer in polymer chains verified by FT-IR, monitoring characteristic azide stretching at 2100 cm-1

Click coupling test

Azided conjugate (4 mg, 0.0396 μmol), propargyl alcohol (9.1 mg, 0.13 mmol), Di-isopropyl-ethyl amine(DIPEA) (9.67 mg, 0.075 mmol) Sodium ascorbate (71.8 mg, 0.36 mmol) Copper sulphate (11.97 mg, 0.075 mmol) was added under argon in 1.5 mL of aqueous PBS (pH=6, 0.1 M). The mixture was stirred for 12 hours at room temperature and then was purified by ultracentrifugation (cutoff tubes membrane≈30 kDa). Purified product was freeze-dried and analysed by FT-IR to estimate conversion degree.

Smart synthesis of charged conjugates

PEG MA 475 (182.0 mg, 0.383 mmol) was purified from inhibitor by celite/neutral alumina column then was bubbled with argon and added under argon in 5 mL flaṣkwith 2-[2-(2-Azidoethoxy)ethyl]Methacrylate (16.22 mg, 0.0658 mmol); α–chymotrypsin macroinitiator (15 mg, 0.00059 mmol) was solved in 5 mL of PBS buffer (0.1 M, pH 6.0) bubbled with argon and this solution added to the monomer flask. Solution of monomers and macroinitiator was transferred under argon in catalyst flask containing CuBr (2.1 mg, 0.014 mmol), CuBr2 (3.12 mg, 0.014 mmol), 2-2'-Bipyridil (5.848 mg, 0.0374 mmol). After 4 hours of stirring in cool room at 4°C was checked D.P. by NMR and were added 300 μL of allyl alcohol. After 30 minutes reaction mixture was divided in four equal parts and three of these were transferred under argon in 2 mL tubes for click coupling. The fourth was exposed to air and was used as Azide Control. In Alcohol tube were propargyl

alcohol (8.0 mg, 0.143 mmol), Sodium Ascorbate (54.0 mg, 0.272 mmol) DIPEA (11.13 mg, 0.0862); in acid and amine tube were propiolic acid (10.0 mg, 0.142 mmol) and propargyl amine (8.0 mg, 0.145 mmol) respectively in addition to the same amount of DIPEA and Sodium Ascorbate. After 12 hours of stirring at room temperature the three click coupling batches and the Azido control were purified by ultracentrifugation (cutoff tubes membrane≈30 kDa). Degree of polymerization (D.P.≈14 monomer unit/initiator group) was estimated by ^{1}H-NMR in D_2O on unpurified conjugate.